पुस्तकालय THE LIBRARY
भौतिक अनुसंधान प्रयोगशाला
PHYSICAL RESEARCH LABORATORY
नवरंगपुरा, अहमदाबाद-380009.
NAVRANGPURA, AHMEDABAD-380009.
भारत/INDIA

043
SOM
15618

Studies on Physical Basis of Luminescence Geochronology and its Applications

Thesis submitted to Nagpur University

for the degree of

Doctor of Philosophy

in

PHYSICS

by

SOMESHWAR RAO L. MAVIDANAM

Earth Science Division

Physical Research Laboratory

Navarangpura, Ahmedabad, India

043
B15618

DEPARTMENT OF PHYSICS

NAGPUR UNIVERSITY

NAGPUR, INDIA

भौतिक अनुसंधान प्रयोगशाला.
PHYSICAL RESEARCH LABORATORY.
कैट सं. 043
Cl. No SOM
लेखा सं
Acc. No 15618
क्रमांक 01/5/96
मूल्य
Price

Certificate

This is to certify that the work presented in the thesis entitled **Physical Basis of Luminescence Geochronology and Its Applications** by Mr.M.Someshwar Rao under my supervision is his own work, and that it is upto the standard of the degree of Doctor of Philosophy.

Place: Nagpur
Date: Feb. 5, 1996

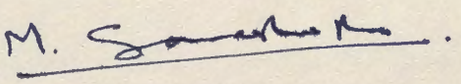
B T Deshmukh

(Prof. B.T.Deshmukh)
(Supervisor)

Declaration

To the best of the author's knowledge and belief, the work in this thesis has not already been accepted in substance for any degree and is not concurrently submitted for any degree. The work is the result of my own investigations unless otherwise stated.

Someshwar Rao L. Mavidanam



(Author)

"na hi kascit ksanam api
jatu tishaty akarmakrt
karyate hy avasah karma
sarvah prakrtijair gunaih"

For no one can remain even for a moment without doing work;
every one is made to act helplessly by the impulses born of nature

Bhagavat Gita, Karma-Yoga, 5

Dedicated to

Amma, Nanna, Anna and Akka

for their affection and inspiration

ACKNOWLEDGEMENT

I was introduced to the field of thermoluminescence by Prof. B.T. Deshmukh and his group at the Department of Physics, Nagpur University. I have had honour and pleasure to be supervised by him. I always admired his his ability to express things in a simple form. I will always be indebted to him for all that he tought me. I acknowledge to him for his personal kindness to me and the moral support during the thesis work.

I express my sincere thanks to Prof.A.K. Singhvi for his invaluable help and support during the thesis work and in its preparation of this thesis. It was his ever encouraging attitude and patience that kept me going at each stage.

Encouragement from Prof. S.Krishnaswami, Prof G.N.Navneeth, and Prof. B.L.K.Somayajulu is also appreciated. I thank the members of the academic committee for their time, intellectual guidance and supervision.

Valuable discussions with Dr. S. Chawla, Dr. Kishan Kumar, Dr. Krbetschek, Prof. M.Lamothe, Dr.K.S.V.Nambi, Dr.R.K.Pant and Dr.S.Sastri are gratefully acknowledged. I wish to thank Dr. B.K.Bisaria, Prof. A.Bronger, Dr.B.K.Sareen and Prof.S.K.Tandon for providing samples for luminescence study.

I am personally grateful to Dr. T.R.Venkatesan, Dr. R.Ramesh, (late)Shri C.S.R.Murthy and Mrs. J.J.Trivedi for their help in the synthesis of the global loess data and Dr. M.M. Sareen for his help in the potassium analysis using AAS.

I am thankful to the members of the library staff for their kind support, Dr. Dinesh Patel for the administrative help, Mr.Girish Ubale and Mr. Nagevadia for their sincere efforts and devotion in the fabrication of the mechanical components of IRSL dating system , Mr. Pandian and Pranav for the electronics help, the members of the glass blowing section and Bhavasar and Waghela.

I benefitted greatly from discussions with Gautam, Himadri, Lambodar, Madhusudan, and Rajan. I thank Debabrata Banerjee, Dr. Cecilia Felix and Navin Juyal for critically going through the manuscript, for constructive suggestions for its improvement and their help at various stages during the thesis work.

I have no words to thank D.P.Raju, Sushma and Varun for their help and all the moral support during the thesis work.

I acknowledge my friends, Biswa, Gopal, Kailash, Manish, Manohar Lal, Manoj, Maqbool Ahmed, Mitaxi, Sam, Sandeep, Seema, Shikha, L.P.Singh, Tarun, Pal, Pareekh, Paulose, Prahlad, Ramani, Supriya and Yadav.

I am grateful in varied ways to the ever charming and informal company of each and every friend and colleague of mine in this institute. The warmth and incense of their friendship made my life here quite a satisfying and memorable experience.

Outside the laboratory, I would like to thank Mrs. Vijaya Mutagi, D.Kameshwara Rao, Dr.Haider, Sunil and their families.

I acknowledge Bhavsar for drafting the figures, Mr. D.R. Ranpura for photography and P.K.Pillai for wordprocessing.

I acknowledge all my teachers and guides who ministered my education.

My parents, Bhaiya-Bhabhi and sister continue to be anchor of stability and support in my studies and my life. The unwavering support of my mother-in-law and father-in-law, close relatives and friends during these many years will remain treasured lifelong memories.

Finally, I thank with love my wife, Sharda who lend her mind, heart and hands in the moments of both frustration and happiness and the maa Sharda and maa Santhoshi for their grace. I owe her my gratitude for the successful completion of the thesis.

M. Someshwar Rao

Contents

List of figures (i)

Index of tables (vi)

Chapter 1: Thermoluminescence and Thermoluminescence dating

1 Introduction 1

1.2 Thermoluminescence 4

1.3 Luminescence Dating 7

1.3 Events dated by TL 9

1.5 Methodological Considerations 11

1) Luminescence measurements, estimation of equivalent dose 14

2) Growth curve 17

3) Stability of the dating signal and anomalous fading 18

4) Dose rate estimation 20

1.6 Objective and scope of the thesis 24

Chapter 2: Experimental Procedures 27

2.1 Sample preparation 27

a) Fine Grain Technique 28

b) Coarse Grain Mineral Inclusion technique (CGT) 28

2.2 Normalization technique 30

2.3 TL measurements 31

2.4 Artificial Irradiations 33

2.5 Measurements of annual dose 34

Chapter 3: Thermoluminescence Dating of Loess-Paleosol sequences

3.1 Introduction 37

3.2 Geological settings and earlier work 41

(a) Luochuan, China 41

(b) Karmaydan, Tadijikstan 43

(c) Dolni Vestonice, Paks and Mende, Central Europe 46

3.3 Experimental details 49

3.4 Results and Discussions 51

(a) Luochuan 61

(b) Tadijikistan 63

(c) Dolni Vestonice, Paks and Mende 64

3.4 Synthesis of TL ages 68

Chapter 4: Studies on Age Underestimation in Thermoluminescence Dating

4.1 Thermoluminescence dating limit and age underestimation 81

4.2 Present Status 81

(a) Change of TL sensitivity with time 84

(b) Change in sensitivity with photo-bleaching 86

(c) Age underestimation to distribution of activation energies 87

4.3 Present studies 88

4.4 Magnitude of underestimation for different sequences 88

4.5 Experimental details 92

4.6 Results 93

(a) Sensitivity with time 93

(b) Effect of dose/dose-rate on sensitivity 94

(c) Change consequent to photobleaching 98

(d) Effect of combined dose/dose-rate and sunbleaching on the sensitivity 101

4.7 Physical basis for sensitivity changes 104

(a) Mineral prior to weathering (geological rock) 106

(b) Sunbleaching (Zero age sediment) 106

(c) Old Sediment 106

(d) Laboratory Zeroing 107

(e) At high laboratory irradiations 107

(f) Zeroing 107

4.8 Summary 108

Chapter 5: Infrared Stimulated Luminescence Dating 111

5.1 Introduction 111

5.2 Instrumentation 115

(c) Age underestimation to distribution of activation energies 87

4.3 Present studies 88

4.4 Magnitude of underestimation for different sequences 88

4.5 Experimental details 92

4.6 Results 93

(a) Sensitivity with time 93

(b) Effect of dose/dose-rate on sensitivity 94

(c) Change consequent to photobleaching 98

(d) Effect of combined dose/dose-rate and sunbleaching on the sensitivity 101

4.7 Physical basis for sensitivity changes 104

(a) Mineral prior to weathering (geological rock) 106

(b) Sunbleaching (Zero age sediment) 106

(c) Old Sediment 106

(d) Laboratory Zeroing 107

(e) At high laboratory irradiations 107

(f) Zeroing 107

4.8 Summary 108

Chapter 5: Infrared Stimulated Luminescence Dating 111

5.1 Introduction 111

5.2 Instrumentation 115

(a) Source 115

(b) Sample chamber 119

(c) Detector 122

5.3 Samples 122

(1) Aeolian environments 124

(2) Fluvial Environments 124

5.4 Analysis 125

5.5 Results and Discussion 128

Chapter 6: Summary and Perspective for Future Research 137

6.1 Summary of the work presented 137

6.2 Future Directions 143

LIST OF FIGURES

Chapter 1

Fig. 1.1(a) Explanation of the basic process of TL induction using the band theory of solids (After Aitken, 1985).

(b) Schematic of simple types of defect such as negative ion vacancy, interstitial defect and impurities in an ionic crystal (After Aitken, 1974).

Fig. 1.2. Events dated by Thermoluminescence

(a) Dating of most recent thermal events
(b) Dating of authegenic growth
(c) Dating of sediments (after Singhvi and Wagner, 1985).

Fig. 1.3. Photo bleaching of Thermoluminescence by sunlight. Important to notice here is the initial rapid bleaching and the asymptotic nature of TL reduction with bleaching time. Typical bleached levels for a 12 hour sunbleaching are ~10-30% which depend on the mineral type, sunlight flux and spectral features of the net sunlight reaching it (after Singhvi and Mejdahl, 1985).

Fig. 1.4. Schematic of methods used in estimation of equivalent dose for sediment. Dose on X-axis refers to the laboratory dose. In a more general (and more commonly encountered) case, the growth curves are non-linear. In view of finite L_0 intensity, it is considered that low dose supralinearity corrections are not necessary for sediment (after Wintle and Proszynska, 1983).

Fig. 1.5(a) TL growth curve of Quartz. The curve has two distinct regions of an exponential + linear growth and a supralinear growth beyond ~500 Gy (after Chawla and Singhvi, 1992).

(b) TL growth of K-feldspar (after Mejdahl, 1985).

Fig. 1.6(a) Components of internal and external doses in different minerals commonly used for TL dating. Typically, all the dose to a ~100μm quartz grain is from external radioactivity; 100μm K-feldspar has ~10% of dose from internal potassium whereas for 100 μm zircons, the internal alpha activity almost accounts for the total dose.

Fig. 1.6(b) Typical contributions to dose rate to a mineral/rock (M) in an environment E. For cases where the size of M is greater than the range of β or α particles the transformation M = E applies for that component.

Chapter 2

Fig. 2.1. Block diagram of the TL apparatus.

Chapter 3

Fig. 3.1. Present day distribution of loess (modified after Williams et al., 1993).

Fig. 3.2. Stratigraphy of Luochuan Loess Profile (Potou section), China. The Brunhes Matuyama boundary occurring at 780 ka is located in soil S_8 (after Bronger and Heinkele, 1989).

Fig. 3.3. Stratigraphy at Karmaydan, along with a correlation with the deep sea oxygen isotope data (After Bronger et al., 1995). The Brunhes Matuyama boundary is located below soil PK IX.

Fig. 3.4. Stratigraphy at Paks and Mende. The Brunhes Matuyama boundary is located below soil F_5 (based on correlation with (after Singhvi et al., 1989).

Fig. 3.5. Ligands for the figures 3.2, 3.2 and 3.4.

Fig. 3.6. Bleaching of TL with sunlight exposure expressed as fraction of natural TL remaining for the sample BCH37.

Fig. 3.7. Plot showing (a) typical glow curve for BCH 11 fine grain sample, (b) typical growth curve (i) additive (ii) regeneration and (c) age plateau

Fig. 3.8. Plot showing (a) typical glow curve for DV135 fine grain sample, (b) typical growth curve and (c) age plateau

Fig. 3.9. Plot showing (a) typical glow curve for J4R fine grain sample, (b) typical growth curve and (c) age plateau

Fig. 3.10. Stratigraphy of Luochuan loess profile along with TL ages obtained in the present thesis (PRL). For comparison, TL ages obtained by Forman et al. (1991) and Lu et al (1987) are also given. A good concordance on ages from different laboratories is seen.

Fig. 3.11. Stratigraphy of loess profile from Dolni Vestonice along with TL ages obtained in the present study (PRL). TL ages reported by Musson and Wintle (1994), Zoller et al (1994) and Zoller et al (1994) are also given for comparison. A good concordance between independently measured ages from different laboratories is seen.

Fig. 3.12. Stratigraphy of TL ages obtained in the present thesis along with other ages reported by Wintle and Packman (1988) and by Zoller and Wagner (1992).

Fig. 3.13. Stratigraphy of TL ages obtained in the present thesis along with other ages reported by Wintle and Packman (1988) and by Zoller and Wagner (1992).

Fig. 3.14 Probability density of occurrence of Loess age (accumulation) for the global data. The figure is constructed by assuming the width of the age gaussian as 1 sigma (Fig. a) and 2 sigma (Fig b).

Fig. 3.15 Probability density of occurrence of Loess age (accumulation) for the loess sequences from Europe. The figure is constructed by assuming the width of the age gaussian as 1 sigma (Fig a) and 2-sigma (Fig.b).

Fig. 3.16. Probability density of occurrence of Loess age (accumulation) for the Chinese loess sequences. The figure is constructed by assuming the width of the age gaussian as 1 sigma (Fig a) and 2sigma (Fig b).

Fig. 3.17. Probability density of occurrence of Loess age (accumulation) for the loess from US. The figure is constructed by assuming the width of the age gaussian as 1 sigma (Fig a) and 2sigma (Fig. b).

Fig. 3.18. Probability density of occurrence of Loess age (accumulation) for loess from New Zealand. The figure is constructed by assuming the width of the age gaussian as 1 sigma (Fig a) and 2sigma (Fig. b).

Fig. 3.19. Power spectrum analysis of Fig. (3.11) unperturbed and (b) perturbed when the hight of the 17 ka peak was arbitrarily reduced to 50%.

Chapter 4.

Fig. 4.1. Comparison of TL ages with geological and other age estimates (After Debenham, 1985).

Fig. 4.2. Plot of TL ages obtained in this study with oxygen isotope stratigraphy as given by Bronger and Heinkele, (1989) and Bronger et.al. (1995). (a)- for Tadjikistan (b)- for Luochuan.

Fig. 4.3. Plot showing normalized glow curves of Tadjikistan loess (a)

N+Sun+Aβ(b) N+Sun.

Fig. 4.4. Normalized TL sensitivity of loess sample with expected age (a) for Tadjikistan, (b) for Luochuan and (c) for K-feldspar mineral separate.

Fig. 4.5. Glow curves of samples J4 for a test dose after incremental laboratory doses followed by sun bleaching.

Fig. 4.6. Normalized TL sensitivity for a test dose following a beta dose and sunbleaching. The data is plotted with respect to laboratory beta dose (a) for Tadjikistan (b) for Luochuan.

Fig. 4.7. Changes in TL sensitivity with multiple sun bleaching cycle each of 12 hr. duration (i) for J4, (ii) for BCH 37 and (iii) for TL7.

Fig. 4.8. Glow curves depicting increase in TL sensitivity for a test dose of 22 Gy after laboratory irradiation followed by a 12 hr sun exposure (i) after laboratory dose of 5.5kGy and (ii) after laboratory dose of 22Gy.

Fig. 4.9. Energy level model showing recombination and charge transfer process during sunbleaching.

Fig. 4.10. Pictorial representation of h_1, h_2 and h_3 centre population at various stages in irradiation and bleaching cycles.

Fig. 4.11. Comparison of "corrected" TL ages with expected ages. The uncorrected ages are also provided to indicate the extent of sensitivity effect (i) for Tadjikistan and (ii) for Luochuan, China.

Chapter 5

Fig. 5.1(a) Stimulated luminescence intensity with excitation wavelength. The resonance at 1.43 eV is used for IRSL dating.

(b) Schematic band structure energy diagram of IRSL process (after Hutt et al. 1988, Hutt and Jaek 1989).

Fig. 5.2(a) Stimulation spectra of K-feldspar with excitation wavelength. The curve differs from Hutt et.al.(1988), in that the luminescence intensity in green blue region is substantially higher (after Clark and Sanderson, 1994)

(b) IRSL energy levelmodel (after Clark and Sanderson, 1994).

Fig. 5.3. Schematic diagram of IRSL measurement system

Fig. 5.4. Infrared excitation peak of K-feldspar, stimulated with a tungsten halogen lamp and the LED TEMT 484 output at 50mA supply current in stabilized condition (After Clark and Sanderson 1994; Spooner and Franks 1990)

Fig 5.5. Reproducibility of infrared source radiance under repetitive measurements.

Fig. 5.6. Schematic diagram of the IRSL dating system developed at PRL. Important parts are,

1) Aluminium flange with oblique slots for infra-red diodes.
2) Aluminium plate with 16 disc equidistant disc slots.
3) Mounting window.
4) Sample change knob

Fig. 5.7. IRSl shine curves (a) disc kept directly under the infrared source (b) disc which is pre-exposed to scattered light for 30 min at a disc slot next to the slot being stimulated. Note that the scattered light caused bleaching of signal by 0.02% in 30min time.

Fig. 5.8. Terrace sequence of Indo-Gangetic alluvium from Kanpur along with the sample locations for the luminescence dating.

Fig. 5.9. Plot showing (a) IRSL shine curves (b) growth curve and (c) shine plateau for polymineralic loess sample J4 (Tadjikstan).

Fig. 5.10. Plot showing (a) IRSL shine curves (b) growth curve and (c) shine plateau for K-feldspar mineral separates for VJPR-5

Fig. 5.11. Plot showing (a) IRSL shine curves (b) growth curve and (c) shine plateau for K-feldspar mineral separates for the surface sediment from the Indo-Gangetic alluvium.

Fig. 5.12. Comparison of IRSL ages on K-feldspar with other ages obtained by TL (quartz, feldspar and polymineral), OSL (quartz) and radiocarbon.

Fig. 5.13. Correlation of IRSL ages (this study) with the oxygen isotope stratigraphy as given by (Bronger et.al., 1995).

Fig. 5.14. Plot showing the comparison of available IRSL and TL ages obtained from various sedimentary deposits (a) regeneration and (b) additive

INDEX OF TABLES

2.1. Comparison between potassium concentration (%) as estimated by AAS and γ-spectrometer.

3.1. Thermoluminescence results and radioactivity data for loess samples from Luochuan.

3.2a. Dose-rate data for Tadjikistan loess.

3.2b. Luminescence dating results for Tadjikistan loess.

3.3. Dose rate data and thermoluminescence results for loess from Dolni Vestonice.

3.4. Luminescence dating results for loess from Paks.

3.5. Thermoluminescence results and radioactivity data for the loess sequence from Mende.

4.1. Comparison of TL ages with the expected ages for the loess profiles from Tadjikistan and China.

5.1. Luminescence dating results of paleofan deposits of Sabarmati river basin.

5.2. TL and IRSL data on samples for the Gangetic alluvium.

Chapter 1

Thermoluminescence and Thermoluminescence dating

1.1. Introduction

With growing concern for man-made climatic changes, an increasing effort is being made to understand the basic climatic system and its natural variability. The available instrumental weather records provide a very limited data set to meaningfully understand the natural variability of the climate system over longer time scales. Consequently, a major emphasis is being placed towards retrieving proxy climatic data from geological sediments, which could then be used to examine and constrain the Global General Circulation Climate Models. The geological record of climate so far has been predominantly

based on ocean cores. It is yet to be established if climate change on land had also the same timing and amplitude. This is important in terms of understanding crucial parameters relating to land albedo changes, vegetational and precipitation changes as also in elucidating orographic effects on climate dynamics.

Unlike oceanic records, terrestrial records are seldom complete. The very agencies that deposit sediments also cause their erosion. Consequently, chronology plays an important role in correlating climate sensitive geological sequences in time and space. A review of chronological methods for the Quaternary period spanning the past 2 Ma of the geological record suggests that only four methods besides luminescence dating can be applied over specific time windows and on specific samples. The **radiocarbon dating** is applicable only to organic remains and carbonates, has a useful range of ~50 ka. Despite the innovation of accelerator mass spectrometry enabling milligram sample analysis, the method suffers from inherent difficulties relating to its calibration beyond the tree ring calibration range of 11 ka, the open system behaviour exhibited by most carbonates often provides only the radiocarbon content of the sample rather than its age. Even in the case of organic rich peat, recent studies have indicated that these are also not close systems in respect of their radiocarbon. Although the advent of thermal ionization mass spectrometry makes the use of **U-series disequilibrium** an attractive proposition for dating events upto ~350 ka, it is generally difficult to find diagenetically unaltered carbonates on the land. Consequently, U-series ages on dirty terrestrial carbonates could often be suspect, due to the presence

of detrital Thorium. Recently, use of ^{10}Be has been proposed to date the wind blown sediments if a constant flux of cosmogenically produced ^{10}Be over geological time can be assumed. However, substantial variations in ^{10}Be content of sample within a strata, difficulties in establishing the constancy of the precipitation of ^{10}Be and variability of ^{10}Be production have hampered its usage in any meaningful chronometry. Though it is possible to use **paleomagnetism** in several terrestrial sequences, the method necessarily requires a secondary calibration age. Extrapolation from the present to Brunhes-Matuyama boundary at 780 ka requires assumption of constant sedimentation rate, a condition that is rarely satisfied in terrestrial sediments.

In this milieu, the advent of the luminescence technique with its applicability to the very minerals (e.g. silicates, carbonates, sulphates etc.) that constitute the sediments, its immunity to cosmic ray flux variability and its range from the present to upto a million years has made it a preferred choice to the extent that during the past decade an estimated 80 luminescence dating systems have become operational. The basic importance of the method stems from the fact that it in principle can provide independent ages to different substrata of a complex stratigraphic sequence that could range from a volcanic tephra layer to an aeolian sand and from a fluvial deposit to a colluvium. This fact allows for a self consistency criterion to be developed for each case. Consequently, the method is currently being applied to date extensively to all possible geomorphic situation and the method from its development barely a decade ago today finds a place in all studies related to recent Earth surface processes and climate dynamics. In respect of the application of luminescence

dating to a variety of situations brought out several new physical phenomena that needed deeper insights into the process of interaction of radiation with matter and luminescence production vis-a-vis defect states participating in it. Thus, phenomena such as anomalous fading, the low efficiency of alphas compared to betas (the LET dependence), TL induction and underestimation of ages were discovered in the context of luminescence dating applications. The research embodied in the present thesis was aimed at both the methodological and application aspects of luminescence dating in respect of its application to one of the most important continental deposits - the wind transported dust - termed as loess.

In the following a brief survey of thermoluminescence (TL) and TL dating is provided along with a brief discussion on the scope of the thesis.

1.2. Thermoluminescence

The phenomenon of stimulated luminescence can be explained using the band theory of solids (fig 1.1a). Typically in silicates, the band gap between the valence band (VB) to the conduction band (CB) is ~8-10 eV. The interaction of ionizing radiations such as α, β, γ or X-rays with a crystal produces an avalanche of electrons and holes. Most of the charges recombine instantaneously by dissipating energy either thermally or optically. A small fraction of these charges, however, gets trapped at various lattice defects in the crystal (Fig 1.1a,b). These defects could be in the form of vacancies, impurities or interstitials, which are either intrinsically present or are created by the

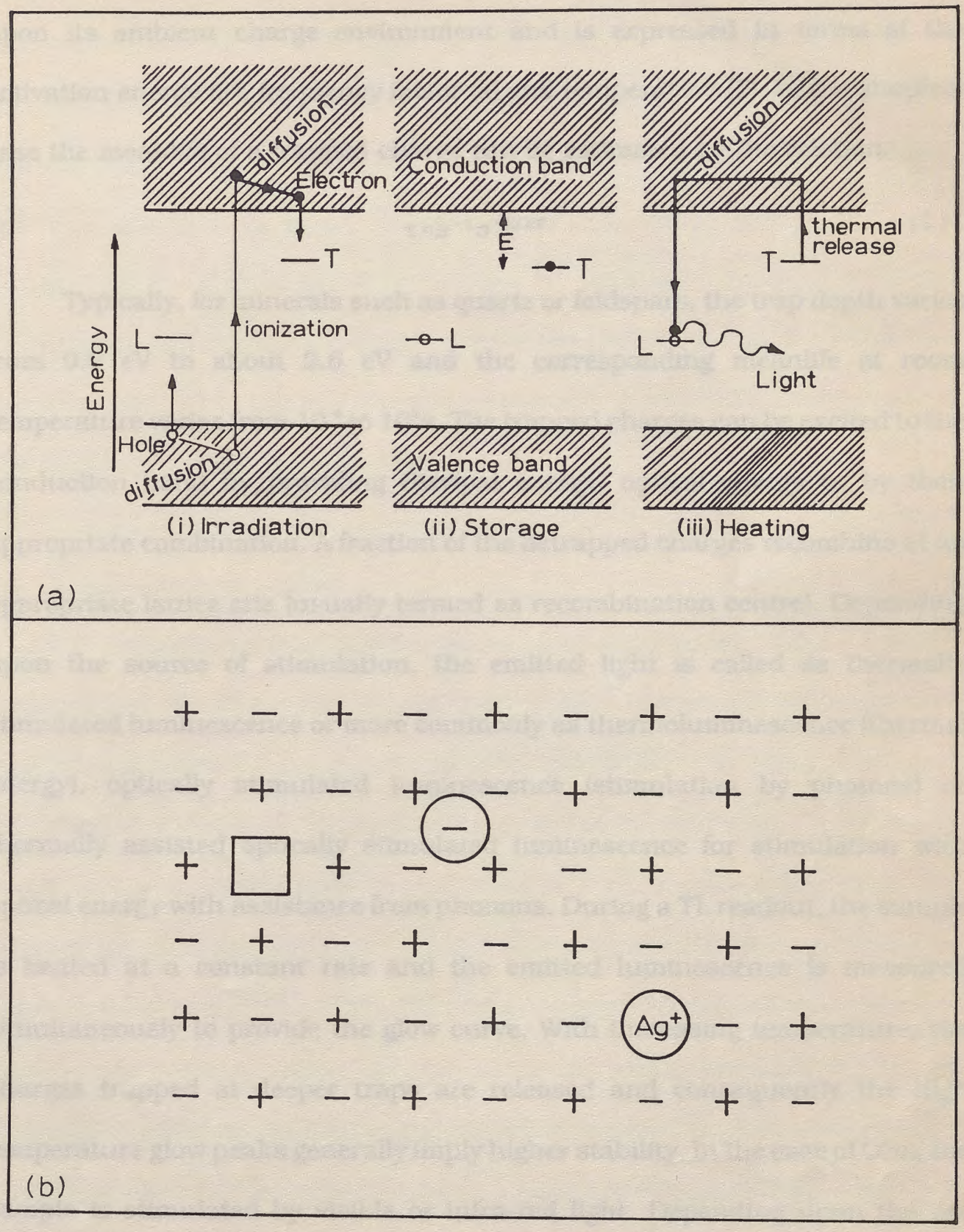


Fig. 1.1(a) Explanation of the basic process of TL induction using the band theory of solids (After Aitken, 1985).

(b) Schematic of simple types of defect such as negative ion vacancy, interstitial defect and impurities in an ionic crystal (After Aitken, 1974).

incident radiation. The residence time (τ) of a trapped charge in a trap depends upon its ambient charge environment and is expressed in terms of the activation energy (E), frequency factor (s) and temperature (T). In the simplest case the meanlife of a trapped charge can be estimated by the relation,

$$\tau = s^{-1} e^{-E/kT} \quad \ldots . \quad (1)$$

Typically, for minerals such as quartz or feldspars, the trap depth varies from 0.6 eV to about 2.6 eV and the corresponding meanlife at room temperature varies from 10^{-4} to 10^{9}a. The trapped charges can be excited to the conduction band by providing thermal energy, optical energy or by their appropriate combination. A fraction of the detrapped charges recombine at an appropriate lattice site (usually termed as recombination centre). Depending upon the source of stimulation, the emitted light is called as thermally stimulated luminescence or more commonly as thermoluminescence (thermal energy), optically stimulated luminescence (stimulation by photons) or thermally assisted optically stimulated luminescence for stimulation with optical energy with assistance from phonons. During a TL readout, the sample is heated at a constant rate and the emitted luminescence is measured simultaneously to provide the glow curve. With increasing temperature, the charges trapped at deeper traps are released and consequently the high temperature glow peaks generally imply higher stability. In the case of OSL, the sample is stimulated by visible or infra-red light. Depending upon the net thermal or photon energy, a set of traps get sampled. Some of the optically stimulated free charges radiatively recombine at the recombination centres to provide luminescence. With a constant source of stimulation, the trapped

charge concentration decreases with time resulting in the decay of luminescence intensity with time. In both TL and OSL the intensity of stimulated luminescence is proportional to the amount of ionization i.e. the dose and the process is cumulative, i.e. the total luminescence increases with dose upto a saturation value. The process of stimulated luminescence also implies that the stimulated emission can be achieved only once after an irradiation as all the trapped charges are evicted on stimulation. A sample has to be re-irradiated to recreate the trapped charge concentration which could then be stimulated to provide luminescence.

1.3. Luminescence Dating

The proportional relationship of luminescence with dose, with a necessity of adhering to the sequence of irradiation, optical or thermal stimulation to observe luminescence formed the basis of its application in radiation dosimetry and dating (Daniels et.al., 1953). In the case of dating application, use is made of the fact that minerals in environment are constantly exposed to the radiation arising from the decay of ubiquitous natural radio isotopes with long half-lives (~10^9 a) viz. ^{238}U, ^{232}Th, ^{40}K and a marginal contribution comes from cosmic rays. Thus as a first approximation the luminescence induction in minerals from such a constant radiation flux [measured as μGy/a (where 1 Gy is 1J/kg of absorbed energy)] occurs at a constant rate such that one could write a simple relationship

$$L = t \times \dot{L} \qquad \ldots . \quad (2)$$

where L is the total stored luminescence, t is the time (Age) and $\dot{L}$ is the annual rate of TL induction.

Thus,

$$t(Age;yrs) = \frac{TL\ acquired}{TL\ acquisition\ per\ year} \qquad \ldots\ (3)$$

This could be simplified to

$$t = \frac{L}{\sum_{\alpha,\beta,\gamma,c} (L/unit\ dose)\ x\ (dose/year)} \qquad \ldots\ (4)$$

$$= \frac{L}{\sum_{\alpha,\beta,\gamma,c} (\chi_i\ D_i)}$$

where the denominator accounts for summation of radiation doses from α, β, γ's emitted in the decay of ^{238}U, ^{232}Th and ^{40}K and cosmic rays. χ's represent the TL sensitivity of a mineral expressed as TL/unit dose.

The above equation is simplified further to write

$$t = \frac{L}{\chi_\alpha D_\alpha + \chi_\beta D_\beta + \chi_\gamma D_\gamma + \chi_c D_c} \qquad \ldots\ (5)$$

D_α, D_β, D_γ and D_c denote the dose rate due to α, β, γ and cosmic rays respectively.

Defining a mineral dependent parameter, the alpha efficiency factor 'a' (Zimmerman, 1971) as,

$$a = \frac{\chi_\alpha}{\chi_\beta} \text{ and } Q = \frac{L}{\chi_\beta} \quad \ldots\ (6)$$

and realizing that, $\chi_\beta = \chi_\gamma = \chi_c$, the age equation can be written as,

$$Age(t; years) = \frac{Q}{aD_\alpha + D_\beta + D_\gamma + D_c} \quad \ldots\ (7)$$

where Q is the laboratory β dose that can induce a TL level identical to that in the virgin sample. The age represents elapsed time elapsed since the zeroing of luminescence intensity to the time of analysis.

A luminescence age determination thus comprises two measurement schedules.

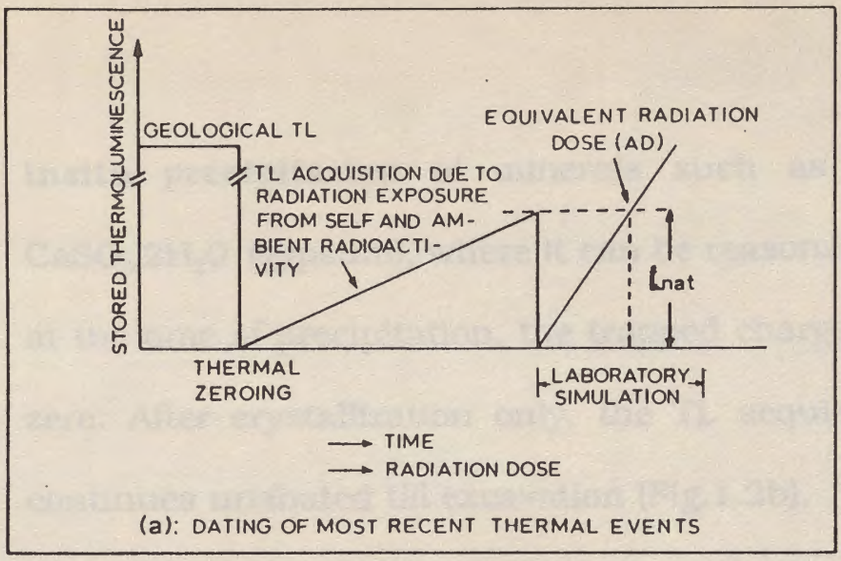
(i) the luminescence measurements to obtain a and Q and,

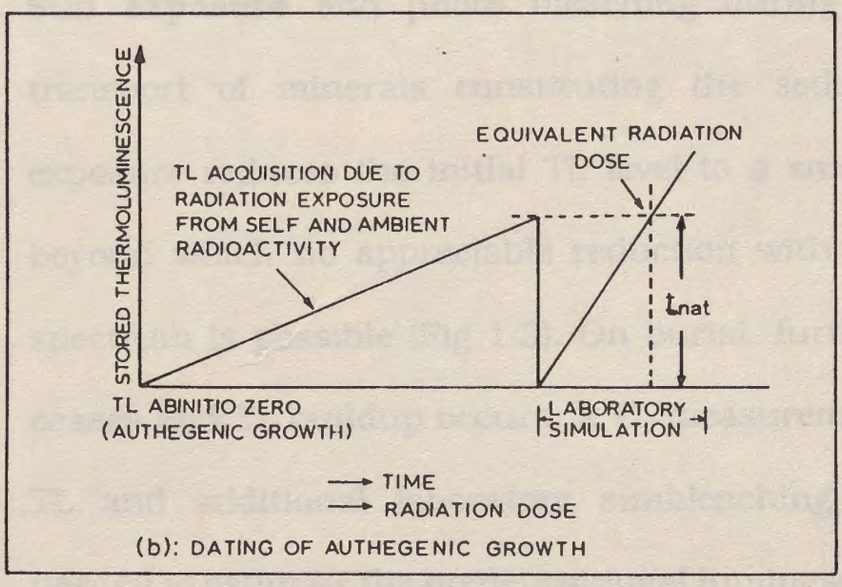
(ii) estimation of concentration of elements viz., U, Th and K for calculation of dose rates.

1.4. Events dated by TL

Three types of events can be dated using the luminescence method (Fig 1.2). All of these refer to events that reset the geological luminescence to zero or a near zero residual level. The events that can be dated are,

(a) **Heating** of mineral grains (to ~400-500°C such as contact heating of sediments by lava flows and the firing event of pottery by ancient man. In this case the previously acquired TL is completely reset to a zero level, and subsequent burial and irradiation from the ambient radiation field results in regrowth of TL which continues unabated till excavation (Fig.1.2a).





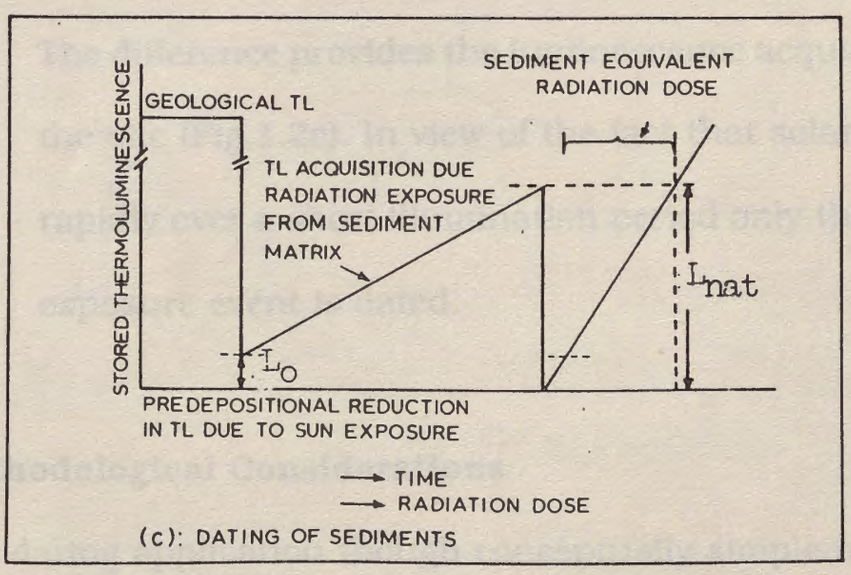


Fig. 1.2. Events dated by Thermoluminescence

(a) Dating of most recent thermal events
(b) Dating of authegenic growth
(c) Dating of sediments (after Singhvi and Wagner, 1985).

(b) **Insitu precipitation** of minerals such as $CaCO_3$ (calcite), $CaSO_4.2H_20$ (gypsum), where it can be reasonably assumed that at the time of precipitation, the trapped charge concentration is zero. After crystallization only, the TL acquisition begins and continues unabated till excavation (Fig.1.2b).

(c) **Sun exposure** and photo bleaching during weathering and transport of minerals constituting the sediments. The sun exposure reduces the initial TL level to a small residual value beyond which no appreciable reduction with the ambient sun spectrum is possible (Fig 1.3). On burial, further sun exposure ceases and TL buildup occurs. A TL measurement provides total TL and additional laboratory sunbleaching experiments are needed to estimate the predepositional luminescence level (i.e. L_o). The difference provides the luminescence acquired since burial at the site (Fig.1.2c). In view of the fact that solar bleaching occurs rapidly over a short illumination period only the most recent sun exposure event is dated.

1.5. Methodological Considerations

The dating application though conceptually simple needs considerable effort in practice. This arises due to several factors such as the difference in the range of α, β and γ radiations and inhomogeneity in the distribution of radioactivity, attenuation of radioactivity by the presence of moisture in

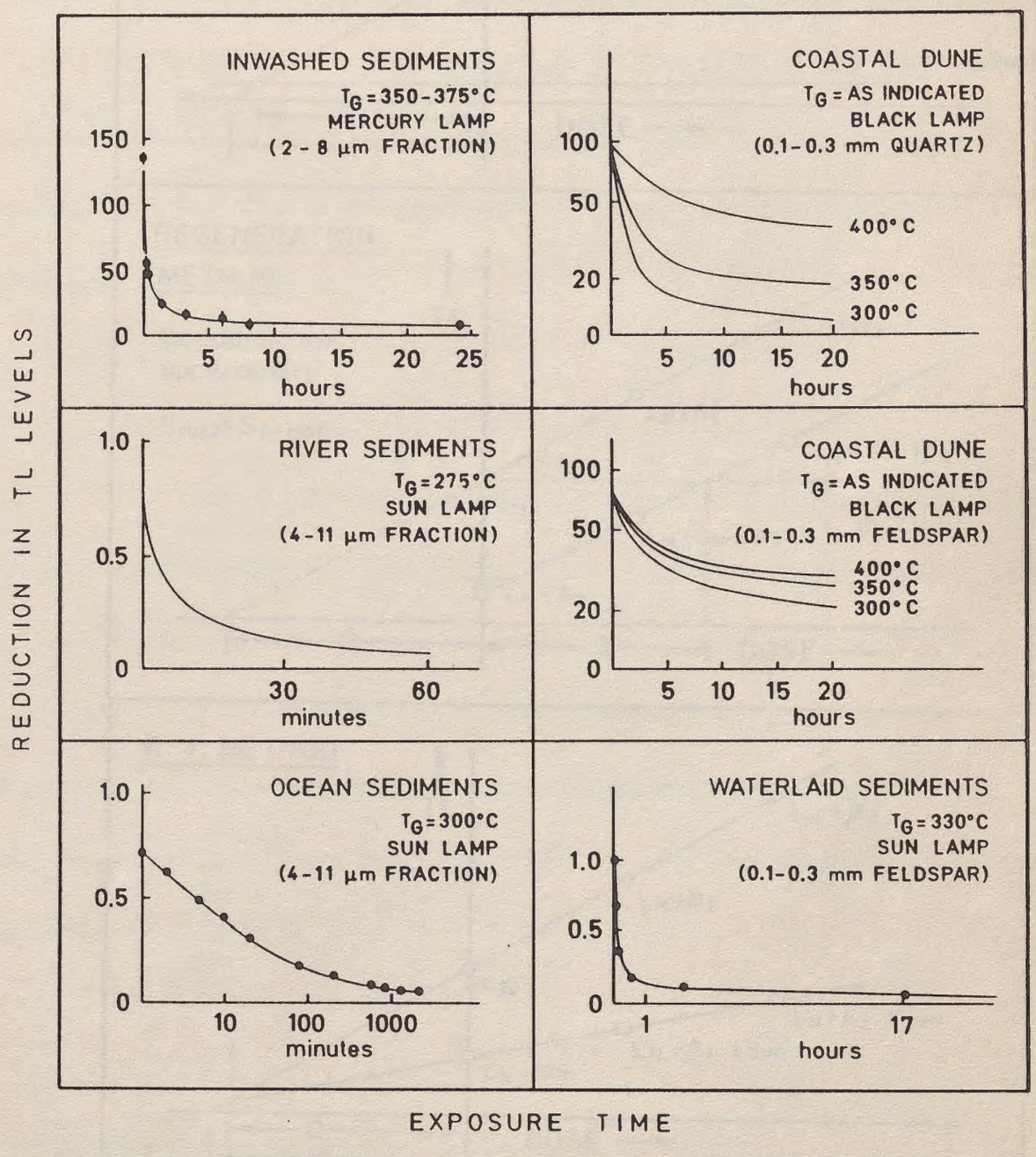


Fig. 1.3. Photo bleaching of Thermoluminescence by sunlight. Important to notice here is the initial rapid bleaching and the asymptotic nature of TL reduction with bleaching time. Typical bleached levels for a 12 hour sunbleaching are ~10-30% which depend on the mineral type, sunlight flux and spectral features of the net sunlight reaching it (after Singhvi and Mejdahl, 1985).

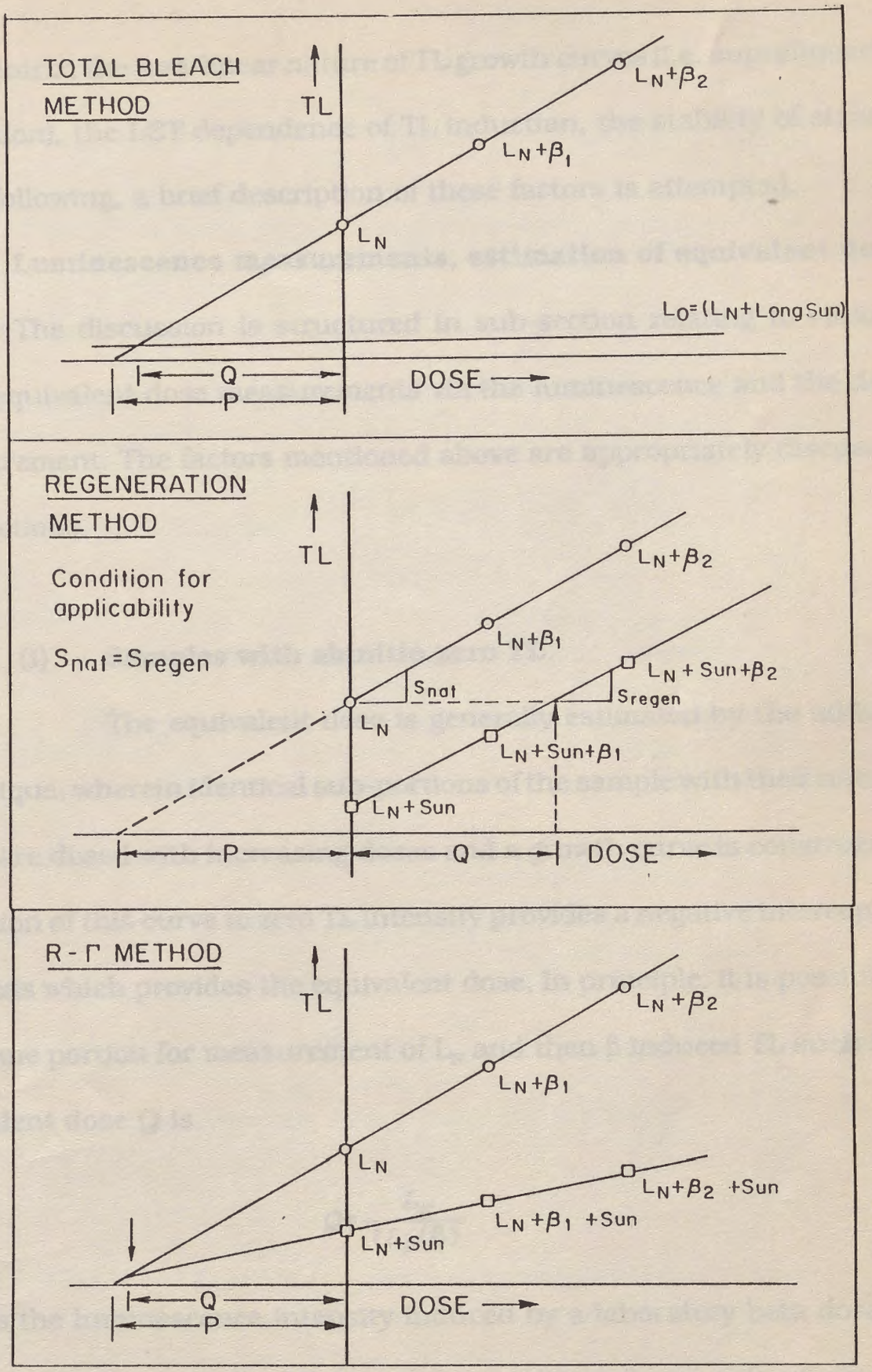


Fig. 1.4. Schematic of methods used in estimation of equivalent dose for sediment. Dose on X-axis refers to the laboratory dose. In a more general (and more commonly encountered) case, the growth curves are non-linear. In view of finite L_0 intensity, it is considered that low dose supralinearity corrections are not necessary for sediment (after WIntle and Proszynska, 1983).

sediment matrix, the non-linear nature of TL growth curves (i.e. supralinearity and saturation), the LET dependence of TL induction, the stability of signals etc. In the following, a brief description of these factors is attempted.

(1) Luminescence measurements, estimation of equivalent dose

The discussion is structured in sub-section relating to various aspects of equivalent dose measurements via the luminescence and the dose rate measurement. The factors mentioned above are appropriately discussed in these sections.

(i) Samples with abinitio zero TL

The equivalent dose is generally estimated by the additive dose technique, wherein identical sub-portions of the sample with their natural signal (L_N) are dosed with increasing doses and a growth curve is constructed. Extrapolation of this curve to zero TL intensity provides a negative intercept on the dose axis which provides the equivalent dose. In principle, it is possible to use the same portion for measurement of L_N and then β induced TL such that the equivalent dose Q is

$$Q = \frac{L_N}{(L_1/\beta)}$$

where L_1 is the luminescence intensity induced by a laboratory beta dose (β). This is, however, normally avoided to circumvent interferences from possible changes of (i) TL response, (ii) crystal phase and (iii) reflectivity of the sample consequent to the heating associated with recording of L_N.

Two factors need to be mentioned here. These are (1) reliable

extrapolation of the additive dose curve, especially for samples having equivalent doses approaching saturation dose or sample phases with complex growth characteristics and, (2) the supralinearity intercept which occurs due to slower growth of TL sensitivity initially followed by substantially enhanced sensitivity. Fleming (1975) has provided an elegant discussion on the procedures for estimation of supralinearity intercept which could be upto a dose of few Gy and occasionally be as large as 20 Gy and is of no consequence for samples beyond the Holocene.

(ii) Sediment with Predepositional Sun Exposure

One of the basic differences in this case compared to the previous one is the fact that in this case a zero age sample has a non-zero TL. Thus it is implicitly assumed that the estimation of equivalent dose includes the estimation of predepositional TL level. Two cases can arise:

(a) totally bleached sample, i.e. with initial level L_0.

(b) partially bleached sample, i.e. those with initial level $>L_0$.

For totally bleached samples, two approaches are used for estimation of Q (Fig.1.4).

(a) **The total bleach or Additive dose - L_0 method** (Singhvi et. al., 1982) relies on the construction of a additive dose growth curve (Fig.1.4a) and then defining a glow curve temperature dependent factor R such that $R = L_0/L_N$ which implies that the dose P acquired since the sedimentation is related to the total dose via the relation

$$P = (1-R)Q$$

The additive dose method works well when the mathematical form of the growth curve is known to effect a realistic extrapolation. To overcome the difficulty in extrapolation, the regeneration method was developed (Debenham and Walton, 1983; Proszynska, 1983). As name implies this method involves laboratory sun exposure and the laboratory β dosing (i.e. L_N + sun exposure + β) (Fig.1.4b). The intensity L_N is then projected on this curve to find out the equivalent dose and is accepted if the sensitivity of the sample is not altered on sun exposure i.e. $\chi_{nat} = \chi_{regen}$. More recently, a combination of the two methods, the slide method is used. In this, the regeneration curve is superimposed on to the additive growth curve by displacing it along the dose axis by an amount equal to the equivalent dose. The resultant curve is used to construct the missing part of the additive dose curve and the paleodose (Huntley et.al., 1993).

(b) **The Partial Bleach (R-T) Method** (Wintle and Huntley, 1979)

In a variety of situations (such as fluvial sediments), the sun exposure is not sufficient to completely bleach the sample to L_0 level. Both the sun exposure duration and the solar spectrum are modified due to sediment load and turbulence, consequently providing a much attenuated light flux of higher wavelengths (with lower efficacy for photo-bleaching) (Fig.1.4c). In such cases, the partial bleach method is used and a equivalent dose plateau with sun exposure is sought. The partial bleach method comprises the evaluation

of the intersection point of additive dose growth curve and the growth curve based on samples identically dosed but additionally exposed to sun for appropriate (small) duration. Besides the tedium of constructing two growth curves, this method suffers from difficulties arising from extrapolation and in assuming that bleaching is not dose dependent. The experimental errors are also higher due to the propagation of errors in estimating the intersection of two curves. As discussed below, a major advancement for dating poorly bleached sediments has been the development of Optically Stimulated Luminescence method which only probes the most optically sensitive signal.

(2) **Growth curve**: An important aspect of equivalent dose estimation is the nature of the growth curve which decides the extrapolated dose used in age estimation. In general, these are complex for fine grain samples where signal is contributed by various mineral phases with differing TL sensitivities, saturation doses and supralinearity intercepts. To an extent these are simplified with selection of appropriate optical windows (to preferentially detect emission from specific mineral phases). For example, Schott UG-11 optical filter with a transmission in 280-380nm band has been used extensively to select the UV emission from K-feldspar in a polyminerallic sample. This filter has also been used to isolate the more rapidly bleachable TL glow peak at 325°C in quartz mineral separates (Debenham and Walton, 1983; Prescott, 1990).

The nature of growth curve in mineral separates is often non-trivial. Thus for example, quartz growth curves have been variously approximated to

(i) a saturating exponential + one or two linear terms, (ii) third order polynomial (Fig 1.5a). On the other hand, most feldspar growth characteristics are reasonably approximated by a saturating exponential (fig 1.5b). Considerable effort has also been expended in optimizing the error from growth curves and several recipes of laboratory irradiation at equal intervals, doubling intervals and exponentially incrementing intervals have been suggested. A discussion of these is given by Grun and Brumby (1994).

(3) Stability of the dating signal and anomalous fading:

Minerals usually contain a distribution of traps associated with various glow peaks with different meanlives ranging from few seconds to few million years. In dating, only those glow peaks which are stable over a period greater than the event being dated are used in the analysis. Conventionally, the stable region in a glow curve is determined by seeking a plateau in the ratio of natural and artificial glow curve intensity. A plateau of this ratio with temperature provides the region of stability. Subsequently, it was considered desirable to obtain a plateau of ages with glow curve temperatures. Since the traps at higher temperatures (beyond 250°C) are generally stable over geological time scales, most samples exhibit a plateau at temperatures beyond 250°C. To felicitate isolation of the stable signal often a preheat at 150-200°C for times ranging upto few hours is used.

Based on TL kinetics, it is expected that the high temperature signal remains stable over geological time scale. But, in some cases loss of TL signal up to 50% was observed within a few weeks. This phenomena was originally

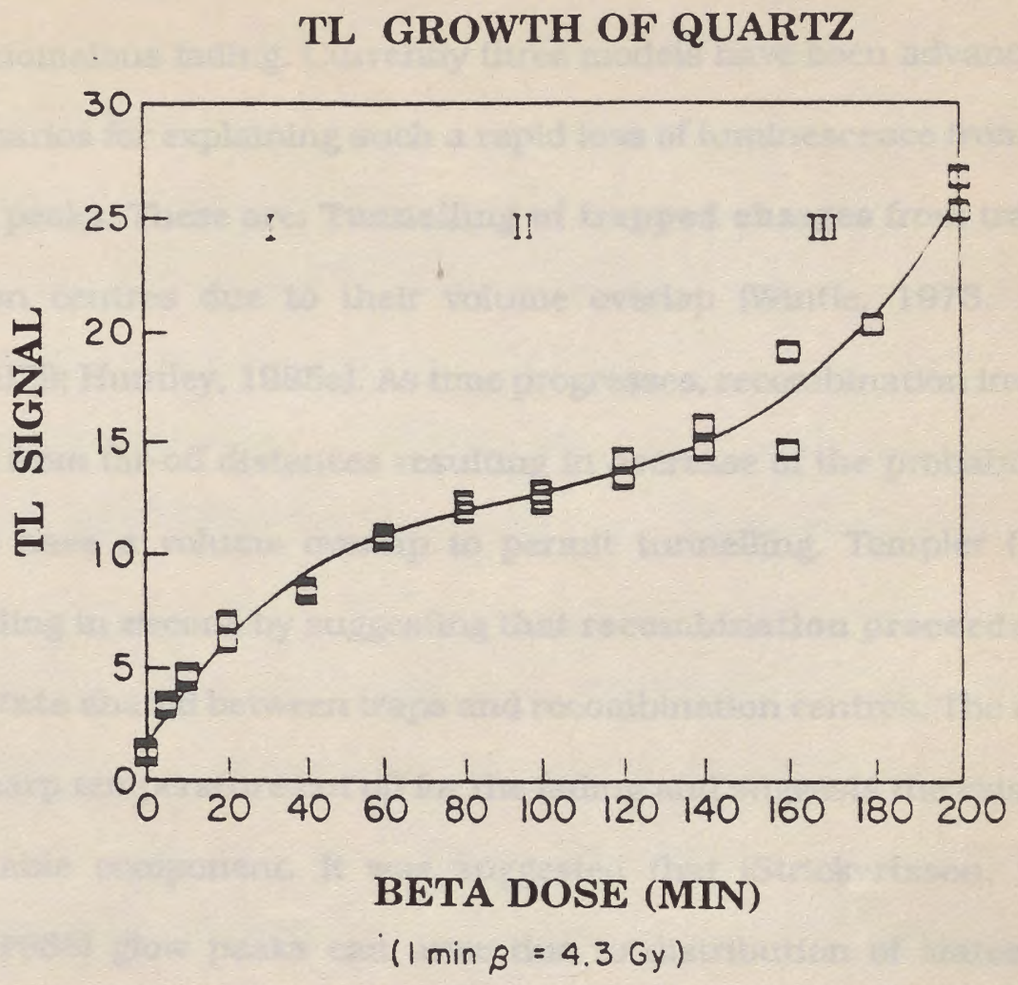


Fig. 1.5(a) TL growth curve of Quartz. The curve has two distinct regions of an exponential + linear growth and a supralinear growth beyond ~500 Gy (after Chawla and Singhvi, 1992).

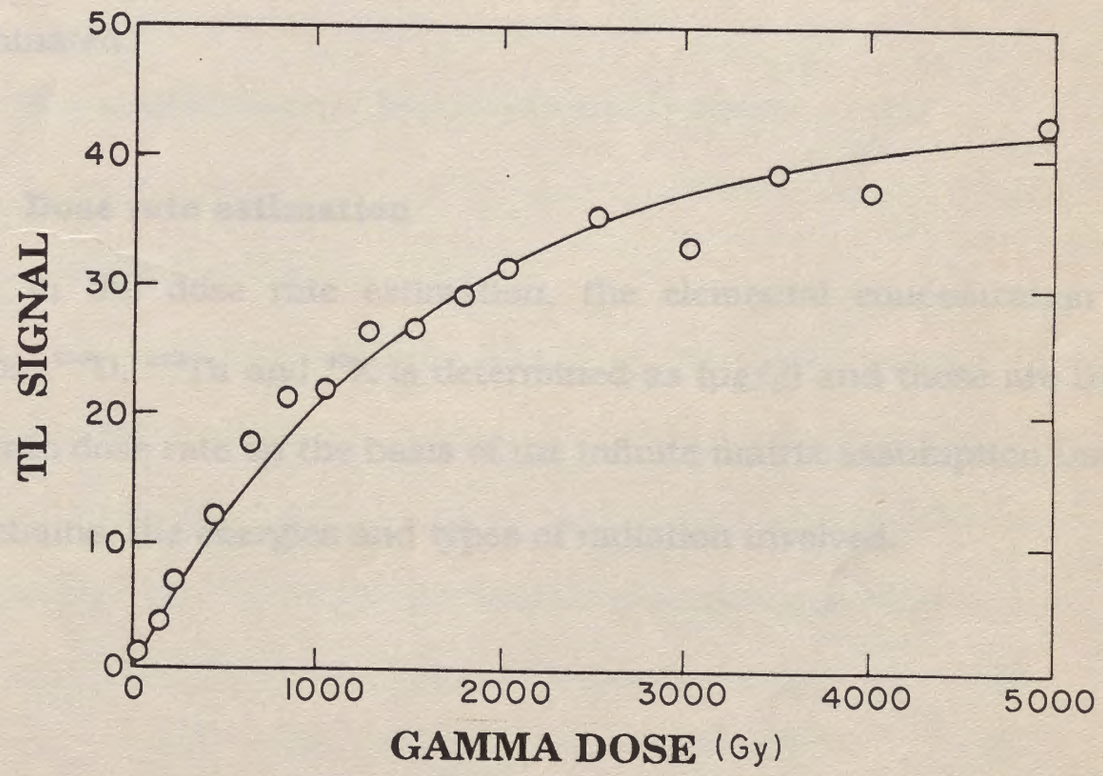


Fig. 1.5(b) TL growth of K-feldspar (after Mejdahl, 1985).

termed as anomalous fading. Currently three models have been advanced as possible scenarios for explaining such a rapid loss of luminescence from high temperature peaks. These are: **Tunnelling of trapped charges** from traps to recombination centres due to their volume overlap (Wintle, 1973, 1977; Visocekas, 1979; Huntley, 1985a). As time progresses, recombination involves charge pairs from far-off distances resulting in decrease of the probability of centres that have a volume overlap to permit tunnelling. Templer (1985) explained fading in zircons by suggesting that **recombination proceeded via an excited state** shared between traps and recombination centres. The model imposes a sharp temperature cut off for the fading and suggests the existence of a true stable component. It was suggested that (Strickertsson, 1985; Sanderson, 1988) glow peaks can arise due to distribution of states with different activation energies and mean lives. The resultant signal therefore shows fading according to the decay of individual components. As indicated above, appropriate pre-heat treatments, each of these unstable components can be eliminated.

(4) Dose rate estimation

In the dose rate estimation, the elemental concentration of elements viz. ^{238}U, ^{232}Th and ^{40}K is determined as (μg/g) and these are then converted into dose rate on the basis of the infinite matrix assumption using the decay chains, the energies and types of radiation involved.

In the estimation of dose rates from a mixed radiation field of α, β, and γ, the important factors are

(i) spatial inhomogeneity of radiation dose

(ii) disequilibrium in the radioactive decay chain and

(iii) water content

Spatial inhomogeneity in radiation dose to a mineral grain arises due to (i) inhomogeneity of radioactivity distribution and (ii) substantial differences in the ranges of α, β and γ rays. Fig.1.6 illustrates these facts by typical examples and provides a generalized dose relationship for each of these components in a typical situation. The large range of γ rays necessitates that both the samples and its ambient strata are analyzed for irradiation. In general, the dosimetry of a natural geological sample becomes complicated with a greater diversity of grain sizes and mineralogy. The analysis is simplified to an extent by selecting specific grain sizes viz.,

(1) **The fine grain technique (FGT)** using 4-11 μm size poly-minerallic fraction (Zimmerman, 1971).

(2) **Mineral inclusion technique** using coarse grains (≥ 90 μm), mineral separates (CGT) for analysis (Flemming, 1970; Mejdahl and Winther-Nielsen, 1982).

In the case of fine grains (4-11 μm), it is assumed that the fine fraction received a full quantum of α dose whereas in coarse grain the α irradiated skin of mineral separates is etched and the etched grain are analyzed with a reasonable assumption that they did not receive any α dose. Absence or presence of α dose

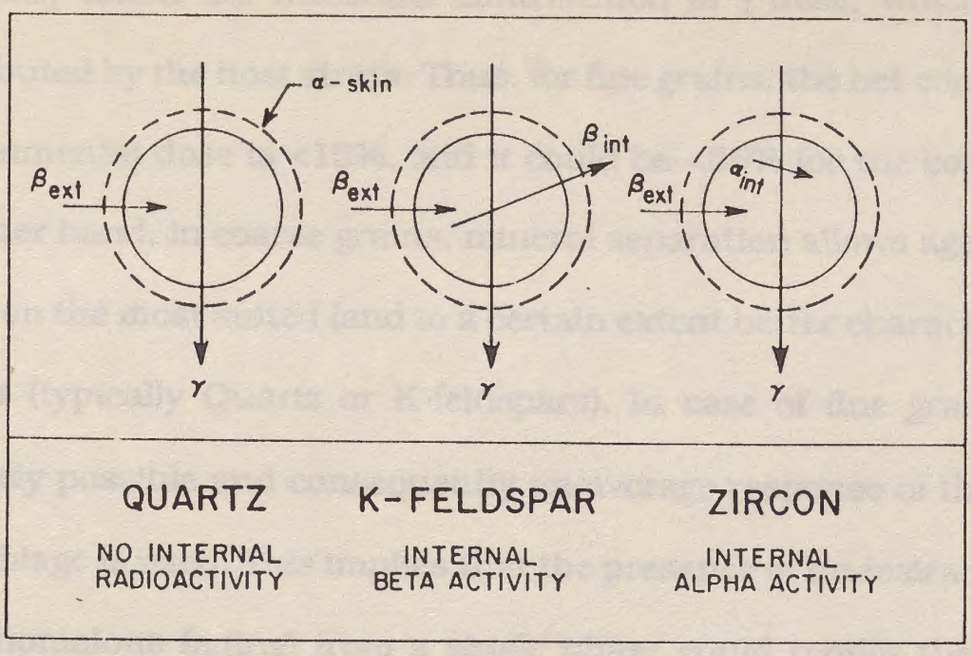


Fig. 1.6(a) Components of internal and external doses in different minerals commonly used for TL dating. Typically, all the dose to a ~100μm quartz grain is from external radioactivity; 100μm K-feldspar has ~10% of dose from internal potassium whereas for 100 μm zircons, the internal alpha activity almost accounts for the total dose.

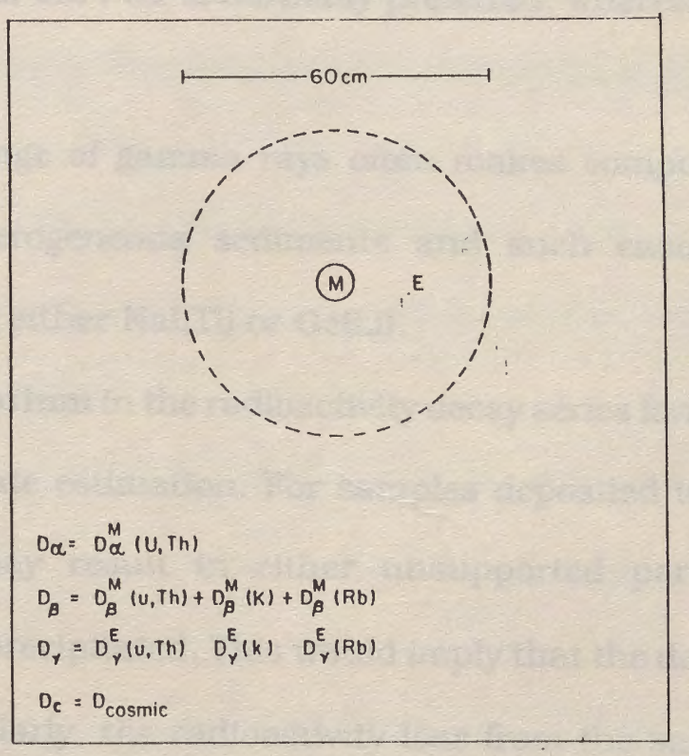


Fig. 1.6(b) Typical contributions to dose rate to a mineral/rock (M) in an environment E. For cases where the size of M is greater than the range of β or α particles the transformation M = E applies for that component.

implicitly alters the fractional contribution of γ dose, which is principally contributed by the host strata. Thus, for fine grains, the net contribution of the environmental dose is <15%, and it could be <35% for the coarse grains. On the other hand, in coarse grains, mineral separation allows age determination based on the most suited (and to a certain extent better characterized) mineral phases (typically Quartz or K-feldspars). In case of fine grains, this is not routinely possible and consequently an average response of the total mineral assemblage is used. This implies that the presence of undesirable TL response (e.g. anomalous fading) from a single phase could render the entire sample unsuitable.

In practice, the choice of the technique is largely governed by the average grain size distribution in the sediment and their depositional environment. Thus, for example, for loess and lacustrine sediments with mean grain size 20 μm, the FGT is normally preferred, whereas for dune sands only CGT is used.

Larger range of gamma rays often makes computation of γ dose rate difficult in heterogeneous sediments and such cases necessitate onsite dosimetry using either NaI(Tl) or Ge(Li).

Disequilibrium in the radioactivity decay series forms another important factor in dose rate estimation. For samples deposited in water, the ambient geochemistry may result in either unsupported parent or unsupported daughter being precipitated. This would imply that the dose rate becomes time dependent. Similarly, the radioactivity loss from the samples forms another important factor. Typically, complete loss of radon can alter the total dose to

the sample by upto 30% and this needs to be established by counting the samples in unsealed and sealed conditions. A good discussion on the dose rate determination is provided by Aitken (1985) and the disequilibrium studies have been described by Wintle (1978) and Readhead (1987).

An important variant in dose rate estimation is the **water content** in the sediment matrix. Devoid of any inherent radioactivity, water efficiently attenuates the radiation flux, diluting thereby the net dose. Typically, a few percent of moisture would alter the net dose by a comparable percentage. Conversion of laboratory determined "dry sample" dose rates to natural "wet" dose rate is computed by using the stopping power ratios of α, β, γ in water and in air. (Zimmerman, 1971). Various parameters that are taken into account for arriving at a realistic estimate of water content through sample history are (i) ground water table, (ii) seasonal changes, (iii) grain size and (iv) pore space volume. In case of extreme situations, the maximum water holding capacity of sediment is estimated and the average water content is assumed at 50% level with ±50% as error. Similarly, standard TLD phosphors are buried for a year to average out seasonal variations in water content. Gamma dose acquired by them during their burial at the site provides a good estimate of the γ dose rate which not only averages over the seasonal fluctuation in water content, but also average over any spatial inhomogeneity in sediment matrix.

1.6. Objective and scope of the Thesis

Theoretically, the upper limit upto which the luminescence technique

can date sediments depends on (i) the dose at which luminescence growth saturates, (ii) the natural dose rate, and (iii) the stability of the dating peak at the ambient temperature. Typically, for loess sequences the dose rate is ~4.5 Gy/ka and saturation dose is ~2.5 kGy. The mean life of the principal TL emitter, K-feldspar high temperature glow peaks is ~10^9a. This suggests that the maximum age limit should be constrained only by the saturation of signal and consequently ages around ~500-600 ka should be obtainable. However, experimentally, early studies on loess-paleosol sequences exhibited a saturation of TL ages at ~100-200 ka which is lower than the saturation limit. The principal objective of this thesis was to identify and understand the physical processes that could give rise to such an age underestimation. The thesis also reports on studies relating to a statistical synthesis of luminescence ages on K-feldspars and new chronology for several loess paleosol sequences. An IRSL dating system constructed and samples from various depositional environments were dated. Additionally, a comparison of IRSL ages obtained in the present study and reported so far with TL and other chronometric ages was also made.

This thesis is structured in six chapters as described below.

Chapter 2 provides a description of experimental methodology used in the dating analysis.

Chapter 3 provides dating results on loess paleosol sequences in China, Tadijikistan and Central Europe along with a summary of the existing dating results in the three regions. Results of synthesis of all the TL ages on loess reported so far (compilation provided as an appendix) also presented.

Implication of this synthesis of global set of TL ages on Loess Paleosol sequences discussed in terms of conventional concepts on synchronicity of loess accumulation, glacial epochs and land-sea correlation is then discussed.

Chapter 4 summarizes our present understanding of age underestimation effect in loess-paleosol sequences including the results discussed in the previous chapter. A series of experiments on changes in TL sensitivity to understand the basic processes leading to age underestimation are then described. A conceptual framework based on one trap and three hole centres is discussed which helps in explaining the observations and provides a basis for the calibration of underestimated ages to true ages.

In **Chapter 5** the basic IRSL process is discussed, and the design of indigenously developed IRSL system is presented. Application of IRSL method to samples from various depositional environments is then demonstrated. A compilation of IRSL data and its comparison with TL ages is then presented which demonstrates that IRSL ages should also experience age underestimation similar to that of TL.

Chapter 6 describes a brief summary of the work presented in the thesis along with a discussion on possible future research directions which could be explored.

Experimental Procedure

Various experimental details, including the sample preparation methodology, the equipment, normalization procedures, error estimation etc. are discussed below.

2.1. Sample preparation

Sediments for the study were collected either in the form of large pieces or in metal cylinders by pushing them into the sediment stratum. Subsequent sample preparation and measurements were carried out under subdued red light to avoid photo-bleaching of thermoluminescence. The outer layer ~10mm of the samples was removed first to eliminate the portions that were sun bleached during sampling. The inner core was then processed either for the

extraction of fine grains (4-11 μm) or for the coarse grain mineral separates (~100-150 μm quartz or feldspars). Usually, the choice of the grain size is determined by the mean grain size of the sediment. Thus, for example, for loess with the mean grain size ~20 μm, fine grain technique was used. On the other hand, for dune sands, coarse grain technique was preferred in view of the mean grain size being ~150 μm.

(a) Fine Grain Technique (FGT): Samples were sequentially treated with 1N HCl (to remove carbonates which are generally post-depositional), 30% H_2O_2 (to dissolve the organic fraction and 0.01N Na-oxalate for deflocculation. During each chemical treatment, samples were given vigorous ultrasonic treatment as also the suspended clay fraction was removed. The separated samples were washed in distilled water and then transferred into an acetone medium for grain size separation and disc preparation. The 4-11 μm grain size, from the bulk sample suspended in 60cm high acetone medium, was separated using Stokes settling time of typically 1.5 minute and 15 minutes. The separated grains were then dispersed either in acetone/alcohol solution and equal volumes (1 ml) of this suspension were pipetted onto small flat bottomed glass tubes, each containing a polished aluminium disc (of 1±.05 cm diameter) at their bottom and about 3cm column of acetone. After drying the solution in an oven (at a temperature of ~45°C for acetone and ~50°C for alcohol), the discs (with thin layer of fine grains) were taken out and transferred into sample holders. Typically ~60 discs from each sample were prepared.

(b) Coarse Grain Mineral inclusion technique (CGT): As discussed above, samples were given chemical pretreatment with 1N HCl and 30% H_2O_2.

The dried samples were sieved for the size fraction 90-150 μm. The sieved fractions were passed through Franz magnetic separator to obtain the non-magnetic fraction which predominantly contained quartz, feldspar and other silicates. The isolation of different mineral phases was done using the sodium polytungstate compound dissolved in water and adjusted to 2.62 g/cm^3 for quartz and 2.58 gm/cm^3 for K-feldspar. The separated quartz and feldspar fractions were etched with HF to remove the alpha exposed layer. The quartz fraction was etched with 40% HF for 80 minutes, followed by 40 minutes with concentrated (12%) HCl to remove fluoride compounds. K-feldspars were extracted after etching the sieved grain size fraction with 10% HF for 40 min followed by 10% HCl treatment to remove the fluoride compounds. The sample purity was also examined using IRSL. Presence of quartz in the feldspar fraction is detected to an extent by the presence of 375°C glow peak superimposed on the smoothly declining glow peaks of K-feldspars beyond 260°C. The K-feldspar contamination in the quartz fraction was readily checked by the presence of infra-red stimulated luminescence (IRSL) as quartz does not exhibit IRSL. In TL also the presence of substantially higher TL signal (~10 times photon/mg) and presence of a broad glow peak between 200°C-300°C provided evidence of K-feldspar contamination. Any feldspar contamination in quartz was removed by a repeat etching. The separated quartz and K-feldspar grains were mounted on stainless steel discs (10 mm) using *Silkospray* with an area defined by an annular disc 5-8 mm dia.

2.2. Normalization techniques

Scatter in luminescence output of identical sub-portions of the same sample can arise either due to the variation in the number of luminescence emitting grains in different aliquots or due to the variability in the luminescence properties of the grains (Franklin and Hornyak, 1990; McFee and Tite, 1994). Thus, normalization between disc becomes essential for all the analyses.

Weight normalization: This technique used for mineral inclusion methods. It is assumed that all the grains are equally sensitive in their luminescence output and have identical paleodose and that the scatter between discs arise solely due to variation in number of grains. Thus the weight of the sample provides a direct measure for normalization. During the course of experiments it was seen that the weight normalization worked well for cases when the sample weight was >5mg, whereas for lower amounts the disc to disc scatter in TL output was higher and the weight normalization did not account for all the scatter in luminescence output. Typically, at sample weights around 3 to 4 mg, the disc to disc scatter in TL intensity scatter was ~10%.

Zero Glow Monitoring (ZGM): In this method, first suggested by Aitken and Bussel (1979), the intensity of glow peak at 110°C, is used to normalize sample amount between discs. Virgin samples with their natural TL and with low temperature peaks are irradiated with a small test dose and the intensity

of 110°C peak is measured. The integrated photon counts in this peak provides a measure of sample amount. For fine grain loess samples, this approach was used routinely. Samples were given a β dose of 22 Gy, and the TL glow was measured following a fixed delay of 4 min between the end of irradiation and glow curve readout. The total intensity between 60°C to 120°C was used for normalization and typical scatter between TL output of different discs for the same sample was ±10%. After the development of IRSL system, short shine normalization was used for loess and feldspar samples. Fresh discs were given infrared stimulation for 1 second and the integrated IRSL counts over this time was used for normalization. Wherever possible, the IRSL normalization for TL intensities was used and found effective. Typical scatter in TL output from disc to disc after normalization ranged for ±3% to ±7%.

2.3. TL measurements

The TL measurements were made on a manual Daybreak TL reader system (Fig.2.1). The system comprised a sensitive photon counting system and a digital ramp based temperature controller system with a reproducibility of <1%. The luminescence was detected by EMI 9635 QA photo-multiplier tube attached to a filter pack normally consisting of HA3 + Corning (5-58+7-59) or HA3+UG11 filters. For brighter samples, fused silica neutral density filters were used and the maximum photon count rate was always kept below 5×10^5 counts/s to avoid any pulse pile up effects. The signal from the PMT was routed through a charge sensitive preamplifier to a ratemeter and through a computer interface to an IBM-PC. The temperature controller worked on a

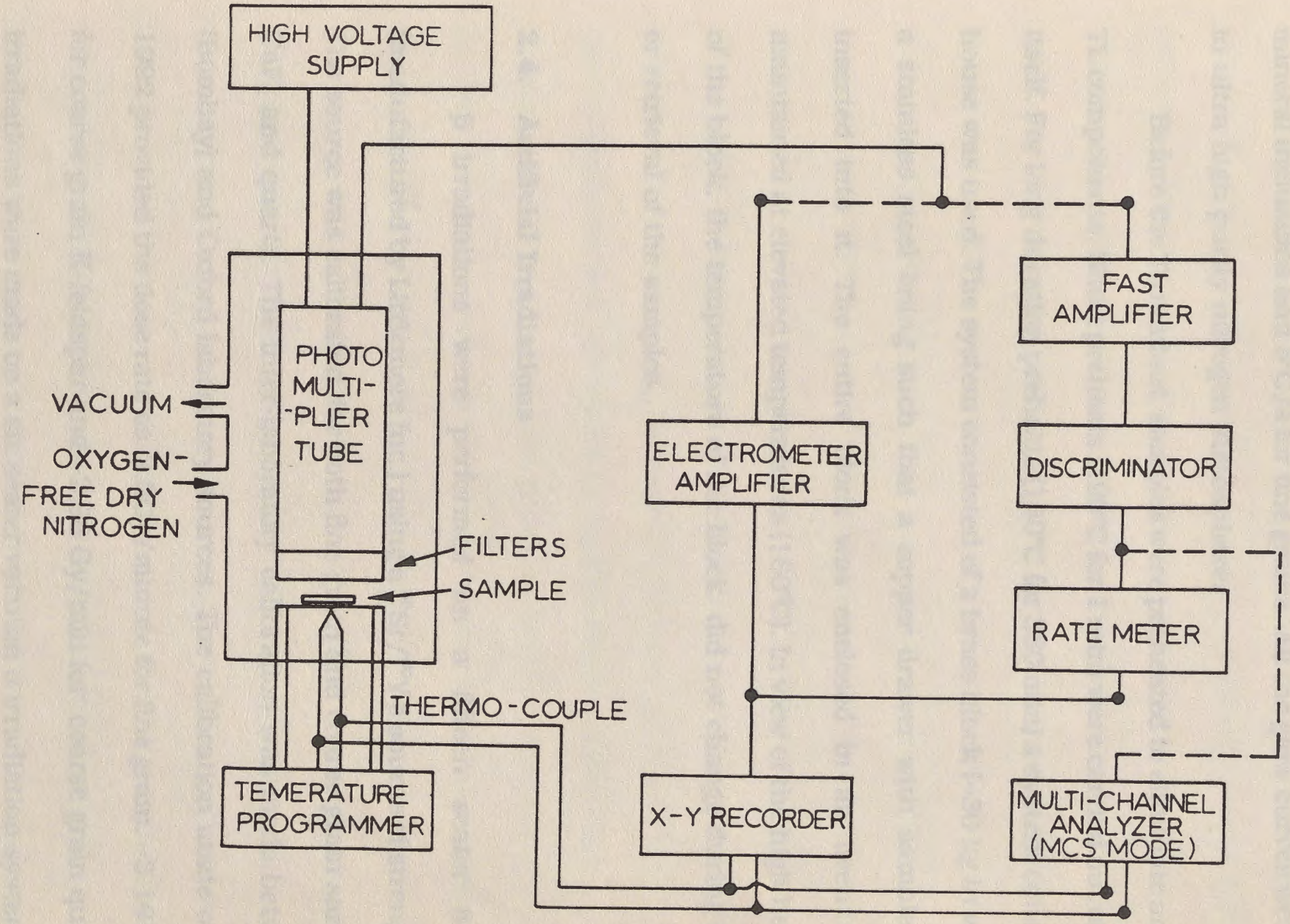


Fig. 2.1. Block diagram of the TL apparatus.

digital ramp that also provided a channel advance pulse for the IBM/PC, used essentially as a multiscaling system. Typical heating rates were 2°C/s for mineral inclusions and 5°C/s for fine grains. All the glow curves were recorded in ultra high purity nitrogen atmosphere.

Before the TL readout, samples were preheated to eliminate any unstable TL components. Short preheats (190°C for 1 min) were carried out on TL reader itself. For long duration preheats (160°C for 330 min) a system constructed in-house was used. The system consisted of a brass block (~30 kg in weight) with a stainless steel lining such that a copper drawer with samples could be inserted into it. The entire block was enclosed in an oven which was maintained at elevated temperatures (160°C). In view of the high heat capacity of the block, the temperature of the block did not change during the loading or retrieval of the samples.

2.4. Artificial Irradiations

β irradiations were performed on a fifteen seater β irradiator (manufactured by Littlemore Inc.) using a $^{90}Sr/^{90}Y$ β source of strength 25 mCi. The source was calibrated for both fine grain and coarse grain samples using CaF_2 and quartz. The inter-laboratory calibration was made between BARC (Bombay) and Oxford laboratory sources. The calibration made on January 1992 provided the dose rate as 2.2Gy/minute for fine grain, ~3.16 Gy/minute for coarse grain K-feldspar and ~2.96 Gy/min for coarse grain quartz. The α irradiations ware made on a six seater vacuum α irradiation system using six ^{241}Am sources (Singhvi and Aitken, 1978) with nominal activity of ~220 μCi.

2.5. Measurement of annual dose

The annual dose rate was evaluated by measuring the elemental concentration of U, Th and K. The uranium and thorium concentrations were measured using thick source α counting. Potassium concentration was estimated using either the atomic absorption spectrometry and also by NaI(Tl) γ-ray spectrometry. Additionally, in the case of heterogeneous complex strata, insitu γ dose rates were measured using a Harwell portable four channel γ ray spectrometer. The γ-ray spectrometer was calibrated using concrete radioactivity block at Oxford.

For measuring uranium and thorium concentrations, fine grain samples were gently crushed, then spread onto a ZnS(Ag) scintillator. For coarse grains, the samples were crushed to powder form and were used for estimation of average radioactivity concentration for determining β dose from U and Th. The counting system was calibrated using NBL Uranium standard BL-3 with 1% U and sand 105A with 10.2 ppm uranium. The counting threshold was set at 83.5% efficiency to allow the efficiency of counting for the two decay chains to be nearly equal (Aitken, 1985). Typical background count rates were ~0.3 counts/ks for a counting area of 13.85cm^2. The counting efficiency of each screen set was measured using a pitchblende source (PB-3) in a resin and used appropriately in computation. Measurements were also made under sealed and unsealed conditions to examine the radon loss. Typically, samples were counted over a period of 200ks and at least for a total count of 1000s. All the measurements were made using the Daybreak 582 alpha counter.

The estimation of ^{40}K was made using 3" x 3" well type NaI(Tl) scintillator

15618

coupled to a standard amplifier and a multi channel analyzer. The energy window was set at 1.46 MeV. The estimation of potassium was made by comparing the count rate per gram of sample with that of the standard (AR grade KCl) for the same geometry. In the comparison, only the photopeak counts significantly upto the full width at half maxima were used. Typically, sample weights were ~15 gm giving a count rate of 4-6 counts per minute compared to a background count rate of 2 counts per minute. The count rate of KCl standard was ~70 counts per minute.

In estimating ^{40}K by atomic absorption spectrometry, samples were digested by sequential treatment of HF, $HClO_4$, HNO_3 and HCL. The solutions were then diluted to bring the concentration to the linear portion of the absorbance curve. The absorption spectra were recorded on the atomic absorption spectrometer (Perkin-Elmer 305). For the measurements, the diluted solutions were aspired through flame and the absorbance was compared with the standard to estimate the potassium percentage. Blank samples were also measured for measuring the background concentrations. A comparison of γ-ray spectrometry results with those of atomic absorption was also made (table 2.1) which indicated a concordance within ±2%. The insitu γ dose from the decay of uranium, thorium and potassium was measured using the 4-channel γ ray spectrometer (Aitken 1985). Stripping factors calculated using Oxford radioactivity blocks were used in the calculations. The cosmic ray dose was estimated using the prescription given by Prescott and Stephan (1982).

Table 2.1. Comparison between potassium concentration (%) as estimated by AAS and γ-spectrometry.

S.N.	Sample code	Estimation by AAS	Estimation by γ-spectrometry
1	DV 127	1.90 ± 0.10	1.73 ± 0.17
2	DV 128	1.50 ± 0.08	1.74 ± 0.17
3	DV 129	1.75 ± 0.09	1.60 ± 0.16
4	DV 130	1.80 ± 0.09	1.50 ± 0.15
5	DV 131	1.78 ± 0.09	1.77 ± 0.18
6	DV 132	1.66 ± 0.08	1.92 ± 0.19
7	DV 133	1.77 ± 0.09	1.81 ± 0.18
8	DV 134	1.94 ± 0.10	2.46 ± 0.25
9	DV 135	1.82 ± 0.09	1.82 ± 0.18
10	DV 136	1.66 ± 0.08	2.04 ± 0.20
11	P 1	1.67 ± 0.08	1.81 ± 0.18
12	BCH 9	1.88 ± 0.09	1.83 ± 0.18
13	BCH 14	2.20 ± 0.11	2.75 ± 0.28
14	BCH 16	1.85 ± 0.09	2.00 ± 0.20
15	BCH 19	1.96 ± 0.10	1.64 ± 0.16
16	BCH 46	1.89 ± 0.09	1.60 ± 0.16
17	TL 6	1.60 ± 0.08	1.80 ± 0.18

Thermoluminescence Dating of Loess-Paleosol Sequences

3.1. Introduction

In global climatology, wind transported dust have been shown to be an important indicator of climate, both on land and in sea. On the land, besides the deserts, extensive deposits of wind transported dust occur and cover about 10% of the land-area (Pye, 1986; Williams, 1993) (Fig.3.1). Some of these dust fall deposits, termed as loess deposits cover a long time span of 2-3 Ma and are considered to be the longest continental archives of climatic change which are comparable to the deep sea oxygen isotopic record. Genetically, loess is a structureless, homogeneous, wind transported dust with mean grain size

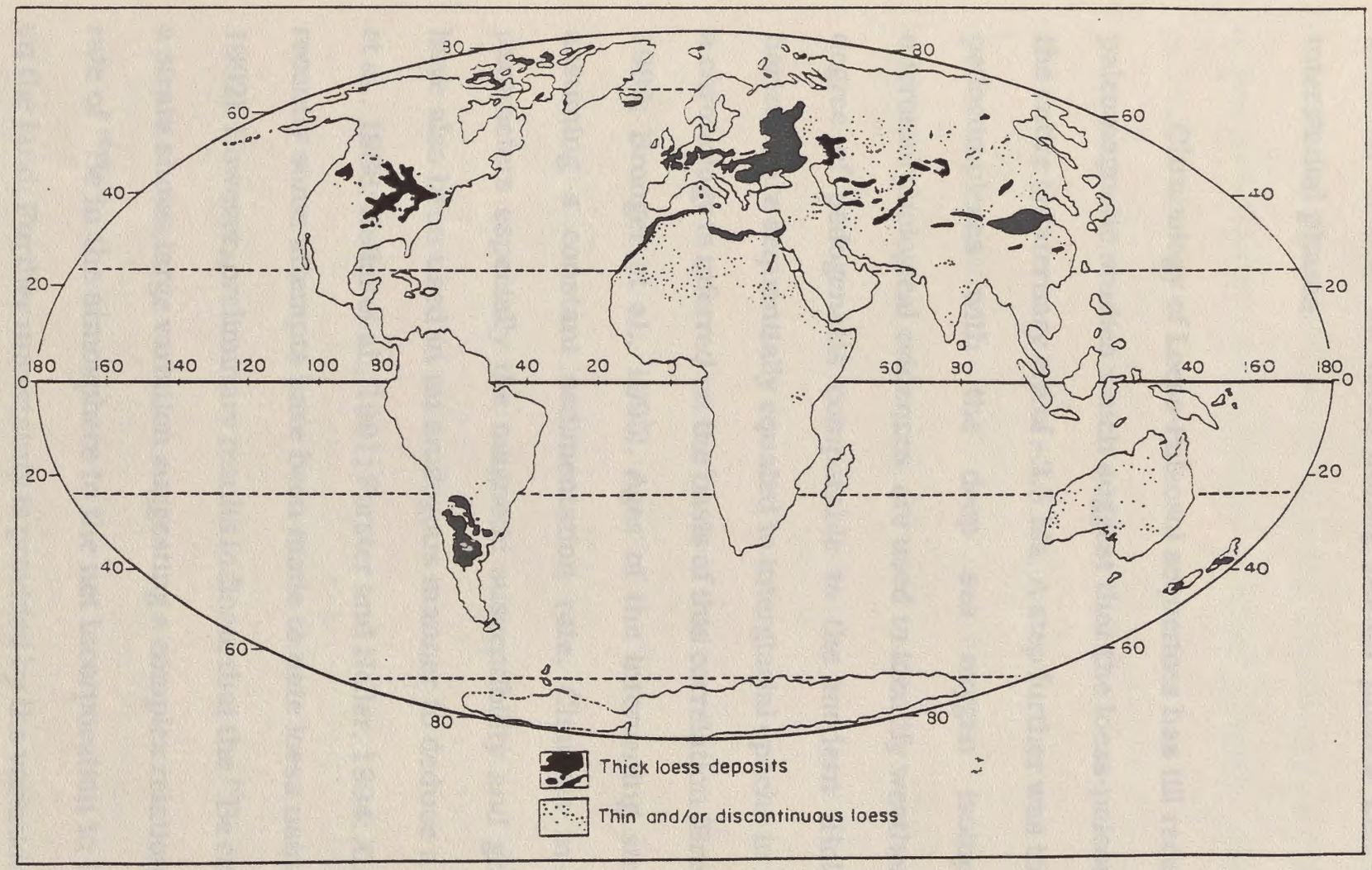


Fig. 3.1. Present day distribution of loess (modified after Williams et al., 1993).

~30μm. A typical loess-paleosol sequence comprises an alternating sequence of loess representing cold, arid, glacial climate and paleosols which are generally formed on loess during humid phases i.e., the interglacial or interstadial phases.

Chronology of Loess-Paleosol sequences has till recently been based on paleomagnetic studies which suggest that the loess-paleosol sequences span the entire Quaternary era of ~2.5 Ma. A step further was the correlation of soil pedocomplexes with the deep sea oxygen isotopic records. Soil micromorphological evidences are used to identify weathered horizons with a degree of pedogenesis comparable to the modern (Holocene) soil. These horizons are sequentially equated to interglacial epochs in isotopic stages and a chronology is inferred on the basis of this correlation (Bronger and Heinkele, 1989; Bronger et al., 1995). Ages of the intervening strata are calculated assuming a constant sedimentation rate. Changes in mineral magnetic parameters especially the magnetic susceptibility and grain size variations have also been used in an analogous manner to deduce a chronology (Kukla et al., 1988; Heller et al., 1991; Forster and Heller, 1994; Xio et al, 1995). More recently some attempts have been made to date loess using ^{10}Be (Shah et al., 1992). However, preliminary results indicate that the ^{10}Be concentration within a strata shows large variation suggesting a complex relationship of scavenging rate of ^{10}Be in the atmosphere to the net incorporation in the loess deposited on the land. Further uncertainty is provided by the variation in cosmic ray flux through this (Gu et al., preprint).

The advent of luminescence dating of sediments provided the first possibility of absolute dating of loess-paleosol sequences. Globally to date ~700 luminescence ages have been reported. The basic merit of this method lies in its ability to date the depositional event of loess and also the formation event of soil A-horizons based on the premise of insitu sunbleaching during pedoturbation.

In the present thesis, an attempt was made to date a loess-deposits in China, Tadijikistan and Central Europe. The TL ages on Tadijikistan are the first set of absolute ages and new sequences from China and Central Europe have been dated. The basic objectives of the present study were

(1) to establish the exact chronology of loess-paleosol sequences to evaluate the epochs of loess accumulation and soil formation,

(2) to determine the amplitude of changes in loess accumulation rates through time,

(3) to determine the extent of correlation with chronology based on deep sea oxygen isotopic stages and estimate the magnitude of age underestimation effect in loess of different provenances (discussed in Chapter 4), and,

(4) to attempt a composite chronology of loess-paleosol sequences by collating all the available luminescence chronological data and attempt a statistical analyses of these data to deduce periods of loess accumulation in order to examine their synchronicity with global climatic events.

The loess-paleosol sequences that were investigated in the present thesis are

(1)	Luochuan	(35°45'N, 109o25'E),	China
(2)	Karmaydan	38(°, 38'N, 68°51'E),	Tadijikistan
(3)	Dolni Vestonice	(48°, 55'N, 16°6'E),	C. Europe
(4)	Paks and Mende	(46°38'N, 18°55'E)	C. Europe
(5)	Mende	(46°50'N, 19°51'E),	C. Europe

In what follows, a brief description of the geological setting and the experimental details is provided. The results are then presented along with comparison of TL ages with available ages on loess. Finally, results of statistical analyses of global loess-paleosol chronological data is presented.

3.2. Geological setting and earlier work

(a) **Luochuan, China**: Loess in China covers ~44,000 sq.km. with average thickness at of the deposit measuring 80m. Paleomagnetic studies suggest that the total loess column dates back to ~2.5 Ma. and that the Brunhes-Matuyama boundary is located in the paleosol S_8 (Fig.3.2). Based on correlation of soil micromorphological data with the deep sea oxygen isotopic record, it has been suggested that Soil S_1 should represent the last interglacial soil (Bronger and Heinkele, 1989; Kukla and An, 1989). More detailed mineral magnetic and grain size data indicated that soil S_1 is a pedocomplex with three distinct horizons (see for example, Derbyshire et al., 1995 and references therein). Efforts on the chronolometry of loess in China were initiated by Li, et al. (1977) and Nishimura et al (1984). Singhvi and Mejdahl (1985) in their

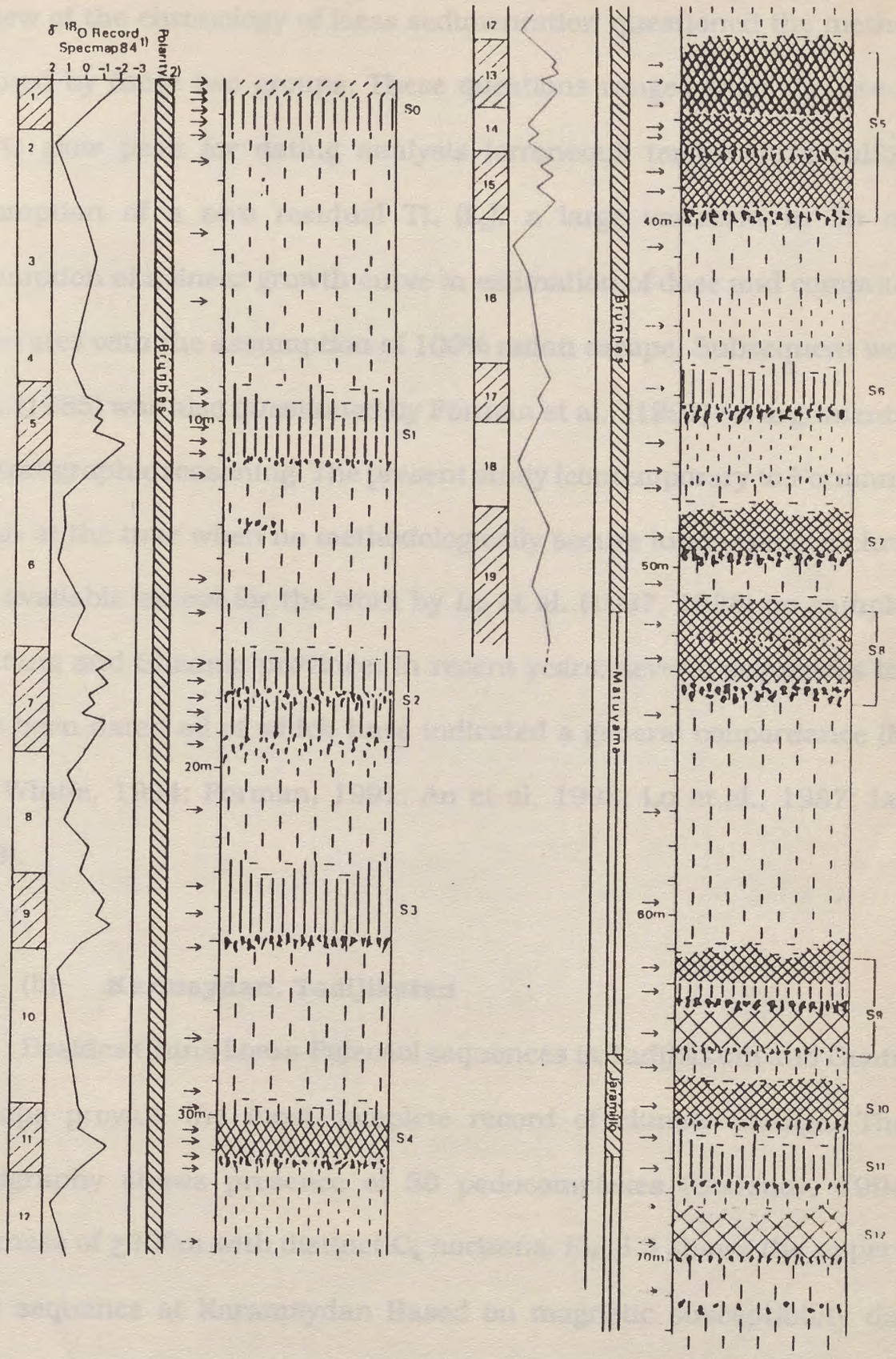


Fig. 3.2. Stratigraphy of Luochuan Loess Profile (Potou section), China. The Brunhes Matuyama boundary occurring at 780 ka is located in soil S_8 (after Bronger and Heinkele, 1989).

review of the chronology of loess sedimentation questioned the methodology adopted by these two groups. These questions ranged from the use of 175-185°C glow peak for dating analysis (erroneous temperature calibration), assumption of a zero residual TL (L_o), a large variation in Th content, assumption of a linear growth curve in estimation of dose and computation of dose-rates with the assumption of 100% radon escape. Subsequent work of Li et al. (1985) was also questioned by Forman et al., (1991) on arguments based on stratigraphic reasoning. The present study (contemporary to Forman (1991)) began at the time when no methodologically secure luminescence chronology was available except for the work by Lu et al. (1987, 1988) on samples from Zhaitang and Shaanxi province. In recent years, several sequences in China have been dated all of which have indicated a general concordance (Musson and Wintle, 1994; Forman, 1991; An et al, 1993; Lu et.al., 1987; Lu et.al., 1988).

(b) Karmaydan, Tadijikstan

Besides China Loess-Paleosol sequences in Tadijikstan and Central Asia perhaps provide the most complete record of climate change. The loess stratigraphy shows presence of 30 pedocomplexes (Dodonov, 1994) in a thickness of $\geq$200m with distinct C_k horizons. Fig.3.3 shows the upper part of loess sequence at Karamaydan Based on magnetic susceptibility data and paleomagnetic studies, Forster and Heller (1994) identified the Brunhes-Matuyama boundary between the 9th and 10th pedocomplexes and correlated it with Xifeng (China) and ODP 677 deep sea core. High magnetic susceptibility

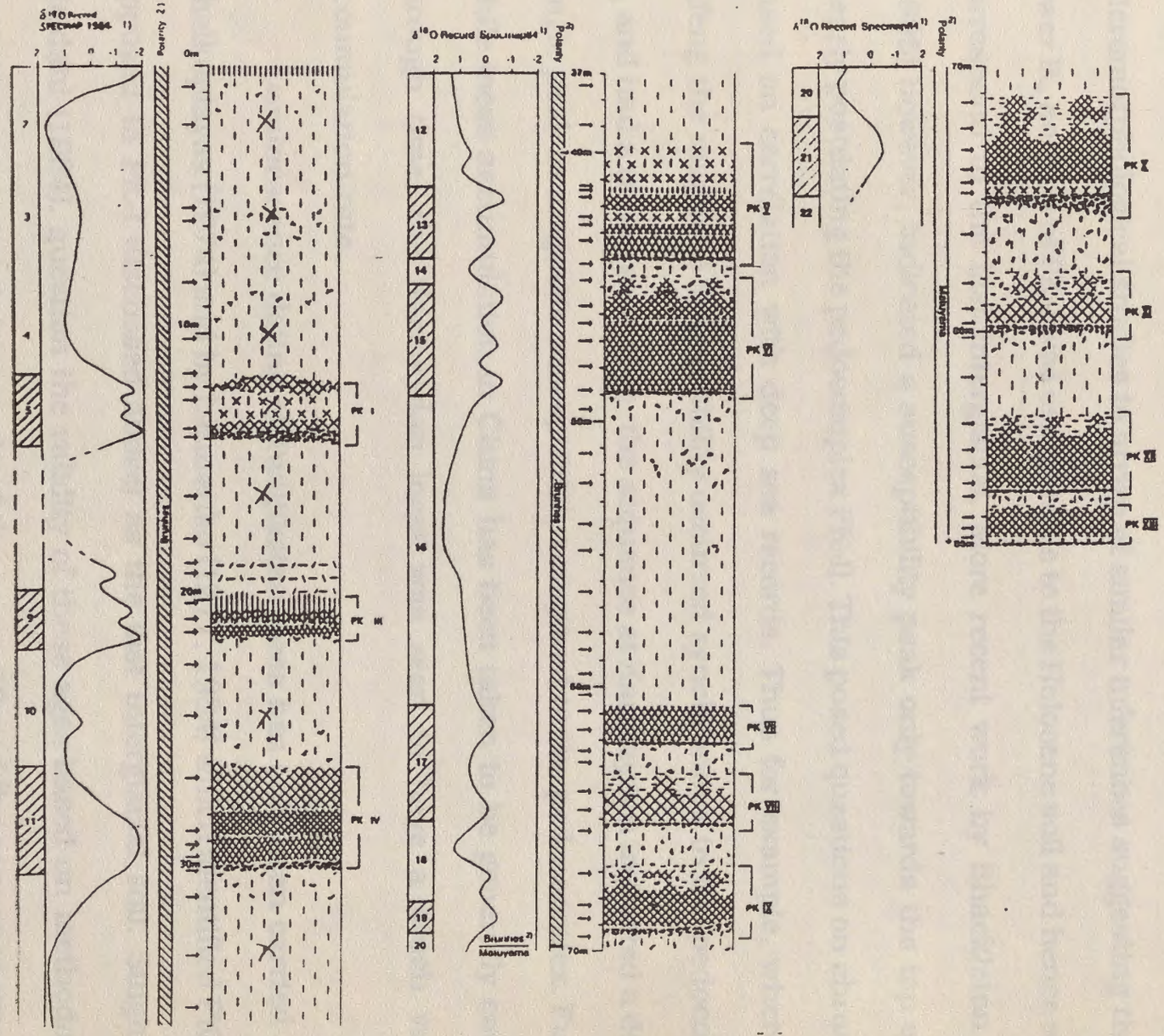


Fig. 3.3. Stratigraphy at Karmaydan, along with a correlation with the deep sea oxygen isotope data (After Bronger et al., 1995). The Brunhes Matuyama boundary is located below soil PK IX.

values were considered to correspond to more humid episodes during which the pedocomplexes developed. The pedocomplex PK-I was inferred to have developed during the last interglacial. Bronger et al., (1995) used soil micromorphological studies to arrive at similar inferences suggesting that the lower B_w horizon of PK-I was comparable to the Holocene soil and hence should correspond to the last interglacial. More recent work by Shackleton et al, (1995) however, indicated a susceptibility peak only towards the top of PK-I (nearly postdating the pedocomplex PK-I). This posed questions on chronology based on correlation with deep sea records. Thus for example, whereas at Xifeng the magnetic susceptibility occurred synchronous to the pedocomplex S_1 and had a triplet structure, the sequence at Karmaydan indicated a delayed single peak in magnetic susceptibility compared to the pedocomplex. Further, while loess accumulation in China has been taken to be generally constant through time, the Karmaydan loess was seen to have a much variable accumulation rate.

Luminescence dating of Tadijikstan loess has only been carried out by Shelkoplayas (1974) and by Lazarenko (1977, 1984) which identified PK-IV (as opposed to PK-I discussed above) as the last interglacial soil. Singhvi and Mejdahl (1984), question the validity of these ages based on methodological grounds. A detailed dating study of the upper 30m of the sequence was taken up to provide an absolute chronology.

(c) Dolni Vestonice, Paks and Mende, Central Europe

The loess-paleosol sequences in Hungary have been the most studied sequence. These sequences are along the R. Danube and until the luminescence dating by Singhvi et al., (1989) considerable debate on the chronology of these sequences existed. These sequences are typically 0-40m thick and have upto 11 paleosols, dating back to ~1 million years. The earlier work by Pecsi (1979, 1985) and INQUA (1961) (International Quaternary Union) adopted a stratigraphic guideline indicating that the youngest brown forest soil (soil F5 in Fig.3.4) represented the last interglacial epoch. On the other hand, Kukla (1977) proposed a correlation of these loess paleosols with deep sea oxygen isotopic records and indicated a much older chronology, with the last interglacial being placed at soil F_2 and the age of soil F_5 was placed at ~500 ka. Butrym and Marusczak (1984) and Borsy et al (1979) reported the first luminescence dates on some of these sequences. However, as discussed by Singhvi and Mejdahl (1985) they were methodologically inadequate and consequently could not be used in any meaningful manner. The early work Singhvi et al., (1989) resolved this issue. In the present thesis, the main objective was to provide further chronology to key horizons from select sites including that at Dolni Vestonice, which depicted a much more detailed record of climatic variation by way of a fine structure in pedocomplex PK-I, II, III. The present results and recent Amino-acid dating results have reconfirmed the luminescence ages provided by Singhvi et al. (1989).

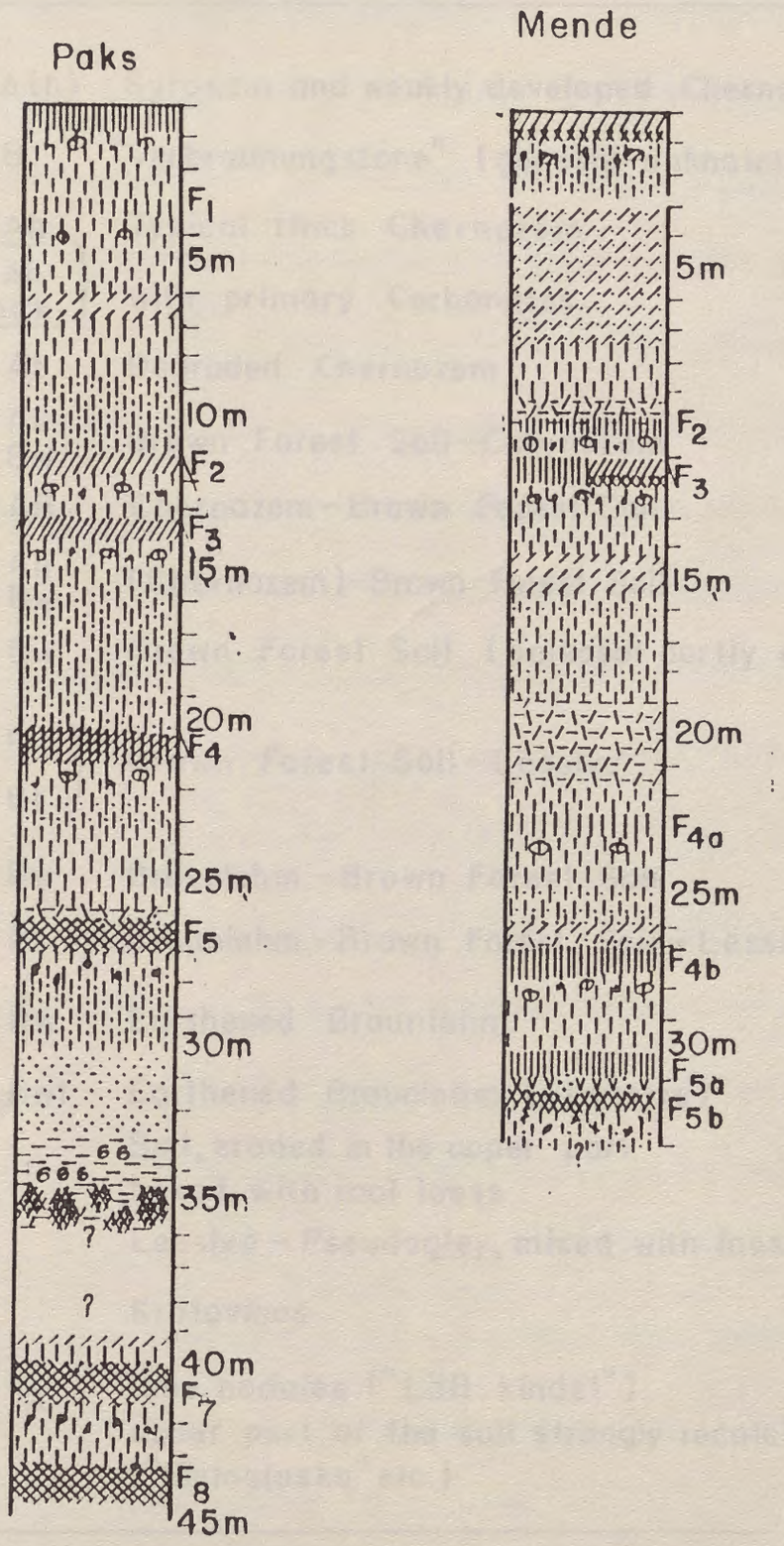


Fig. 3.4. Stratigraphy at Paks and Mende. The Brunhes Matuyama boundary is located below soil F_5 (based on correlation with (after Singhvi et al., 1989).

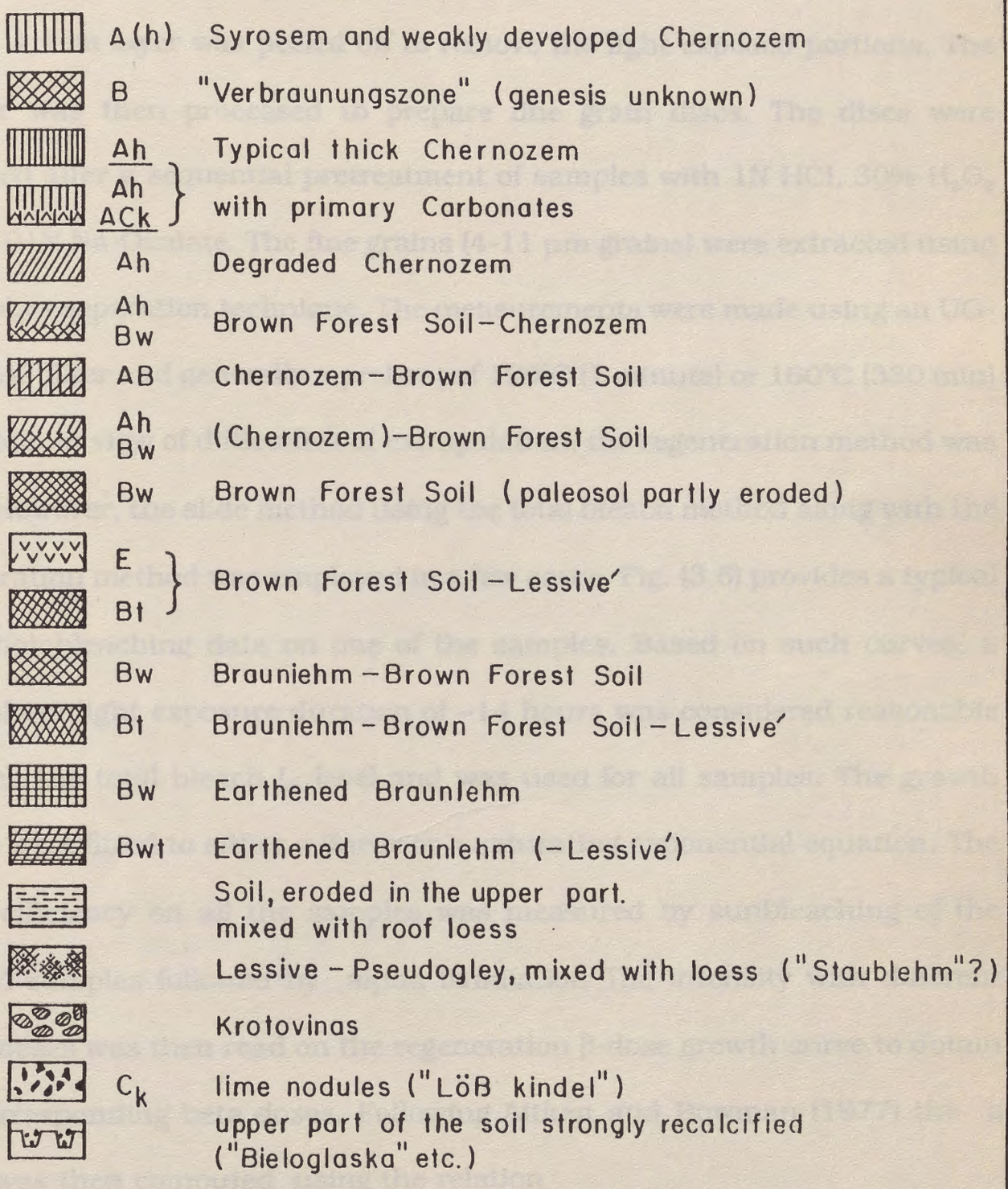


Fig. 3.5. Ligands for the figures 3.2, 3.2 and 3.4.

3.3. Experimental Details

In all the cases the samples were obtained through the courtesy of Prof.A.Bronger, who provided the samples as ~3 cm x 3 cm x 3 cm cubes, from which a 1cm layer was peeled off to remove the light exposed portions. The interior was then processed to prepare fine grain discs. The discs were prepared after a sequential pretreatment of samples with 1N HCl, 30% H_2O_2 and 0.01N Na-Oxalate. The fine grains (4-11 μm grains) were extracted using the Stokes separation technique. The measurements were made using an UG-11 + HA3 filter and generally a preheat of 190°C (1 minute) or 160°C (330 min) was used. In view of difficulties of extrapolation, the regeneration method was used. However, the slide method using the total bleach method along with the regeneration method was employed in a few cases. Fig. (3.6) provides a typical sun photobleaching data on one of the samples. Based on such curves, a natural sunlight exposure duration of ~14 hours was considered reasonable to reach the total bleach L_0 level and was used for all samples. The growth curves were fitted to either a linear or a saturating exponential equation. The alpha efficiency on all the samples was measured by sunbleaching of the natural samples followed by alpha irradiation The intensity with different alpha doses was then read on the regeneration β-dose growth curve to obtain the corresponding beta doses. Following Aitken and Bowman (1977) the a value was then computed using the relation

$$a = \frac{\beta\ (Gy)}{13.S.y} \qquad \ldots\ (9)$$

where β is the beta dose that gives the TL intensity equal to that given by y

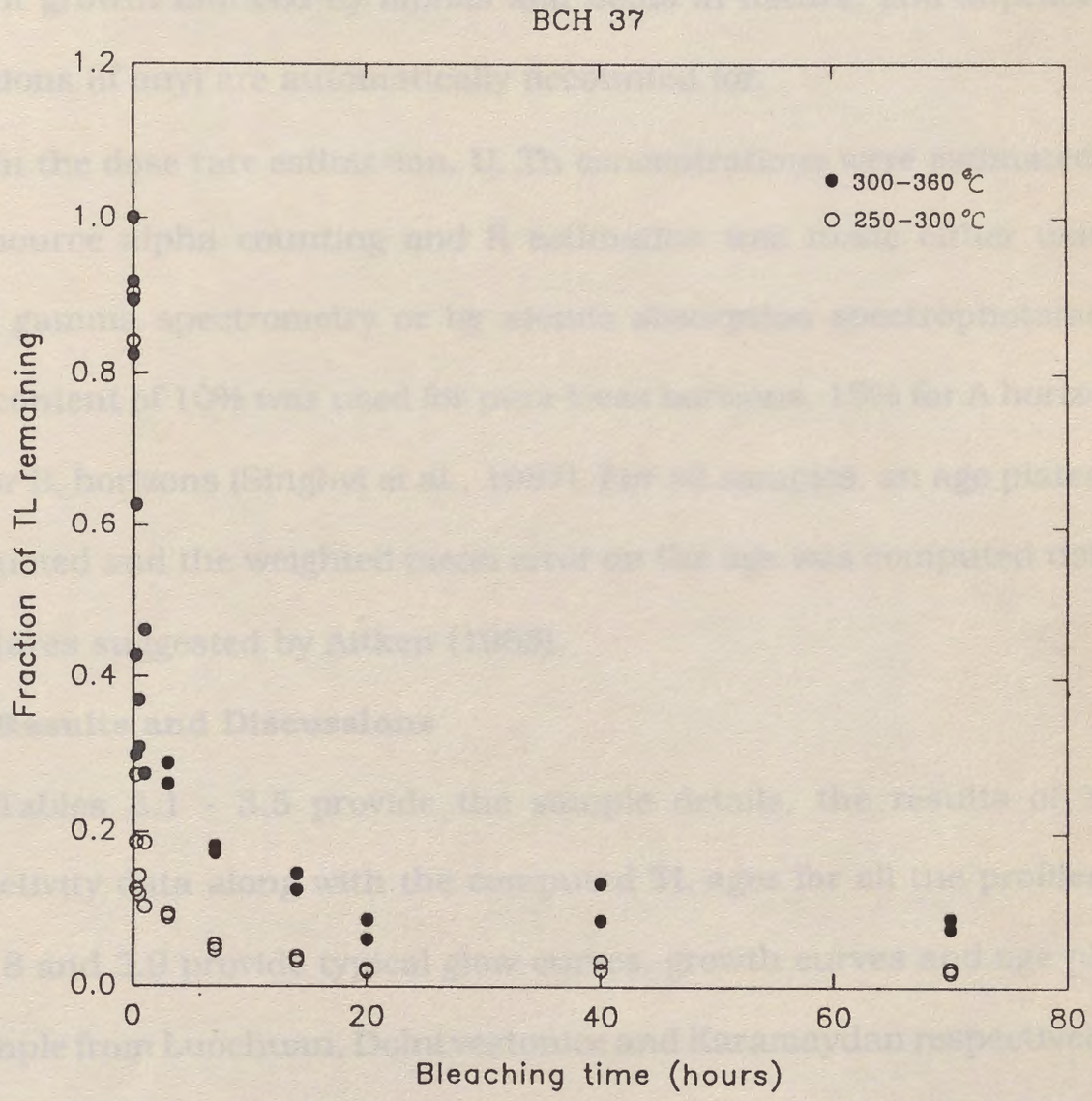


Fig. 3.6. Bleaching of TL with sunlight exposure expressed as fraction of natural TL remaining for the sample BCH37.

(minutes) of alpha-exposure from an ^{241}Am source of strength "S" (given in μm^{-2} min^{-1}). In this scheme, sensitivity changes on sunbleaching, effects of different growth induced by alphas and betas in nature, and supralinearity corrections (if any) are automatically accounted for.

In the dose rate estimation, U, Th concentrations were estimated using thick source alpha counting and K estimation was made either using the NaI(Tl) gamma spectrometry or by atomic absorption spectrophotometry. A water content of 10% was used for pure loess horizons, 15% for A horizon and 20% for B_t horizons (Singhvi et al., 1987). For all samples, an age plateau was constructed and the weighted mean error on the age was computed using the procedures suggested by Aitken (1985).

3.4. Results and Discussions

Tables 3.1 - 3.5 provide the sample details, the results of TL and radioactivity data along with the computed TL ages for all the profiles. Figs. 3.7, 3.8 and 3.9 provide typical glow curves, growth curves and age plateaus for sample from Luochuan, Dolni vestonice and Karamaydan respectively. Figs. 3.10, 3.11, 3.12 and 3.13 provide a comparison of the TL ages obtained in the present study along with other TL age estimates from equivalent loess profiles, wherever available. In all the cases the TL ages show a general consistency and also indicate a limiting TL age of ~100-200 ka. Figs. 4.2a,b shows a comparison of TL ages on Luochuan and Karamaydan sequences with the age estimates inferred from the correlation of pedostratigraphy with deep sea oxygen isotope chronology. It is clearly seen that all TL ages are underestimated beyond 100 ka. Similar underestimation of ages has been

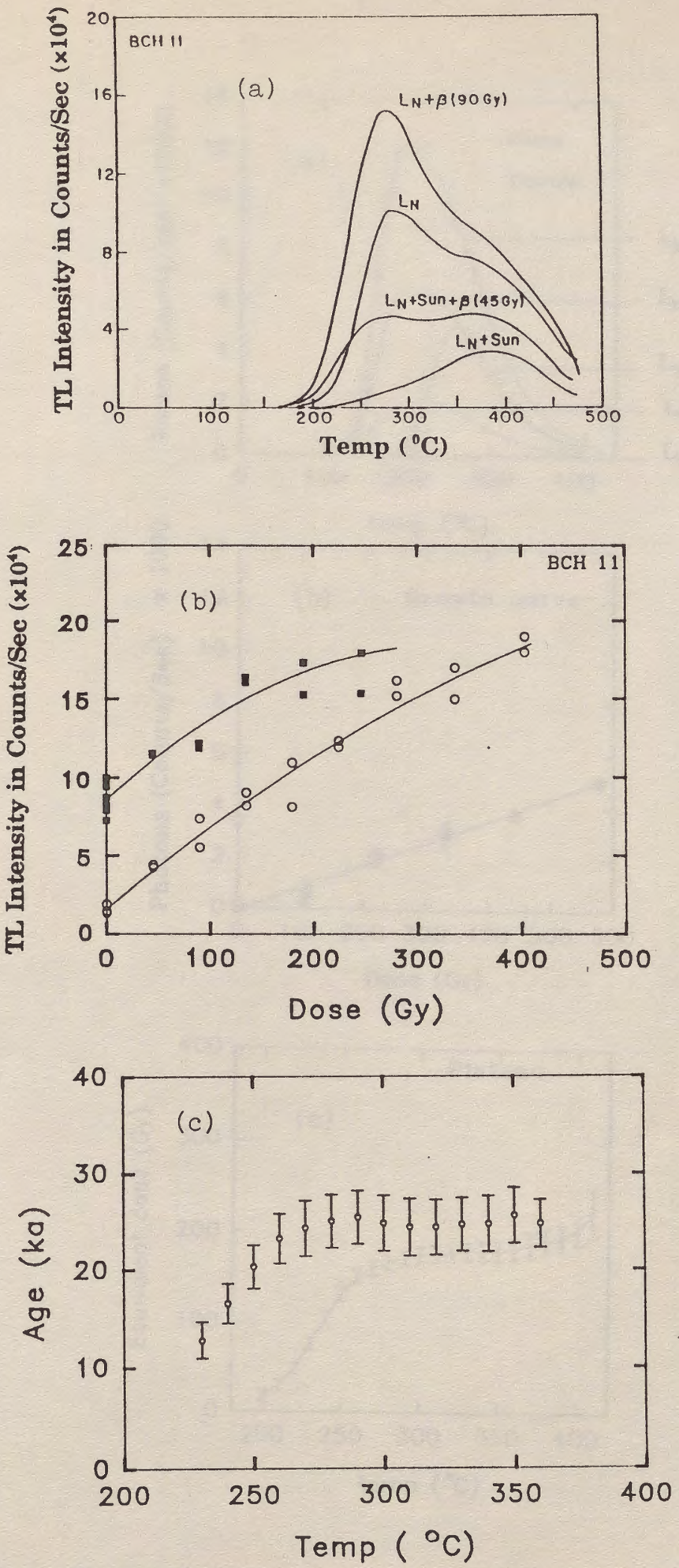


Fig. 3.7. Plot showing (a) typical glow curve for BCH 11 fine grain sample, (b) typical growth curve (i) additive (ii) regeneration and (c) age plateau

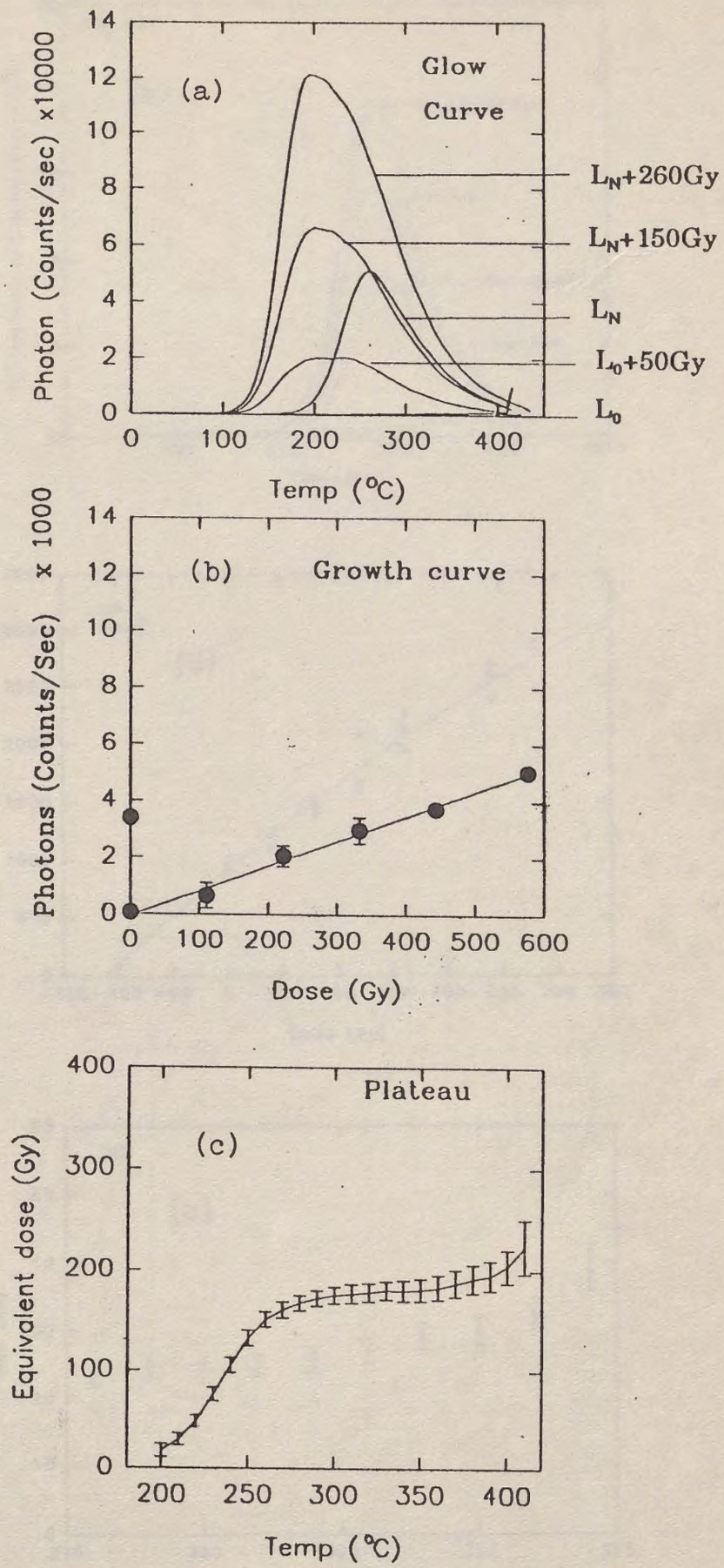


Fig. 3.8. Plot showing (a) typical glow curve for DV135 fine grain sample, (b) typical growth curve and (c) age plateau

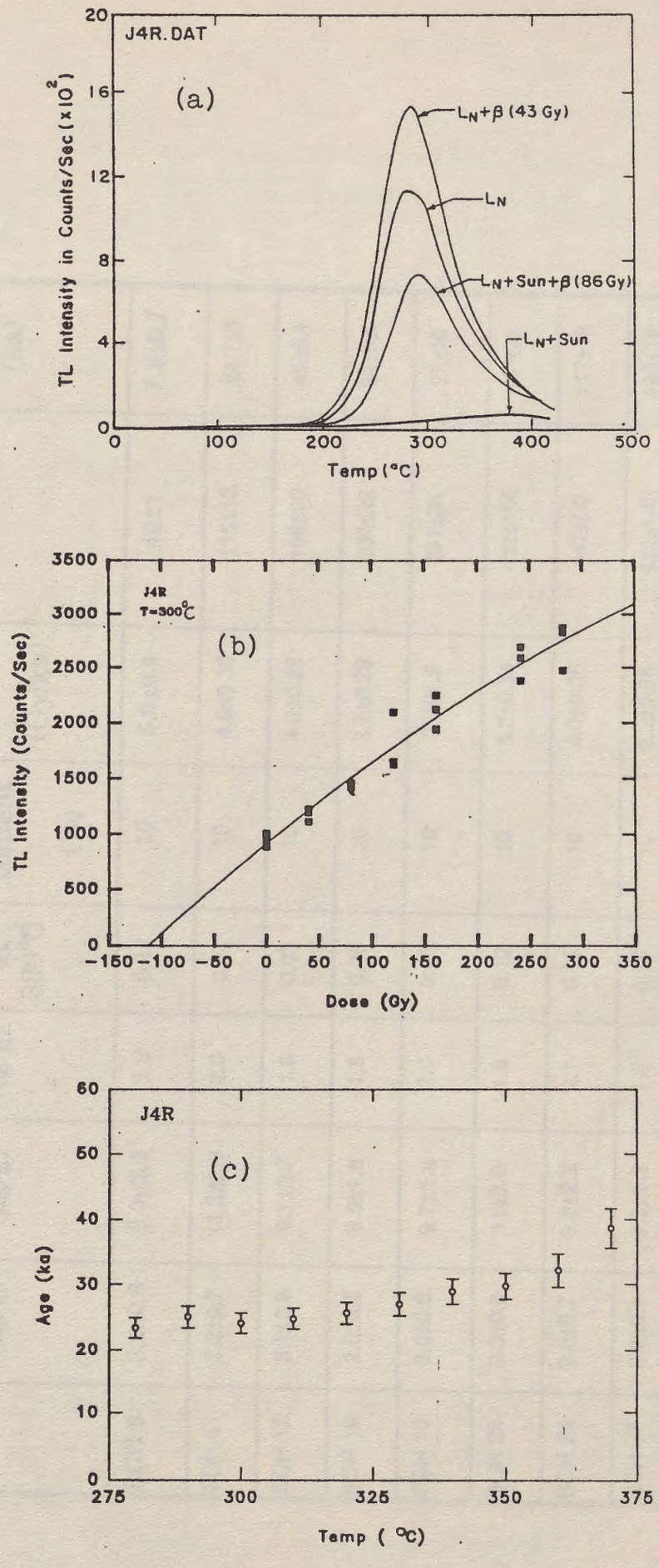


Fig. 3.9. Plot showing (a) typical glow curve for J4R fine grain sample, (b) typical growth curve and (c) age plateau

Table 3.1 Thermoluminescence results and radioactivity data for loess samples from Luochuan

Sample code	U (μg/g)	Th (μg/g)	K (cg/g)	a value at 300°C	Assumed moisture content (%)	Dose Rate (Gy/ka)	Equivalent dose at 300°C	Age (ka)
BCH 9	3.2±0.8	9.0±2.6	1.9	0.11	10	5.0±0.4	49±1	7.8±0.7
BCH 11	2.2±0.7	11.3±2.3	2.0	0.11	10	4.8±0.38	115±13	24.7±3
BCH 12	3.1±0.8	9.7±2.7	1.6	0.03	10	4.0±0.28	168±20	49±6.4
BCH 16	2.5±0.5	9.5±1.8	1.8	0.08	20	3.7±0.29	306±29	83±9.6
BCH 19	3.0±0.5	9.7±1.8	2.0	0.03	10	3.8±0.3	381±31	97±16
BCH 25	3.3±0.8	11±3.0	1.9	0.12	10	5.2±0.34	452±156	87±20
BCH 29	2.8±0.7	9.3±2.2	2.1	0.05	10	4.0±0.35	447±50	117±16
BCH 37	2.8±0.4	9.3±1.2	1.8	0.19	10	5.2±0.35	922±143	160±18
BCH 46	2.7±0.8	10.5±2.6	1.9	0.19	10	5.7±0.38	816±204	155±22

Table 3.2a. Dose rate data for Tadjikistan loess

Site	Sample code	Depth (m)	Horizon	U (µg/g)	Th (µg/g)	K (cg/g)	a value at 300°C	Assumed moisture content (%)	Dose rate (Gy/ka)
Kara maydan	J4R	2	loess	3.66±0.07	9.99±3.33	1.74	0.08±0.02	10	4.5±0.4
	J5	6	loess	2.56±0.58	6.52±1.99	1.74*	0.08±0.02	10	4.5±0.3
	J6	10	loess	3.91±0.75	6.5±2.56	1.91	0.08±0.03	10	4.4±0.4
	J15	13	PK-I	3.42±0.63	8.87±1.67	1.7*	0.08±0.03	15	4.04±0.3
	J7	16	loess	2.61±0.79	9.26±2.7	2.18	0.09±0.03	10	4.5±0.4
	J8	24	loess	2.81±0.8	9.44±2.79	1.61	0.05±0.03	10	3.7±0.3
	J11	33	loess	3.02±0.77	6.93±2.63	1.65	0.08	10	3.8±0.3
Chashma Nigar	J13	8.5	loess	2.86±0.54	5.3±1.86	1.77*	0.08	10	3.7±0.3
	J14	>13	loess	3.04±0.7	7.97±2.38	1.77	0.07±0.008	10	4.0±0.3

Table 3.2(b). Luminescence dating results for Tadjikistan loess

Sample code	Equivalent Dose (Gy)				Age (ka)				Age (ka)
	IRSL		TL		IRSL		TL		
	Additive	Slide	Additive	Slide	Additive	Slide	Additive	Slide	
J4 R	68±3		113±7		15±1.2		25±2		
J5	-		147±15		-		33±3.5		
J6	179^{+47}_{-23}		277±79		41^{+9}_{-5}		63±14.5		
J15	304^{+180}_{-89}	296±30	341±55	432±59	75^{+33}_{-17}	73±7.3	84±11	107±13	
J7	551^{+624}_{-218}	339±55	652±65	654±79	123^{+105}_{-38}	75±10.5	145±14.5		
J8	508^{+63}_{-29}		373±121		137^{+16}_{-11}		101±8	145±17	
J11	847^{+79}_{-50}		1013±92		223^{+22}_{-18}		267±27		
J13	289^{+17}_{-10}		275±25		78^{+7}_{-6}		74±7		
J14	252^{+33}_{-21}		294±62	350±60	63^{+7}_{-6}		73±15	87±13	

Table 3.3 Dose rate data and thermoluminescence results for loess from Dolni Vestonice

Dolni Vestonice

Sample code	U (µg/g)	Th (µg/g)	K (cg/g)	a value at 300°C	Assumed moisture content (%)	Dose Rate (Gy/ka)	Equivalent dose at 300°C	Age (ka)
DV 127	2.8±0.8	9.9±2.6	1.9	0.1	15	4.3±0.3	180±15	43±4
DV 128	3.0±0.6	7.0±2.2	1.5	0.06	20	3.1±0.2	170±23	55±7
DV 129	2.4±0.9	12.8±3.2	1.8	0.12	15	3.4±0.3	234±28	47±8
DV 130	2.3±0.8	11.4±2.6	1.8	0.12	20	4.2±0.3	309±27	74±7
DV 132	3.4±1.0	13.4±3.5	1.7	0.1	20	4.6±0.3	326±31	71±7
DV 133	3.5±0.6	6.0±2.1	1.8	0.06	15	3.5±0.2	336±80	89±15
DV 134	3.9±0.8	6.5±2.7	1.8	0.06	15	3.8±0.26	407±29	106±9.5
DV 135	2.9±0.7	9.3±2.2	1.8	0.07	20	3.8±0.3	382±28	102±9

Table 3. Luminescence dating results for loess from Paks

Paks

Sample code	U (µg/g)	Th (µg/g)	K (cg/g)	a value at 300°C	Assumed moisture content (%)	Dose Rate (Gy/ka)	Equivalent dose at 300°C	Age (ka)
Soil F_1 (P4)	4.2±0.9	9.0±3.0	1.5	0.13	15	4.9±0.3	377±28	82±7
Loess below F_2 (P5)	2.3±0.7	9.2±2.5	1.3	0.1	10	3.9±0.3	372±39	104±11
Soil F_3 (P2)	2.6±0.8	10.6±2.7	1.3	0.05	10	3.4±0.2	407±46	131±15
Soil F_4 (P3)	2.3±0.8	13.7±3.9	1.4	0.13	20	4.3±0.3	626±32	144±12

Table 3.5 Thermoluminescence results and radiactivity data for the loess sequence from Mende.

Mende

Sample code	U (µg/g)	Th (µg/g)	K (cg/g) (assumed)	a value at 300°C	Assumed moisture content (%)	Dose Rate (Gy/ka)	Equivalent dose at 300°C	Age (ka)
Soil F_3- A_{hw} (J9)	4.4±1.1	7.0±3.9	1.5	0.15	20	4.9±0.3	257±87	52±10
Soil F_3- B_{hw} (J10)	3.8±0.8	7.7±2.8	1.5	0.07	15	3.7±0.2	282±38	84±10

described previously (Debenham, 1985; Wintle et al, 1985). The physical basis of the age underestimation was also examined in depth. Chapter 4 provides the experimental details and a conceptual framework to correct the underestimated luminescence ages is also provided. Figs. 4.11 and 4.12 show that the underestimation of ages upto 20 ka is negligible.

(a) Luochuan

(1) The TL ages evaluated using the regeneration method indicated a limiting value at 160 ka. These were on samples with expected ages of 400-500 ka. Studies by Forman (1991) indicated that the total bleach method (Singhvi et al., 1982) provided ages of 170 ka and 290 ka on horizons where the expected ages are 125 ka-240 ka. This suggests that the age underestimation occurs to a lesser degree in the total bleach method compared to that in the regeneration method.

(2) A general agreement on TL ages from different groups exists and despite the fact that soil stratigraphy implicitly assumes a constant sedimentation rate, the ages indicate distinct accumulation episodes. This is clearly seen in Luochuan where TL ages indicate accumulation episodes at ~30 ka and ~55ka. Implication of this observation is discussed later in the chapter.

(3) The above observation also indicates that loess

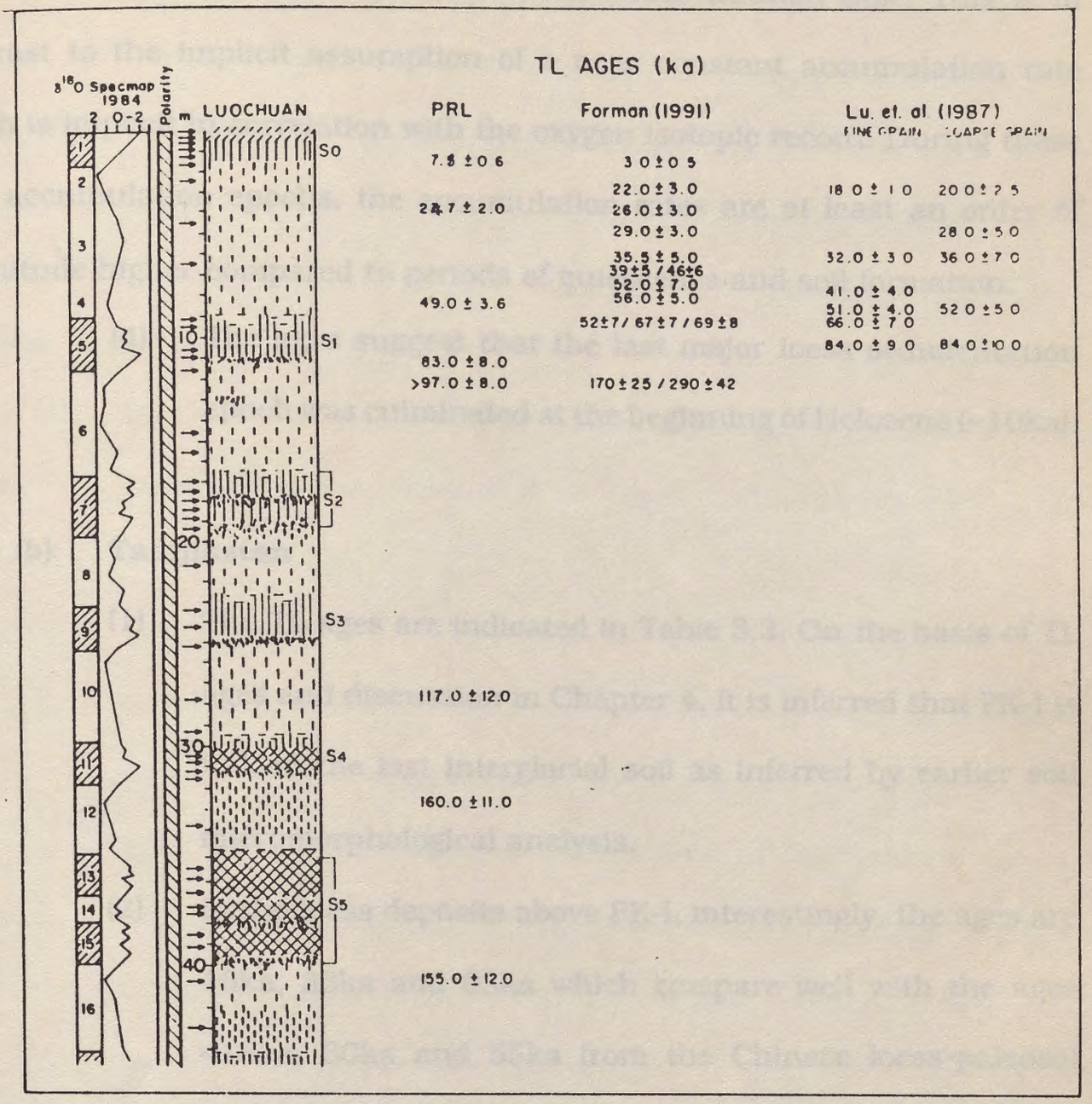


Fig. 3.10. Stratigraphy of Luochuan loess profile along with TL ages obtained in the present thesis (PRL). For comparison, TL ages obtained by Forman et al. (1991) and Lu et al (1987) are also given. A good concordance on ages from different laboratories is seen.

accumulation does not occur at a constant rate through time. This is in contrast to the implicit assumption of a near constant accumulation rate which is implicit in correlation with the oxygen isotopic record. During these high accumulation epochs, the accumulation rates are at least an order of magnitude higher compared to periods of quiescence and soil formation.

(4) The ages suggest that the last major loess sedimentation epoch was culminated at the beginning of Holocene (~10ka).

(b) Tadijikstan

(1) The TL ages are indicated in Table 3.3. On the basis of TL ages and discussion in Chapter 4, it is inferred that PK-I is indeed the last interglacial soil as inferred by earlier soil micromorphological analysis.

(2) In the loess deposits above PK-I, interestingly, the ages are 16ka, 33ka and 63ka which compare well with the ages ~18ka, 30ka and 55ka from the Chinese loess-paleosol sequences (Musson and Wintle, 1994; Forman, 1991) suggesting that these were deposited under an identical climatic regime.

(4) The loess accumulation in the region ceased at ~15ka which again reflects a global trend.

(c) Dolni Vestonice, Paks and Mende

Fig. 3.11, 3.12 and 3.13 provide a compilation of loess TL ages along with those reported by other groups (Musson and Wintle, 1994; Zoller et al., 1994a,b). Results on Dolni Vestonice obtained simultaneously by Musson and Wintle (1994) and Zoller et al., (1994) show good concordance and suggest that

(1) The soil complex PK-I is chronologically too young to represent the last interglacial. Instead it is PK-III that qualifies as the last interglacial soil.

(2) The above results also imply that PK-III, PK-II and PK-I were developed in the period around 70-20 ka ago. This is closely paralleled by the loess record at Kashmir in India (Singhvi et al., 1987). It is of interesting to observe such a fine structure in loess-paleosol sequence and it perhaps represents delicately balanced thresholds in climatic regimes which with a marginal variability permits either the loess accumulation or provides conditions conducive for landscape stability and soil formation.

(3) If indeed loess TL ages are underestimated, a correction for a meanlife of ~ 160 ka provides ages of 82ka for PK-II and 136 ka for PK-III suggesting these to be comparable to oxygen isotopic stages 5c and 5e respectively.

(4) The TL ages at Paks and Mende show a general concordance with TL dates reported by other groups (Wintle and Packman, 1988;

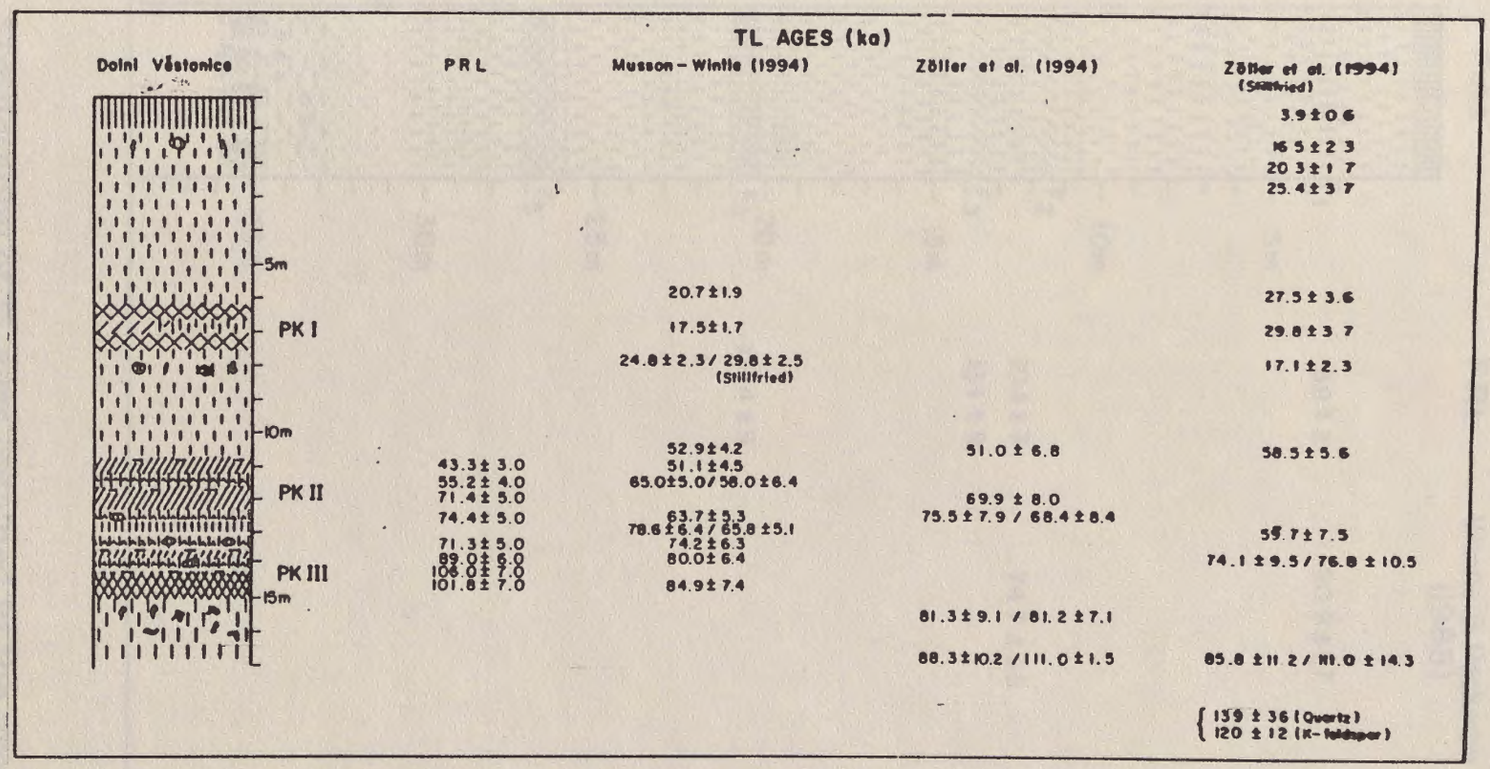


Fig. 3.11. Stratigraphy of loess profile from Dolni Vestonice along with TL ages obtained in the present study (PRL). TL ages reported by Musson and Wintle (1994), Zoller et al (1994) and Zoller et al (1994) are also given for comparison. A good concordance between independently measured ages from different laboratories is seen.

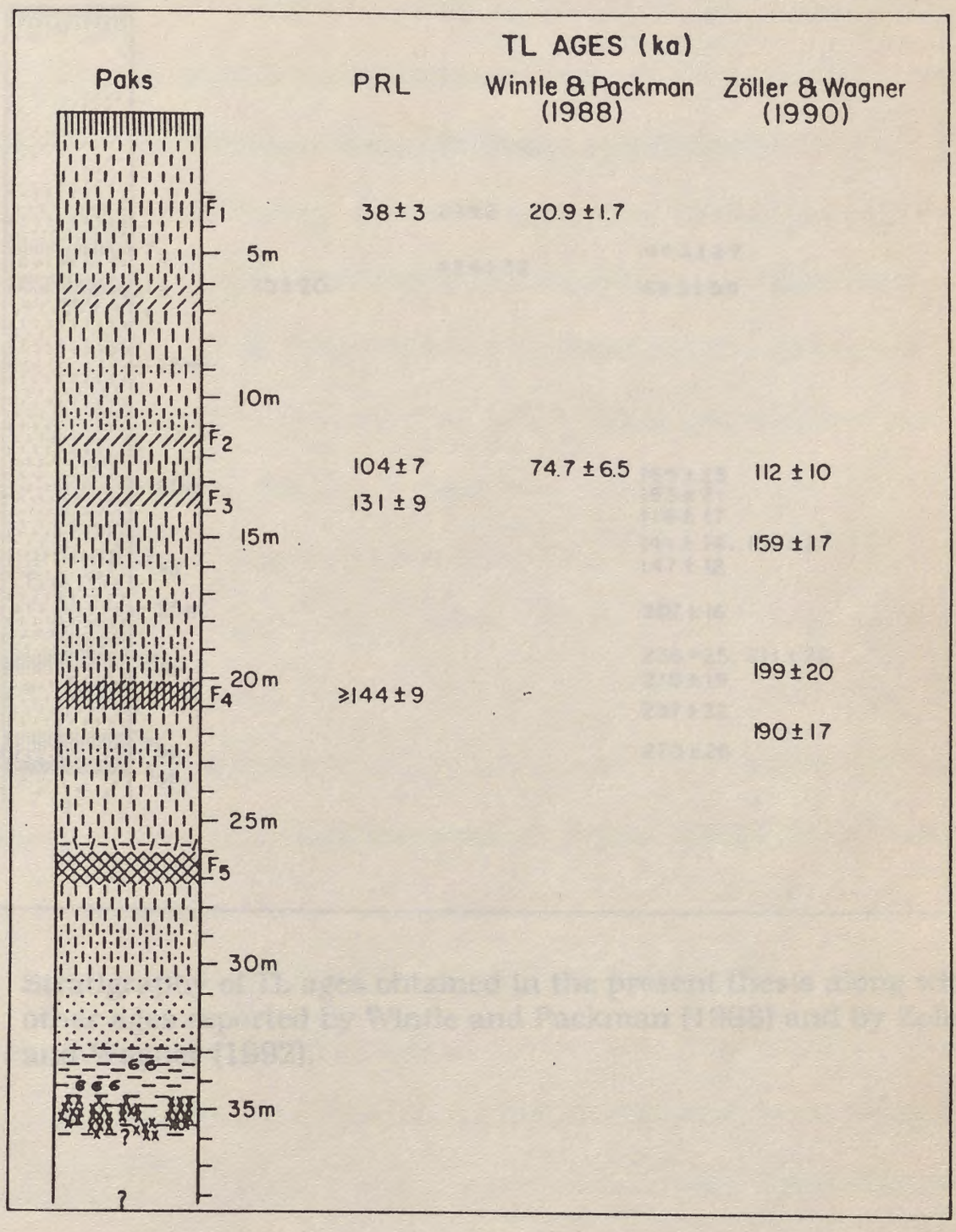


Fig. 3.12. Stratigraphy of TL ages obtained in the present thesis along with other ages reported by Wintle and Packman (1988) and by Zoller and Wagner (1992).

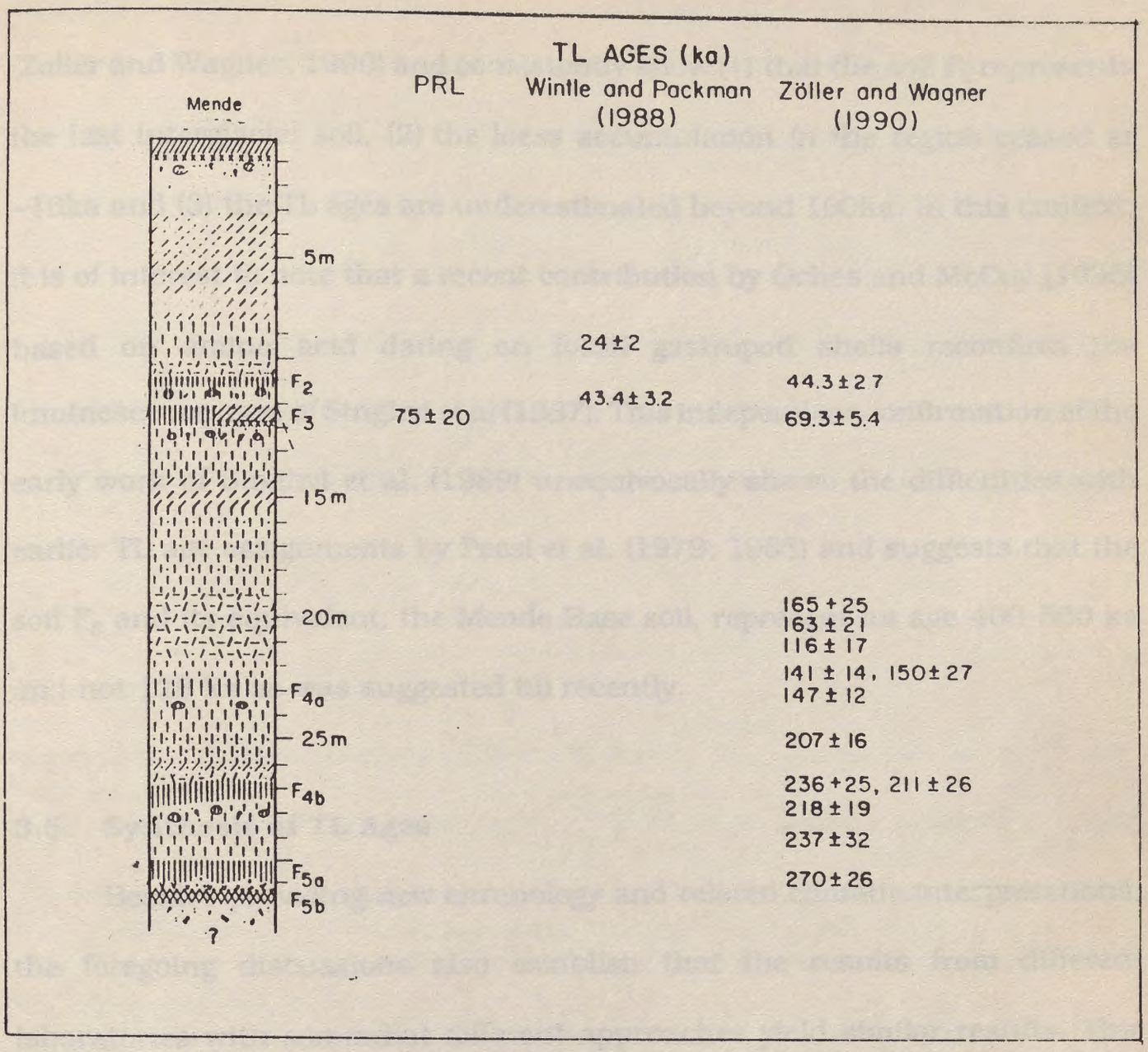


Fig. 3.13. Stratigraphy of TL ages obtained in the present thesis along with other ages reported by Wintle and Packman (1988) and by Zoller and Wagner (1992).

Zoller and Wagner, 1990) and consistently show (1) that the soil F_2 represents the last interglacial soil, (2) the loess accumulation in the region ceased at ~16ka and (3) the TL ages are underestimated beyond 100ka. In this context, it is of interest to note that a recent contribution by Oches and McCoy (1995) based on amino acid dating on fossil gastropod shells reconfirm the luminescence ages of Singhvi et al (1987). This independent confirmation of the early work of Singhvi et al. (1989) unequivocally shows the difficulties with earlier TL age assignments by Pecsi et al. (1979; 1985) and suggests that the soil F_5 and its equivalent, the Mende Base soil, represent an age 400-500 ka and not 128 ka as was suggested till recently.

3.5. Synthesis of TL Ages

Besides providing new chronology and related climatic interpretations, the foregoing discussions also establish that the results from different laboratories with somewhat different approaches yield similar results. This indicates that the physical principles underlying the TL dating are basically sound and that the ages could indeed be used to date paleoclimatic events.

In order to deduce the paleoclimatic information from loess TL ages, all the TL ages on loess paleosol sequences were collated and methodologically assessed. Of these all, those ages which were on pure loess horizons obtained on soil B or C horizons were compiled (Appendix-1). TL ages on A horizons were not included as these indicated the event of soil formation and not of loess accumulation. This is in view of the fact that during the process of A-horizon development, faunal pedoturbation causes churning of strata,

resulting in an onsite sun exposure. Approximately 500 methodologically reliable TL ages depicting the age of loess accumulation were available for a statistical analysis. These were then analyzed in a probability density approach following Venkatesan and Ramesh (1993). In this analysis if T_i is the age of ith sample with σ_i its 1σ experimental error, a histogram can be constructed which also takes in to cognizance of the error σ_i. To plot the histogram from time T_1 to T_2, the internal $T_2 - T_1$ is divided into sub-intervals such that the number of classes is

$$N = \frac{T_2 - T_1}{\Delta t} \quad \ldots\ (10)$$

where Δt is the class interval (500 yrs in the present case). Now for each age a gaussian variable is generated such that its mean occurs at t_i and σ_i is its *fwhm* then the contribution to the probability density of each age to each class interval can be computed. The probability density for the mean T_j of the jth interval is then computed by subdividing the class intervals to sub-intervals into smaller intervals Δt (50 years in the present case). The PD at either end of sub-interval is then calculated as

$$P_k = \sum_{i=1}^{n} \frac{1}{\sigma_i \sqrt{2\pi}} \exp -\left(\frac{1}{2} \frac{t_i - T_k}{\sigma_i}\right)^2 \quad \ldots\ (11)$$

where k indicates the lower subclass limited, thus T_k is the lower limit of an interval and T_{k+1} the upper limit. t_i is the age of ith sample and n is the number of dates used in the analysis. The area under each sub-interval is then calculated using the trapezoidal rule, i.e.

This is done for each sub-interval within the class interval j. The sum of these

$$Area = \Delta t_{sub} \times \left(\frac{P_k + P_{K+1}}{2}\right) \quad \ldots\ (12)$$

class intervals is then divided by class interval Δt to yield PD for each class interval, i.e.

$$PD\ for\ class\ interval = \frac{\sum_{i=1}^{k} PD_{sub\text{-}interval\,i}}{\Delta t_{class\ interval}} \quad \ldots\ (13)$$

The PD for class interval is represented at its mid-point and the procedure is repeated for all the classes within the limits of time range (0-250ka). To obtain a normalized distribution the total probability was then divided by n. Fig.3.14 gives the PD density obtained for global data set with 1σ errors and 2σ error intervals. It may also be pertinent to point out the following.

In the above analysis, it is reasonably assumed that the data set is unbiased based on the fact that the samples were collected by different groups with different objectives.

Since it is difficult to locate a long complete sequence extending over a large time span, most of the dates are confined to the last 50 ka and very few dates relate to loess deposition after 100ka. Consequently, the peak in probability density is to an extent reflects higher number of ages in 10-20 ka range. Erosional processes if any would imply voids in TL age sequence and these are not accounted for. However, this was examined by creating regional data sets with the assumption that erosional epochs should not be globally synchronous. Further, although the analysis was carried out for past 200 ka, the results have been interpreted only for the most recent climatic epoch, thereby ensuring that any effect due to underestimation of ages does not affect

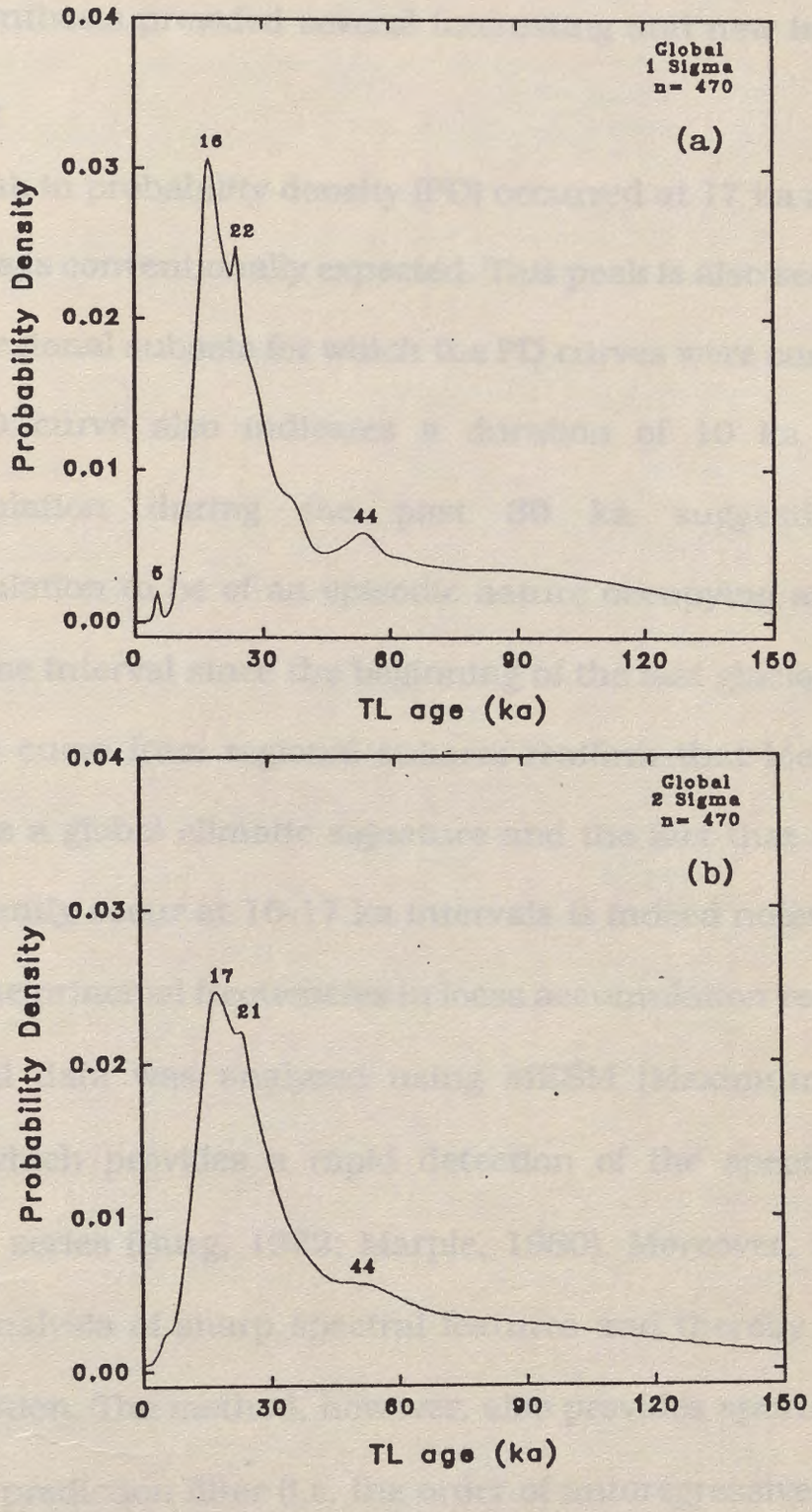


Fig. 3.14 Probability density of occurrence of Loess age (accumulation) for the global data. The figure is constructed by assuming the width of the age gaussian as 1 sigma (Fig. a) and 2 sigma (Fig b).

the conclusions. Figs. 3.15-3.18 provide results on probability density analysis for the regional data sets.

The global synthesis provided several interesting and new insights on loess accumulation.

(1) The peak in probability density (PD) occurred at 17 ka and not at 22 ka as is conventionally expected. This peak is also seen in each of the regional subsets for which the PD curves were constructed.

(2) The PD curve also indicates a duration of 10 ka for loess accumulation during the past 30 ka suggesting loess accumulation to be of an episodic nature occupying at best 25-30% time interval since the beginning of the last glacial epoch.

(3) The PD curve from regional subsets reaffirm that loess indeed provides a global climatic signature and the fact that the peaks consistently occur at 16-17 ka intervals is indeed noteworthy.

To estimate the principal frequencies in loess accumulation records, the PD curve for global data was analyzed using MESM (Maximum Entropy Spectral Method) which provides a rapid detection of the spectral peaks present in the time series (Burg, 1972; Marple, 1980). Moreover, it has the property of being analysis of sharp spectral features and thereby providing good spectral resolution. The method, however, also provides spurious peaks with increasing the prediction filter (i.e. the order of autoregressive model).

From the PD data, 1113 points were obtained at an uniform interval. The data set was examined for randomness test after dividing the data into series of various widths. The turning point test showed that the series were not

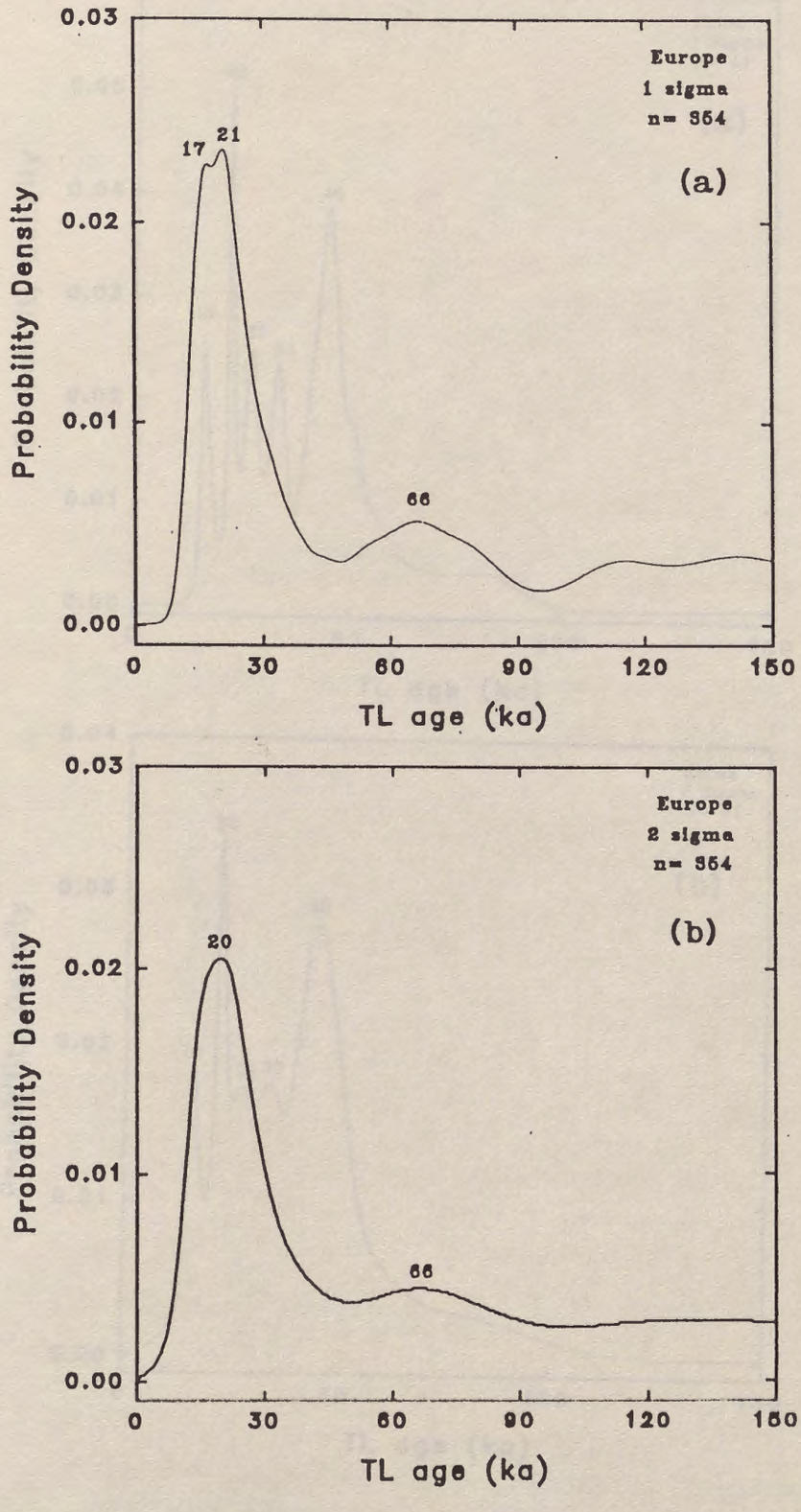


Fig. 3.15 Probability density of occurrence of Loess age (accumulation) for the loess sequences from Europe. The figure is constructed by assuming the width of the age gaussian as 1 sigma (Fig a) and 2-sigma (Fig.b).

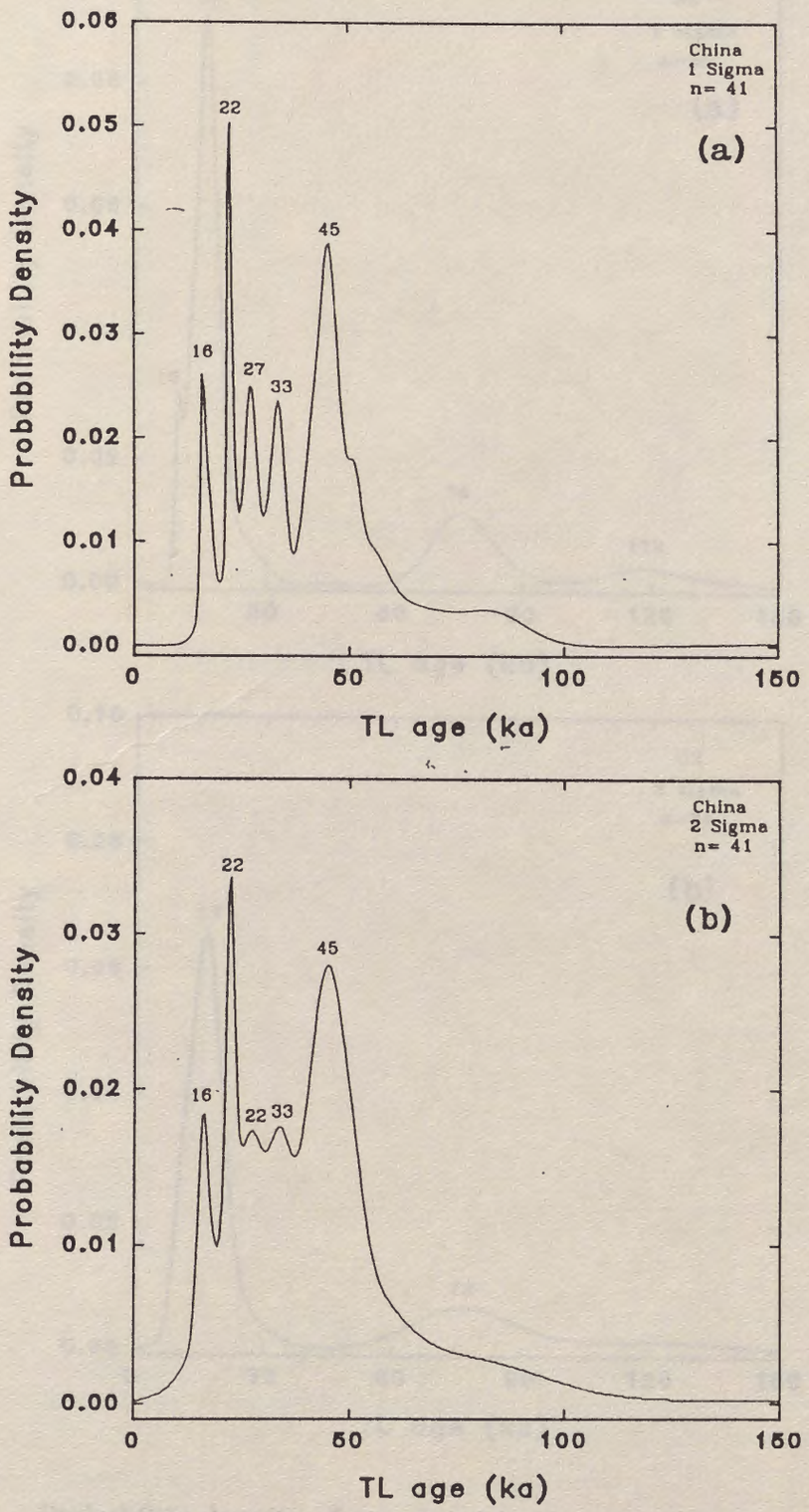


Fig. 3.16. Probability density of occurrence of Loess age (accumulation) for the Chinese loess sequences. The figure is constructed by assuming the width of the age gaussian as 1 sigma (Fig a) and 2sigma (Fig b).

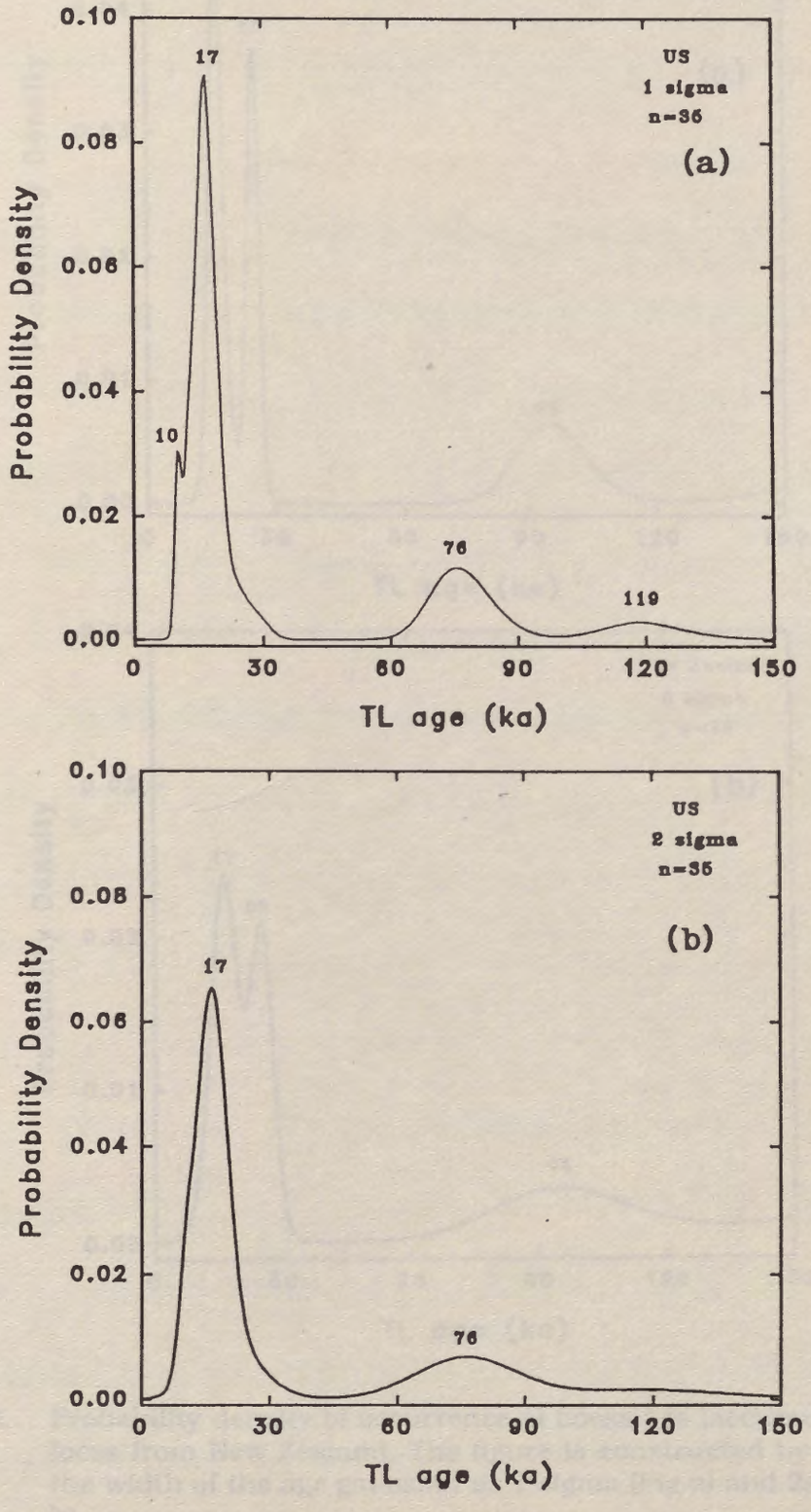


Fig. 3.17. Probability density of occurrence of Loess age (accumulation) for the loess from US. The figure is constructed by assuming the width of the age gaussian as 1 sigma (Fig a) and 2sigma (Fig. b).

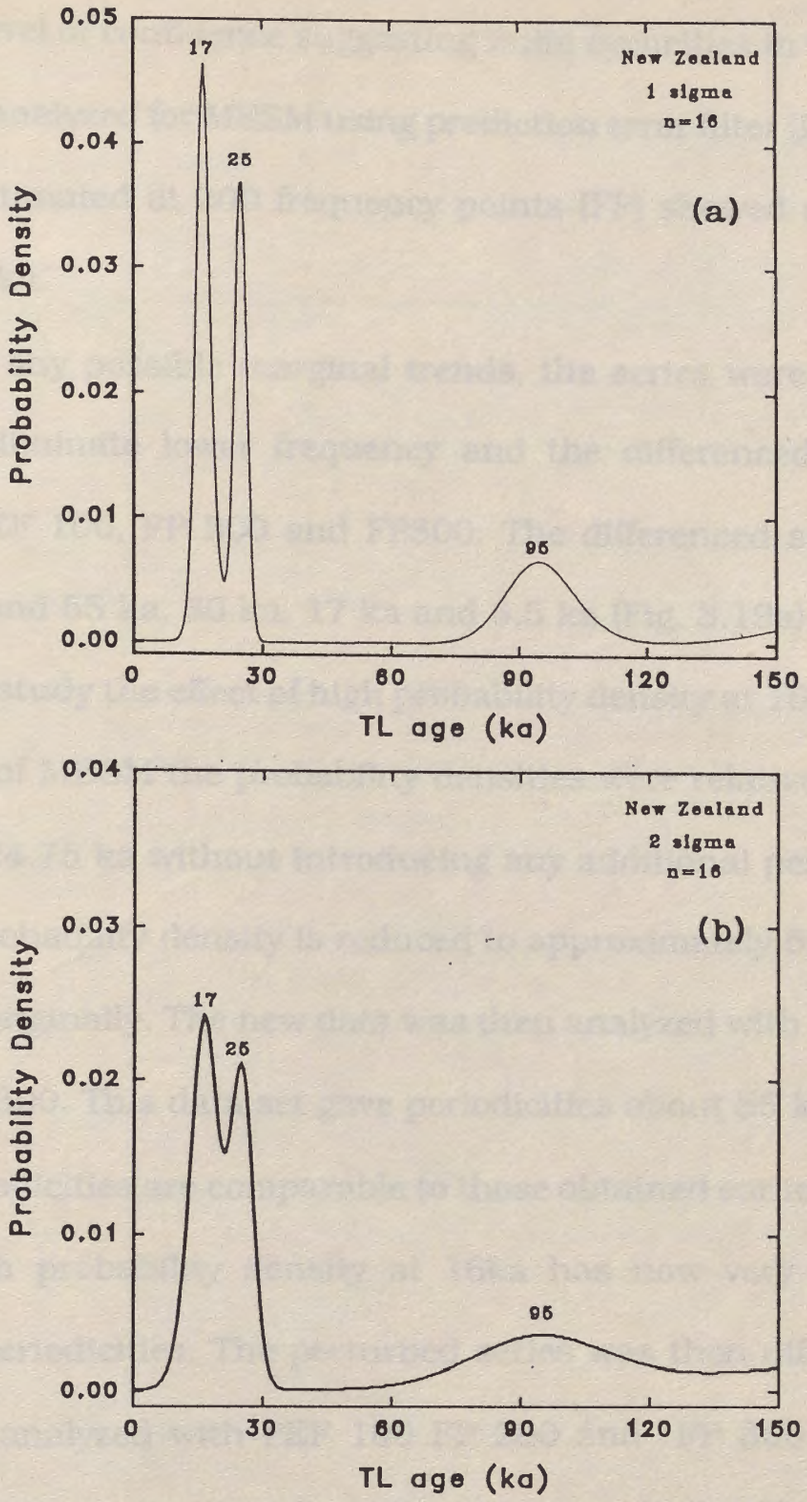


Fig. 3.18. Probability density of occurrence of Loess age (accumulation) for loess from New Zealand. The figure is constructed by assuming the width of the age gaussian as 1 sigma (Fig a) and 2sigma (Fig. b).

random at 1% level of confidence suggesting finite cyclicities in the data. The series were then analyzed for MESM using prediction error filter (PEF) 100. The power density estimated at 200 frequency points (FP) showed an additional periodicity of 50 ka.

To remove any possible marginal trends, the series were subjected to differencing to eliminate lower frequency and the differenced series were analyzed with PEF 100, FP 200 and FP300. The differenced series showed periodicities around 55 ka, 30 ka, 17 ka and 5.5 ka (Fig. 3.19a).

In order to study the effect of high probability density at 16.75 ka on the power spectrum of MESM the probability densities were relatively perturbed from 9.25 ka to 24.75 ka without introducing any additional peak or trough. The maximum probability density is reduced to approximately 50% of what it was at 16.75 ka originally. The new data was then analyzed with PEF 100 and FP 200 and FRP 300. This data set gave periodicities about 55 ka, 23 ka and 16 ka. These periodicities are comparable to those obtained earlier, suggesting the effect of high probability density at 16ka has now very little role in influencing the periodicities. The perturbed series was then differenced and which was then analyzed with PEF 100 FP 200 and FP 300. The results indicated periodicities around 55 ka, 29 ka, 16 ka and 5.36 ka which were similar to differenced series generated without perturbing the data (Fig.3.19b).

The probability density spectrum in combination with spectral analysis showed that the loess deposition occurred during short time windows which is also supported by the TL dates at individual locations. The delayed peak in the loess accumulation compared to glacial maxima indeed expected if the

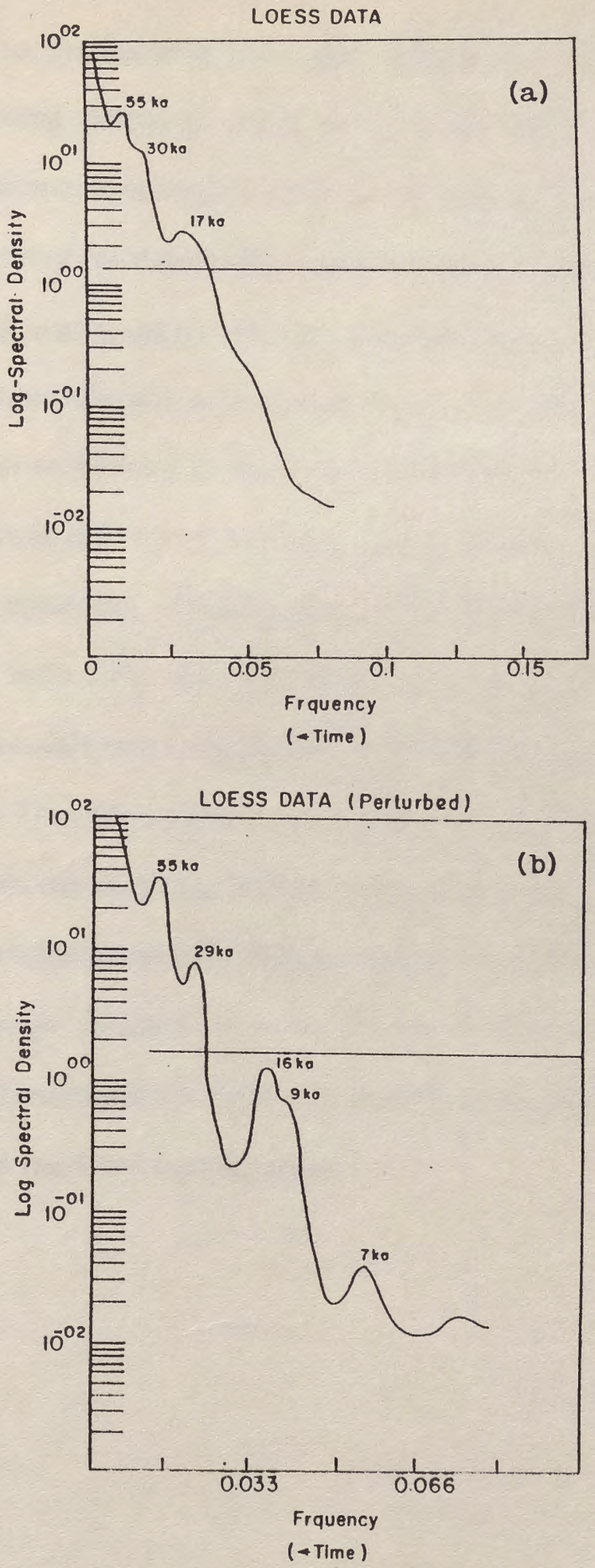


Fig. 3.19. Power spectrum analysis of Fig. (3.11) unperturbed and (b) perturbed when the hight of the 17 ka peak was arbitrarily reduced to 50%.

process leading to production, transport and accumulations of loess are considered. Assuming glacial grinding as the principal mechanism for loess formation, it is reasonable to expect that the silt became available for deflation only after the ice cover retreated and this could have happened only after the glacial maxima. The transport conditions could be considered identical, but the accumulation of loess should have commenced only after glacial maxima as loess accumulation requires a finite amount of moisture/vegetation in order to trap the silt. This is also borne out by the wind tunnel experiments of Cegla (1972). Thus, an optimum configuration of conditions for loess deposition became available only after the glacial epochs, and that it was of short duration also reasonable due to reduction in dust supply and in enhancement of vegetation cover. This observation necessitates a close look at the correlation so far made between the deep sea isotopic records and the continental records because such a correlation would imply a comparison between a continuously accumulating system (ocean) with a punctuated accumulation system (continental). The luminescence ages and their analyses question the validity of the conventional land sea correlations.

Chapter 4

Studies on Age Underestimation in Thermoluminescence dating

In this Chapter, results of a detailed study on the physical processes that could lead to the observed underestimation of TL ages on Loess-Paleosol sequences are presented. The current status is briefly summarized. Subsequently result of a detailed study on possible causes of underestimation of ages are described. A band-structure scenario involving a single trap and three recombination centres is described which explains the changes in TL sensitivity and can be used to provide a basis for the correction of the TL ages.

4.1. Thermoluminescence dating limit and age underestimation

With the advent of thermoluminescence dating of sediments (Wintle and Huntley, 1979), chronometry of a large variety of sedimentary deposits is being attempted. The application of the luminescence method also suggests that the maximum limit upto which the technique can provide ages is much smaller compared to the expected upper limit to age based on the saturation dose, the dose rate and the mean life of the dating signal. Thus, for example, luminescence dating of loess sequences using feldspar emission indicated a limiting age of 100-200 ka and not ~ 1 Ma as was previously considered. The first systematic description of age underestimation of TL ages on loess was given by Debenham (1985) and is shown in Fig.4.1 which indicates that the TL ages systematically showed a limiting age (Debenham, 1985; Wintle, 1990; Musson and Wintle, 1994; Zoller and Wagner, 1994).

4.2. Present Status

The limiting age obtainable by the TL method has attracted considerable attention for long. Process such as anomalous fading (athermal loss of TL) can cause a severe underestimation of TL ages in samples exhibiting this phenomena (Wintle, 1973; Visocekas, 1976). In one of the early studies, Nambi (1983a, 1983b, 1984) identified an additional limiting factors in long range TL dating limits in some detail. Based on the synthesis of a variety of datasets on quartz, gypsum, calcrete etc., Nambi inferred that, "TL buildup in nature reaches a dynamic equilibrium much ahead of the lifetime of the TL traps concerned and is solely determined by the radioactivity of the sample; the

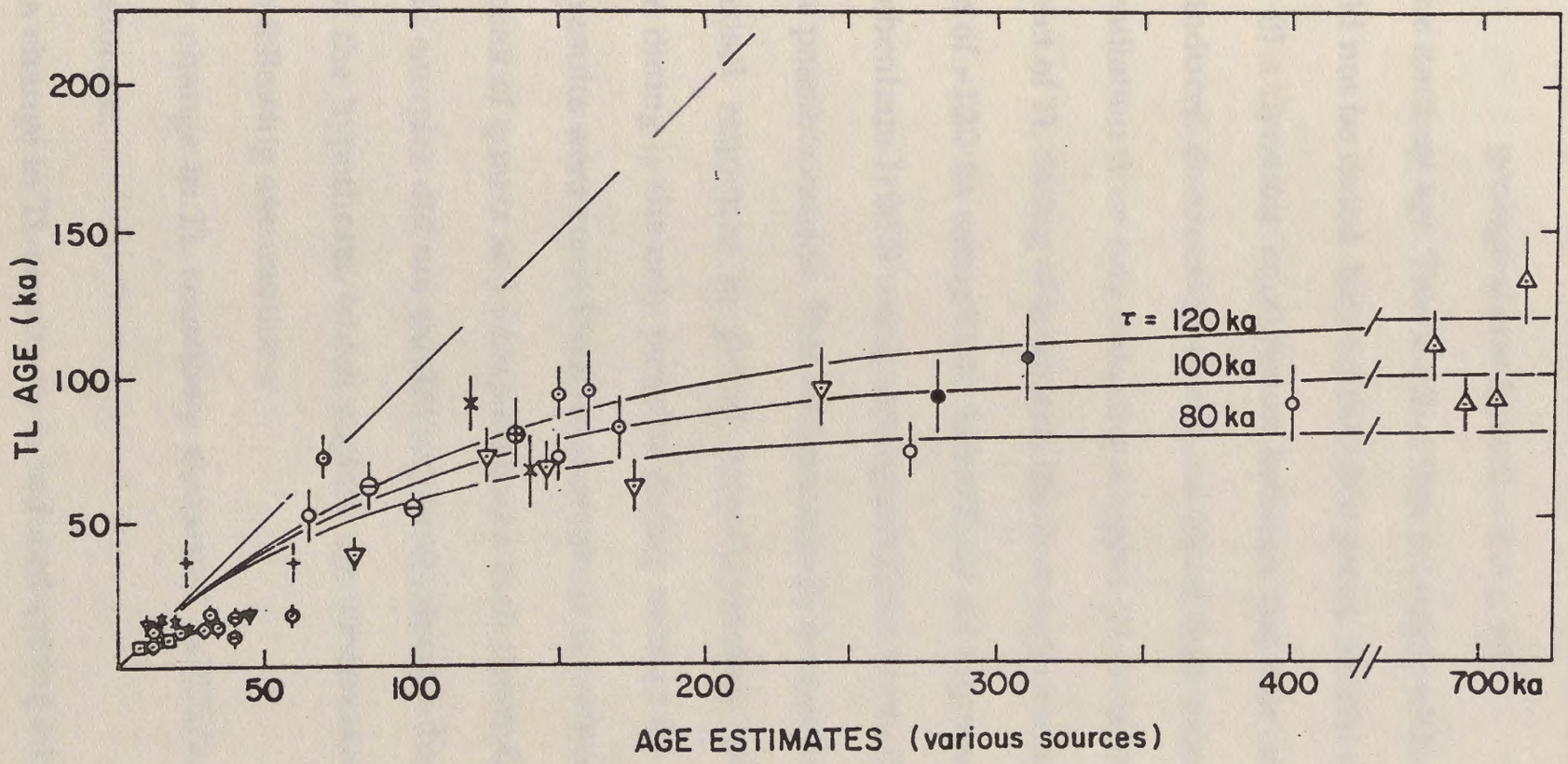


Fig. 4.1. Comparison of TL ages with geological and other age estimates (After Debenham, 1985).

validity of TL dating does not exist once such an equilibrium is reached". Nambi also concluded that the relation,

Surface alpha emission rate (counts per hour for 13.86cm counting area) x geological age (years) = 4.5 x 10^6

determined the limiting age. This implied that a sample with 1 ppm of natural uranium could not be dated beyond 500,000 years. Nambi hypothesized this to be due to (i) a dynamic equilibrium between the rate of trap filling and (ii) radiation induced destruction at natural alpha dose rate and due to high laboratory irradiation dose rate inducing a higher TL sensitivity.

In respect of TL dating of sediment, the first experimental observation of a limiting age of ~120 ka using TL in loess/Paleosol sequences from western Europe by Debenham (1985) using the regeneration method initiated several studies on the possible causes. This was principally because of the importance of loess/paleosol sequence in global paleoclimatology and the fact that luminescence dating is the only possible dating method for such sequences. Further, the results were considered as anomalous in view of the fact that the dating glow peak of quartz and feldspars had a high thermal stability (Aitken, 1985) and the samples did not exhibit any anomalous fading.

Most of the hypotheses which explain age underestimation have been based on the following assumptions:

(1) a change in TL sensitivity measured as (TL/mg, Gy) occurs on storage,

(2) a change in TL sensitivity is induced during laboratory bleaching and/or irradiation,

(3) the age underestimation is a consequence of a larger distribution of trapping levels, some of which have a lower stability.

(a) Change of TL sensitivity with time

Debenham (1985) attributed the underestimation of TL ages to the decay of recombination centres (over a lifetime of 80-100 ka). The above hypothesis, however, suffered from three basic difficulties viz., (i) if the mean life of centres is assumed to be ~100 ka, then over the period since the mineral was formed, all the accumulation centres should have been lost making the mineral non-luminescent, (ii) the loss of centres would uniformly reduce the sensitivity of both the natural and regenerated growth curves, and (iii) it does not agree with the fact that minerals older than 100 ka do show an increase in their TL growth on being given additional dose. Rendell and Townsend (1988), Mejdahl (1988) suggested that decay of TL sensitivity occurs due to thermal loss of signal over the time scale of ~10^5 ka. This was suggested on the basis of an observation of higher saturation limit for the TL from samples irradiated in the laboratory compared to those exposed in nature. Xie and Aitken (1991) extended this concept and explained the age underestimation by examining the growth of stable and unstable components. The unstable component decays with time over the geological storage period but remains intact under laboratory irradiations. Consequently the laboratory induced TL grows with higher sensitivity. Possibility of the existence of such transient centres was also hypothesized by Wintle and Packman (1988) who argued that presence of shallow traps along with the dose rate difference between natural

and laboratory irradiation can give rise to age underestimation. Under natural irradiation, shallow traps are maintained at a very small equilibrium population of trapped charges (over geological time scales). On the other hand, in laboratory irradiation after bleaching, shallow traps are filled rapidly and may go into saturation. Irradiation beyond this dose provides excess charges (that were filling the shallow traps) to deeper traps causing an enhancement in TL sensitivity. The underestimation is therefore expected to occur beyond a certain laboratory equivalent dose. In an interesting experiment to examine this hypothesis, Wintle and Packman (1988) irradiated samples at different elevated temperatures to ensure that shallow traps remain unfilled. However, in the samples studied by them no change in sensitivity beyond 270° C was detectable. On the other hand, Mejdahl et al (1992) reported that equivalent doses (ED) estimated by irradiating K-feldspar samples at elevated temperatures (~130°C) (for keeping shallow traps unfilled) exhibited higher values (by ~35%) compared to the ED's obtained for samples irradiated at room temperature and thus concluded that "shallow traps could well be the main cause of underestimation". The different results by Wintle and Mejdahl et al (1992) perhaps could be due to the fact that different TL centres were being sampled. Further, the procedure of irradiation of samples at elevated temperature may alter the TL sensitivity, but this is yet to be investigated in some detail.

b. Changes in TL sensitivity with photo-bleaching

A scenario, alternative to the loss of TL sensitivity with time is an enhancement of TL sensitivity during laboratory simulation. This occurs due to intra-centre charge transfer by photo-bleaching. The basic premise in this approach relates to an enhancement of TL response consequent to laboratory photobleaching. Thus the growth of regenerated TL occurs at higher TL sensitivity and consequently a lower equivalent dose is estimated. Based on Rendell et al's (1983) observation on complex photo bleaching behaviour in Potwar loess, Wintle (1985) hypothesized that the dose dependent sensitivity changes on photobleaching would result in an enhanced sensitivity and consequently would cause an age underestimation. A basic difficulty with this suggestion arises because during weathering of rocks, the dose (geological TL) is highest and when the mineral is first photobleached and consequently as per the model, the sensitivity enhancement on photobleaching will also be the highest. As natural doses imparted in the laboratory are substantially smaller than geological dose (<1%), the sensitivity changes should be relatively insignificant to explain the underestimation of ages. The only recourse to this is to assume that the sensitivity enhancement decays with time so that the memory of positive enhancement is lost. Rendell and Townsend (1988) thus hypothesized the presence of a transient signal based on the observation of a change of TL sensitivity on storage. They also suggested temporary conversion of non-radiative centres to radiative centres by photo exposure. Rendell and Townsend (1988) thus suggested that, ".....Overall conclusion is that the regeneration method may be seriously flawed". More recently, Zhou and Wintle

(1994) suggested that sensitivity change on photobleaching may be related to previous dose. The sensitivity was seen to change at a prior dose having a threshold of ~200 Gy and a maximum change of 30% was seen in all the emission windows. However, in none of the approaches a clear cut recipe for correction of ages was provided.

(c) Age underestimation due to distribution of activation energies

In an interesting experiment relating to archaeological application of TL, Hornyak et al., (1993) picked up the experimental evidence that typical quartz when exposed to a laboratory dose equal to the natural dose provided higher signal compared to signal acquired during antiquity. Hornyak et al. (1993) proposed a model based on a thermal release of electrons trapped at centres possessing different activation energies. In a detailed computational exercise, the authors showed that in such case a systematic underestimation based on burial temperature could occur. For example, for activation energy 1.4eV, width of activation energy distribution of ~0.186eV and burial temperature of ~15°C, underestimation by upto 40 ka could arise for a 200 ka sample. Although the authors presented convincing computational results, it is not yet clear as to how a plateau test fails to detect such an underestimation even with an activation energy distribution. There must exist traps which have increasingly higher stability and the plateau test should locate these without any ambiguity. This study, however, was not extended to K-feldspar the principal TL emitter in loess-paleosol sequences and no routine recipe was made available to correct for the possible underestimation of ages.

4.3. Present Studies

Although, all the above studies though presented important concepts in understanding the age under estimation process, they were rarely followed by rigorous experimental analysis. Consequently a more quantitative data base was needed and the present thesis aimed at systematically examining various factors that could lead to the underestimation of ages. This basic premise of our approach was to reconcile with the theoretical estimate of the stability of TL signal based on the kinetics analysis and at the same time provide a physical basis that would be in conformity with experimental observations of limiting ages. To ascertain that the underestimation effect was universal and existed in the fine grain loess sample of different provenances, detailed studies on the extent of the magnitude of the underestimation of age was made on samples from China and Tadijikstan. Subsequently, studies on the luminescence sensitivity were carried out under various laboratory conditions and the results were used to provide a scenario for the underestimation of ages. These studies were based on the premise that K-feldspar dominates the TL signal from fine grain samples on the basis of (1) the substantially higher luminescence sensitivity of K-feldspar, and (2) choice of optical window that helped optimize in the detection of K-feldspar signal.

4.4. Magnitude of underestimation for different sequences

The Loess-Paleosol sequences from China and Tadjikistan were chosen as they provided independent chronostratigraphy based on correlation with the deep sea oxygen isotope record. Consequently, a comparison was possible

between TL ages and "expected ages". The stratigraphy and sampling points are shown in Fig.3.2 and 3.3. The topmost loess sample was collected from the layer immediately below the top soil (Holocene) and the bottom sample was collected from the loess horizon below a few paleosol layers (below 4th paleosol pedocomplex in China and below the 3rd pedocomplex in Tadijikstan). In the absence of absolute chronology for these sequences, a chronology based on the correlation of the loess/paleosol stratigraphy with the glacial/interglacial stages in the marine oxygen isotope record (Bronger and Heinkele, 1989; Bronger et al., 1995) was considered to be a reasonable first-order estimate. This stratigraphy is based on sequential associations of well developed soils beneath the Holocene soil to interglacials epochs. The age of the intermediate horizon is deduced by interpolation assuming a constant sedimentation rate. In assigning the ages a 10% error was assumed in each case. The TL ages of loess were determined using the regeneration and/or the total bleach method. The details of the dating analyses are described in the Chapter 3. The table 4.1 compares the TL ages with the expected ages derived from the deep sea oxygen isotope data with correlations. Fig. 4.2a and 4.2b show that the TL ages for Tadjikistan and the Chinese sequence "saturate" at 130 ka and 160 ka respectively. These are similar to the ages first reported by Debenham (1985) for the European loess samples and suggest that age underestimation the effect is a universal one and is related to the basic TL characteristics of K-feldspar emission.

Table 4.1. Comparison of TL ages with the expected ages for the loess profiles from Tadjikistan and China

Country	Site	Sample code	TL age (ka)		Expected age (Bronger and Heinkele 1989; Bronger et.al., 1995)
			Estimated	Corrected for sensitivity decay	
TADJIKI STAN	Karmaydan	J4	25 ± 2	25 ± 3	15 ± 10
		J6	63 ± 7	105 ± 37	65 ± 20
		J7	145 ± 16	241 ± 48	220 ± 85
		J8	101 ± 12	202 ± 23	350 ± 20
	Chashma nigar	J13	74 ± 7	145 ± 14	140 ± 30
		J14	73 ± 15	146 ± 30	250 ± 40
CHINA	Luochuan	BCH 9	7.5 ± 0.6	7.5 ± 0.6	15 ± 0.7
		BCH 11	27.7 ± 2	-	42 ± 0.7
		BCH 12	49 ± 3.6	69 ± 6	69 ± 0.7
		BCH 16	83 ± 8	147 ± 16	130 ± 3
		BCH 19	97 ± 8	-	137 ± 0.5
		BCH 25	117 ± 12	-	350 ± 1
		BCH 37	160 ± 11	302 ± 40	449 ± 1
		BCH 46	155 ± 12	-	540 ± 1

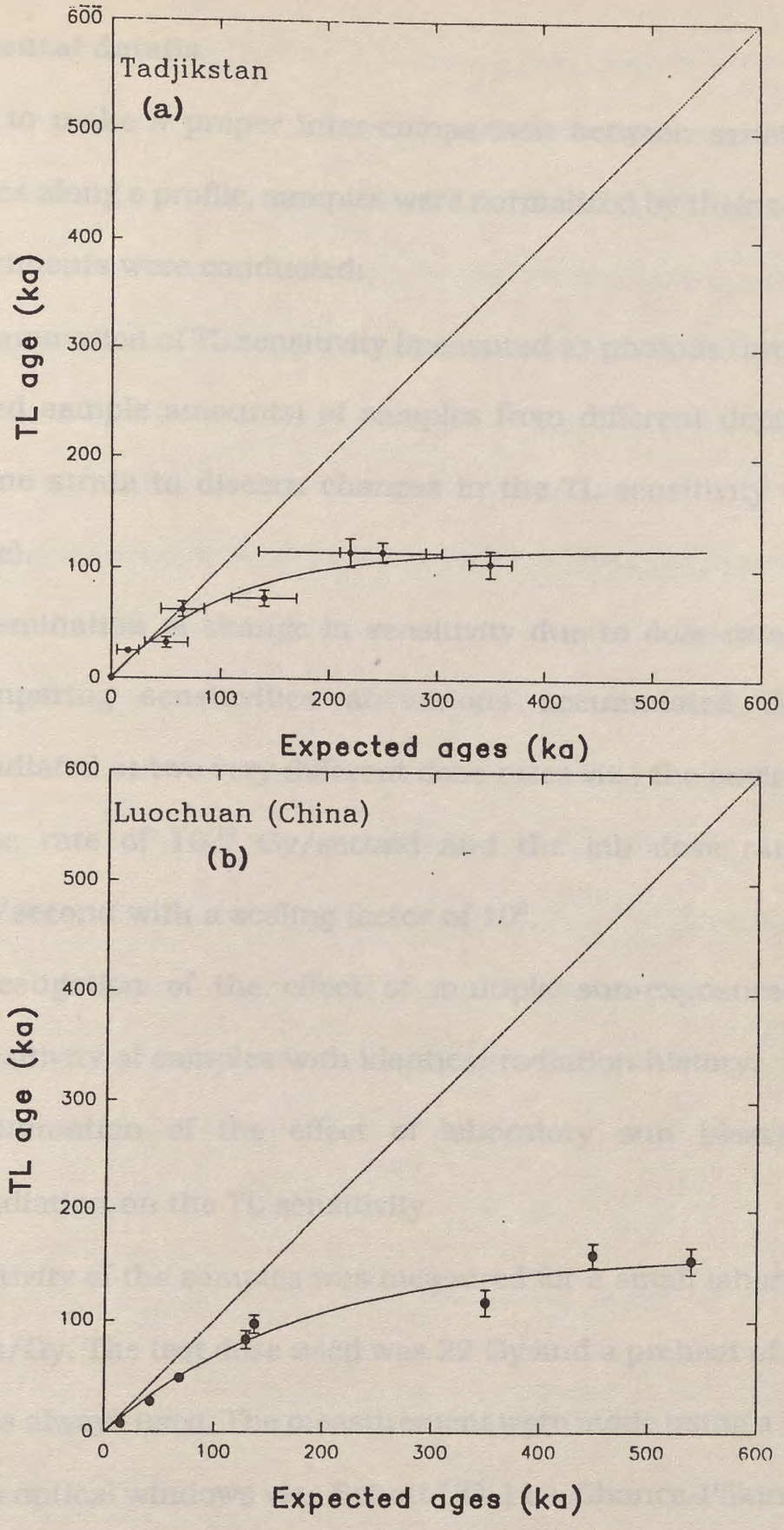


Fig. 4.2. Plot of TL ages obtained in this study with oxygen isotope stratigraphy as given by Bronger and Heinkele, (1989) and Bronger et.al. (1995). (a)- for Tadjikistan (b)- for Luochuan.

4.5. Experimental details

In order to make a proper inter-comparison between sensitivities of different samples along a profile, samples were normalized by their zero glows. Following experiments were conducted:

1. Examination of TL sensitivity (measured as photons/unit dose for fixed sample amounts) of samples from different depths in the same strata to discern changes in the TL sensitivity with time (age).
2. Examination of change in sensitivity due to dose-rate effect by comparing sensitivities at various accumulated doses but irradiated at two very different dose-rates viz., the environmental dose rate of 10^{-10} Gy/second and the lab dose rate of 10^{-2} Gy/second with a scaling factor of 10^{8}.
3. Investigation of the effect of multiple sun-exposures on the sensitivity of samples with identical radiation history.
4. Examination of the effect of laboratory sun bleaching and irradiation on the TL sensitivity.

The sensitivity of the samples was measured for a small laboratory test dose as photons/Gy. The test dose used was 22 Gy and a preheat of 160°C for 330 minutes was always used. The measurement were made using a Daybreak TL reader in two optical windows viz., Schott UG-11 + Chance-Pilkington HA3 (loess samples) and Corning 5-58 + Chance-Pilkington HA3 (coarse grain K-feldspars). Due to the high TL response of K-feldspars in the selected emission window and the general glow curve shapes, it is considered that a UG 11 +

HA3 filter combination emission window principally samples the K-feldspar emissions. However, to further confirm the results, pure K-feldspar mineral separates from a desert dune sequence were also studied. An important aspect in these studies was the normalization between the samples especially since neither the weight normalization, nor the short shine normalization could be used. Weight normalization in fine grain disc is generally impractical on account of sub-milligram sample amounts. Further as a specific mineral emission was being probed, it was considered that the measured weight (which also includes the weight of non-luminescent grains and the grains emitting in other optical windows) would provide higher scatter. The short shine normalization could not be considered as it depended on the sample dose which is different for different samples. Thus, the only possibility was to use the zero glow normalization as it still represented the intrinsic concentration of TL emitters in a disc in the emission region of interest. The errors in each measurement were computed using standard procedures on propagation of errors.

4.6. Results

(a) Sensitivity with time: The long term change in luminescence sensitivity was examined by comparing the initial TL sensitivity (S_1) for the samples of different ages in the same loess-paleosol profile. The sensitivity S_1 for the sample was measured as,

$$S_1 = \left[\frac{(L_N+Sun+\Delta\beta) - (L_N+Sun)}{\Delta\beta}\right] \cdot \frac{1}{ZG} \qquad \ldots\ldots(14)$$

where L_N denotes the natural TL of a sample, sun denotes a 14 hr sun bleaching $\Delta\beta$ is the test dose and ZG is the zero glow intensity. The term in the parenthesis provided the TL sensitivity which was scaled with the zero glow intensity to provide normalized sensitivity. This was done to enable intercomparison between the samples. Typical normalized glow curves are given in Fig.4.3 and Fig. 4.4a,b,c depicts the variation in TL sensitivity with age.

(b) Effects of dose/dose-rate on sensitivity

The second aspect of the study related to study of possible changes in sensitivity to dose/dose rate effects. This was done in view of the fact that laboratory dose rates are 10^8 times higher compared to the natural environmental dose rates and the recent data on a possible defect creation in quartz that has been attributed to a dose dependent dose rate effect (Chawla et al., 1996, preprint).

In this study, doses of increasing magnitude upto 1 or 2 kGy were administered to various sub-portions which were then sunbleached and the sensitivity to a test dose was measured and normalized to zero glow intensity. In this way it was possible to ensure that all the changes in sensitivity (S_2) could be attributed to dose/dose rate.

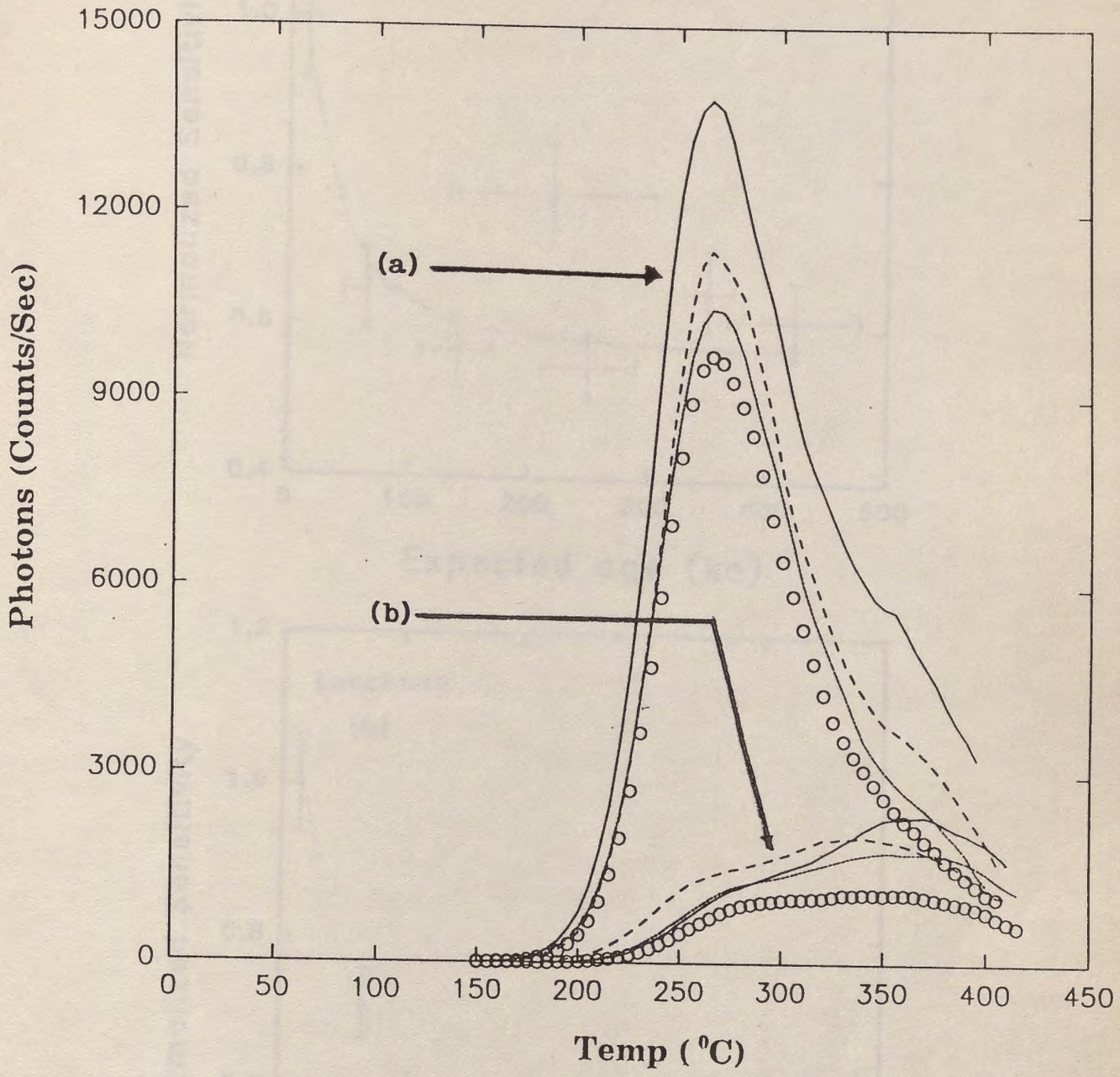


Fig. 4.3. Plot showing normalized glow curves of Tadjikistan loess (a) N+Sun+β (b) N+Sun.

(i) ——— J4

(ii) ------ J7

(iii) ——— J8

(iv) oooooooo J11

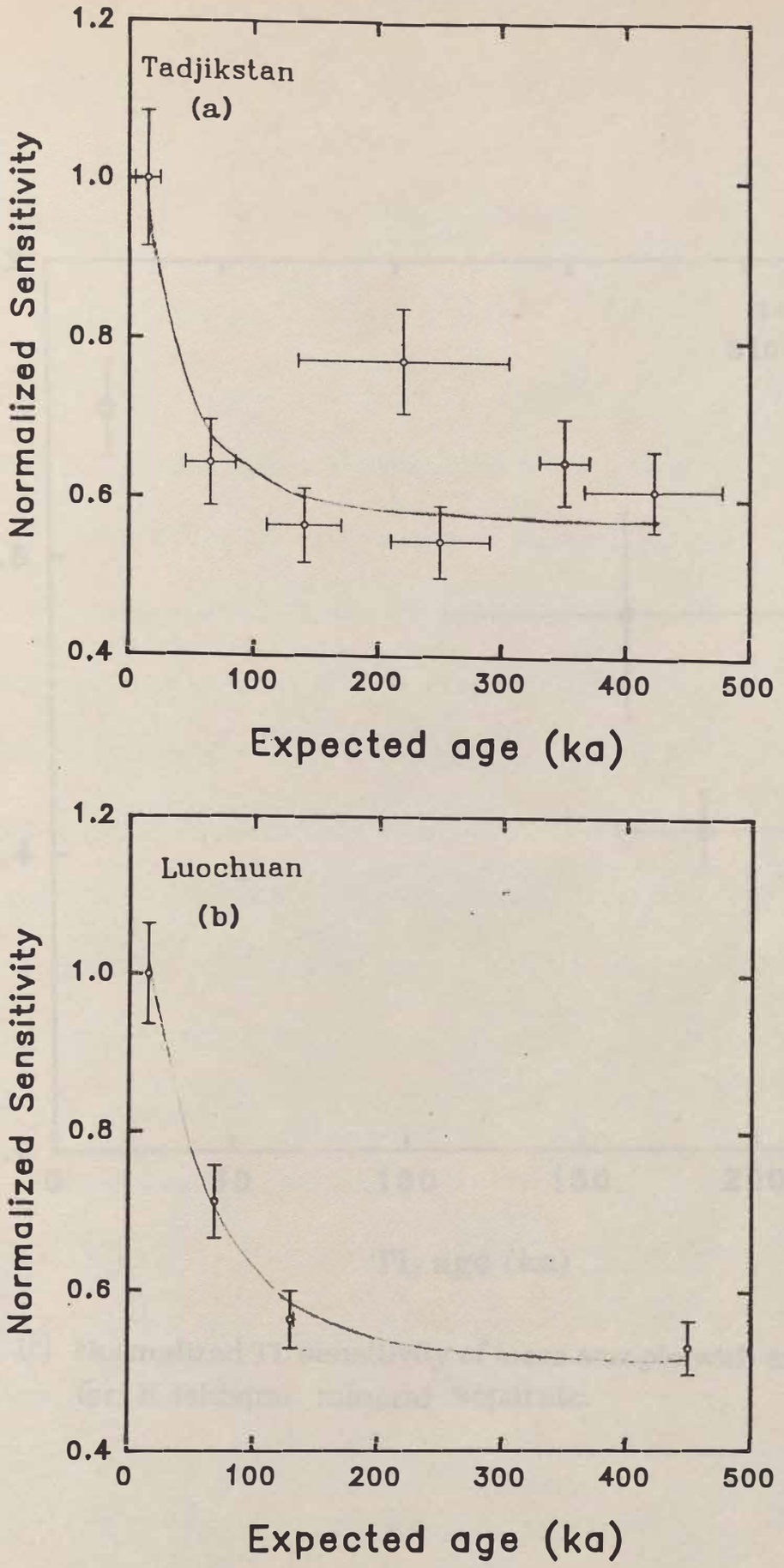


Fig. 4.4. Normalized TL sensitivity of loess sample with expected age (a) for Tadjikistan, and (b) for Luochuan

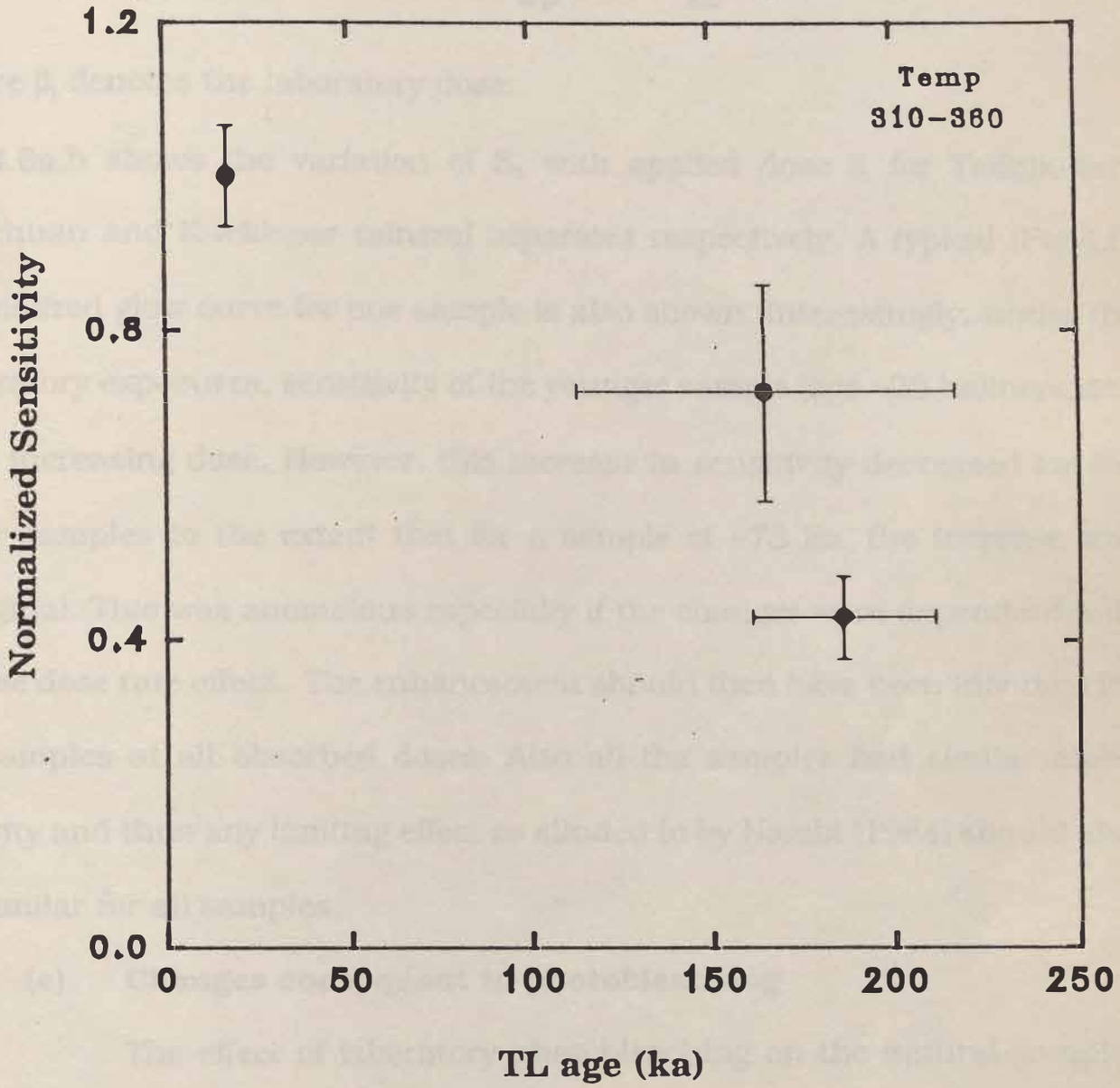


Fig. 4.4. (c) Normalized TL sensitivity of loess sample with expected age for K-feldspar mineral separate.

$$S_2 = \left(\frac{L_N+\beta_J+Sun+\Delta\beta}{\Delta\beta}\right)\frac{1}{ZG} \qquad \ldots\ (15)$$

where β_j denotes the laboratory dose.

Fig.4.6a,b shows the variation of S_2 with applied dose β_i for Tadijikstan, Luochuan and K-feldspar mineral separates respectively. A typical (Fig.4.5) normalized glow curve for one sample is also shown. Interestingly, under the laboratory exposures, sensitivity of the younger sample (age ~25 ka)increased with increasing dose. However, this increase in sensitivity decreased for the older samples to the extent that for a sample of ~73 ka, the increase was marginal. This was anomalous especially if the changes were dependent only on the dose rate effect. The enhancement should then have been identical for all samples at all absorbed doses. Also all the samples had similar alpha activity and thus any limiting effect as alluded to by Nambi (1984) should also be similar for all samples.

(c) Changes consequent to photobleaching

The effect of laboratory photobleaching on the natural samples (with different TL ages) was examined by measuring the TL sensitivity after multiple photobleaching. The measurement sequence was,

$$S_3 = \frac{(L_N+Sun+\Delta\beta)_k - (Sun+\Delta\beta)_k}{\Delta\beta} \qquad \ldots\ (16)$$

where, k indicates the sunbleaching cycle and it ranges from 1 to 4. The 'sun bleached' sensitivity also depicted a decreasing trend with age, reconfirming that a the loss of TL sensitivity occurs with time. The repeated cycles of

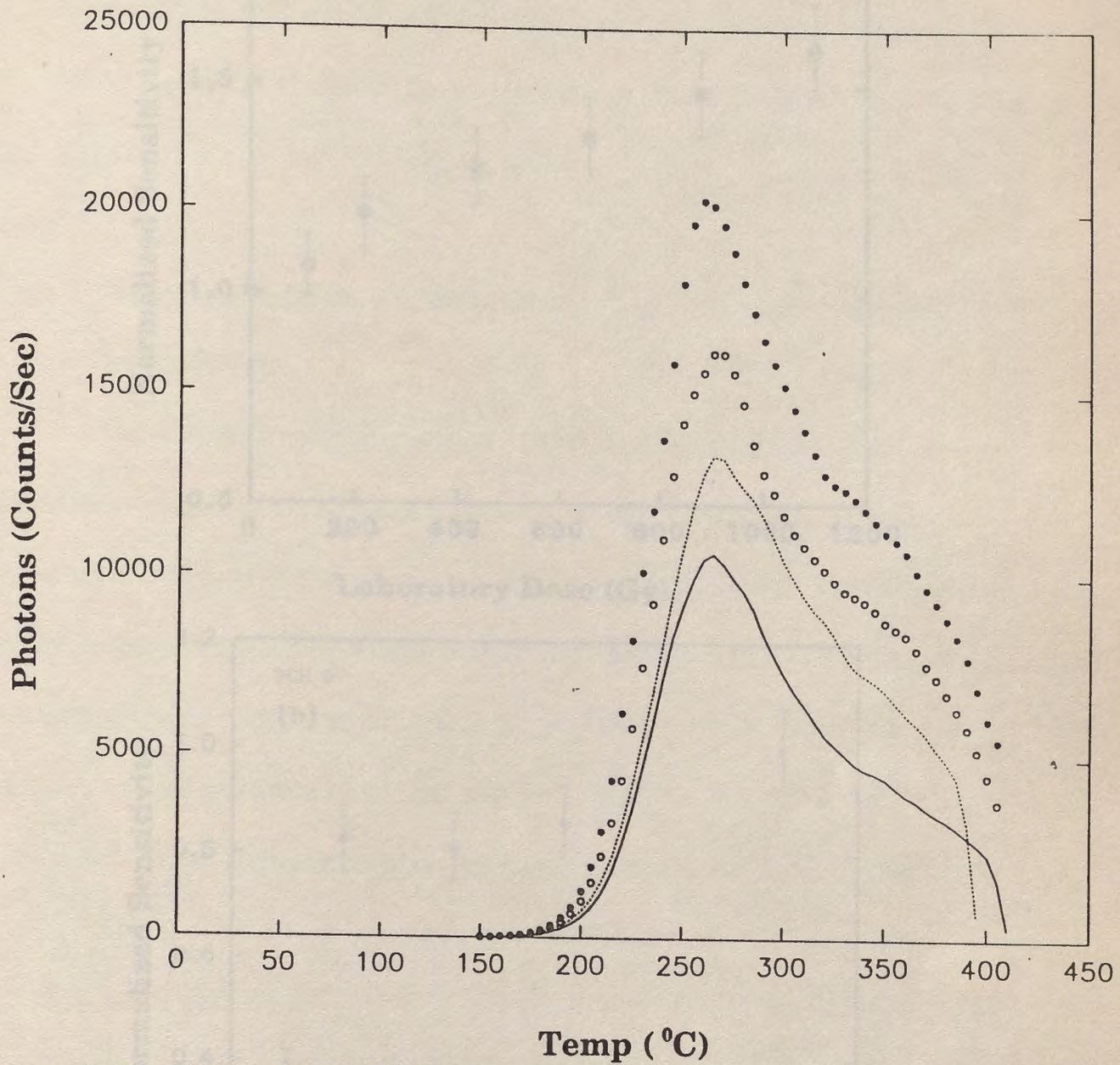


Fig. 4.6. Glow curves of samples J4 for a test dose after incremental laboratory doses followed by sun bleaching.

(i) ····· N+Beta (600)

(ii) ooooo N+Beta(500)

(iii) ····· N+Beta (300)

(iv) ——— N

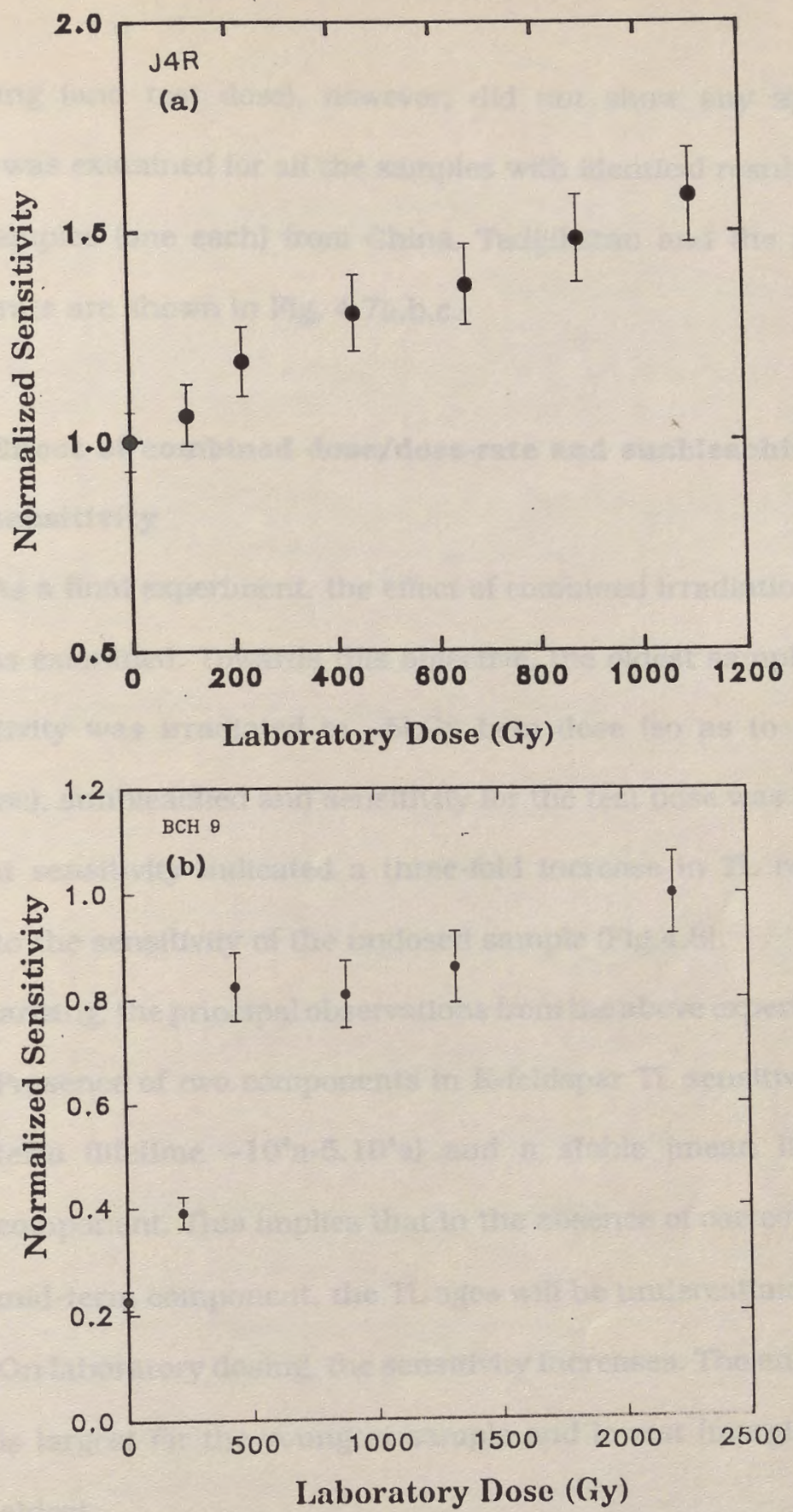


Fig. 4.7 Normalized TL sensitivity for a test dose following a beta dose and sunbleaching. The data is plotted with respect to laboratory beta dose (a) for Tadjikistan (b) for Luochuan.

photobleaching (and test dose), however, did not show any appreciable change. This was examined for all the samples with identical results. Typical results for samples (one each) from China, Tadijikstan and the K-feldspar mineral separate are shown in Fig. 4.7a,b,c.

(d) Effect of combined dose/dose-rate and sunbleaching on the sensitivity

As a final experiment, the effect of combined irradiation and sun bleaching was examined. Towards this objective, the oldest sample with the lowest sensitivity was irradiated to ~5kGy beta dose (so as to mimic the geological dose), sunbleached and sensitivity for the test dose was measured. The resultant sensitivity indicated a three-fold increase in TL response in comparison to the sensitivity of the undosed sample (Fig.4.8).

Summarizing, the principal observations from the above experiments are:

1. Presence of two components in K-feldspar TL sensitivity, a mid-term (lifetime ~10^4a-5.10^4a) and a stable (mean life ~10^{8-9}a) component. This implies that in the absence of correction for the mid-term component, the TL ages will be underestimated.
2. On laboratory dosing, the sensitivity increases. The enhancement is largest for the youngest sample and lowest (marginal) for the oldest.
3. Multiple sun bleaching does not alter TL sensitivity of the minerals.
4. Irradiation of minerals with a large dose followed immediately by

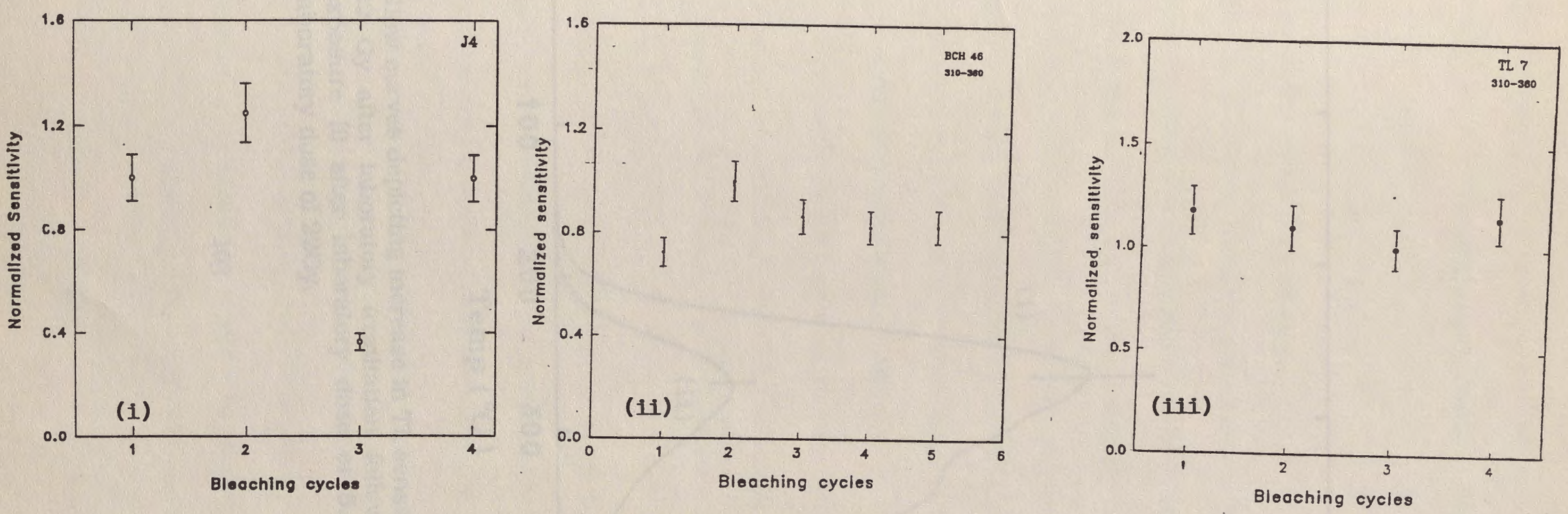


Fig. 4.7. Changes in TL sensitivity with multiple sun bleaching cycle each of 12 hr. duration (i) for J4, (ii) for BCH 37 and (iii) for TL7.

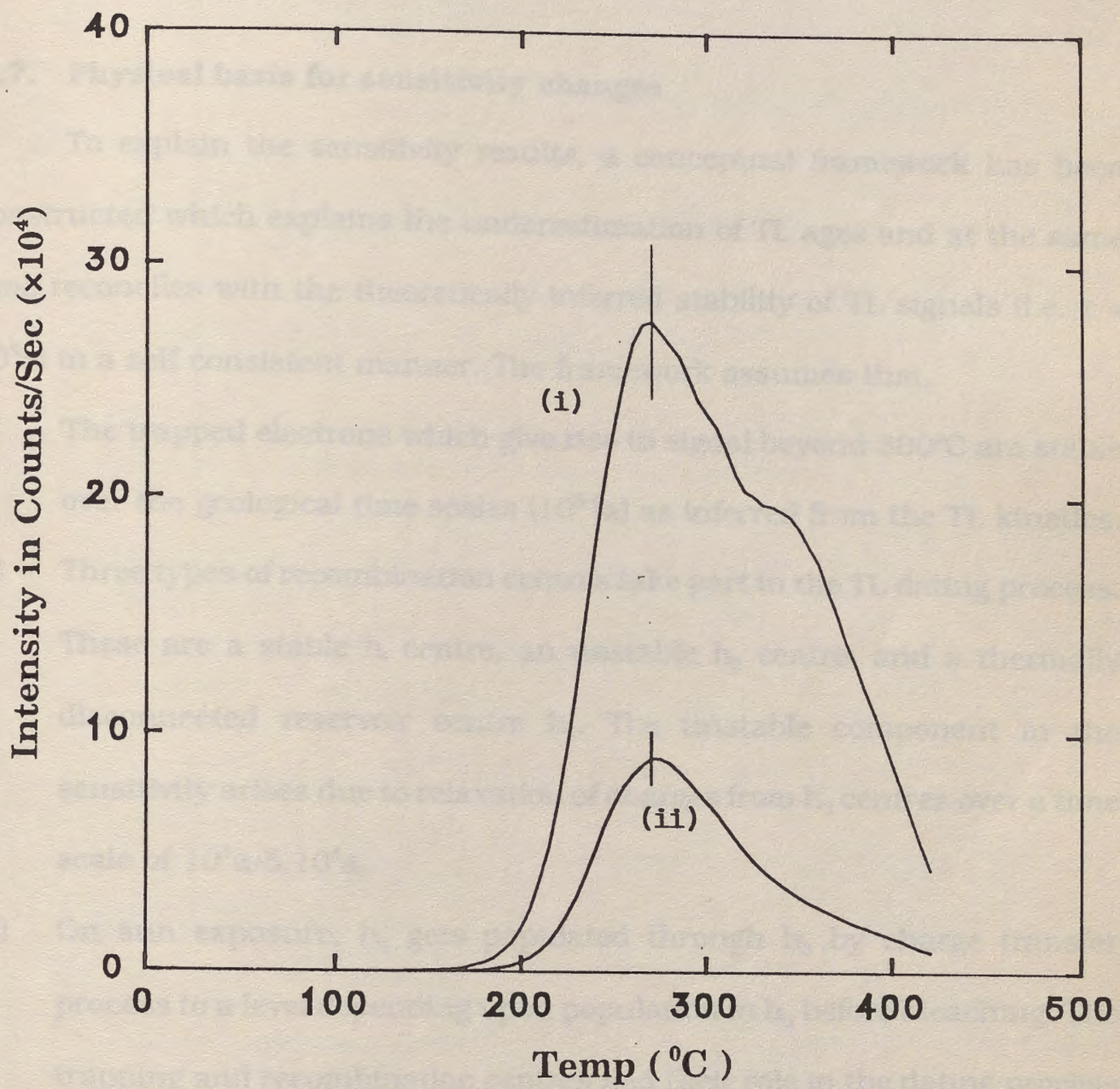


Fig. 4.8. Glow curves depicting increase in TL sensitivity for a test dose of 22 Gy after laboratory irradiation followed by a 12 hr sun exposure (i) after laboratory dose of 5.5kGy and (ii) after laboratory dose of 22Gy.

sun exposure causes enhancement in TL sensitivity and this phenomena can be used to determine the pristine sensitivity of sediment during the deposition.

4.7. Physical basis for sensitivity changes

To explain the sensitivity results, a conceptual framework has been constructed which explains the underestimation of TL ages and at the same time reconciles with the theoretically inferred stability of TL signals (i.e. $\tau \simeq 10^9$a) in a self consistent manner. The framework assumes that,

(i) The trapped electrons which give rise to signal beyond 300°C are stable over the geological time scales ($10^{8\text{-}9}$a) as inferred from the TL kinetics.

(ii) Three types of recombination centres take part in the TL dating process. These are a stable h_1 centre, an unstable h_2 centre, and a thermally disconnected reservoir centre h_3. The unstable component in the sensitivity arises due to relaxation of charges from h_2 centres over a time scale of 10^4a-5.10^4a.

(iii) On sun exposure, h_2 gets populated through h_3 by charge transfer process to a level depending upon population in h_3 before bleaching. The trapping and recombination centres and their role in the dating process is schematically explained in the Fig.4.9.

Fig.4.10 shows the trapped charge concentration in the centres h_1, h_2 and h_3. This is indicated by letters 'Low', 'High' and 'medium'. The trapped charge concentration in each of these centres at various stages in the history of the sample is discussed below. At this stage of analysis only a qualitative

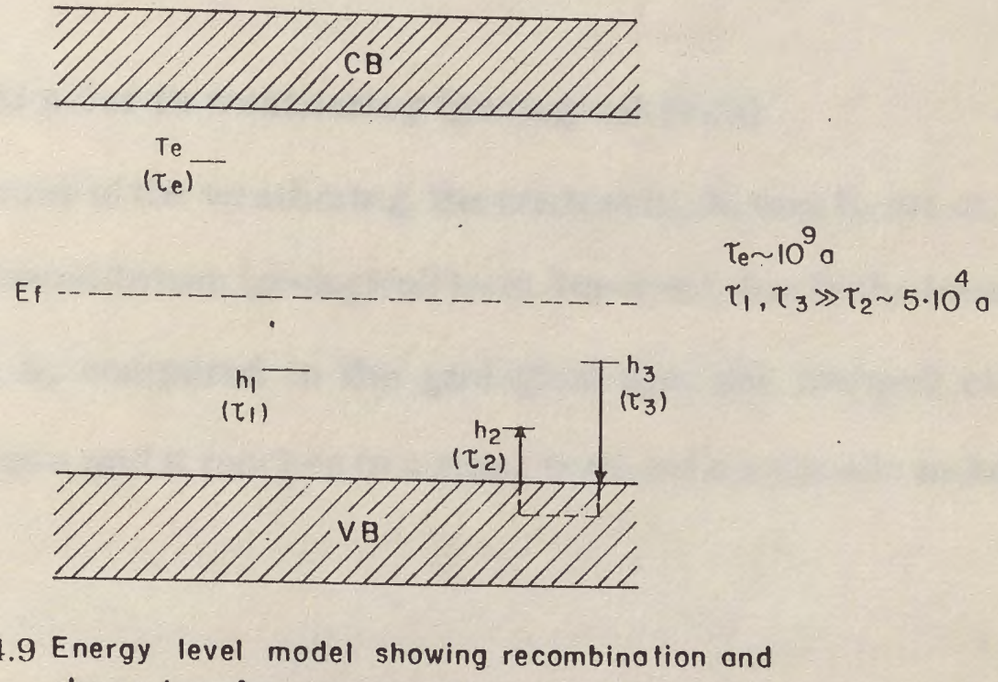


Fig. 4.9 Energy level model showing recombination and charge transfer processes during Sun bleaching

		h_1	h_2	h_3
(1)	Pristine Sample	High	Low	High
(2)	Sunbleaching (Zero age Sediment)	Low	High	Low
(3)	Old Sediment	High	Low	High
(4)	Laboratory Zeroing	Low	Medium	Low
(5)	At high laboratory irradiations	High	High	High
(6)	Zeroing	Low	High	Low

Fig. 4.10 Pictorial representation of h_1 h_2 and h_3 centre population at various stages in irradiation and bleaching cycles

description is attempted and studies such as optical absorption, ESR etc. would be needed to quantify these descriptions. This aspect is discussed in Chapter 6.

(a) Mineral prior to weathering (geological rock)

At the time of the weathering, the centres h_1, h_2 and h_3 are at their natural saturation/equilibrium (geological) level. However, due to the lower life time of the centre h_2 compared to the geological age, the trapped charge population in it decays and it reaches to a small level, schematically indicated as 'Low'.

(b) Sunbleaching (Zero age sediment).

The pre-depositional sun exposure bleaches the signal from h_1, h_2 and h_3 bringing their level to low value. However, the charge transfer during the photo bleaching from h_3 to h_2 builds up the signal in h_2. Since, before photobleaching the reservoir trap h_3 is at its natural saturation limit, the charge transfer would also be optimum and hence the centre h_2 attains a higher value (shown by 'high'). Since the sensitivity depends on the concentration of recombination centres, the higher charge in h_2 results in enhancement of sensitivity or in other words, the zero age sediment would show a higher sensitivity.

(c) Old Sediment

Subsequent to burial, the centre h_2 undergoes thermal relaxation of its charges and accordingly the sample shows decay in its sensitivity. Beyond the age of 10^5a, the sensitivity becomes low and the mineral acquires a constant

sensitivity due to the effective growth of signal taking place only in the h_1 centre.

(d) Laboratory Zeroing

The laboratory zeroing does not affect the sensitivity of zero age sediment as it is already under the sunlight while being collected, whereas in older sample since the centre h_3 has a low population compared to the mineral before weathering, the sunbleaching causes a marginal increase in the population of the centre h_2 (shown by Low +). This is in agreement with the observation of constant value in sensitivity under multiple sun-bleaching experiments.

(e) At high laboratory irradiations

At high laboratory doses, all the centres reach their saturation values (because of non-availability of time for charge relaxation) and is indicated by 'High' in all the three 'boxes'.

(f) Zeroing

Since the centre h_3 is at its saturation limit, the sun exposure causes h_2 to attain its optimum value which is the case similar to the zero age sample.

The scenario thus explains all the experimental observations. However, any increase in sensitivity due to creation of defects by the dose rate effect is not considered.

The framework also explains the difference in sensitivity in photobleached (regenerated growth curve) and additive dosed samples. The regenerated sensitivity is higher due to the dose dependent phototransfer of charges from h_3 to h_2. The present framework thus suggests that age underestimation should occur in both the methods. A first order correction in TL ages can be made by multiplying the natural TL level L_N (or the corresponding paleodose P) by a factor representing the fractional loss of sensitivity during the geological storage and re-estimating the regenerated TL age for the corrected L_N. In doing so, it is intrinsically assumed that TL properties of all samples along the depth for a given sediment column is identical. The essential requirement for this new method is the requirement of zero age sample which fixes the value of initial TL response for sample with unfaded signal. The method would also assume that the sample received a photobleaching of its geological TL only at the time of deposition. In cases of multiply reworked sample the present prescription would provide an upper estimate to the age. The corrected ages for some of the loess samples by this new method are compared with the expected ages in Fig.4.11 and 4.12.

4.8. Summary

In the literature, several explanations can be found for explaining the observed age underestimation in TL dating. But, most of these either lacked experimental support or were stated without a firm physical basis. Based on four systematic experiments we proposed a framework which explains age underestimation in a self consistent manner without violating the theoretically

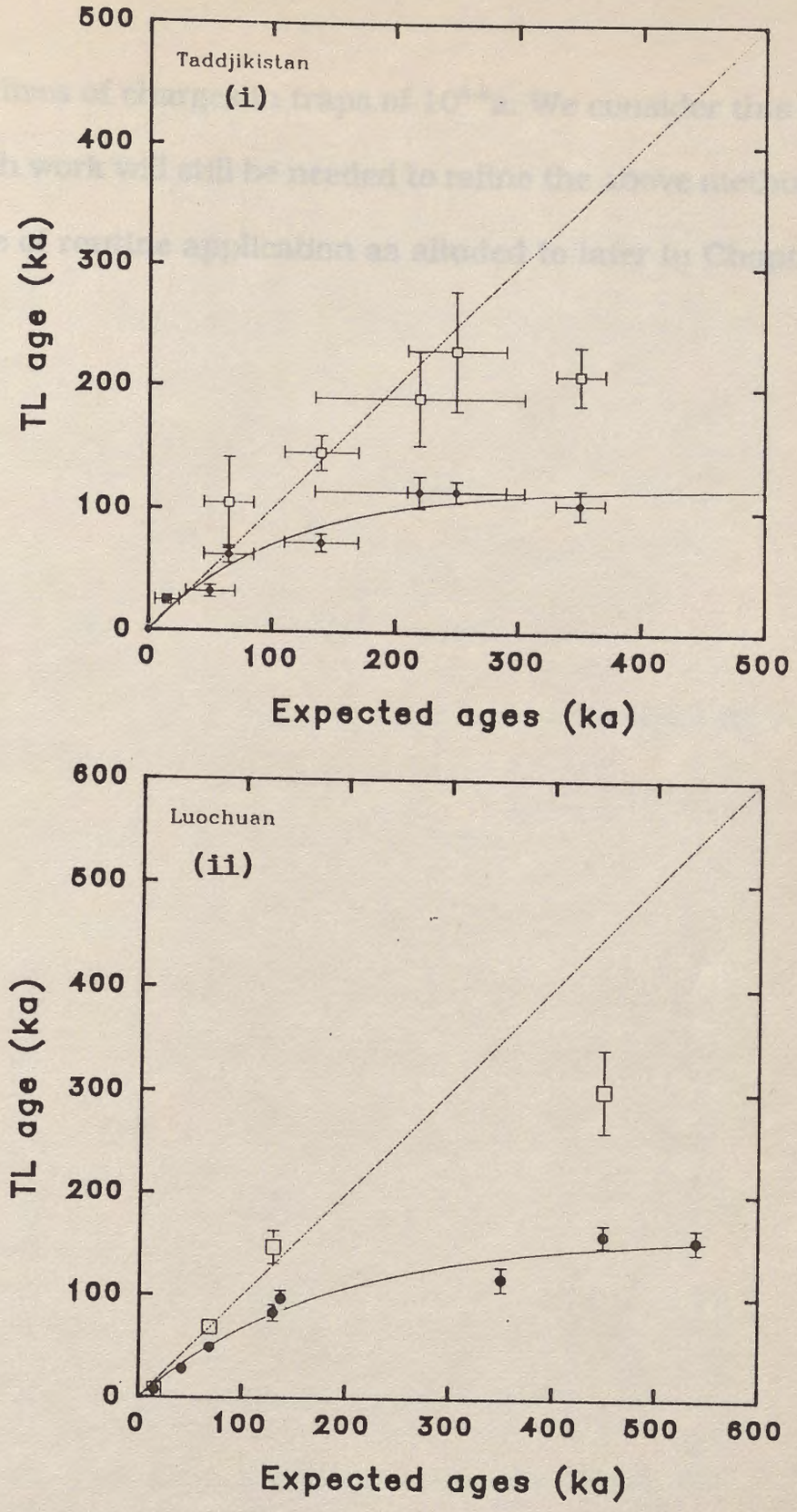


Fig. 4.11. Comparison of "corrected" TL ages with expected ages. The uncorrected ages are also provided to indicate the extent of sensitivity effect (i) for Tadjikistan and (ii) for Luochuan, China.

estimated mean lives of charges in traps of 10^{8-9}a. We consider this as a first attempt and much work will still be needed to refine the above methodology to bring it to a stage of routine application as alluded to later in Chapter 6.

Chapter 5

Infrared Stimulated Luminescence Dating

5.1. Introduction

The basic premise of TL dating of sediments is the photobleaching of geological TL of constituent minerals to a small residual value (L_o) during weathering and transport. On deposition, TL level builds up over and above L_o to a value L_d such that the age is given by the ratio of the difference in radiation dose corresponding to (L_d-L_o) to the annual dose rate (i.e. rate of TL induction). Thus, estimation of L_o is a crucial component of luminescence dating of sediments. The presence of L_o implicitly signifies that the TL signal comprises two components (1) optically bleachable, and (2) optically

unbleachable (L_o) (Wintle and Huntley, 1980; Singhvi et.al., 1982). Huntley et al. (1985) provided the concept of optical stimulation of luminescence as opposed to thermal stimulation which implied that only the optically sensitive traps are sampled. A successful application of this concept was demonstrated by Huntley et al. (1985) where green light at 514.6 nm from an Argon ion laser was used to excite luminescence in sediment samples and the emitted luminescence was observed in the blue UV region. The emitted luminescence exhibits a decay with illumination time and is called as shine down curve. The intensity at any point is dependent on the dose and consequently a growth curve based on integrated luminescence intensity at various time intervals is constructed to obtain an age. With the absence of heating and the stimulation being optical, this method (now termed as optical dating) has provided several advantages over conventional TL dating of sediments. These are;

(1) Avoidance of need of a strict control of the inertness of the oven atmosphere as no heating is involved,

(2) Elimination of processes such as thermal quenching,

(3) No interference from black body radiation. This fact additionally in principle allows a probing of deeper traps that are otherwise inaccessible due to interference from black body radiation and thermal quenching effect,

(4) Applicability to minerals, organic compounds and polymers that change phase on heating in TL.

In a comparison of OSL with TL bleaching characteristics, it was seen that with OSL, the zeroing of signal occurs at a much faster rate (Godfrey-

Smith et al., 1988). Thus for example, whereas it typically takes a few hours to reduce a TL signal to 20% of its original level, for OSL only ~20 seconds or less are needed to achieve the same reduction. This implies that even for cases such as fluvially transported sediments whose TL is only partially bleached, a complete zeroing of the geological OSL can be reasonably assumed. However, these advantages must be weighed against the fact that no information can be deduced on the stability of the signal. Thus for example, in TL the glow curve temperature generally provides a measure of the stability of the luminescence signal, no such information is available from a shine down curve. Godfrey-Smith et al. (1988) suggested two possible avenues for examining the stability of OSL signals. These are (1) a preheat of sample after irradiation to remove the unstable components and (2) stimulation by a range of wavelengths with increasing photon energy. The former is used more routinely though a debate exists on the effects of preheat on intertrap change transfer (Stokes, 1994; Roberts et al., 1994).

An interesting experiment on thermally assisted optical bleaching was reported by Hutt et al (1988). It was demonstrated that in the stimulation of K-feldspar with varying stimulation energies ranging from 1.2 eV to 2.4 eV two resonance peaks at 1.43 eV and 1.33 eV are seen (Fig.5.1a). The resonance peak at 1.43 eV appeared especially enigmatic as the trap depth energy of 1.55 eV was higher compared to the excitation wavelength 1.4 eV. It is now reasonably well established that the IR stimulation of luminescence (IRSL) proceeds in two steps (Fig. 5.1b), (1) infrared excitation to a metastable state, and (2) further excitation into the conduction band through the lattice energy

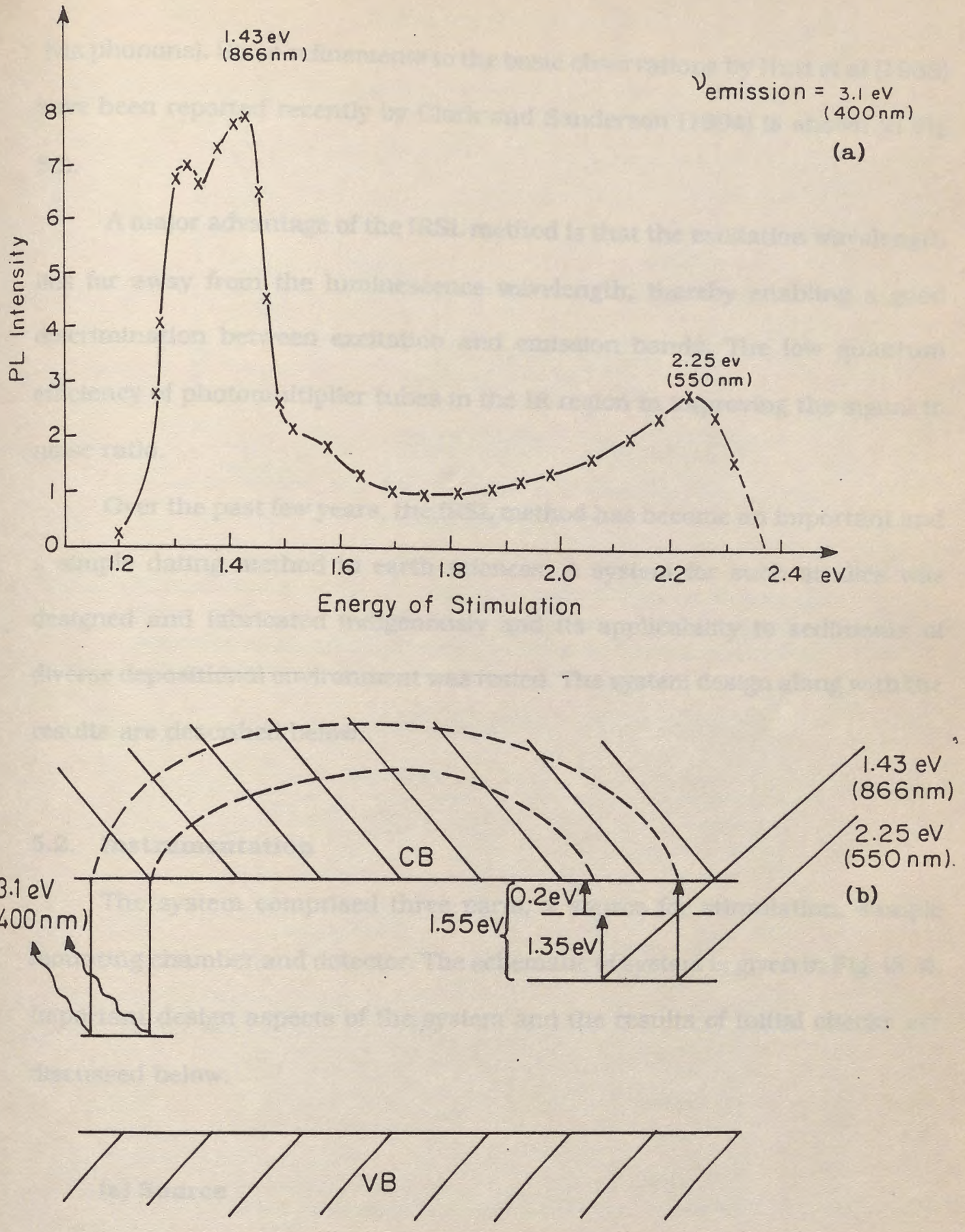


Fig. 5.1 (a) Stimulated luminescence intensity with excitation wavelength. The resonance at 1.43 eV is used for IRSL dating.

(b) Schematic band structure energy diagram of IRSL process (after Hutt et al. 1988, Hutt and Jaek 1989).

(via phonons). Some refinements to the basic observations by Hutt et al (1988) have been reported recently by Clark and Sanderson (1994) is shown in Fig 5.2.

A major advantage of the IRSL method is that the excitation wavelength lies far away from the luminescence wavelength, thereby enabling a good discrimination between excitation and emission bands. The low quantum efficiency of photomultiplier tubes in the IR region in improving the signal to noise ratio.

Over the past few years, the IRSL method has become an important and a simple dating method in earth sciences. A system for such studies was designed and fabricated indigenously and its applicability to sediments of diverse depositional environment was tested. The system design along with the results are described below.

5.2. Instrumentation

The system comprised three parts, a source for stimulation, sample mounting chamber and detector. The schematic of system is given in Fig. (5.3). Important design aspects of the system and the results of initial checks are discussed below.

(a) Source

The source was made by connecting fourteen GaAs high power IR LED's in series. These diodes emit light at 880±80nm that matches well with the stimulation spectrum of K-feldspar (Fig.5.4). The source output was

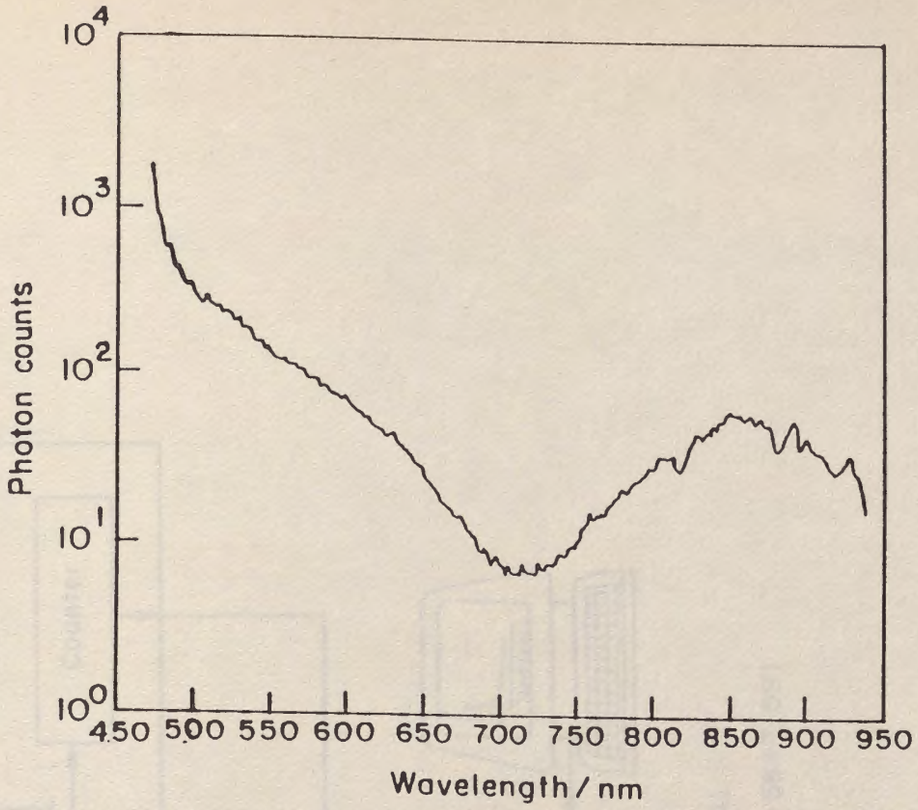


Fig. 5.2(a) Stimulation spectra of K-feldspar with excitation wavelength. The curve differs from Hutt et.al.(1988), in that the luminescence intensity in green blue region is substantially higher (after Clark and Sanderson, 1994)

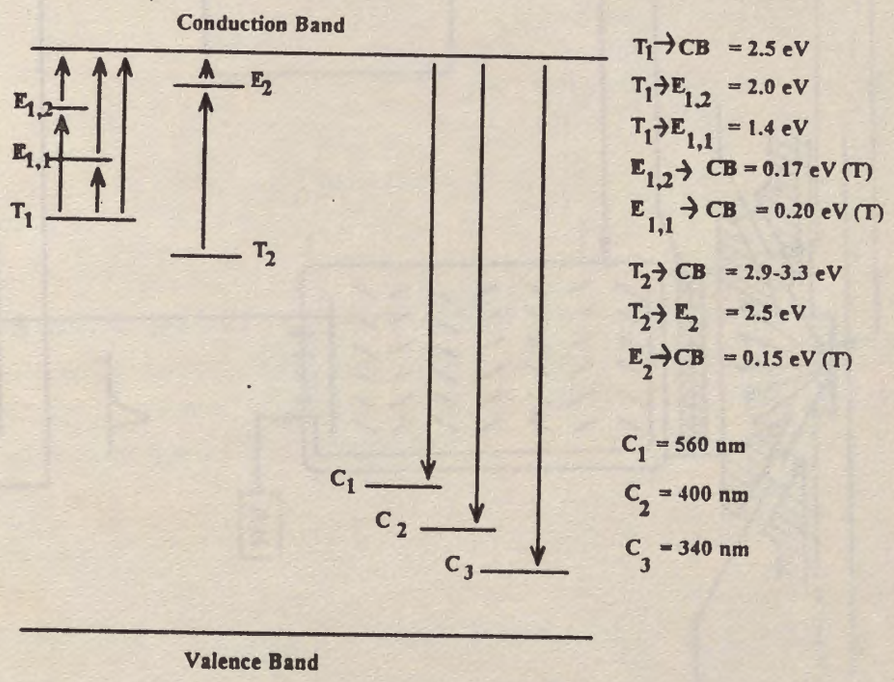


Fig. 5.2(b) IRSL energy levelmodel (after Clark and Sanderson, 1994).

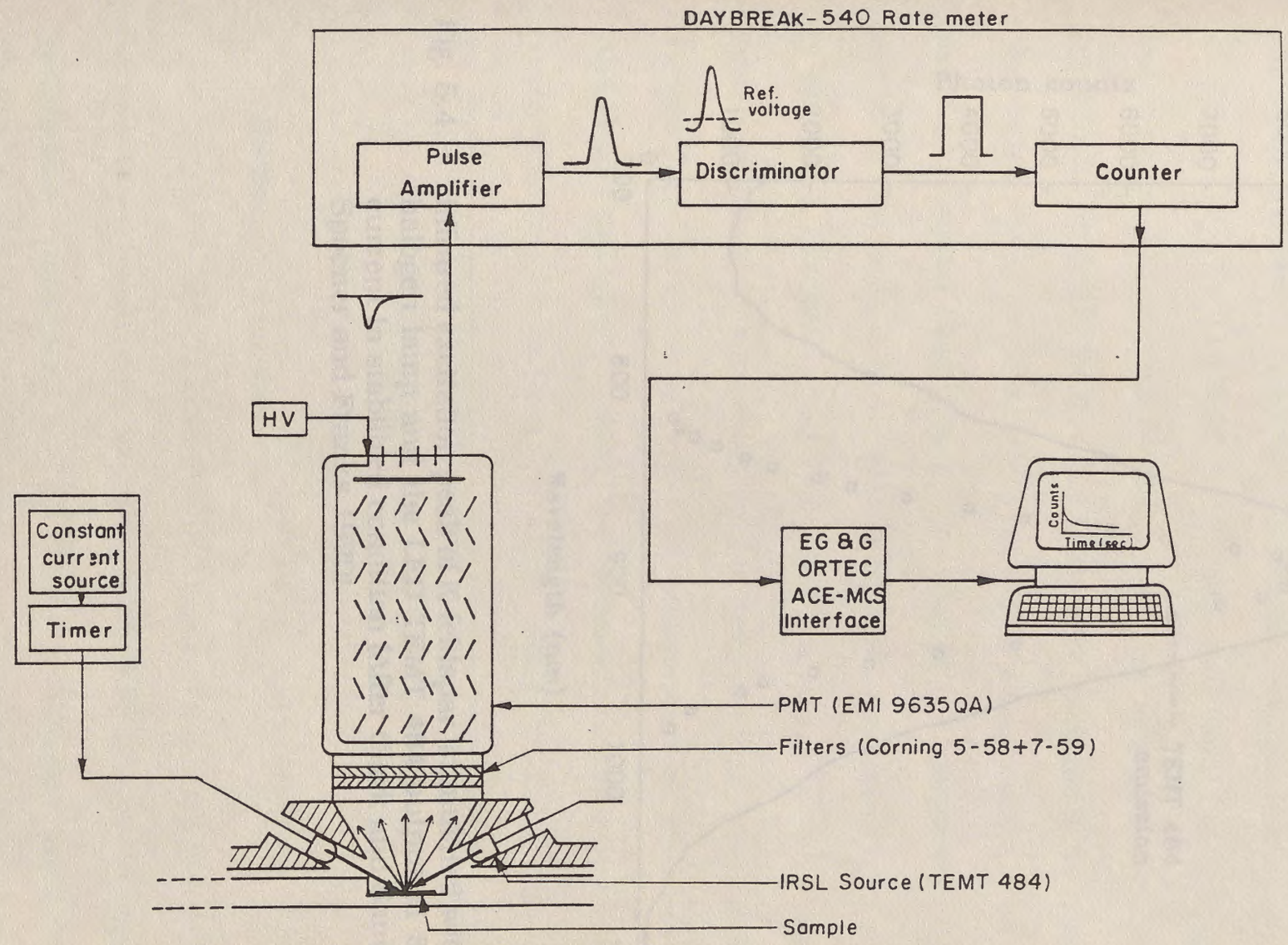


Fig. 5.3. Schematic diagram of IRSL measurement system

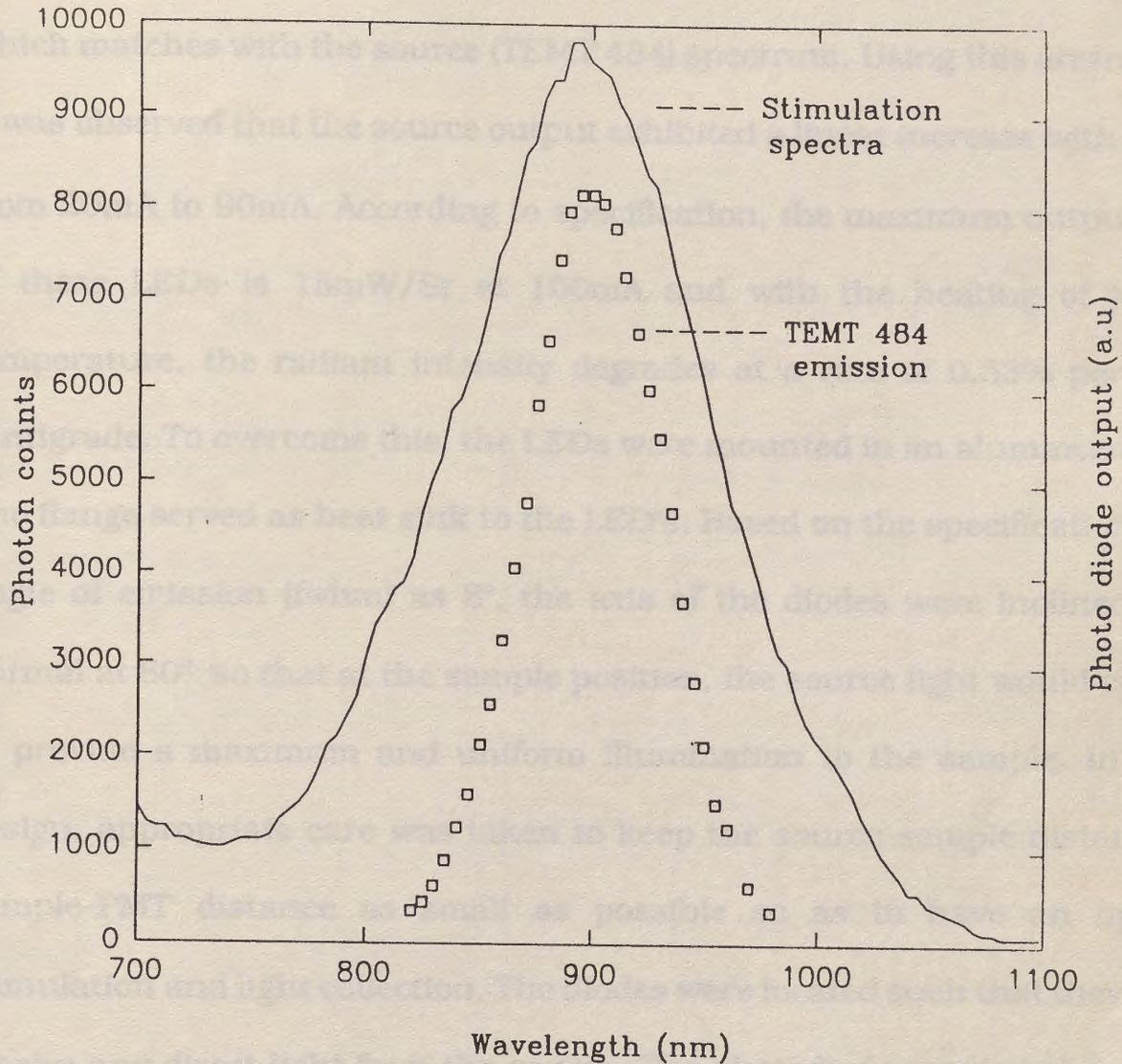


Fig. 5.4. Infrared excitation peak of K-feldspar, stimulated with a tungsten halogen lamp and the LED TEMT 484 output at 50mA supply current in stabilized condition (After Clark and Sanderson 1994; Spooner and Franks 1990)

controlled by programmable constant current DC supply. The source intensity was monitored using a photodiode, BPX 65 (RS 304-346), the response of which matches with the source (TEMT 484) spectrum. Using this arrangement it was observed that the source output exhibited a linear increase with current from 20mA to 90mA. According to specification, the maximum output power of these LEDs is 15mW/Sr at 100mA and with the heating of junction temperature, the radiant intensity degrades at a rate of 0.53% per degree centigrade. To overcome this, the LEDs were mounted in an aluminum flange. The flange served as heat sink to the LED's. Based on the specification of half angle of emission (fwhm) as 8°, the axis of the diodes were inclined to the normal at 60° so that at the sample position, the source light would converge to provide a maximum and uniform illumination to the sample. In source design, appropriate care was taken to keep the source-sample distance and sample-PMT distance as small as possible so as to have an optimum stimulation and light collection. The diodes were located such that they did not receive any direct light from the source. The photodiode reading showed that the fluctuations in the source intensity with time was less than 5% and on rapid *on and off*, cycling the reproducibility was 99% (Fig.5.5).

(b) Sample chamber

The sample chamber was made of a revolving metal disc enclosed between two metal flanges, as shown in Fig.(5.6). The revolving plate contained equidistant sample slots for disc mounting. The distance between two slots was adjusted so as to have a maximum number of slots on a given

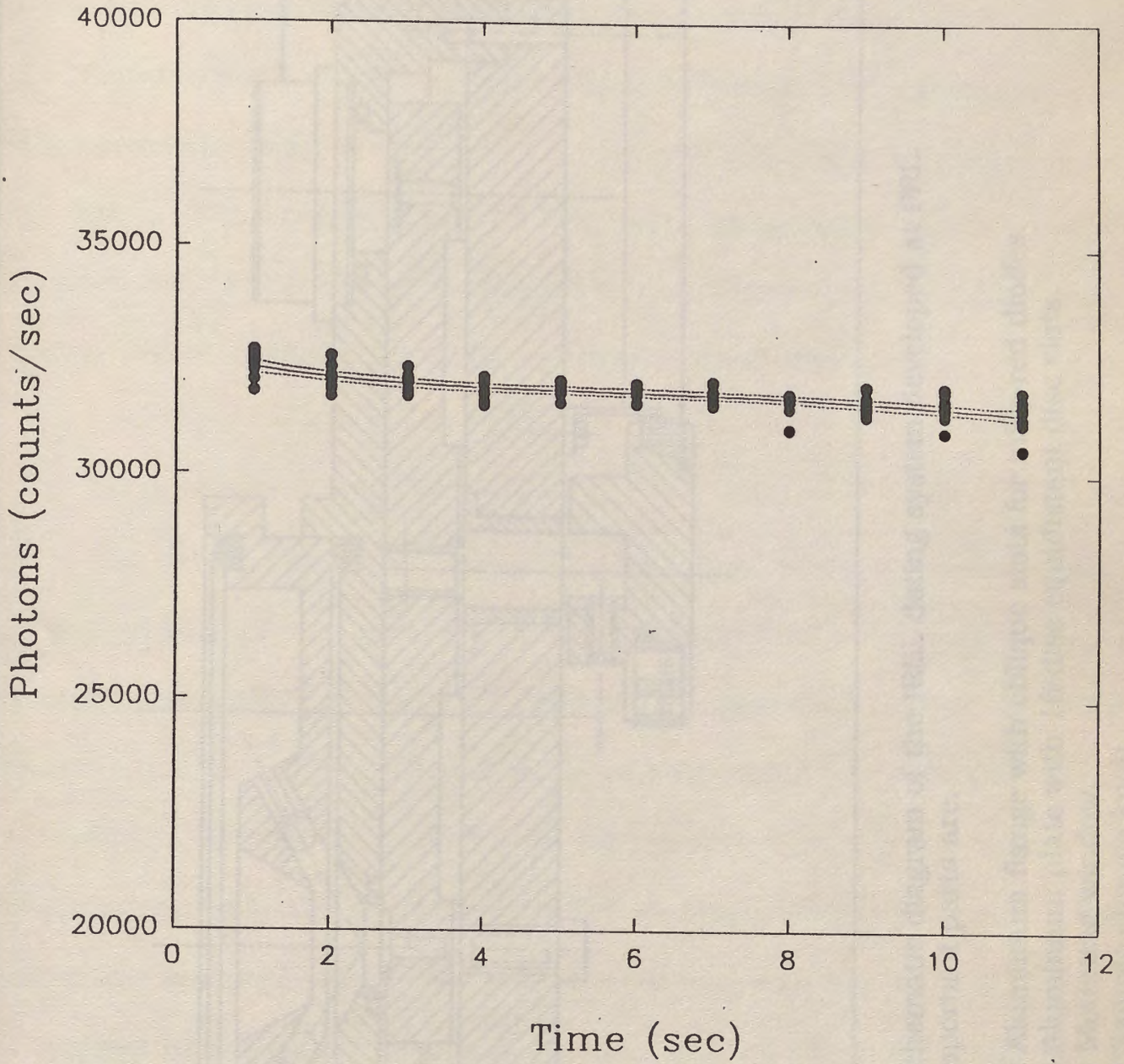


Fig 5.5. **Reproducibility of infrared source radiance under repetitive measurements.**

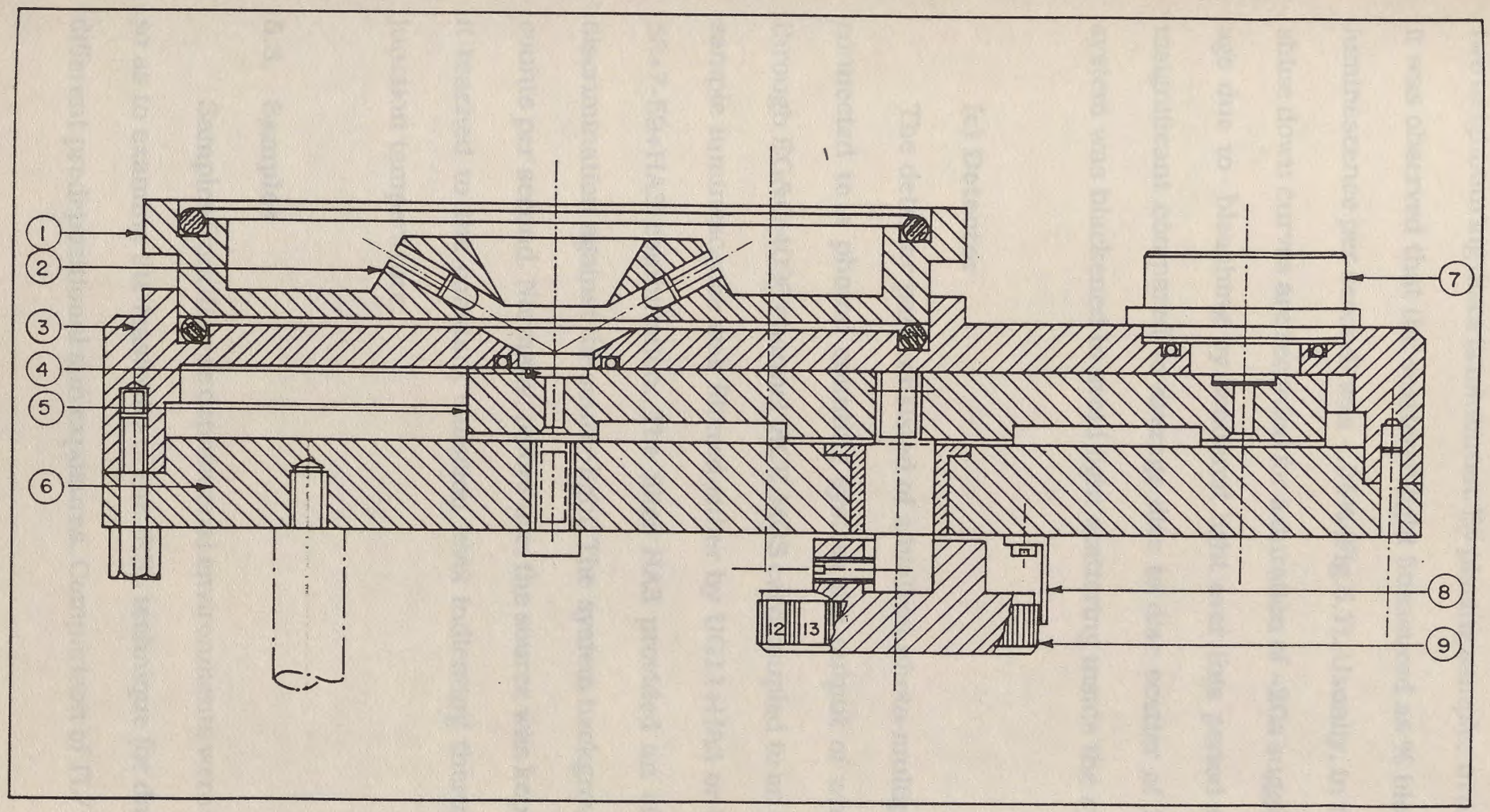


Fig. 5.6. Schematic diagram of the IRSL dating system developed at PRL. Important parts are,

1) Aluminium flange with oblique slots for infra-red diodes.
2) Aluminium plate with 16 disc equidistant disc slots.
3) Mounting window.
4) Sample change knob

circumference and at the same time to ensure that the cross talk between any two neighbouring discs is minimum. By placing samples in neighbouring discs, it was observed that the scattered light (measured as % bleaching of samples luminescence per second) was <.04% (Fig.5.7). Usually, in the dating studies, shine down curves are recorded for a duration of ~20s suggesting that error in age due to bleaching by scattered light over this period is <0.1% which is insignificant compared to average disc to disc scatter of 2-5%. The entire system was blackened to avoid light scattering inside the system.

(c) Detector

The detector part consisted of a bialkali photo-multiplier tube 9635QA connected to a photon counting system the output of which was recorded through EG&G 4096 channel ACE-MCS card coupled to an IBM/PC-486. The sample luminescence was filtered either by UG11+HA3 or by the Corning 5-58+7-59+HA3 combination. The filter HA3 provided an effective means for discrimination against the source light. The system background was ~100-200 counts per second. Normally, before use, the source was kept on until the time it reached to the constant emission level indicating thermal equilibrium of junction temperature.

5.3. Samples

Samples from diverse depositional environments were selected for dating so as to examine the feasibility of the IRSL technique for dating samples with different predepositional sun exposures. Comparison of TL/^{14}C with IRSL ages

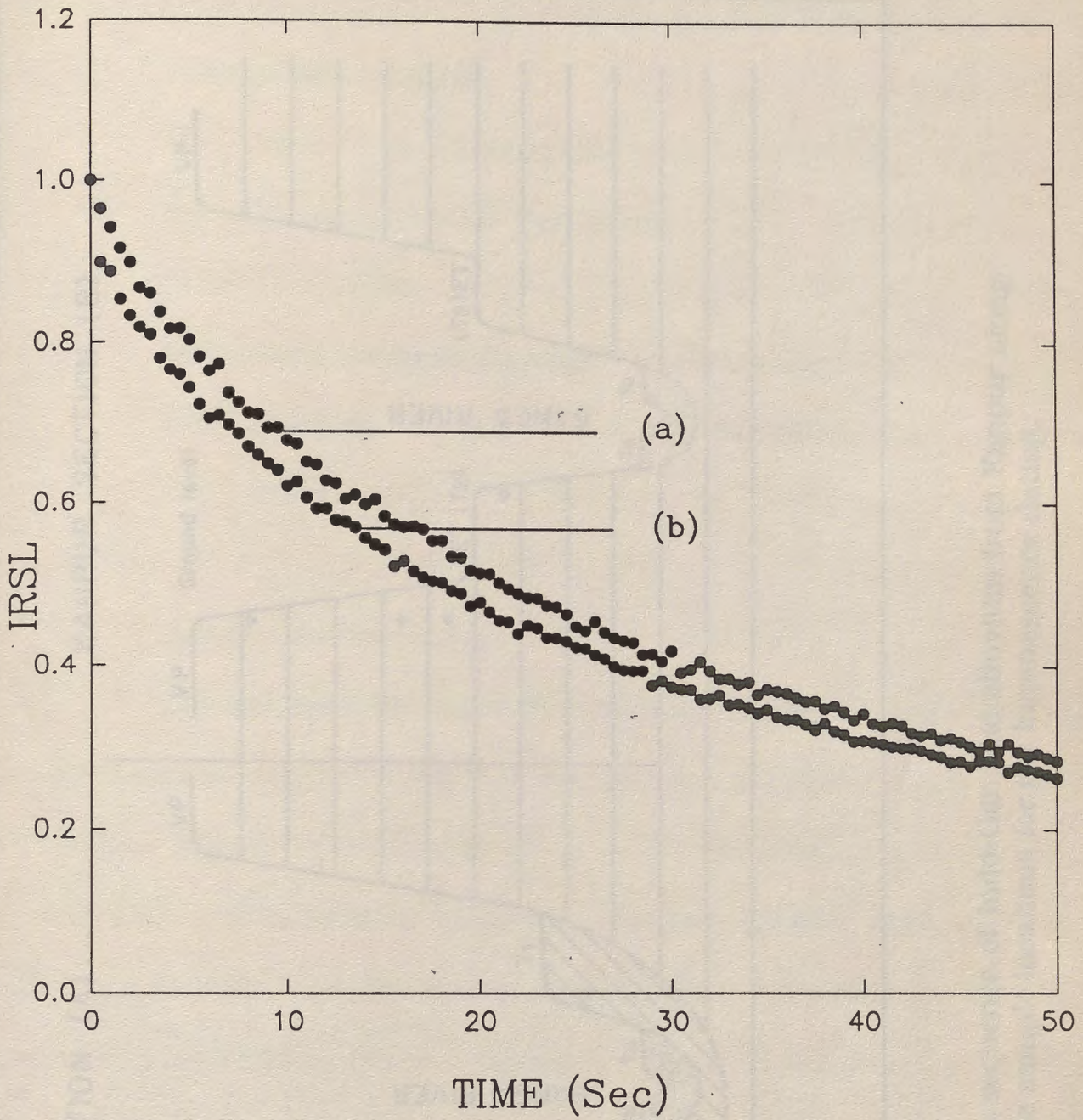


Fig. 5.7. IRSl shine curves (a) disc kept directly under the infrared source (b) disc which is pre-exposed to scattered light for 30 min at a disc slot next to the slot being stimulated. Note that the scattered light caused bleaching of signal by 0.02% in 30min time.

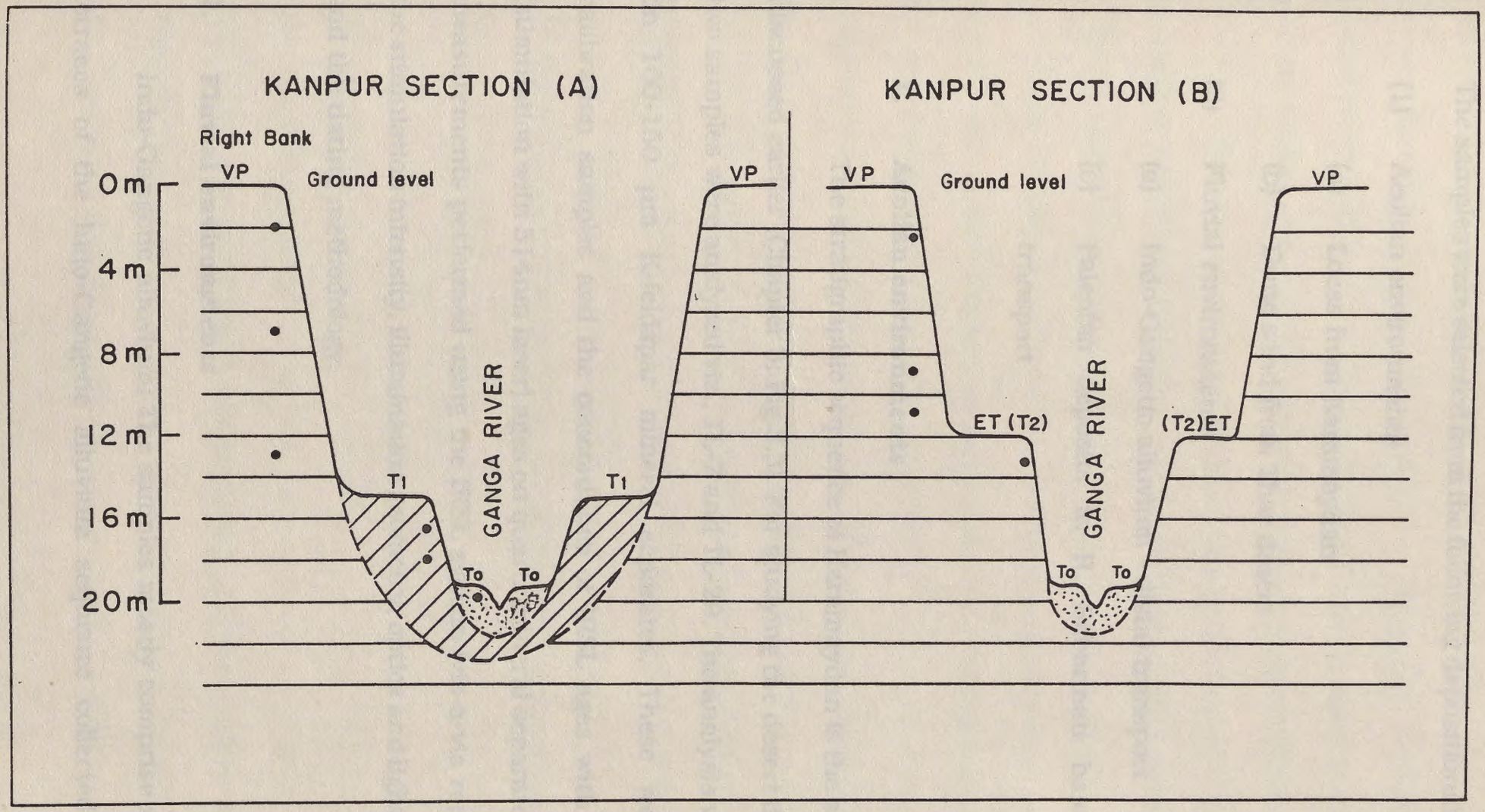


Fig 5.8. Terrace sequence of Indo-Gangetic alluvium from Kanpur along with the sample locations for the luminescence dating.

was also attempted.

The samples were selected from the following depositional environments:

(1) Aeolian environments

(a) Loess from Karamaydan

(b) Dune sand from Thar desert

(2) Fluvial environments

(a) Indo-Gangetic alluvium - distal transport

(b) Paleofan deposits in R. Sabarmati basin - proximal transport

1. Aeolian environments

The stratigraphic sequence at Karamaydan is the same as the one discussed earlier (Chapter 3; Fig.3.3). For studying the desert dune sequence, two samples were analyzed viz., TL-7 and TL-29. The analysis was carried out on 100-150 μm K-feldspar mineral separates. These were essentially calibration samples and the concordance of IRSL ages with TL and GLSL (stimulation with 514nm laser) ages on quartz mineral separates validates the measurements performed using the IRSL system (vis-a-vis reproducibility in the stimulation intensity, illumination geometry, optics and light collection etc.) and the dating methodology.

2. Fluvial environments

Indo-Gangetic alluvium: The samples mostly comprise sands from the terraces of the Indo-Gangetic alluvium sequence collected from various

locations along the downstream of the Ganga plain. A typical terrace sequence with the sample location is shown in the Fig.5.8. These terraces provide an unique opportunity to understand the interplay between Himalayan orogeny/tectonics and the sea level changes. Rajagopalan (1992) used ^{14}C method to date the carbonate nodules embedded in the terrace sediments. These ages provide a baseline for this study. Additionally, to check the lower age limit of IRSL dating technique (i.e., the zeroing of IRSL), a surface sediment of the terrace was also analyzed.

Paleofan deposits: These were sedimentary deposits laid down in the form of colluvial fans during the Quaternary. One such paleofan was sampled at Vijapur near Ahmedabad. These sediments were exposed due to incision by R. Sabarmati. Dating analyses were carried out on samples from red-sand unit and the horizon immediately below in which occurrence of paleolithic stone tools were reported (Zeuner, 1950). Since these deposits fall in the desert margins, they are considered to be important in understanding the climatic variation through time. TL and IRSL chronology obtained from these deposits have helped in identifying and correlating the climatic changes during the past 300ka.

5.4. Analysis

From loess, polymineral fine grain samples were extracted using fine grain technique and from dune sand samples, 90-150 μm K-feldspar was extracted. The luminescence output from the sample discs was normalized by their short shine intensities for 1 second. For dating additive dose method was

used. The unstable component in the luminescence signal generated due to laboratory irradiations was removed by preheating samples at 160°C for 5 hours. This treatment has been found to be an optimum one since no draining of natural IRSL signal occurs. In the detection optics, the filters 5-58+7-59+HA3 were used. The growth curve data were fitted to a linear or a saturating exponential equation. Typical IRSL shine down curve, growth curves and equivalent dose plateaus are shown in the Fig.5.9, 5.10 and 5.11. In the case of Tadjikistan, two samples J7 and J15 were also analyzed using the *slide method* (see Huntley et al., 1993). Table 3.1 and 5.1 provide the radioactivity data and the computed luminescence ages.

5.5. Results and Discussion

The surface sediment of the river terrace from Kanpur provided the IRSL age ~150 years suggesting it to be the lower age limit for the IRSL technique in dating these fluvial deposits. Fig.5.12 shows the correlation between IRSL and other ages (TL, OSL, ^{14}C etc.). The graph shows a good concordance between various techniques. However, in this plot, the ages that were compared with ages on the sediments that are older than 10 ka were dated by TL or OSL method, suggesting a similar underestimation effect in the IRSL ages. This is more explicitly borne out by Fig.5.13 where the IRSL ages obtained on Tadjikistan sequence are compared to the expected ages derived on the basis of correlation of pedocomplexes with interglacial epochs in deep sea oxygen isotope stratigraphy. In order to confirm the universality in the underestimation, a collation IRSL and TL dates was made from the published

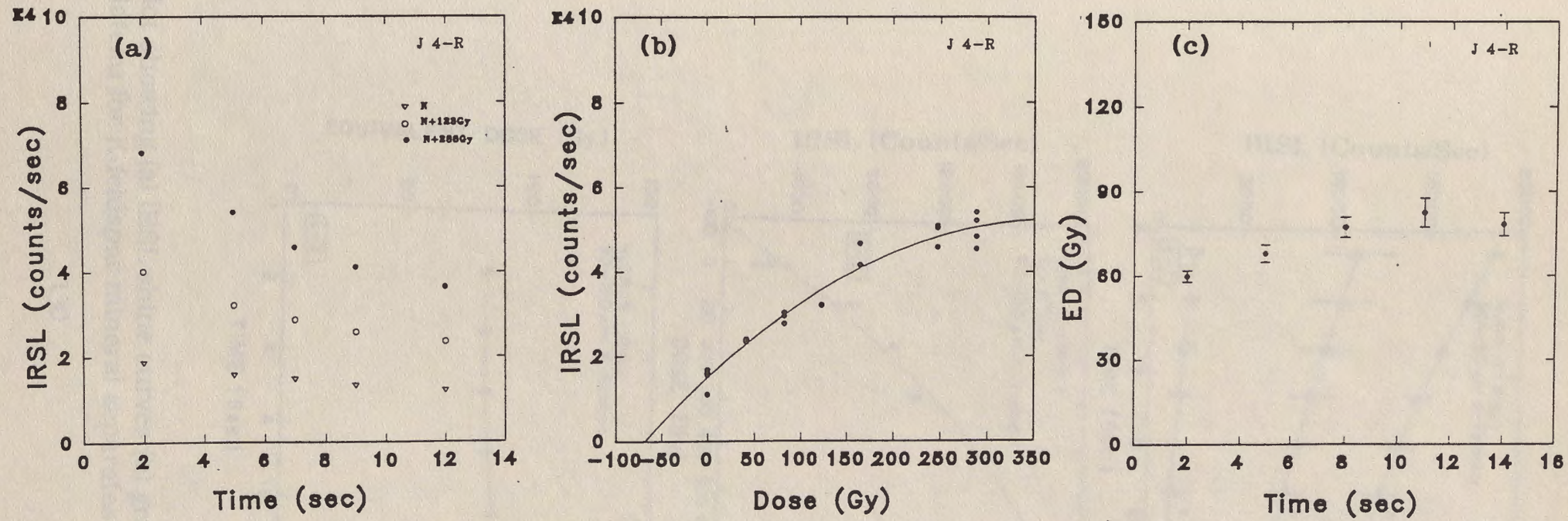


Fig. 5.9. Plot showing (a) IRSL shine curves (b) growth curve and (c) shine plateau for polymineralic loess sample J4 (Tadjikstan).

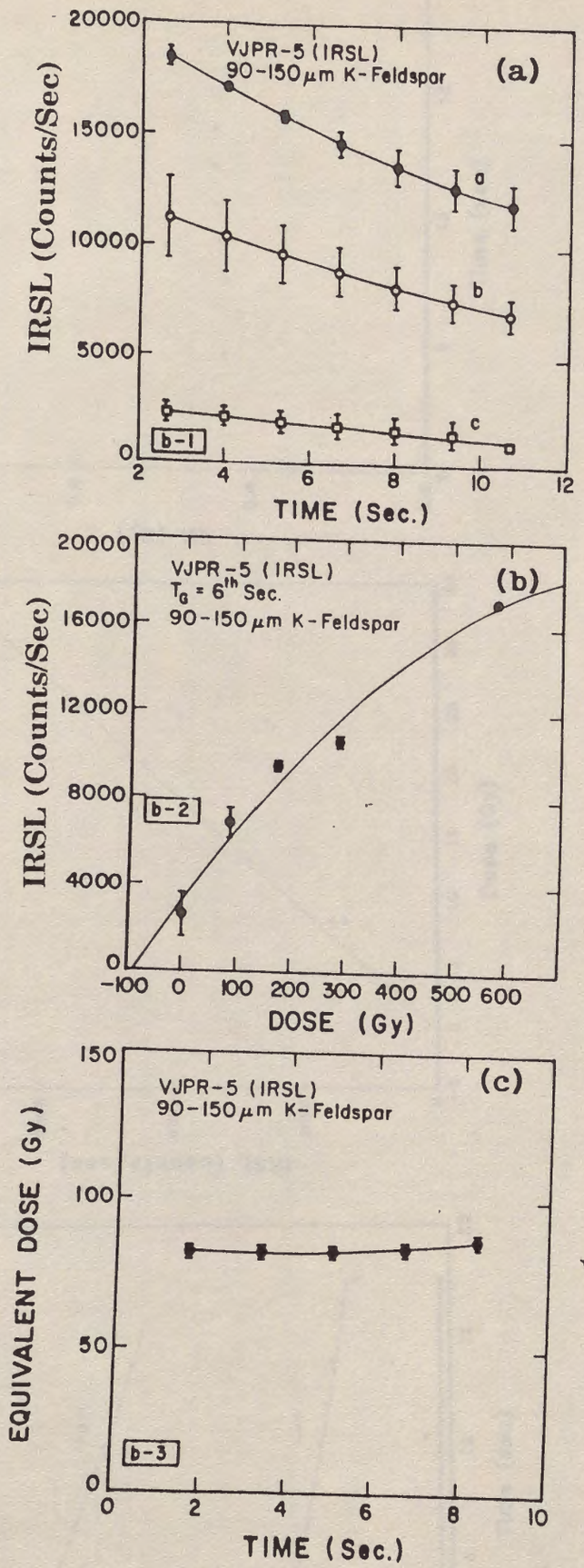


Fig. 5.10. Plot showing (a) IRSL shine curves (b) growth curve and (c) shine plateau for K-feldspar mineral separates for VJPR-5

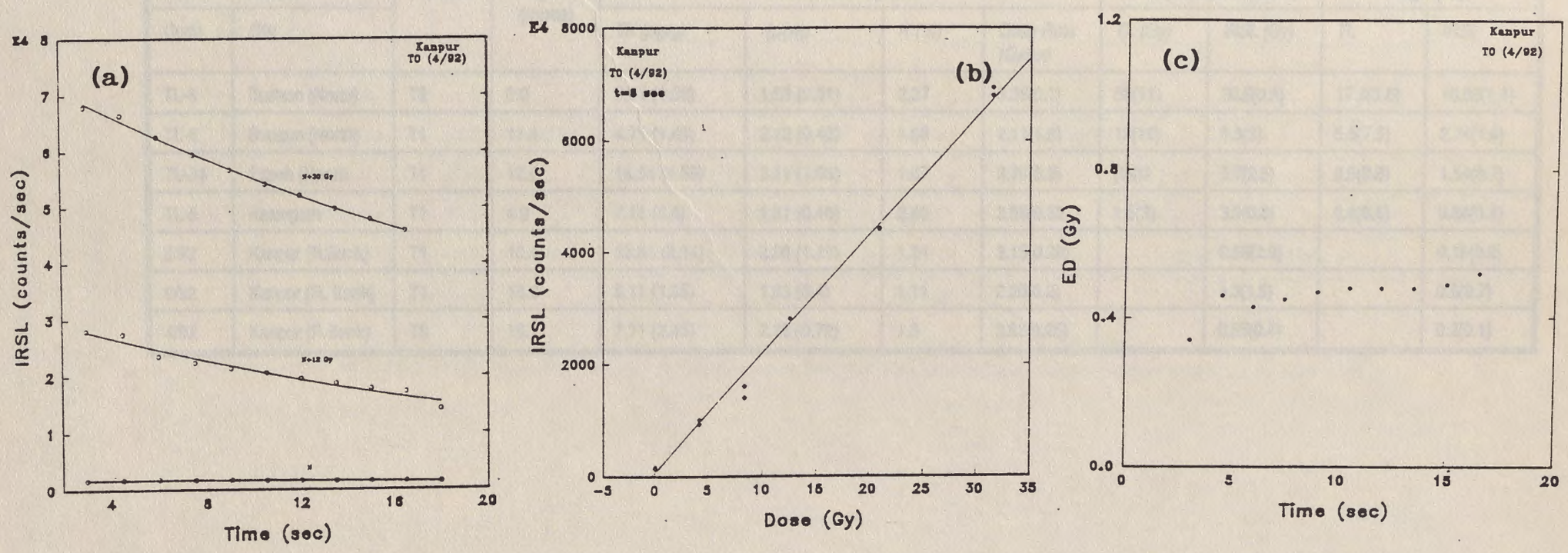


Fig. 5.11. Plot showing (a) IRSL shine curves (b) growth curve and (c) shine plateau for K-feldspar mineral separates for the surface sediment from the Indo-Gangetic alluvium.

Table 5.2 TL and IRSL data of samples for the Gangetic alluvium

Sample		Terrace	Depth (mbas)	Radioactivity data				Equivalent Dose		Age (ka)	
Code	*Site*			*Th (µg/g)*	*(µg/g)*	*K (%)*	*Dose Rate (Gy/ka)*	*TL (Gy)*	*IRSL (Gy)*	*TL*	*IRSL*
TL-8	Budaun (North)	T2	8.0	5.51 (1.06)	1.63 (0.31)	2.37	3.36(0.3)	58(11)	36.5(0.8)	17.3(3.6)	10.86(1.1)
TL-6	Budaun (North)	T1	11.4	4.71 (1.49)	2.12 (0.43)	1.08	2.11(1.9)	12(16)	5.8(3)	5.5(7.5)	2.74(1.4)
TL-34	Etawh (North)	T1	12.9	14.54 (4.56)	3.11 (1.06)	1.67	3.70(0.3)	(14)3	5.7(2.5)	3.8(0.8)	1.54(0.7)
TL-5	Azamgarh	T1	4.0	7.13 (1.6)	1.81 (0.46)	2.40	3.56(0.32	1.5(3)	3.0(0.8)	0.4(0.8)	0.84(0.1)
5/92	Kanpur (R.Bank)	T1	16.4	13.84 (3.94)	2.86 (1.15)	1.24	3.15(0.28)		0.58(2.9)		0.18(0.9)
6/92	Kanpur (R. Bank)	T1	18.0	6.11 (1.35)	1.93 (0.4)	1.11	2.20(0.2)		1.3(1.5)		0.6(0.7)
4/92	Kanpur (R.Bank)	T0	19.7	7.11 (2.45)	2.13 (0.72)	1.3	2.82(0.25)		0.55(0.4)		0.2(0.1)

Table 5.1 Luminescence dating results of paleofan deposits of Sabarmati River basin

Sample Code	Mineral	Method	$D(I_d)$ (Gy)	U(µg/g)	Th (µg/g)	K(%)	Dose Rate** (Gy/ka)	Age (ka)	Age Wt. mean (ka)
VJPR5	Quartz	TL/R-β	79(16)	1.16(0.04)	3.81(0.13)	1.32(0.03)	2.03(0.31)	39.0(8.0)	39.0(4.0)
	Feldspar	TL/R-β	136(24)	1.16(0.04)	3.81(0.13)	1.32(0.03)#	2.38(0.32)	57.2(12.7)	
	Feldspar	IRSL (Additive)	64(2)	1.16(0.04)	3.81(0.13)	1.32(0.03)#	2.38(0.3)	36.7(5.2)	
VJPR4	Quartz	TL/Rβ	218(16)	2.98(0.05)	9.82(0.17)	3.0(0.07)	5.16(0.65)	42.0(12.0)	58.0(5.2)
	Feldspar	TL/R-β	415(30)	2.98(0.05)	9.82(0.17)	3.0(0.07)#	5.5(0.65)	75.3(10.4)	
	Feldspar	IRSL (Additive)	307(25)	2.98(0.05)	9.82(0.17)	3.0(0.07)#	5.5(0.65)	55.8(8.0)	

\+ The numbers in parenthesis provide errors of each measurement. Thus 1.32(0.03) in 1.32 ± 0.03.

++ In dose-rate computation U and Th concentrations were estimated using Zns (Ag)alphs counting and K% was estimated using AA and/or NaI (Tl) spectrometry. 5% average water content was assumed and cosmic ray dose rate were calculated using Prescott & Stephan (1982)

\# Internal K assumed as 10%

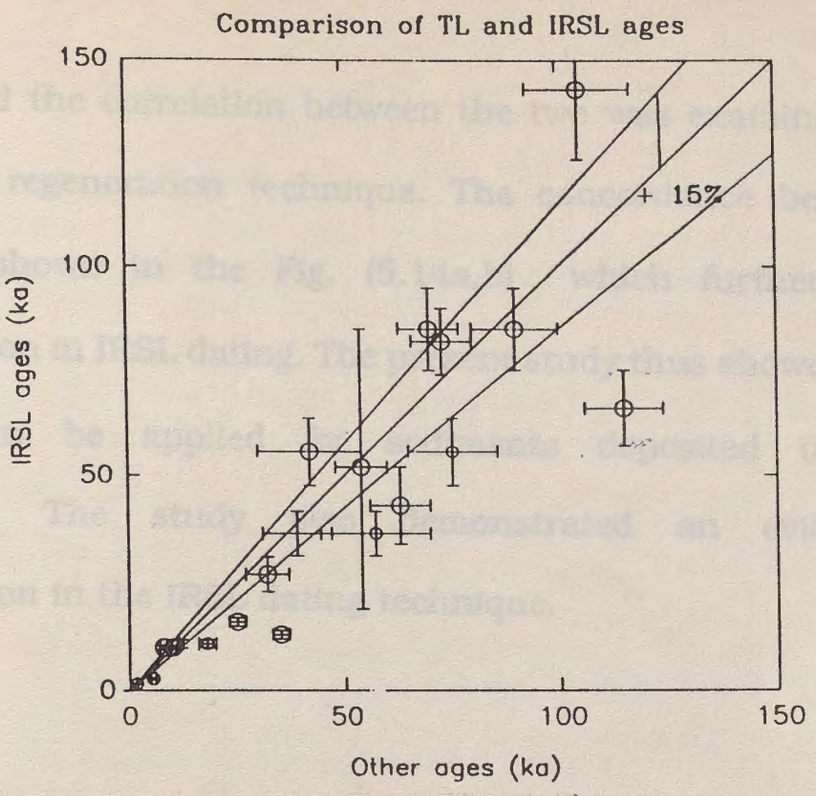


Fig. 5.12 Comparison of IRSL ages on K-feldspar with other ages obtained by TL (quartz, feldspar and polymineral), OSL (quartz) and radiocarbon.

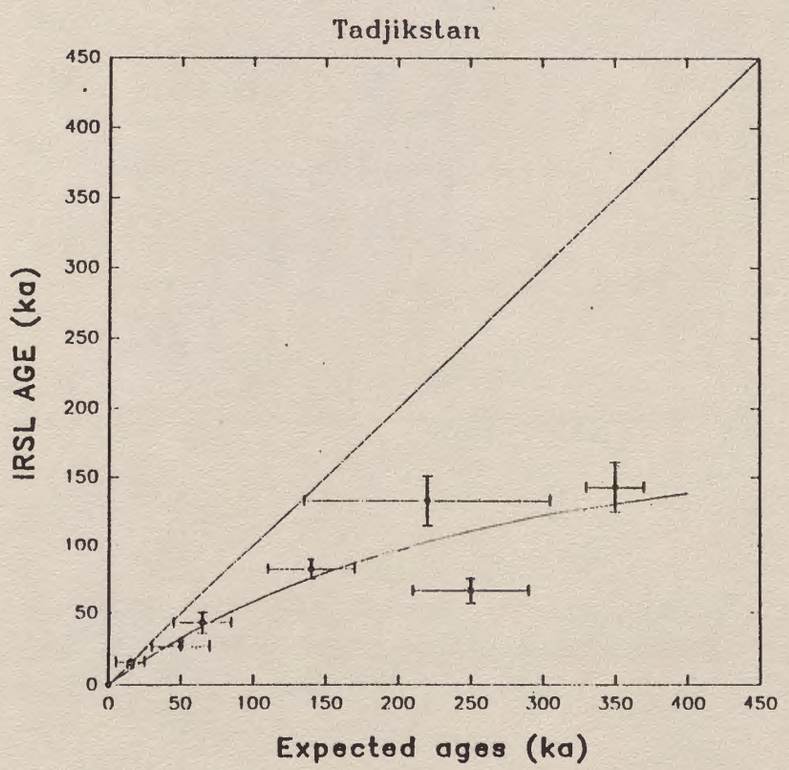


Fig 5.13. Correlation of IRSL ages (this study) with the oxygen isotope stratigraphy as given by (Bronger et.al., 1995).

literature and the correlation between the two was examined for both the additive and regeneration technique. The concordance between the two methods is shown in the Fig. (5.14a,b) which further confirms the underestimation in IRSL dating. The present study thus showed that the IRSL technique can be applied for sediments deposited under different environments. The study also demonstrated an evidence of age underestimation in the IRSL dating technique.

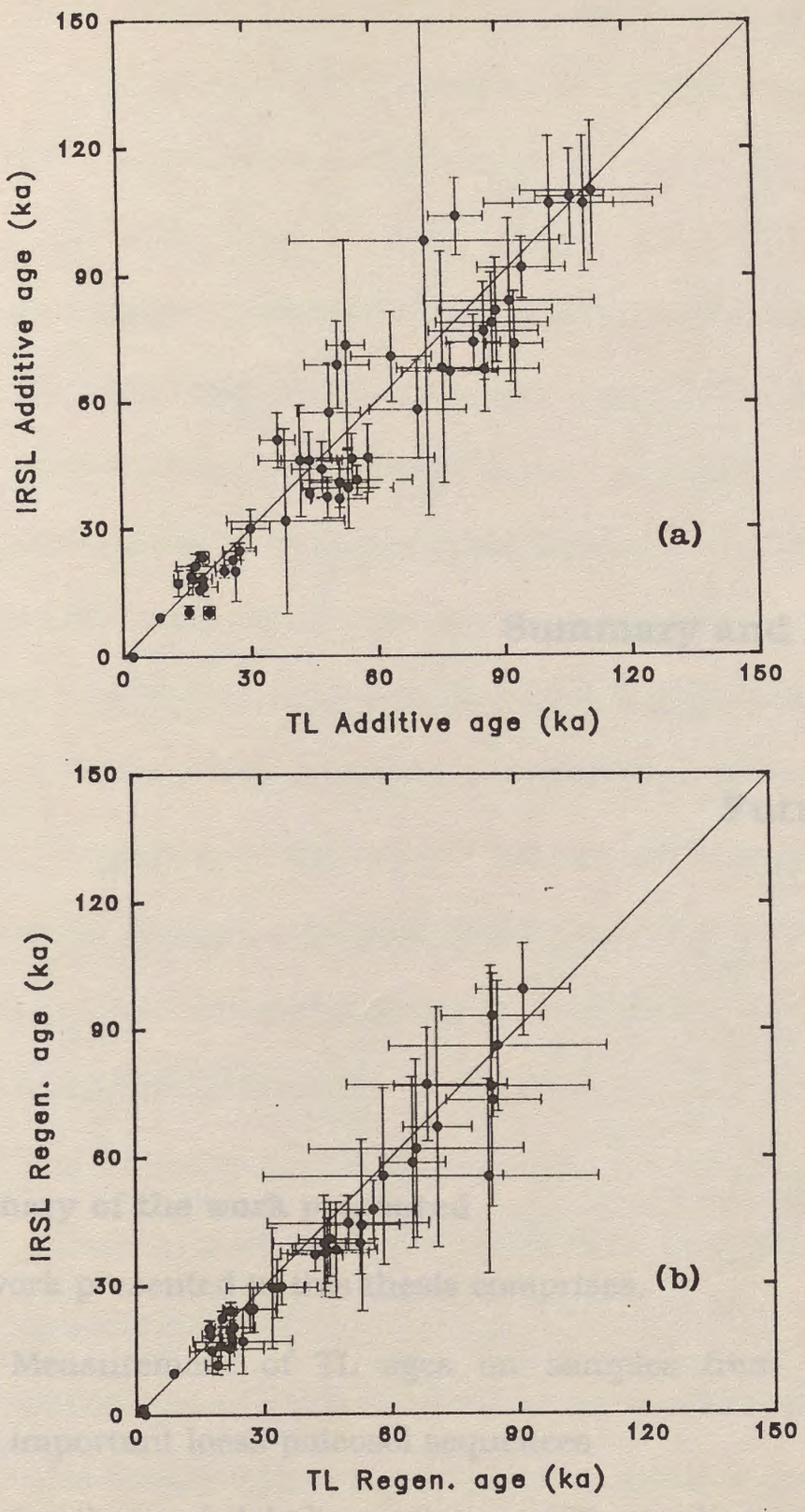


Fig 5.14 Plot showing the comparison of available IRSL and TL ages obtained from various sedimentary deposits (a) regeneration and (b) additive

Chapter 6

Summary and Perspectives for Future Research

6.1. Summary of the work presented

The work presented in this thesis comprises,

(1) Measurement of TL ages on samples from several globally important loess-paleosol sequences

(2) Synthesis of global compilation of TL ages in a probability density approach

(3) Methodological studies on the physical processes leading to the underestimation of TL ages beyond 100 ka and development of

(i) a band-structure based scenario that could explain the observed underestimation of TL ages and

(ii) an experimental procedure to correct the underestimated age.

(4) Development of Infrared Stimulated Luminescence dating system, its application to samples from different depositional environments including loess paleosol sequences and demonstration of TL like underestimation of IRSL ages.

Detailed chronology on five globally important loess-paleosol sequences viz. Luochuan (China), Karmaydan (Tadijikstan), Dolni -Vestonice. (The Czech Republic) and Paks - Mende (Hungary) was provided. Of these, the dating of loess paleosol sequences at Karmaydan was the first ever attempt to provide luminescence chronology both by TL and by IRSL methods. The studies at other sequences was contemporary to other groups. The study provided several important results such as,

(1) The identification of interglacial soils in each region thereby providing a chronological basis for a regional correlation of climatic events.

(2) Chronological evidence of loess accumulation being episodic as TL ages from long sequences always showed a stepwise behaviour with depth indicating that conditions conducive for loess production, transport and eventual deposition were reached only for very limited periods of time. This observation has significant implications for global land-sea correlations and for paleoclimatic

deductions.

(3) The establishment of the fact that the correlation of pedocomplexes with the interglacials in the deep-sea oxygen isotopic records appears reasonable. However, any chronological extrapolation on loess chronology based on this correlation may not be rigorously correct.

(4) The data also showed a general synchronicity of paleosol chronologies in China and Tadijikstan and of Dolni-Vestonice with Kashmir. This reemphasises the truly Global nature of loess records.

(5) The comparison of TL ages with deep sea oxygen isotope chronology indicates a limiting behaviour of TL ages beyond ~100 ka. The present study provided results similar to that of Debenham (1985) on West European loess-paleosol sequences. This was an anomalous observation since on the basis of dose-rate, saturation dose and kinetics of trapped charges from K-feldspars, the limiting ages should have occurred at time >500 ka.

In a synthesis of all the ~700 TL ages reported so far in the literature, the loess accumulation episodes examined using a probability density formulation provided results that are in sharp contrast to conventional concept of genesis of loess-paleosol sequences. In this synthesis, a gaussian was defined for each age with its width taken as 1σ or 2σ, σ being the total experimental error (random + systematic, cf. Aitken, 1985). Broadly speaking,

these gaussians were then superimposed on the age (time) axis and with appropriate normalization a probability density curve was constructed for the total data set as also for the regional data sets. All the probability density curves showed sharp peaks around 16-17 ka with smaller epochs at 30 ka and 50 ka. The peak at 16-17 ka was unexpected as conventionally the peak in loess accumulation has been considered to be synchronous with the glacial epochs. Further, the existence of the peak by itself was anomalous as it went against the widely used correlation of loess accumulation record (an episodic record) with that of oxygen isotopic record from deep sea cores (with constant sedimentation rates). Considerations on the mechanism of loess genesis and prerequisites for transport and accumulation suggest that a post-glacial peak in loess accumulation is indeed logical. The present analysis thus offered new insights on the loess accumulation and has provided a caveat in correlation with deep sea records based on wind tunnel studies.

An important aspect of the present thesis was investigation of the physical processes leading to the underestimation of TL ages beyond 100 ka which is unexpected based on the saturation dose level, annual dose rate for loess and the stability of charges in traps being $\geq 10^8$ ka. Several mechanisms which have been proposed to explain the underestimation are the decay of recombination centres, change of TL sensitivity during photo bleaching, presence of transient centres and distribution of activation energies. However, none of these provided a physical mechanism or a basis on which the underestimated TL ages could be corrected. The studies presented in this thesis have helped in formulating a first order scenario based on a series of

experimental observations for the basic physical process that could lead to underestimation of TL ages. These studies also provide a simple experimental basis to measure an age correction factor for each sample. Preliminary results for this approach appear promising. The basic premise in this study was to examine a possible mechanism that could alter the TL sensitivity of a sample - either with age or with laboratory simulation, (i.e. with laboratory dose rate/or photobleaching) and at the same time reconcile with the inferred stability of TL signal from the kinetic studies. For this study, two loess-paleosol sequences in different geographical locations and which provided a long stratigraphical record with some independent estimate on these ages were chosen. TL sensitivity of various samples of different inferred ages were measured under different laboratory simulation conditions of photobleaching and irradiation. It was seen that TL sensitivity of samples decreased with sample age reducing to a ~50% level beyond which no decrease was seen. TL sensitivity increased with laboratory dose but the magnitude of increase reduced with the total dose in the sample. This not only ruled out the presence of any dose rate effect but at the same time suggested the presence of a "medium-term" decaying factor in TL sensitivity. Finally, observation of a recovery of sensitivity in samples after a large dose and a long sunbleach provided a basis for the development of a physical scheme to explain the underestimation of TL ages. In this scheme, a simple trap and three recombination centres are hypothesised. Two hole centres take part in TL processes and the third is a reservoir centre. It is further assumed that the charge concentration in one of the recombination centres participating in the TL process undergoes thermal

relaxation over time periods of ~10^4 years. Based on these observations, a procedure has been suggested to correct the underestimated ages. The factor is estimated by calculating the inverse of the ratio of TL sensitivity of a sample as received and the TL sensitivity of the same sample but after a large dose followed by a long sunbleach. Preliminary results on samples from Karmaydan and Luochuan have been encouraging.

In the second phase of the thesis a system for infra-red stimulated luminescence was developed using infra-red diodes, a constant current timer controlled supply and a multiple sample illumination chamber which allowed for a change of sample without any light exposure. The system was standardized and its reproducibility and stability were verified using standard techniques and multiple readouts. In this study, samples from various depositional environments ranging from aeolian sands and silts to fluvial sands and soils were investigated. The IRSL ages on K-feldspar extracts from aeolian sands from Thar Desert and samples from the Karmaydan loess-paleosol sequences provided ages that were consistent with TL ages on the same sequences. The dating of fluvially transported K-feldspar extracts from Indo-Gangetic alluvium gave ages in the range of 1 ka-20 ka.

It is noteworthy to point out that the IRSL ages on the Karamaydan sequence and the Indo-Gangetic alluvium (IGA) are the first ever absolute ages. The study successfully demonstrated the feasibility of dating the IGA deposits of the Indian Quaternary and it should lead to the establishment of a chronological basis for deciphering the relative influence of sea level change, climatic change and the role of Himalayan tectonics on the sedimentation

pattern in North India. Though several conjectures existed so far, no conclusive scenario could be evolved and in this context the present work should be providing a new direction.

A compilation of TL and IRSL ages was also made including the results obtained in this thesis and a general concordance was seen which suggests that IRSL ages are also underestimated in a manner analogous to that in TL.

Thus, it is considered that the present thesis contributes to both the methodological and the applicational aspects of thermally and optically stimulated luminescence in respect of their applications in Earth Sciences.

6.2. Future Directions

One of the important outcomes of the present thesis is the development of the physical basis to explain the underestimation of TL ages. This proposed scenario involves the presence of a centre (the h_2 centre) which is hypothesized to have a relaxation time of ~10^4-5.10^4 a. Though considerable evidence already exists to support this contention, a direct experimental evidence of its existence and characterization is necessary. Three possible ways of detection are (1) spectral studies of TL with the possibility of emission of h_1 and h_2 being in different spectral bands, (2) by electron spin resonance provided h_2 centre is paramagnetic, and (3) by optical absorption or by photo acoustic spectrometric studies. It may not be easy to observe h_2 centre directly, but a conjuctive use of the three possible methods may perhaps provide evidence for such a centre. The future work would also need a much larger data base on sensitivity changes and utility of the proposed approaches. It will also be

instructive to examine the sensitivity change with different laboratory doses to simulate geological doses despite the fact that experimental evidence suggests a saturation in enhancement. It will also be prudent to validate the above approaches on sequences that have independent and reliable age control.

The global synthesis of loess ages provide new concepts in loess accumulation epochs. Though ample evidence exists, there is still a need for chronology on very densely sampled sequences between the Holocene soil and the last interglacial soil. Chronology on the phases of loess accumulation in each of the basins could then be effectively used in climate modelling efforts. The thesis has also raised basic questions on the processes of aeolian dust accumulation vis-a-vis glacial aridity, dust production, its deflation and the role of moisture in its accumulation. Increasing evidence has accrued that in general aeolian dust and sand accumulation on land postdate glacial aridity and is climate specific, but the relative importance of controlling factors such as the dust supply and the vegetation needs to be established. In these studies, a controlled precision luminescence dating will help to define exact climatic conditions that favoured accumulation of loess in various parts of the world.

In respect of IRSL dating, perhaps the most significant, the most satisfactory and also the most disturbing observation is the concordance of TL and IRSL ages. This implies that IRSL is also affected by age underestimation. This needs to be elucidated and such studies would require development of an adequate normalization procedure between samples to measure IRSL sensitivities of different samples within the same profile. This may be non-

trivial. On the other hand, it would also be instructive to compare Green Light Stimulated Luminescence (GLSL) and examine if the GLSL age is limited identically or on different time scales. If it is affected on a different time scale then the ratio of IRSL/GLSL itself could perhaps be used as a chronometer. Finally, the successful demonstration of the feasibility of luminescence dating of Indo-Gangetic alluvium by itself provides a basis for new possibilities in the Indian context. In respect of methodology, it is necessary to examine effects of various preheat treatments and their implications on IRSL ages.

References

Aitken M.J. (1974) Physics and Archeology. Clarendon Press, Oxford.

Aitken M.J. (1985) Thermoluminescence dating. Academic press, London.

Aitken M.J. and Bussel A.J. (1979) Zero-glow monitoring (ZGM), *Ancient TL*, **6**, 13-15

Aitken M.J. and Bowman S.G.E. (1975) Thermoluminescence dating: assessment of alpha particle contribution, *Archeometry*, **17**, 132-138

An Z., Porter S.C., Zhou W.J., Lu Y.C, Donahue D.J., Head M.J., Wu X.H., Ren Jianzhang and Zheng Hongbo (1993) Episode of strengthened summer monsoon climate of Younger Dryas age on the loess plateau of Central China, *Quaternary Research*, **39**, 45-54

Berger G. W. (1990) Effectiveness of natural zeroing of the thermoluminescence in sediments, *Journal of Geophysical Research.*, **95**, 12375-12397

Borsy Z, Felszerfalvy J and Szabo P.P. (1979), Thermoluminescence dating of several layers of loess sequences at Paks and Mende (Hungary). *Acta Geolo. Acad. Sci. Hung.*,**26**, 131-154.

Bronger A. and Th. Heinkele (1989) Paleosol as witness of Pleistocene climatic history, in *Catena Supplement*, **16**, Crelinger 163-186.

Bronger A., Winter R., Derevjanko O. and Aldag S. (1995), Loess-paleosol sequences in Tadjikistan as a paleoclimatic record of the Quaternary in Central Asia, *Quaternary Proceedings*, **4**, 69-81

Burg J.P. (1972), The relationship between maximum entropy spectra and maximum likelihood spectra, *Geophysics* , **37**, 375-376.

Butrym J and Muruszczak H (1984), Thermoluminescence chronology of younger and older loesses. In: M. Pecsi (Editor), *Lithology and Stratigraphy of Loesses and Paleosol* , Hung. Acad. Sci. , Budapest, pp 195-199.

Cegla J. (1972) Loess sedimentation in Poland, *Acta Univ Wratislav., Geogr*, **17 (168)**, 53-71

Chawla S. and Singhvi A.K. (1992) Thermoluminescence dating: Some unresolved enigmas. In *Thermoluminescence and its applications, Tata McGraw Hill Publ. Co. Ltd.* 308-328.

Chawla S., Gundu Rao T.K. and Singhvi A. K. Quartz thermoluminescence: Dose and dose rate effects and their implications (pre-print)

Clark R.J. and Sanderson D.C.W. (1994) Photostimulated luminescence excitation spectroscopy of feldspars and micas, *Radiation Measurements*, **23**, 641-646

Daniel F., Boyd C.A. and Saunders D.F. (1953) Thermoluminescence as a research tool, *Science* , **117**, 349

Debenham N.C.(1985) Use of UV emission in TL dating of sediments, *Nuclear Tracks*, **10** 717-724

Debenham N.C. and Walton A.J. (1983) TL properties of some wind blown sediments *PACT J.*,**9** 531-538

Derbishire E., Kenn D.H., Kemp R.A., Rolph T.A. Shaw J. and Xingmin Meng (1995) Loess-Paleosol sequences as records of paleocilmatic variations during the last glacial and interglacial cycle: Some problems of correlation in North-Central China, *Quat. Proc.*,**4**,7-18

Dodonov A.E. (1994), Loess stratigraphy in Central Asia, Abstracted in Inter.Conf. on Wind blown sediments in the Quaternary records, Organized by INQUA and QRA, held at Royal Holloway Uni, London, Jan 1994.

Fleming S.J. (1970), Thermoluminescence dating, refinement of the quartz inclusion method, *Archeometry*,**12**, 133-147

Fleming S.J. (1975) Supralinearity correction in fine grain thermoluminescece dating: a re-appraisal, *Archeometry*, **16**, 91-95

Forman S.L. (1991), Late Pleistocene chronology of loess deposition near Luochuan, China, *Quaternary Research* **36** 19-28

Forster Th. and Heller F. (1994) Loess deposits from the Tajik depression (Central Asia): Magnetic properties and paleoclimate. *Earth and Planetary Science Letters* **128**, 501-512.

Franklin A.D. and Hornyak W.F (1990) Isolation of the rapidly bleaching peak in quartz TL glow curves, *Ancient Tl*, **9**, 29-31.

Franklin A.D. and and Hornyak W.F. (1992) Normalization of inclusion size quartz TL data. *Ancient TL* **10** 1-6

Godfrey-Smith D.G., Huntley D.J. and Chen W.H. (1988) Optical studies of quartz and feldspar sediment extracts, *Quaternary Science Review*, **7**, 373-380

Grun R. and Brumby S. (1994) The assessment of errors on past radiation dose extrapolated from ESR/TL dose-response data, *Radiation Measurement*, **23**, 307-315

Gu Y.C., Lal D., Liu T.S., Southan J., Caffe M.W., Finkel R.C. and Guo Z.T. A study of cosmogenic ^{10}Be in dust deposits from the Chinese loess plateau: inference on weathering of dust layer and past climatic variation (preprint)

Heller F., Liu X.M., Liu T.S. and Xu T.C. (1991) Magnetic susceptibility of loess in China, *Earth Plaetary Science Letters* **103** 301-310

Hornyak W., Franklin A. and Chen R. (1993) A model for mid-term fading in TL dating, *Ancient TL*, **11** 21-27

Huntley D.J. (1985) A note on temperature dependence of anomalous fading. *Ancient TL*, **3**, 20-21

Huntley D.J., Godfray-Smith D.I. and Thewalt M.L.W. (1985) Optical dating of sediments *Nature* **313** 105-107

Huntley D.J., Hutton J.T. and Prescott J.R. (1993) The stranded beach dune sand sequence of south-east south Australia: a test of thermoluminescence dating 0-800 ka, *Quaternary Science Review*, **12**, 1-20.

Hutt G., Jaek I. and Tchonka J.(1988) Optical dating: K-feldspar optical response stimulation spectra *Quaternary Science Reviews* **7** 381-385

Hutt G. and Jaek I. (1989) Infrared photoluminescence (PL) dating of sediments: Modification of physical model, equipment and some dating results. In: *Long and short range limits in Luminescence dating*, Occasional publication No. 9 of the Research Laboratory for Archaeology and the History of Art, Oxford, 21-25

Kukla G. (1977), Pleistocene land sea correlations, I. Europe., *Earth Science Reviews*, **13**, 307-374.

Kukla G., Heller F., Liu X.M., Xu T. G., Liu T.S. and An Z.S. (1988) Pleistocene climates in China dated by magnetic susceptibility, *Geology* **16**, 811-814

Kukla G. and An Z.S. (1989) Loess stratigraphy in central China. *Palaeogeography, Palaeoclimatology, Palaeoecology* **72** 203-225

Lazarenko A.A. (1977) Loess cover of the Tadjik depression (stratigraphy, lithology, problems of genesis), In:*Abstracts of the ICCP International symposium on the Neogene Quaternary Boundary*, Moscow , pp 35-37

Lazarenko A.A. (1984) The loess of Central Asia. In: Velinchko (ed.). *Late Quaternary Environments of the Soviet Union*, University of Minessota Press, Minneapolis, pp 125-131

Li J-L., Pei J-X., Wang Z.-Z and Lu Y.C. (1977) A preliminary

study of both the thermoluminescence of the quartz silts in loess and the age determination of the loess layers, *Kexue Tongbao*, **7**, 498-502

Li J. (1985a) Thermoluminescence dating of loess, in Loess and environment (ed., Liu T.S.) pp 231-238, Ocean Press, Beijing, China

Li J. (1985b) Formation age of Malan loess dated by thermoluminescence (TL) of Quartz, *Kenxue Tongbao*, **30 (8)**, 1091-1094

Lu Yanchou, Prescott J.R., Robertson G.B. and Hutton J.T. (1987) Thermoluminescence dating of the Zhaitang Section of the Malan loess, China. In: *Aspects of loess research* Ed. by Liu Tungsheng, China Ocean Press, Beijing pp. 259-273

Lu Y.C., Prescott J.R., and Hutton J.T. (1988) Sunlight bleaching of the thermoluminescence of Chinese loess *Quaternary Science Review.* **7** 335-338

Lu Y.C., Zhang J-Z and Xie J. (1988) Thermoluminescence dating of loess and paleosols from the Lantian section Shaanxi Province, China, *Quaternary Science Review*, **7**, 245-250

Marple L. (1980) A new autoregressive spectral analysis algorithm, *IEEE Transaction on ASSP*, **28**, 441-454

McFee C.J. and Tite M.S. (1994) Investigation into the thermoluminescence properties of single quartz grains using an imaging photon detector, *Radiation Measurement*,**23**, 355-360

Mejdahl V. (1985a) Further comments on extrapolation methods of of dating sediments, *Ancient TL*, **3**, 21-27

Mejdahl V. (1985b) Thermoluminescence dating based on feldspar. *Nucl.Tracks. and Radiat. Meas.* **10** 133-136

Mejdahl V. (1988) Long term stability of TL signal in alkali feldspar. *Quatern. Sci. Rev.* **7**, 357-360

Mejdahl V. and Winther-Nielson M. (1982), Thermoluminescence dating based on feldspar inclusion, *PACT*, **6**,

Mejdahl V. Shlukov A.I. Shakhovets S.A., Voskovskaya L.T. and Lyashenko H.G. (1992) The effect of shallow traps: a possible source of error in TL dating of sediments. *Ancient TL* **10** 22-25

Musson M.F. Wintle A.G. (1994) Luminescence dating of the loess profile at Dolni Vestonice, Czech Republic, *Quaternary Geochronology*. **13**, 411-416

Nambi K.S.V. (1983) The problem of low thermoluminescence age estimates in geological dating,*PACT* **9 (II)**, 479-485

Nambi K.S.V. (1984) Alpha - radioactivity - related upper limit for thermoluminescence dating? *Proc. Indian Acd. Sci. (Earth Planetary Sciences)* **93**, 47-56.

Nishimura S., Miao J.V. and Sasajima S. (1984) Thermoluminescence dating of paleosol in the Luochuan loess sequences. In Recent Research of loess in China (Ed. by Sasajima S. and Yong Yan W.) pp-69-78, Kyoto University, Japan.

Oches E.A. and Mccoy W.D (1995) Aminostratigraphic evolution of conflicting age estimates for the "Young Loess" of Hungary, *Quaternary Research*, **44**, 160-170

Pecsi M. (1985) Chronostratigraphy of Hungarian loesses and the underlying Subaerial Formations, in *Loess and the Quaternary: Chinese and Hungarian case study, edited by, Pecsi M.*, Academiai Kiado, Budapest, 33-49.

Pecsi M. Pevezner M.A. and Szebenyl E. (1979) In: Guide Book for conference and Field, Workshop on the stratigraphy of loess and Alluvial Deposits, Geophys. Res. Inst. Budapest, pp 11-38.

Prescott J. R. Stephan L.G.(1982) Contribution of cosmic radiation to environmental dose *PACT*, **6**, 17-25

Proszynska H. (1983) TL dating of some sub-areal sediments from Poland *PACT*, 9 539-546

Pye K. (1987) Aeolian dust and dust deposits. Academic Press. pp 333

Rajgopalan G. (1992) Radiocarbon ages of carbonate materials from gangetic alluvium, *Gangetic Plain: Terra Incognita*, (ed. I.B. Singh), Geol.Dept. Lucknow Univ. pp 45-48

Readhead M.L. (1987) Thermoluminescence dose rate data and dating equations for the case of disequilibrium in the decay series, *Nuclear Tracks and Radiation Measurements and Radiation Measurements*, **13**, 197-207

Rendell H.M., Gamble I.J.A. and Townsend P.D. (1983) Thermoluminescence dating of loess from the Potwar Plateau, Northern Pakistan *PACT J* **9**, 555-562.

Rendell H.M. and Townsend P.D. (1988) Thermoluminescence dating of a 10m. loess profile from Pakistan. *Quatrnary Science Reviews* **7** 251-255

Roberts R.D., Spooner N.A. and Questiaux D.G (1994) Palaeodose underestimates caused by extended duration of preheats in the optical dating of quartz, *Radiation Measurements*, **23**, 647-653

Sanderson D.C.W. (1988) Fading of thermoluminescence in feldpsars: characteristics and corrections, *Nuclear Tracks and Radiation Measurements and Radiat. Meas.*, **14**, 155-161

Shakleton N.J., An Z., Dodonov A.E., Gavin J., Kukla G.J., Ranov V.A. and Zhou L.P. (1995) Accumulation rate of loess in Tadjikistan and China: Relationship with Global ice volume cycles, *Quaternary Proceedings*, **4**, 1-4

Shen C.D. , Beer J., Liu T.S., Oeschger H., Bonani G., Suter M., and Wolfli E. (1992). ^{10}Be in Chinese loess. *Earth and Planetary Science Letters* **109**, 169-177

Shelkoplyas V.N. (1974), Geokhronologiya lessovoy formatsii po dannyam termolyuminestsentogo metoda (*Loess formation geochronology based on thermoluminescence method data*). in Materialy po chetvertichnomu priodu Ukrainy, Kiev, 89-120.

Singhvi A.K. and Aitken M.J. (1978) Americium-241 for alpha irradiations, *Ancient TL*, no. 3, 2-9

Singhvi A.K., Sharma Y.P. and Agrawal D.P.(1982) Thermoluminescence dating of sand dunes in Rajasthan, India. *Nature*, London **295** 313-315

Singhvi A.K. and Mejdahl V. (1985), Thermoluminescence dating of sediments *Nuclear Tracks and Radiation Measurements*, **10 (1-2)**, 137-161.

Singhvi A.K. and Wagner G.A. (1985) Thermoluminescence dating and its applications to young sedimentary deposits, In, Hrurford A.J., Jagar E. and Tencate L.A. M. eds. Dating young sediments, Bangkok, Thailand U.N. CCOP Technical Secretariat p 159-197

Singhvi A.K., Bronger A., Pant R.K. and Sauer W. (1987) Thermoluminescence dating and its implication for the chronostratigraphy of loess-paleosol sequences in the Kashmir Valley (India) *Chem. Geo.* **65** 45-56

Singhvi A.K., Bronger A., Sauer W. and Pant R. K. (1989), Thermoluminescence dating of loess-paleosol sequences in the Carpathian Basin (East-Central Europe): A suggestion for a revised chronology, *Chem. Geol.(Isotope Geoscienece Section*, **73**, 307-317.

Spooner N.A. and Franks M. (1990) Some characteristics of infrared emitting diodes relevant to luminescence dating *Ancient TL* **18** 16-19

Stokes S. (1994) The timing of OSL sensitivity changes in a natural quartz, *Radiation Measurements*, **23**, 601-605

Strickertsson (1985) The thermoluminescence of potassium feldspars- glow curve characterstics and initial rise measurements, *Nuclear Tracks and Radiation Mesurements*, **10** 613-617

Templer R.H. (1985) The removal of anomalous fading in zircon *Nuclear Tracks and Radiation Measurements and Radiation Measurements*, **10**, 531-537

Venkatesan T.R. and Ramesh R. (1993) Consideration of analytical uncertainties while plotting histograms, *Journal of Geological Society of India*, **14**, 313-317

Vesoceka R (1979) Miscellaneous aspect of artificial TL of calcite: emission spectra, athermal detrapping and anomalous fading, *PACT* **3**, 258-265

Williams M.A.J., Dunkerley J.L., Decker P.De., Kershaw A.P. and Stokes T. (1993) Quaternary environment. in Edward Arnold, New York pp. 322

Wintle A.G. (1973) Anomalous fading of TL in mineral samples *Nature*, **245** 143-145

Wintle A.G. (1977) Detailed study of TL minerals exhibiting anomalous fading, *J. Lum.* **15**, 385-393

Wintle A.G.(1978) A thermoluminescence dating study of some Quaternary calcite: potential and problems, *Canadian Journal of Earth Sciences*, **15**, 1977-1986

Wintle A.G.(1985) Sensitization of TL signal by exposure to light. *Ancient TL* **3** 16-21

Wintle A.G. (1990) A review of current research on TL dating of loess, *Quaternary Science Review* **9**, 385-398

Wintle A.G. and Huntley D.J. (1979) Thermoluminescence dating of deep sea sediment core, *Nature*, **279**, 710-712

Wintle A.G. and Huntley D.J. (1980) Thermoluminescence dating of ocean sediment, *Canadian Journal of Earth Sciences* **17**, 348-360

Wintle A.G. and Huntley D.J. (1982) Thermoluminescence dating of sediments, *Quaternary Science Review*, **1** , 31-53

Wintle A.G. and Proszynska H. (1983) TL dating of loess in Germany and Poland, *PACT*, **9**, 547-554

Wintle A.G. and Packman S.C. (1988) Irradiation of loess at elevated temperatures. *Ancient TL*, **6** 22-23

Wintle A and Packman S.C. (1988), Thermoluminescence ages for three sections in Hungary, *Quaternary Science Reviews*, **7**, 315-320.

Xie and Aitken (1991) The hypothesis of mid-term fading and its trial on Chinese loess. *Ancient TL* **9**, 21-25

Xio J., Porter S.C., An Z.S., Kumai J. and Yoshikawa S. (1995) Grain size of quartz as an indicator of winter monsoon strength of the loess plateau of Central China during the last 130, 000 yrs, *Quat. Res*, **43**, 22-29

Zeuner F.E. (1950) Stone age Pleistocene chronology of Gujrat. Deccan Collage Monograph, Series 6, Poona pp 46.

Zimmerman D.W. (1971) Thermoluminescence dating using fine grains from pottery. *Archeometry* **13** 29-52

Zhou L.P. and Wintle A.G. (1994), Sensitivity change of thermoluminescence signals after laboratory bleaching: experiments with loess fine grains, *Quaternary Geochronology* , **13**, 457-463.

Zhu, X., Liu,Z., and Zang, S. (1983) Soils of the loess region in China. *Geoderma*, **29** 237-255.

Zoller L. and Wagner G. (1990), Thermoluminescence dating of loess- recent developments, *Quaternary International*, **7/8**, 119-128.

Zoller L., Oches E.A. and McCoy W.D. (1994), Towards a revised chronostratigraphy of loess in Austria with respect to key sections in the Czech Republic and Hungary, *Quaternary Science Review.*, **13**, 465-472.

Appendix

Country: America
Site: Half Way house site, Alaska
Source: Berger et.al., Test of thermoluminescence dating of loess from New Zealand and Alaska, 1994. *Quaternary Science Review*, **13**, 309-333

Laboratory Sample Code	Stratigraphic Unit	Soil Horizon	Depth mbas	TL age (years)	Method	Other Ages/Controls/Remarks
QTL 71A				110000 ± 32000	PB	≤140000 ± 10000(*)
QTL 71A				204000 ± 30000	ADD	≤140000 ± 10000(*)
QTL 71H				≥140000 ± 30000	PB	≥ 140000 ± 10000(*)
QTL 71H				< 229000 ± 37000	ADD	≥ 140000 ± 10000(*)

* Wastgate, J.A.; Stemper, B.A. and Pewe, T.L. (1990), A 3m.y. record of Pleiocene-Pleistocene loess in interior Alaska, Geology, **18**, 858-861

Country: America
Site: Half Way house site, Alaska
Source: Wintle A.G. and Wastgate J.A. (1986), Thermoluminescence age of Old Crow tephra in Alaska, *Geology*, **14**, 594-597

Laboratory Sample Code	Stratigraphic Unit	Soil Horizon	Depth mbas	TL age (years)	Method	Other Ages/Controls/Remarks
QTL 71A				77000 ± 7000	RGN	
				79000 ± 8000	RGN	
QTL 71H				83000 ± 9000	RGN	

Country: America
Site: Vicksburg, Loc. V1
Source: Pye, K. and Johnson, R. (1988). Stratigraphy, Geochemistry and Thermoluminescence ages of Lower Missicippi Valley. *Earth Surf. Processes and Landforms*, **13**, 1103-124.

Laboratory Sample Code	Stratigraphic Unit	Soil Horizon	Depth mbas	TL age (years)	Method	Other Ages/Controls/Remarks
V1(ii)	Loess Unit 1	A	1* 1.5	8070 ± 660 -	R-β	Leached Zone ^{14}C 8760 ± 90 (UM-3002)
V1(i)	Loess Unit 1	C	3 4.0	12360 ± 920 -	R-β	^{14}C 13660 ± 200 (UM-3002)
V1(B)	Loess Unit 1	C	10*	16460 ± 1400	R-β	-
V1(F)	Loess Unit 1	C	12.0* 12.5*	17890 ± 1600 -	R-β	^{14}C 19910 ± 320 (UM-3004)
V1(H)	Loess Unit 2		13.0*	20490 ± 600	R-β	Farmdale Loess ^{14}C 23390±340 (UM-2576)
V1(K)	Loess Unit 3		14.5*	79610 ± 5400	R-β	Pre-farmdale highly weathered Loess
V1(N)	Loess Unit 3		16.0*	76100 ± 5690	R-β	- do -
V1(P)	Loess Unit 3/4		16.9*	85090 ± 5860	R-β	- do -
V1(R)	Loess Unit 4		?	172770 ± 11980	R-β	- do -
V1(R)	Loess Unit 4		18.0*	122570 ± 10030	RGN	- do -
V1(T)	Loess Unit 4		?	196100 ± 12330	R-β	- do -
V1(R)	Loess Unit 4		19.0	>132000	RGN	- do -

*Depths estimated from authors stratigraphic diagrams.

Country: America
Site: Vickburg Loc. V-2
Source: Pye, K. and Johnson, R. (1988). Stratigraphy, Geochemistry and Thermoluminescence ages of Lower Missicippi Valley. *Earth Surf. Processes and Landforms*, **13**, 1103-124.

Laboratory Sample Code	Stratigraphic Unit	Soil Horizon	Depth mbas	TL age (a)	Method	Other ages/Controls/Remarks
V2A	1S	A	0.3*	5800 ± 400	R-β	Leached Zone
-	1	C	1.7*	-	-	^{14}C 39900 ± 100 (UM-3001)
-	1	C	2.2	-	-	^{14}C 10000 ± 100 (UM-2570)
V2G	1	C	2.8*	10470 ± 860	R-β	-
V	1	C	5.9*	-	-	^{14}C 16620 ± 130 (UM-2572)
V20	1	C	6.0*	15580 ± 1090	R-β	-
-	1	C	9.5*	-	-	^{14}C 17130 ± 200 (UM-2573)
V2W-1	1	C	9.6*	17380 ± 1260	R-β	-
V2W-2	1	C	9.6*	17190 ± 1120	R-β	-
V2F	1	C	14.0*	20020 ± 1240	R-β	-
-	2	?	14.9	-	-	^{14}C 20800 ± 210 (UM-2575)
V2JJ	2T	?	16.0* 16.0*	27240 ± 1940 30690 ± 2060	R-β R-β	- -
V2KK	2T	?	16.5*	34470 ± 2490 36870 ± 2600	R-β R-β	- -

Country: America
Site: Natchez (N1)
Source: Pye, K. and Johnson, R. (1988). Stratigraphy, Geochemistry and Thermoluminescence ages of Lower Missicippi Valley. *Earth Surf. Processes and Landforms*, **13**, 103-124.

Laboratory Sample Code	Stratigraphic Unit	Soil Horizon	Depth mbas	TL age (years)	Method	Other Ages/Controls/Remarks
N1C	Leached zone	A*	0.4*	5150 ± 360	R-β	-
N1F	Loess 1	C	1.8*	14220 ± 910	R-β	-
N1G	Loess 1	C	3.0*	15660 ± 1105	R-β	-
N1G	Loess 1	C	3.0*	16320 ± 1220	R-β	-
N1H	Loess 1	C	4.0*	16980 ± 1180	R-β	-
N1I	Loess 1	C	5.0*	18640 ± 1400	R-β	-
-	Loess 1	C	6.2*	-	-	^{14}C 19300 ± 360 (UM-2579)
-	Weathered loess 2	?	7.0	-	-	^{14}C 18620 ± 250 (UM-2578)
N1K	Weathered loess	?	7.0*	21240 ± 1430	R-β	-
N1M	Weathered loess-3	?	7.6*	76840 ± 6340	β	-
N1M	Weathered loess-3	?	7.6*	74441 ± 9760	β	-
N1M	Weathered loess-3	?	7.6*	74720 ± 5670	RGN	-
N10	Weathered loess 4	?	8.4*	117250 ± 7300	RGN	-
N1O	Weathered loess 4	?	8.4*	237830 ± 20100	β + RGN	

Country: America
Site: Natchez (N2)
Source: Pye, K. and Johnson, R. (1988). Stratigraphy, Geochemistry and Thermoluminescence ages of Lower Missicippi Valley. *Earth Surf. Processes and Landforms*, **13**, 103-124.

Laboratory Sample Code	Stratigraphic Unit	Soil Horizon	Depth mbas	TL age (years)	Method	Other Ages/Controls/Remarks
N2A	Loess 1	C	2.3*	10150 ± 760	β	-
N2B	Weathered Loess 2	?	10.2*	21630 ± 1460	β	-
N2B	Weathered Loess 2	?	10.2*	21800 ± 1790	β	-
-	Weathered loess 2	?	10.2*	-	-	^{14}C 21400 ± 390 (UM-2580)
-	Weathered loess 2	?	10.8*	-	-	^{14}C 21680 ± 250 (UM-2581)
N2D	Weathered loess-2T	?	11.9*	36240 ± 2750	β	-
N3A	Loess-1	C	?	19220 ± 1260	β	-

Country: America
Site: Idaho Natn. Eng. Lab. NR29E Sect. 19
Source: Forman, S.L. et al (1993). Timing of Late Quaternary Glaciations in the Western United States based on age of Loess on the Eastern Snake River Plain, Idaho.

Laboratory Sample Code	Stratigraphic Unit	Soil Horizon	Depth mbas	TL age (years)	Method	Other Ages/Controls/Remarks
OTL	L-A	C	1.4	28000 ± 3000	T-B	-
ITL-307	L-A	C	1.4	2500 ± 300	T-B	-

Country: America
Site: Natchez (N2)
Source: Pye, K. and Johnson, R. (1988). Stratigraphy, Geochemistry and Thermoluminescence ages of Lower Missicippi Valley. *Earth Surf. Processes and Landforms*, **13**, 103-124.

Laboratory Sample Code	Stratigraphic Unit	Soil Horizon	Depth mbas	TL age (years)	Method	Other Ages/Controls/Remarks
N2A	Loess-1	C	2.3*	10150 ± 760	β	-
N2B	Weathered Loess-2	?	10.2*	21630 ± 1460	β	-
N2B	Weathered Loess-2	?	10.2*	21800 ± 1790	β	-
-	Weathered Loess-2	10.2*	-	-	-	^{14}C 21400 ± 390 (UM-2580)
-	Weathered Loess-2	?	10.8*	-	-	^{14}C 21680 ± 250 (um-2581)
N2D	Weathered Loess-2T	?	11.9*	36240 ± 2750	β	-
N3A	Loess-1	C	?	19220 ± 1260	β	-

Country: America
Site: Idaho Natn. Eng. Lab. NR29E Sect. 19
Source: Forman, S.L. et al (1993). Timing of Late Quaternary Glaciation in the Western United States based on age of Loess at the Eastern Snake River Plain, Idaho.

Laboratory Sample Code	Stratigraphic Unit	Soil Horizon	Depth mbas	TL age (years)	Method	Other Ages/Controls/Remarks
OTL-337	L-A	C	1.4	28,00 ± 3000	TB	-
ITL-307	L-A	C	1.4	2500 ± 300	TB	-

Country: America
Site: Idaho Natn. Engg. Lab., T2 N.R. 29E, Sect. 18
Source: Forman, S.L. et al (1993). Timing of Late Quaternary Glaciation in the Western United States based on age of Loess at the Eastern Snake River Plain, Idaho.

Laboratory Sample Code	Stratigraphic Unit	Soil Horizon	Depth mbas	TL age (years)	Method	Other Ages/Controls/Remarks
OTL-340	B	C_b	3.8	71600 ± 5000	TB	-
OTL-340b	B*	C_b*	3.8*	79000 ± 6000	TB	-
ITL-306	B	C_b	3.8	7400 ± 6000	TB	-
-	Lava Flow	-	4.4	-	-	K/Ar: 95000 ± 25000[1]
-	C	A_b	5.6	-	-	^{14}C >32,000 (B-41481)
-	C	A_b	5.6	-	-	^{14}C >33,750 (GX-16547)
ITL-305	C	B_{wb}	6	101000 ± 7000	TB	-
OTL-336	C	B_{wb}	6.2	108000 ± 13000	TB	-

*Horizon, depth inferred.
[1]Champion et al. 1981. *Geophy. Res. Lett.* **8**, 1055-58.

Country: America
Site: Treynor 1A
Source: Norton, D.L. and Bradford, J.M., 1985. Thermoluminescence Dating of Loess from W. Iowa. *Soil Sc. Am. J.*, **49**, 708-712.

Laboratory Sample Code	Stratigraphic Unit	Soil Horizon	Depth mbas	TL age (years)	Method	Other Ages/Controls/Remarks
Alpha Analy.514	Upper Wis. 1	B*	0.91	24130 ± 2900	RGN	-
Alpha Analy. 517	Upper Wisc. 1	B*	1.83	15890 ± 1700	RGN	-
Alpha Analy. 523	Upper Wisc. 1	B*	2.8	13270 ± 1780	RGN	-
Alpha Analy. 520	Upper Wisc. 1	B*	3.71	15830 ± 2900	RGN	-
Alpha Analy. 524	Upper Wisc. 1	B*	4.63	16500 ± 2290	RGN	-
Alpha Analy. 515	Upper Wisc.[1]	B*	5.54	13150 ± 1160	RGN	-
Alpha Analy. 522	Upper Wisc.[2]	B/C/ Loess*	6.45	20260 ± 2730	RGN	-
Alpha Analy. 521	Upper Wisc.[2]	B/C/ Loess*	7.37	23630 ± 2520	RGN	-
Alpha Analy. 514	Upper Wisc.[2]	B/C/ Loess*	8.28	16640 ± 2090	RGN	-
Alpha Analy. 512	Upper Wisc.[2]	B/C/ Loess*	9.19	20320 ± 2450	RGN	-
Alpha Analy. 518	Farmdale	B*	10.11	46720 ± 5180	RGN	-
Alpha Analy. 513	Farmdale	B*	11.02	45960 ± 8310	RGN	-
Alpha Analy. 516	Loveland	B*	11.53	80200 ± 9230	RGN	Overestimation possible due to linear extrapolation of growth curves.

*Inferred
[1]Oxideached
[2]Unoxidized - unleached

Country: Austria
Site: Stillfried
Source: Zoller et.al., (1994), Towards a revised chronology of loess of Austria with respect to key sections in the Czech Republic and in Hungary, *Quaternary Geochronology*, **13**, 465-472

Laboratory Sample Code	Stratigraphic Unit	Soil Horizon	Depth mbas	TL age (years)	Method	Other Ages/Controls/Remarks
STILL1-4	Holocene soil			3900 ± 600	RGN	
STILL5a	Loess			16500 ± 2300	RGN	
STILL5b	Loess			20300 ± 1700	RGN	
STILL5c	Loess			25400 ± 3700	RGN	
STILL5d	Loess			17100 ± 2300	RGN	
STILLB2	Loess			27500 ± 3600	RGN	
STILLB1	Stillfried B Paleosol			29800 ± 3700	RGN	
STILLA4	Loess (Stillfried A pedocomplex)			59100 ± 5700	RGN	
STILLA3	Loess (Stillfried A pedocomplex)			59700 ± 7500	RGN	
STILLA2	Loess (Stillfried A pedocomplex)s			74100 ± 9500	RGN	
STILLA2 PTW	Loess (Stillfried A pedocomplex)			76800 ± 10500	RGN	
STILLA1	Loess			85800 ± 11200	RGN	
STILLA1 PTW	Loess			111000 ± 14000	RGN	
STILLA0Q	Loess			139000 ± 36000	RGN	
STILLA0 KF	Loess			119000 ± 12000	RGN	

Country: Austria
Site: Wels
Source: Zoller et.al., (1994), Towards a revised chronology of loess of Austria with respect to key sections in the Czech Republic and in Hungary, *Quaternary Geochronology*, **13**, 465-472(TL ages after Stremme, H.E.; Zoller, L.; and Krause W. (1991) Boden stratigraphic und Thermolumineszez-Datierungen fur das Mittel und Jungpleistozan des Alpenvorlandes, Saunderveroff Geol. Inst. Univ. zu Koln **83** (Brunnacker Festchrift), 301-315)

Laboratory Sample Code	Stratigraphic Unit	Soil Horizon	Depth mbas	TL age (years)	Method	Other Ages/Controls/Remarks
	Humic colluvial loess			24000 ± 3000	RGN	
	Loess			21000 ± 2000	RGN	
	Humic colluvial loess	fAh		81000 ± 8000	RGN	
				136000 ± 13000	RGN	
	Loess			128000 ± 15000	RGN	
		f2Bt		233000 ± 35000	RGN	
	Loess			245000 ± 51000	RGN	
				202000 ± 30000	RGN	

Country: Austria
Site: Paudorf
Source: Zoller et.al., (1994), Towards a revised chronology of loess of Austria with respect to key sections in the Czech Republic and in Hungary, *Quaternary Geochronology*, **13**, 465-472

Laboratory Sample Code	Stratigraphic Unit	Soil Horizon	Depth mbas	TL age (years)	Method	Other Ages/Controls/Remarks
PAU4	Loess above Paudorf soil PAII			54400 ± 6500	RGN	
PAU3	Loess below PAII			103000 ± 11000	RGN	
PAU2PTW	Loess above PAI pedocomplex			100000 ± 12000	RGN	
PAU1	Loess below PAI			197000 ± 23000	RGN	

Country: Austria
Site: Gotweig-Furth
Source: Zoller et.al., (1994), Towards a revised chronology of loess of Austria with respect to key sections in the Czech Republic and in Hungary, *Quaternary Geochronology*, **13**, 465-472

Laboratory Sample Code	Stratigraphic Unit	Soil Horizon	Depth mbas	TL age (years)	Method	Other Ages/Controls/Remarks
GOT4	Loess above Gottweig pedocomplex GO I			28000 ± 3600	RGN	
GOT5	Loess below GO I			107000 ± 10000	RGN	
GOT5add	Loess below GO I			119000 ± 13000	TB	
GOT2	Loess above GO II			256000 ± 46000	RGN	
GOT3	Colluvial loess below GO II			240000 ± 28000	RGN	

Country: Austria
Site: Stratzing
Source: Zoller et.al., (1994), Towards a revised chronology of loess of Austria with respect to key sections in the Czech Republic and in Hungary, *Quaternary Geochronology*, **13**, 465-472

Laboratory Sample Code	Stratigraphic Unit	Soil Horizon	Depth mbas	TL age (years)	Method	Other Ages/Controls/Remarks
STRATZ3	Loess			25400 ± 2500		
STRATZ2	Loamy loess, semicalcareous			26200 ± 2500		
STRATZ1	Reddish brown loess, semi calcareous			46400 ± 4400		
STRATZ4				30200 ± 3500		

Country: Belgium
Site: Rocourt
Source: Wintle, A.G. Thermoluminescence Dating of Loess at Rocourt, Belgium, 1987. *Geol. en Mijnbow*, **66**, 35-42.

Laboratory Sample Code	Stratigraphic Unit	Soil Horizon	Depth mbas	TL age (years)	Method	Other Ages/Controls/Remarks
QTL-89B	Holocene Soil (I)	A*	0.8*	13500 ± 1100	RGN	-
QTL-89D	Loess (I)	-	1.6*	13200 ± 1100	RGN	-
QTL-89F	Loess (I)	-	2.2*	13500 ± 1100	RGN	-
QTL-89G	Loess (II)	-	-	13500 ± 1200	RGN	-
QTL-89H	Loess (II)	-	2.8*	17100 ± 1400	RGN	-
QTL-89I	Loess (III)	-	3.0*	24800 ± 2100	RGN	-
QTL-89J	Loess (II)	-	3.3*	38000 ± 3200	RGN	-
QTL-89K	Loess (III)	-	0.8*	44300 ± 3700	RGN	-
QTL-89L	Loess (III)	-	1.0	42500 ± 3500	RGN	-

Country: Belgium
Site: Rocourt
Source: Juvigne, E.H. and Wintle, A.G., 1988. A new chronostratigraphy of the late Weichselian Loess Units in middle Europe based on thermoluminescence dating. *Elszeitalt.u.Gegenw.*, **38**, 94-105.

Laboratory Sample Code	Stratigraphic Unit	Soil Horizon	Depth mbas	TL age (years)	Method	Other Ages/ Controls/Remarks
QTL-103A	Loess between tongued horizon and Eltville tephra	?	?	15900 ± 1300	RGN	-
QTL-103B	Loess between Eltville tephra and E-2 Nassboden	?	?	16600 ± 1300	RGN	-
QTL-78A	- do -	?	?	17200 ± 1700	RGN	-
QTL-78B	Loess from tongued horizon	Soil (?)		15300 ± 1300	RGN	-
QTL-77B	Paleosol		-	15800 ± 1300		

Country: Belgium
Site: Lixhe
Source: Juvigne, E.H. and Wintle, A.G., 1988. A new chronostratigraphy of the late Weichselian Loess Units in middle Europe based on thermoluminescence dating. *Eiszeitalt.u.Gegenw.*, **38**, 94-105.

Laboratory Sample Code	Stratigraphic Unit	Soil Horizon	Depth mbas	TL age (years)	Method	Other Ages/ Controls/Remarks
QTL-77B	Paleosol tongued horizon and Eltville tephra	?	?	15800 ± 1300	RGN	-

Country: China
Site: Zhaitang
Source: Lu Yanchou, Mortlock A.J.; Price D.M. and Readhead M.L. (1987) Thermoluminescence dating of quaertz from the Malan loess at Zhaitang section, China. *Quaternary Research*, **28**, 356-363.

Laboratory Sample Code	Stratigraphic Unit	Soil Horizon	Depth mbas	TL age (years)	Method	Other Ages/Controls/Remarks
Z-08	Loess		1.9	17800 ± 2500	TB+RGN (FG)	-
Z-08	Loess		1.9	19800 ± 2500	TB+RGN (CG)	-
Z-07	Loess		2.7	27800 ± 4700	TB+RGN(CG)	-
Z-06	Paleosol		3.5	35600 ± 6500	TB+RGN(CG)	-
Z-06	Paleosol		3.5	32400 ± 3500	TB+RGN(FG)	-
Z-04	Loess		6.0	41100 ± 4200	TB+RGN(FG)	-
Z-03	Loess		6.7	51800 ± 5200	TB+RGN(CG)	
Z-03	Loess		6.7	50700 ± 4200	TB+RGN(FG)	
Z-02	Loess	?	7.5	65600 ± 7300	TB+RGN(FG)	-
Z-01	Loess	?	9.4	84000 ± 9000	TB+RGN(FG)	-
Z-01	Paleosol	?	9.4	84000 ± 10500	TB+RGN(CG)	-

Country: China
Site: Lantin Section, Shaanxi
Source: Lu Yanchou, Zang Jingzhao and Xie Jun (1988), Thermoluminescence dating of loess paleosols from the lantian section, Shaanxi provinance, China. *Quaternary Science Reviews*, **7**, 245-250.

Laboratory Sample Code	Stratigraphic Unit	Soil Horizon	Depth mbas	TL age (years)	Method	Other Ages/Controls/Remarks
01	Loess		2.0	34300 ± 1700	RGN	-
02	Paleosol		3.1	33500 ± 2400	RGN	-
03	Loess		4.1	41900 ± 2600	RGN	-
04	Paleosol		5.5	50000 ± 3700	RGN	-
05	Weathered Loess		6.8	121200 ± 10200	RGN	-
06	Loess		7.8	144000 ± 11800	RGN	-
07	Loess		10.3	150200 ± 12700	RGN	
08	Paleosol		10.9	130700 ± 14000	RGN	
09	Loess	?	11.7	156300 ± 15900	RGN	-
10	Paleosol	?	13.0	137100 ± 13600	RGN	-

Country: China
Site: Luochuan
Source: Forman S.L., (1991) Late Plaistocene chronology of loess deposition near Luochuan, China, *Quaternary Research*, **36**, 19-28.

Laboratory Sample Code	Stratigraphic Unit	Soil Horizon	Depth mbas	TL age (years)	Method	Other Ages/Controls/Remarks
ITL-73 S0	Soil	Ah	0.3*	3000 ± 500	TB	
ITL-73 S0	Soil	Ah	0.3*	2000 ± 400	R-β	-
ITL-81 (L1)	Loess		1.9*	26000 ± 3000	TB	-
ITL-53 (L1)	Loess		2.7*	35000 ± 5000	TB	-
ITL-53 (L1)	Loess		3.5*	34000 ± 5000	TB	-
ITL-93 (L1)	Loess		3.5*	39000 ± 5000	TB	-
ITL-92 (L1)	Loess		6.0*	52000 ± 7000	TB	-
ITL-92 (L1)	Loess		6.7*	45000 ± 6000	TB	
ITL-94 (L1)	Loess		6.7*	56000 ± 5000	TB	
ITL-52 (L1)	Loess	?	7.5*	67000 ± 7000	TB	-
ITL-52 (L1)	Loess	?	9.4*	72000 ± 9000	TB	-
ITL-95 (L2)	Paleosol	?	9.4*	290000 ± 42000	TB	-

Country: China
Site: Heimugou Brickyard
Source: Forman S.L., (1991).Late Plaistocene chronology of loess deposition near Luochuan, China, *Quaternary Research*, **36**, 19-28.

Laboratory Sample Code	Stratigraphic Unit	Soil Horizon	Depth mbas	TL age (years)	Method	Other Ages/Controls/Remarks
ITL-96(L1)	Loess		2.5*	22000 ± 3000	TB	
ITL-96(L1)	Loess		2.5*	25000 ± 4000	TB	-
ITL-148(L1)	Loess		2.9*	29000 ± 3000	TB	-
ITL-148(L1)	Loess		2.9*	30000 ± 4000	R-β	-

Country: China
Site: Lower Heimugou
Source: Forman S.L., (1991). Late Plaistocene chronology of loess deposition near Luochuan, China, *Quaternary Research*, **36**, 19-28.

Laboratory Sample Code	Stratigraphic Unit	Soil Horizon	Depth mbas	TL age (years)	Method	Other Ages/Controls/Remarks
ITL-147 (L1)	Loess		5.0*	46000 ± 6000	TB	-
ITL-146 (L1)	Loess		8.3*	52000 ± 7000	TB	-
ITL-146 (L1)	Loess		8.3*	54000 ± 8000	RB	-
ITL-140 (L1)	Loess		8.5*	69000 ± 8000	TB	-
ITL-140 (L1)	Loess		8.5*	70000 ± 9000	R-β	-
ITL-142 (L1)	Loess		12.0*	170000 ± 25000	TB	

Country: China
Site: Baxie
Source: An Zhisheng, Porter S.C., Zhou Weijian, Lu Yanchou, Douglas J. Donhue, Head M.J., Wu Xihuo, Ren Jianzhang and Zheng Hongbo (1993)Episodes of strengthened summer monsoon climate of younger dryas age on the loess plateau of Central China, *Quaternary Research*, **39**, 45-54.

Laboratory Sample Code	Stratigraphic Unit	Soil Horizon	Depth mbas	TL age (years)	Method	Other Ages/Controls/Remarks
BX-8805	Paleosol		7.9	9950 ± 580	TB, RGN, PB	10559-10039 ^{14}C
BX-8802	Paleosol		7.8	11000 ± 820	TB, RGN, PB	13279-12779 ^{14}C
BX-8801	Loess		15.0	17020 ± 890	TB, RGN, PB	

Country: China
Site: Liujiapo
Source: Musson F.M., Clarke M.L. and Wintle A.G., (1994). Luminescence dating of loess from the Liujiapo section, Central China, *Quaternary Geochronology*, **13**, 407-410

Laboratory Sample Code	Stratigraphic Unit	Soil Horizon	Depth mbas	TL age (years)	Method	Other Ages/Controls/Remarks
	Loess		0.5	18900 ± 900	RGN	-
	Loess		0.5	15300 ± 600	TB	-
	Loess		0.8	22600 ± 1200	RGN	-
	Loess		0.8	25700 ± 800	TB	-
	Loess		0.9	22300 ± 800	RGN	-
	Loess		1.0	21900 ± 600	RGN	-
	Loess		1.0	23700 ± 800	TB	-
	Loess		1.1	26400 ± 1500	RGN	-
	Loess		1.1	27300 ± 1100	TB	-
	Loess		1.2	27200 ± 1300	RGN	-

	Loess		1.4	32800 ± 1600	RGN	-
	Loess		1.4	26300 ± 1000	TB	-
	Loess		1.6	33800 ± 1500	RGN	-
	Loess		2.0	41800 ± 2000	RGN	-
	Loess		2.0	51000 ± 2100	TB	-
	Loess		2.2	31700 ± 2400	RGN	-
	Loess		2.2	44000 ± 1200	TB	-
	Loess		2.4	45400 ± 2000	RGN	-
	Loess		2.8	43900 ± 2700	RGN	-
	Loess		2.8	38300 ± 3000	TB	-
	Loess		3.0	40100 ± 2200	RGN	-
	Loess		3.1	44700 ± 2000	RGN	-
	Loess		3.1	58000 ± 3400	TB	-
	Loess		3.6	44100 ± 2400	RGN	-
	Loess		3.6	48200 ± 1500	TB	-
	Loess		4.1	47900 ± 2400	RGN	-
	Loess		4.3	55500 ± 2900	RGN	-
	Loess		4.3	55300 ± 3500	TB	-
	Loess		4.8	46800 ± 2200	RGN	-
	Loess		4.8	53200 ± 2500	TB	-
	Paleosol		5.0	51100 ± 2000	RGN	-
	Paleosol		5.3	55200 ± 3700	RGN	-

Errors in age were calculated directly from the dose rate and equivalent dose data.

Country: Czech Republic
Site: Dolni Vestonice
Source: Musson F.M. and Wintle A.G., (1994), Luminescence dating of loess profile at Dolni Vestonice, Czech Republic, *Quaternary Geochronology*, **13**, 411-416

Laboratory Sample Code	Stratigraphic Unit	Soil Horizon	Depth mbas	TL age (years)	Method	Other Ages/Controls/Remarks
a				19700 ± 800	RGN	
a				17000 ± 1000	TB	
b				21600 ± 1600	RGN	
b				18700 ± 800	TB	
c	Occupation layer			17600 ± 1000	RGN	
c				16300 ± 900	RGN	
d				24800 ± 2000	TB	
e				52900 ± 2300	RGN	
e				36600 ± 1300	TB	
f	Soil Complex II (B2g)			52400 ± 1600	RGN	
f	Soil Complex II (B2g)			51100 ± 2000	TB	
g	Soil Complex II (B2g)			49700 ± 4000	RGN	
g	Soil Complex II (B2g)			48900 ± 2000	TB	
h	Loess in Soil Complex II (B2b)			65000 ± 2600	RGN	
h	Loess in Soil Complex II (B2b)			53100 ± 1800	TB	
i	Loess in Soil Complex II (B2b)			58000 ± 6700	RGN	
i	Loess in Soil Complex II (B2b)			41900 ± 2500	TB	
j	Soil Complex II (B2b)			83000 ± 5400	RGN	
j	Soil Complex II (B2b)			76100 ± 3000	TB	

k	Soil Complex II (B2b)			65200 ± 2500	RGN	
k	Soil Complex II (B2b)			62500 ± 3600	TB	
l	Loess			65900 ± 5100	RGN	
l	Loess			70100 ± 2900	TB	
o	Soil complex III (B1d)			70900 ± 2500	RGN	
o	Soil complex III (B1d)			72400 ± 6400	TB	
p	Loess in Soil complex III			80000 ± 3600	RGN	
q	Soil complex III (B1d)			84300 ± 3200	RGN	
q	Soil complex III (B1d)			92200 ± 4800	TB	
r	Soil complex III (B1d)			85400 ± 5600	RGN	
r	Soil complex III (B1d)			79400 ± 3600	TB	
s	Loess			68600 ± 4500	RGN	
s	Loess			57400 ± 1900	TB	
t	Loess			83900 ± 4200	RGN	
u	Loess			84500 ± 3300	RGN	

Errors in age were calculated directly from the dose rate and equivalent dose data.

Country: Czech Republic
Site: Dolni Vestonice
Source: Zoller et.al., (1994), Towards a revised chronology of loess of Austria with respect to key sections in the Czech Republic and in Hungary, *Quaternary Geochronology*, **13**, 465-472

Laboratory Sample Code	Stratigraphic Unit	Soil Horizon	Depth mbas	TL age (years)	Method	Other Ages/Controls/Remarks
DV6	Loess in PKII			51000 ± 6800	RGN	
DV5	PKII			69900 ± 8000	RGN	
DV4	Loess in PKII			75500 ± 9700	RGN	
DV3	Loess in PKIII			68400 ± 8400	RGN	
DV2	Loess below PKIII			81300 ± 7100	RGN	
DV1	Loess below PKIII			88300 ± 10200	RGN	
DV1KF	Loess below PKIII			111000 ± 15000	RGN	

Country: Hungary (Carpathian Basin)
Site: St.Slankamen
Source: Singhvi A.K., Bronger A., Saur W. and Pant R.K.(1989) Thermoluminescence dating of loess-paleosol sequences in the Carpathian Basin (East-Central Europe): A suggestion for a revised Chronology, *Chemical Geology*, **73**, 307-317.

Laboratory Sample Code	Stratigraphic Unit	Soil Horizon	Depth mbas	TL age (years)	Method	Other Ages/Controls/Remarks
S-50 F2		Ah		75000 ±	RGN	-
S-30 F2		Ah		63000 ±	RGN	-
S-29 F2		Ah		82000 ±	RGN	-
S-120 F2		Ah		85000 ±	RGN	-
S-26 F3		Ah		128000 ±	RGN	-
S-25	Loess below F3	-		121000 ±	RGN	-
S-23	Loess below F4	-		186000 ±	RGN	-
S-22 F5		Bt		≥314000 ±	RGN	-

Country: Hungary (Carpathian Basin)
Site: Erdut
Source: Singhvi A.K., Bronger A., Saur W. and Pant R.K.(1989) Thermoluminescence dating of loess-paleosol sequences in the Carpathian Basin (East-Central Europe): A suggestion for a revised Chronology, *Chemical Geology*, **73**, 307-317.

Laboratory Sample Code	Stratigraphic Unit	Soil Horizon	Depth mbas	TL age (years)	Method	Other Ages/Controls/Remarks
Er-43 F1	Loess			29000 ±	RGN	-
Er-45	Loess below F1			45000 ±	RGN	-

Country: Hungary (Carpathian Basin)
Site: Titel/Mosorin
Source: Singhvi A.K., Bronger A., Saur W. and Pant R.K.(1989) Thermoluminescence dating of loess-paleosol sequences in the Carpathian Basin (East-Central Europe): A suggestion for a revised Chronology, *Chemical Geology*, **73**, 307-317.

Laboratory Sample Code	Stratigraphic Unit	Soil Horizon	Depth mbas	TL age (years)	Method	Other Ages/Controls/Remarks
TM-30	Loess below F2			71000 ±	RGN	-
TM-32 F2	Loess			125000 ±	RGN	-

Country: France
Site: Achenheim
Source: Packman S.C. and Grun R. (1992) TL anaysis of loess samples from Achenheim, *Quaternary Science Review*, **11**, 103-107.

Laboratory Sample Code	Stratigraphic Unit	Soil Horizon	Depth mbas	TL age (years)	Method	Other Ages/Controls/Remarks
J2a	Kesselt Horizon		2.5*	15600 ± 1900	RGN (5-58)	
J2a	Kesselt Horizon		2.5*	16400 ± 1900	RGN (BG12)	-
J2a	Kesselt Horizon		2.5*	12900 ± 2700	TB(5-58)	-
J2a	Kesselt Horizon		2.5*	14800 ± 2300	TB(BG12)	-
L1	Loess		4.0*	26500 ± 3400	RGN(5-58)	-
L1	Loess		4.0*	22600 ± 2800	RGN(BG12)	-
L1	Loess		4.0*	27000 ± 4900	TB(5-58)	-
L1	Loess		4.0*	26900 ± 5300	TB(BG12)	

O2	Loess		23.0*	72500 ± 9300	RGN(5-58)NP	
O2	Loess	?	23.0*	60200 ± 7500	RGN(BG12)	-
O2	Loess		23.0*	47100 ± 13700	TB(5-58)NP	
O2	Loess		23.0*	55800 ± 17700	TB(BG12)	
O2	Loess		23.0*	74600 ± 8700	RGN(5-58)PH	
O2	Loess		23.0*	99200 ± 60000	TB(5-58)PH	
O2	Loess		23.0*	56200 ± 7000	RGN(UG11)NP	
O2	Loess		23.0*	66100 ± 31800	TB(UG11)NP	
T1	Loess		33.0*	147100 ± 2100	RGN(5-58)	
T1	Loess		33.0*	118100 ± 18100	RGN(BG12)	
T1	Loess	?	33.0*	127900 ± 31200	TB(5-58)	-
T1	Loess	?	33.0*	86600 ± 10900	TB(BG12)	-

Country: France
Site: Achenheim 1
Source: Buraczynski and Butrym J. (1987) Thermoluminescence stratigraphy of the loess in Alsace (France), *Catena Suppliment*, **9**, 81-94.

Laboratory Sample Code	Stratigraphic Unit	Soil Horizon	Depth mbas	TL age (years)	Method	Other Ages/Controls/Remarks
	Loess Vistulian		2.0	15400 ± 2200		-
Lub 31	Loess Vistulian		6.0	38500 ± 4600		-
Lub 32	Loess Vistulian		10.0	56000 ± 7000		-
Lub 33	Loess Warthanian		13.0	159000 ± 20000		-
Lub 34	Soil Holsteinian upper	Bt	20.7	265000 ± 35000		-

Country: France
Site: Achenheim 2
Source: Buraczynski J. and Butrym J. (1987) Thermoluminescence stratigraphy of the loess in Alsace (France), *Catena Suppliment*, **9**, 81-94.

Laboratory Sample Code	Stratigraphic Unit	Soil Horizon	Depth mbas	TL age (years)	Method	Other Ages/Controls/Remarks
Lub 35	Loess Vistulian Solifluction		3.0	27500 ± 33000		-
Lub 36	Loess Vistulian Solifluction		5.0	39000 ± 4700		-
Lub 37	Loess Vistulian		6.9	48400 ± 5800		-
Lub 38	Loess Warthanian		10.0	118000 ± 15000		-
Lub 39	Loess Warthanian		13.0	176000 ± 23000		-
Lub 40	Soil Drenthanian	Bt	18.0	222000 ± 29000		-
Lub 41	Drenthanian Decal.loess		22.0	244000 ± 31000		
Lub 42	Holsteinian upper loess		26.5	278000 ± 36000		

Country: France
Site: Bischoffsheim 3
Source: Buraczynski J. and Butrym J. (1987) Thermoluminescence stratigraphy of the loess in Alsace (France), *Catena Suppliment*, **9**, 81-94.

Laboratory Sample Code	Stratigraphic Unit	Soil Horizon	Depth mbas	TL age (years)	Method	Other Ages/Controls/Remarks
Lub 442	Soil Warthanian	Bt	2.4	176000 ± 26000		-
Lub 443	Loess Warthanian		3.0	236000 ± 35000		-
Lub 444	Soil Drentanian	Bt	4.0	248000 ± 37000		-

Country: France
Site: Griesheim 4
Source: Buraczynski J. and Butrym J. (1987) Thermoluminescence stratigraphy of the loess in Alsace (France), *Catena Suppliment*, **9**, 81-94.

Laboratory Sample Code	Stratigraphic Unit	Soil Horizon	Depth mbas	TL age (years)	Method	Other Ages/Controls/Remarks
Lub 445	Loess Vistulian		1.0	35000 ± 5000		-
Lub 446	Soil Holsteinian upper	Bt	1.9	330000 ± 49000		-
Lub 447	Loess Holsteinian upper		2.7	359000 ± 54000		-

Country: France
Site: Neiderbtschdorf
Source: Buraczynski J. and Butrym J. (1987) Thermoluminescence stratigraphy of the loess in Alsace (France), *Catena Suppliment*, **9**, 81-94.

Laboratory Sample Code	Stratigraphic Unit	Soil Horizon	Depth mbas	TL age (years)	Method	Other Ages/Controls/Remarks
Lub 448	Colluvial deposit Warthanian		5.0	147000 ± 22000		-
Lub 449	Soil Drentanian	Bt	9.5	242000 ± 3600		-
Lub 450	Loess Drentanian		10.6	26700 ± 40000		-
Lub 451	Decal.Loess Holsteinian		16.0	351000 ± 53000		-

Country: France
Site: Equischem 6
Source: Buraczynski J. and Butrym J. (1987) Thermoluminescence stratigraphy of the loess in Alsace (France), *Catena Suppliment*, 9, 81-94.

Laboratory Sample Code	Stratigraphic Unit	Soil Horizon	Depth mbas	TL age (years)	Method	Other Ages/Controls/Remarks
Lub 439	Loess Drentanian		5.0	248000 ± 37000		-
Lub 440	Soil Holsteinian	Bt	5.2	306000 ± 46000		-
Lub 441	Soil Holsteinian	Bt	6.4	1494000 ± 224000		-

Country: France
Site: Botzingen 7
Source: Buraczynski J. and Butrym J. (1987) Thermoluminescence stratigraphy of the loess in Alsace (France), *Catena Suppliment*, 9, 81-94.

Laboratory Sample Code	Stratigraphic Unit	Soil Horizon	Depth mbas	TL age (years)	Method	Other Ages/Controls/Remarks
Lub 438	Loess Wartheinian		11.0	141000 ± 21000		-
Lub 436	Colluvial deposit Drentanian		12.4	284000 ± 42000		-
Lub 437	Soil Holsteinian upper	Bt	14.0	487000 ± 73000		-

Country: France
Site: Normandy (St.Romain)
Source: Wintle, A.G., Shakleton N.J. and Lautridou J.P. (1984) Thermoluminescence dating of periods of loess deposition and soil formation in Normandy, *Nature*, **310**, 491-493

Laboratory Sample Code	Stratigraphic Unit	Soil Horizon	Depth mbas	TL age (years)	Method	Other Ages/Controls/Remarks
QTL-20 a	Modern Soil		0.3*	12600 ± 1300	RGN	-
QTL-20 b	Loess	-	0.6*	14400 ± 1300	RGN	-
QTL-20 c	Loess	-	0.9*	13700 ± 1200	RGN	-
QTL-20 d	Loess	-	1.2*	14200 ± 1300	RGN	-
QTL-20 e	Loess	-	1.5*	11100 ± 1000	RGN	-
QTL-20 f	Loess	-	1.78*	16400 ± 1500	RGN	-
QTL-20 g	Loess	-	1.82*	75000 ± 6500	RGN	-
QTL-20 h	Loess		2.1*	80000 ± 7000	RGN	
QTL-20 i	Inter- stadial soil		2.4*	88000 ± 8000	RGN	
QTL-20 j	Inter- stadial soil		2.7*	86000 ± 8000	RGN	
QTL-20 k	Inter- stadial soil		3.0*	83000 ± 7000	RGN	
QTL-20 l	Inter-glacial soil		3.3*	120000 ± 10000	RGN	
QTL-20 m	Inter-glacial soil		3.6*	111000 ± 10000	RGN	
QTL-20 n	Inter-glacial soil		3.9*	114000 ± 10000	RGN	
QTL-20 o	Inter- stadial soil	-	4.2*	125000 ± 11000	RGN	-
QTL-20 p	Inter- stadial soil	-	4.5*	139000 ± 12000	RGN	-

Country: Germany
Site: Niederbieber
Source: Wintle, A.G. (1987) Thermoluminescence dating of loess at Rocourt, Belgium. *Geologie en Mijnbouw*, **66**, 350-420

Laboratory Sample Code	Stratigraphic Unit	Soil Horizon	Depth mbas	TL age (years)	Method	Other Ages/Controls/Remarks
	Laacher sea ash					11000 ^{14}C
QTL-51b	Loess	-		13000 ± 1100	RGN	-

Country: Germany
Site: Rheinhessen
Source: Wintle, A.G. and Brunnacker K. (1982). Ages of volcanic tuff in Rheinhessen Obtained by thermoluminescence dating of loess, *Naturwissenschaften*, **69**, -181

Laboratory Sample Code	Stratigraphic Unit	Soil Horizon	Depth mbas	TL age (years)	Method	Other Ages/Controls/Remarks
QTL-32 a	Loess	-	1.5	19200 ± 1900	RGN	-
QTL-32 b	Loess	-	2.5	19000 ± 1900	RGN	-
QTL-32 c	Loess	-	3.3	20200 ± 2000	RGN	-
QTL-32 d	Loess	-	3.5	18600 ± 1900	RGN	-
QTL-32 e	Loess	-	4.5	43200 ± 4300	RGN	-

Country: Germany
Site: Ringen
Source: Juvigne E.H. and Wintle, A.G., (1988) A new chronostratugraphy of the Late Weichselian loess units in Middle Europe based on thermoluminescence dating, *Elszeitalter u. Geg*, **38**, 94-105

Laboratory Sample Code	Stratigraphic Unit	Soil Horizon	Depth mbas	TL age (years)	Method	Other Ages/Controls/Remarks
QTL-55 A	Loess	-		16100 ± 1400	RGN	-
QTL-55 B	Loess	-		16400 ± 1400	RGN	-

Country: Germany
Site: Riegel
Source: Zoller L., Stremme H.E. and Wagner G.A. (1988) Thermolumineszenz-Datierung an Loess-Paleoboden-Sequenzen von Niedr-, Mittel- und Oberrhein, *Chemical Geology*, **73**, 39-62
Zoller L., and Wagner G.A. (1990) Thermoluminescence dating of loess-Recent developments, *Quaternary International*, **7/8**, 119-128

Laboratory Sample Code	Stratigraphic Unit	Soil Horizon	Depth mbas	TL age (years)	Method	Other Ages/Controls/Remarks
RI 12	Loess	-	3.5*	25200 ± 2200	RGN	-
RI 11	Loesskindl Gerollhorizont	-	14.6*	32600 ± 3000	RGN	-
RI 10	Loess mit loesskindl	-	16*	153000 ± 14000	RGN	-
RI 9	Loess	-	16.7*	184000 ± 1900	RGN	-
RI 8			20.7*	259000 ± 26000	RGN	
RI 7			21.6*	254000 ± 24000	RGN	
RI 6	Obergangsbildung zwischen bzw ober Bodenhorizont		23.2*	273000 ± 23000	RGN	
RI 2	Loess		30.8*	390000 ± 47000	RGN	
RI 0	Loess		34.5*	361000 ±	RGN (STW)	
RI 0	Loess	-	34.5*	425000 ±	RGN (PTW)	-

Country: Germany
Site: Heilbronn-Bockingen
Source: Zoller L., and Wagner G.A. (1990) Thremoluminescence dating of loess-Recent developments, *Quaternary International*, **7/8**, 119-128

Laboratory Sample Code	Stratigraphic Unit	Soil Horizon	Depth mbas	TL age (years)	Method	Other Ages/ Controls/Remarks
HN 0	Loess	-	0.9*	22000 ± 2000	RGN (STW)	-
HN 0	Loess	-	0.9*	23000 ± 2000	RGN (PTW)	-
HN 1	Vernaste Umalagerungszone	-	2.4*	30000 ± 3000	RGN (STW)	-
HN 1	Vernaste Umalagerungszone	-	2.4*	26000 ± 3000	RGN (PTW)	-
HN 2	Lohne soil		3.2*	41000 ± 4000	RGN (STW)	
HN 2	Lohne soil		3.2*	36000 ± 3000	RGN (PTW)	
HN 3	Loess		4.4*	50000 ± 5000	RGN (STW)	
HN 3	Loess		4.4*	66000 ± 6000	RGN (PTW)	
HN 4	Humic Zone		5.7*	63000 ± 7000	RGN (STW)	
HN 4	Humic Zone		5.7*	68000 ± 6000	RGN (PTW)	
HN 5			7.2*	110000 ± 10000	RGN (STW)	
HN 5			7.2*	ca.109000 ±	RGN (PTW)	
HN 6	Loess		8.6*	138000 ± 12000	RGN (STW)	
HN 6	Loess		8.6*	140000 ± 12000	RGN (PTW)	
HN 6	Loess		8.6*	160000 ± 16000	RGN (PTW)	
HN 7	Loess		10*	134000 ± 12000	RGN (STW)	
HN 7	Loess		10*	131000 ± 13000	RGN (PTW)	
HN 7	Loess		10*	149000 ± 13000	RGN (PTW)	
HN 8	Loess		11.7*	142000 ± 13000	RGN (STW)	
HN 9	Loess		12.6*	145000 ± 13000	RGN (PTW)	

HN 10	Soil	fBt	14.8*	168000 ± 28000	RGN (STW)	
HN 10	Soil	fBt	14.8*	ca. 207 ±	RGN (PTW)	
HN 11	Bokinger Humuszone		15.5*	173000 ± 15000	RGN (STW)	
HN 12	soil	fBt	16.7*	170000 ± 15000	RGN (STW)	
HN 12			16.7*	ca.190000 ±	RGN (PTW)	
HN 12	Loess	-	16.7*	ca.256000 ±	RGN (PTW)	

Country: Germany
Site: Rheindahlen
Source: Zoller L., Stremme H.E. and Wagner G.A. (1988) Thermolumineszenz-Datierung an Loess-Paleoboden-Sequenzen von Niedr-, Mittel- und Oberrhein, *Chemical Geology*, **73**, 39-62
Stremme H.E. (1989) Thermoluminescence dating of the Pedostratigraphy of the Quaternary Period in NW Germany. *Geoderma*, **45**, 185-195

Laboratory Sample Code	Stratigraphic Unit	Soil Horizon	Depth mbas	TL age (years)	Method	Other Ages/ Controls/Remarks
RD2	Verbraung/schwach verbraunt (loess loam)	BvC	2.1*	77200 ± 6600	RGN	-
RD3	Stzuhorizont/ staunasse	f1 A1 Sw	2.7*	13700 ± 13000	RGN	-
RD6	Verraung/schwash verbraunt (Fleckenlehm) (loess loam)	f1BvtSd	4.1*	167000 ± 15000	RGN	-
RD8	Stauhorizont/Staunasse (Staublehm)	f2Sd1	5.7*	239000 ± 26000	RGN	-

Country: Germany
Site: Ariendorf
Source: Zoller L., Stremme H.E. and Wagner G.A. (1988) Thermolumineszenz-Datierung an Loess-Paleoboden-Sequenzen von Niedr-, Mittel- und Oberrhein, *Chemical Geology*, **72**, 39-62

Laboratory Sample Code	Stratigraphic Unit	Soil Horizon	Depth mbas	TL age (years)	Method	Other Ages/Controls/Remarks
AR-1	Loess		0.5*	30800 ± 3100	RGN	-
AR-10	Loess		3.7*	199000 ± 18000	RGN	-
AR-12	Sandloess	f2C	7.0*	235000 ± 42000	RGN	-
AR-15K	Sandloess	f2C	7.4*	244000 ± 25000	RGN	-
AR-16	Sandloess	f2C	7.8*	300000 ± 34000	RGN	
	Interglazial Selbergit-tuff	f4Bs	14.2*		RGN	420000 ± 20000 $^{40}Ar/^{39}Ar$

Country: Germany
Site: Toenchesberg
Source: Zoller L. and Wagner G.A. (1989). Strong or partial thermal washing in TL dating of sediments? *Long and Short range limits in Luminescence dating*, The research Laboratory for Archeology and History of Art, Oxf. Univ.,Occasional Publi. no.9

Laboratory Sample Code	Stratigraphic Unit	Soil Horizon	Depth mbas	TL age (years)	Method	Other Ages/Controls/Remarks
	Loess		3.3*	65800 ± 5800	RGN	-
	H3 Humic zone		4.2*	65500 ± 5500	RGN	-
	H2 Humic Zone		5.0*	114000 ± 9000	RGN	-
	Loess		5.5*	114000 ± 17000	RGN	-
	H1 Humic Zone		7.0*	108000 ± 17000	RGN	-
	Loess		9.0*	≥121000 ± 11000	RGN	-
	Loess		9.5*	≥129000 ± 12000	RGN	-

Country: Germany
Site: Nussloch
Source: Zoller L., Stremme H.E. and Wagner G.A. (1988) Thermolumineszenz-Datierung an Loess-Paleoboden-Sequenzen von Niedr-, Mittel- und Oberrhein, *Chemical Geology*, **72**, 39-62

Laboratory Sample Code	Stratigraphic Unit	Soil Horizon	Depth mbas	TL age (years)	Method	Other Ages/Controls/Remarks
NU-1	Eltviller tuff		2.9*	22100 ±	RGN	-
NU-2	Loess		11.5*	66900 ± 5100	RGN	-
NU-4	soil	Bt	12.7*	110000 ± 12000	RGN	-
NU-5	Loess		15*	162000 ± 15000	RGN	-
NU-7	Lohner	Bt		34800 ± 3700	RGN	-

Country: Germany
Site: Rotenberg
Source: Zoller L., Stremme H.E. and Wagner G.A. (1988) Thermolumineszenz-Datierung an Loess-Paleoboden-Sequenzen von Niedr-, Mittel- und Oberrhein, *Chemical Geology*, **72**, 39-62

Laboratory Sample Code	Stratigraphic Unit	Soil Horizon	Depth mbas	TL age (years)	Method	Other Ages/Controls/Remarks
RO-1	Loess		0.7*	27900 ± 2600	RGN	-
RO-2	Loess		2.4*	24000 ± 2400	RGN	-
RO-3	Loess		4.8*	29900 ± 3000	RGN	-
RO-5	Lohner Boden Vorausgegangene		8.0*	34500 ± 3500	RGN	
RO-6	Loess		9.6*	53300 ± 5100	RGN	
RO-7	Humuszone		11.4*	63500 ± 6700	RGN	
RO-8	Humuszone		12.5*	75900 ± 7500	RGN	

Country: Germany
Site: Bad Soden
Source: Zoller L., Stremme H.E. and Wagner G.A. (1988) Thermolumineszenz-Datierung an Loess-Paleoboden-Sequenzen von Niedr-, Mittel- und Oberrhein, *Chemical Geology*, **72**, 39-62

Laboratory Sample Code	Stratigraphic Unit	Soil Horizon	Depth mbas	TL age (years)	Method	Other Ages/Controls/Remarks
SO-1	Lohner Boden	AhBv	1.2*	28600 ± 2900	RGN	-
SO-2	Hochriszeitliche Loess	Bvt	4.9*	150000 ± 13000	RGN	-
SO-3	Humuszone	Ah	6.0*	149000 ± 12000	RGN	-
SO-4	Weilbacher Humuszone	Ah	7.5*	157000 ± 13000	RGN	
SO-5	Tuffband		8.8*	253000 ± 31000	RGN	
SO-6	Tuffband		8.9*	236000 ± 26000	RGN	

Country: Germany
Site: Rheinheim
Source: Zoller L., Stremme H.E. and Wagner G.A. (1988) Thermolumineszenz-Datierung an Loess-Paleoboden-Sequenzen von Niedr-, Mittel- und Oberrhein, *Chemical Geology*, **72**, 39-62

Laboratory Sample Code	Stratigraphic Unit	Soil Horizon	Depth mbas	TL age (years)	Method	Other Ages/Controls/Remarks
RH-1	Lohner Boden	Bv	2.0*	27000 ± 2600	RGN	-
RH-2	Lohner Boden	Bv	2.5*	27800 ± 2800	RGN	-
RH-6	Rheinheimer tuff		14.0*	228000 ± 37000	RGN	-
RH-7	Rheinheimer tuff		14.8*	216000 ± 23000	RGN	

Country: Germany
Site: Karlich
Source: Zoller L., Stremme H.E. and Wagner G.A. (1988) Thermolumineszenz-Datierung an Loess-Paleoboden-Sequenzen von Niedr-, Mittel- und Oberrhein, *Chemical Geology*, **72**, 39-62

Laboratory Sample Code	Stratigraphic Unit	Soil Horizon	Depth mbas	TL age (years)	Method	Other Ages/Controls/Remarks
KAE-4	Weilbacher Humuszone		5.0*	152000 ± 15000	RGN	-
KAE-2	Loess		7.0*	232000 ± 28000	RGN	-
KAE-1	Loess		7.5*	222000 ± 25000	RGN	-

Country: Germany
Site: Die Hangendfolge des Quartarprofils in der Ziegeleigrube Hagelsstadt Nordwand;
Source: Buch M.W. and Zoller L. (1990) Gliederung und Thermolumineszenz Chronologie der Wurmloesse im Raum Regensberg. *Eiszeitalter U.Gegenwart*, **40**, 63-84

Laboratory Sample Code	Stratigraphic Unit	Soil Horizon	Depth mbas	TL age (years)	Method	Other Ages/Controls/Remarks
Hg1	Nasboden in typ. Loess		0.8*	25100 ± 2300	RGN	-
Hg2	Loess		2.1*	58000 ± 5000	RGN	
Hg3	Pseudovergleyter Lehm (Basisfließerde) with Hozkohle und Fe/Mn Konerlionen		2.5*	74000 ± 7400	RGN	
Hg4	Loesslehm		4.9*	138000 ± 14000	RGN	
Hg4B	Loesslehm		5.1*	141000 ± 16000	RGN	

Country: Germany
Site: Raum Regensburg/Donau im Vergleich Gliederungsschema
Source: Buch M.W. and Zoller L. (1990) Gliederung und Thermolumineszenz Chronologie der Wurmloesse im Raum Regensberg. *Eiszeitalter U.Gegenwart*, **40**, 63-84

Laboratory Sample Code	Stratigraphic Unit	Soil Horizon	Depth mbas	TL age (years)	Method	Other Ages/Controls/Remarks
Roh-1			0.2*	16200 ± 1500	RGN	-
Ob-1	Loess		1.3*	20000 ± 2000	RGN	
Ob-2	initial Verbraunnung	fCv	2.7*	21400 ± 2000	RGN	
Ob-3	Nasboden in sandloess		2.1*	21600 ± 1900	RGN	
Le1	sandloess		2.3*	24100 ± 2400	RGN	
Le2	Sandloes/loessabfoldge	fCv	2.3*	25400 ± 2400	RGN	

Country: Germany
Site: Rheindahlen
Source: Frechen M. Bruckner H. and Radtke. (1992) A comparison of different TL-techniques on loess from Rheindahlen (F.R.G.). *Quaternary Science Review*, **11**, 109-113

Laboratory Sample Code	Stratigraphic Unit	Soil Horizon	Depth mbas	TL age (years)	Method	Other Ages/Controls/Remarks
RHE 9	Sandy Reworked loess		1.5*	10300 ± 9000		-
RHE 8	Sandy Reworked Loess		2.5*	99000 ± 9000		
RHE 7	Loess clay		3.2*	163000 ± 14000		
RHE 6	Loess clay		3.8*	142000 ± 12000		
RHE 5	Loess clay		5.0*	176000 ± 15000		
RHE 4	Loess clay		5.1*	194000 ± 17000		
RHE 3	Loess clay		5.9*	172000 ± 14000		
RHE 2	Loess clay		7.1*	194000 ± 15000		
RHE 1	Loess clay		7.5*	172000 ± 14000		

Country: Germany
Site: Rheindahlen
Source: Frechen M. Bruckner H. and Radtke. (1992) A comparison of different TL-techniques on loess from Rheindahlen (F.R.G.). *Quaternary Science Review*, **11**, 109-113

Laboratory Sample Code	Stratigraphic Unit	Soil Horizon	Depth mbas	TL age (years)	Method	Other Ages/Controls/Remarks
AR1 1	Reworked loess		0.1*	59000 ± 6000	RGN	-
AR1 1	Reworked Loess		0.1*	41000 ± 4000	TB	
AR1 5	Reworked loess		0.8*	105000 ± 19000	RGN	
AR1 5	Reworked loess		0.8*	56000 ± 14000	TB	
AR1 10	Reworked loess		1.7*	106000 ± 16000	RGN	

AR1 10	Reworked loess		1.7*	133000 ± 14000	TB	
AR1 16	Reworked loess		2.5*	101000 ± 13000	RGN	
AR1 16	Reworked loess		2.5*	90000 ± 13000	TB	
AR1 20	Reworked loess		2.6*	87000 ± 11000	RGN	
AR1 20	Reworked loess		2.6*	159000 ± 28000	TB	
AR1 25	Reworked loess		3.7*	139000 ± 16000	RGN	
AR1 25	Reworked loess		3.7*	81000 ± 14000	TB	
AR1 30	Reworked loess		4.4*	122000 ± 13000	RGN	
AR1 30	Reworked loess		4.4*	125000 ± 13000	TB	
AR1 34	Reworked loess		8.0*	142000 ± 14000	RGN	
AR1 34	Reworked loess		8.0*	198000 ± 22000	TB	
AR1 37	Reworked loess		9.0*	153000 ± 17000	RGN	
AR1 37	Reworked loess		9.0*	140000 ± 19000	TB	

Country: Germany
Site: Toenchesberg
Source: Frechen M. Bruckner H. and Radtke. (1992) A comparison of different TL-techniques on loess from Rheindahlen (F.R.G.). *Quaternary Science Review*, **11**, 109-113

Laboratory Sample Code	Stratigraphic Unit	Soil Horizon	Depth mbas	TL age (years)	Method	Other Ages/Controls/Remarks
T1	Loess		0.5*	13500 ± 1700	RGN	-
T15	Colluvium		2.0*	40000 ± 4000	RGN	-
T25	Colluvium		4.0*	59000 ± 7000	RGN	-
T30	Reworked Loess		7.0*	84000 ± 9000	RGN	-
T40	Reworked Loess		8.4*	85000 ± 9000	RGN	-
T60	Reworked Loess		10.0*	80000 ± 10000	RGN	
T75	Reworked Loess		14.0*	103000 ± 11000	RGN	
T80	Reworked Loess		19.0*	106000 ± 11000	RGN	

Country: Germany
Site: Graselberg
Source: Buschbeck H. M, Chun H.-U., Donig R. and Gesler R. (1992) Thermoluminescence dating of loess horizones in Wiesbaden-Graselberg and Wallertheim by the quartz inclusion method. *Quaternary Science Review*, **11**, 19-23

Laboratory Sample Code	Stratigraphic Unit	Soil Horizon	Depth mbas	TL age (years)	Method	Other Ages/Controls/Remarks
GR 90	Loess		1.1*	20300 ± 2900	TB+RGN	-
GR 135	Loess		1.7*	21400 ± 2500	TB+RGN	-
GR 150	Loess		1.8*	24000 ± 3000	TB+RGN	-
GR 190L	Loess		2.1*	27400 ± 3400	TB+RGN	-
GR 190R	Loess		2.1*	26900 ± 3300	TB+RGN	-

Country: Germany
Site: Weisbaden
Source: Bushbeck H. M., Chun H.-U., Donig R. and Gesler R. (1992) Thermoluminescence dating of loess horizones in Wiesbaden-Graselberg and Wallertheim by the quartz inclusion method, *Quaternary Science Review*, **11**, 19-23

Laboratory Sample Code	Stratigraphic Unit	Soil Horizon	Depth mbas	TL age (years)	Method	Other Ages/Controls/Remarks
W10	Loess		1.7*	31400 ± 3500	TB+RGN	-
W14	Loess		1.7*	27500 ± 3000	TB+RGN	-
W9	Loess		2.3*	30000 ± 3000	TB+RGN	
W11	Loess		2.3*	31500 ± 3600	TB+RGN	
W13	Loess		2.3*	33000 ± 3900	TB+RGN	
W125	Loess		3.2*	31200 ± 3200	TB+RGN	
W151	Loess		3.7*	29300 ± 3300	TB+RGN	-
W215	Loess		3.8*	33000 ± 3600	TB+RGN	-
W245	Loess		4.3*	31200 ± 3600	TB+RGN	-

Country: Hungary
Site: Paks
Source: Wintle A.G. and Packman S.C. (1988), Thermoluminescence ages for three sections in Hungary. *Quaternary Science Review*, **7**, 315-320

Laboratory Sample Code	Stratigraphic Unit	Soil Horizon	Depth mbas	TL age (years)	Method	Other Ages/Controls/Remarks
QTL 86B	Loess		4.2*	20900 ± 1700	RGN	-
QTL 86C	Loess		6.3*	74700 ± 6500	RGN	-

Country: Hungary
Site: Mende
Source: Wintle A.G. and Packman S.C. (1988), Thermoluminescence ages for three sections in Hungary . *Quaternary Science Review*, **7**, 315-320

Laboratory Sample Code	Stratigraphic Unit	Soil Horizon	Depth mbas	TL age (years)	Method	Other Ages/Controls/Remarks
QTL 85DD	Loess			24000 ± 2000	RGN	-
MO 422	MF1					29800 ± 600 ^{14}C
I-3130	MF2					27200 ± 1400 ^{14}C
HV-5422	MF2					27000 ± 1589 ^{14}C
QTL-85DB	Loess			43400 ± 3800	RGN	
	BD1					32000 ± ^{14}C

Country: Hungary
Site: Tapiosuly
Source: Wintle A.G. and Packman S.C. (1988), Thermoluminescence ages for three sections in Hungary. *Quaternary Science Review*, **7**, 315-320

Laboratory Sample Code	Stratigraphic Unit	Soil Horizon	Depth mbas	TL age (years)	Method	Other Ages/Controls/Remarks
QTL 84AA	Loess		1.6*	15800 ± 1300	RGN	-
QTL 84Z	Loess		1.7*	17700 ± 1600	RGN	
QTL 84N	Loess		2.5*	23200 ± 1900	RGN	
QTL 84G	Loess		5.1*	74400 ± 6600	RGN	
QTL 84D	Loess		6.1*	79200 ± 6100	RGN	

Country: Hungary
Site: Paks
Source: Zoller L. and Wagner G. (1990) Thermoluminescence dating of loess-Recent developments. *Quaternary Inrenational*, **7/8**, 119-128

Laboratory Sample Code	Stratigraphic Unit	Soil Horizon	Depth mbas	TL age (years)	Method	Other Ages/Controls/Remarks
	Loess		9.5	112000 ± 10000	STW	
	Loess		10.5	114000 ± 11000	PTW	
	Loess		12.0	114000 ± 14000	PTW	
	Loess		13.5	159000 ± 17000	STW	
	Loess		20.7	199000 ± 20000	STW	
	Loess		20.7	172000 ± 18000	PTW	
	Loess		25.0	190000 ± 17000	STW	

Country: Hungary
Site: Mende
Source: Zoller L. and Wagner G. (1990). Thermoluminescence dating of loess-Recent developments, *Quaternary Inrenational*, **7/8**, 119-128

Laboratory Sample Code	Stratigraphic Unit	Soil Horizon	Depth mbas	TL age (years)	Method	Other Ages/Controls/Remarks
	MF1		10.0	44300 ± 2700	PTW	
	MF2		11.0	69300 ± 5400	PTW	
	Loess		17.3	165000 ± 25000	STW	
	Loess		17.3	163000 ± 21000	PTW	
	BD1		18.0	116000 ± 17000	PTW	
	Loess		19.0	150000 ± 27000	STW	
	Loess		19.0	141000 ± 14000	PTW	
	BD2		21.0	147000 ± 12000	PTW	
	Loess		22.0	207000 ± 16000	PTW	
	BA		23.0	211000 ± 26000	STW	
	BA		23.0	236000 ± 25000	PTW	
	BA		25.0	218000 ± 19000	PTW	
	Loess		27.0	237000 ± 32000	PTW	
	Loess		27.8	270000 ± 26000	PTW	

Country: Hungary
Site: Tapiosuly
Source: Zoller L. and Wagner G., (1990). Thermoluminescence dating of loess-Recent developments *Quaternary Inrenational*, **7/8**, 119-128

Laboratory Sample Code	Stratigraphic Unit	Soil Horizon	Depth mbas	TL age (years)	Method	Other Ages/Controls/Remarks
	h1 (Weakhumus Horizon)		2.1	21000 ± 1600		
	Loess		2.5	23500 ± 2000		

Country: India
Site: Burzahom, Kashmir
Source: Singhvi,A.K.; Bronger, A.; Pant, R.K. and Saur, W . (1987), Thermoluminescence dating and its implications for the chronostratigraphy of loess-plaeosol sequences in Kashmir, *Chemical Geology*, **65**, 45-56
Bronger et.al., 1987. *Quaternary Research*, **27**, 167-181

Laboratory Sample Code	Stratigraphic Unit	Soil Horizon	Depth mbas	TL age (years)	Method	Other Ages/Controls/Remarks
B-1	Loess		0.3	48800 ±	RGN	
B-3	Soil	Bw	1.3	64700 ±	RGN	
B-9	Soil	Bt	2.8	101300 ±	RGN	

Country: India
Site: Dilpur, Kashmir
Source: Singhvi, A.K.; Bronger, A.; Pant, R.K. and Saur, W (1987), Thermoluminescence dating and its implications for the chronostratigraphy of loess-plaeosol sequences in Kashmir. *Chemical Geology*, **65**, 45-56
Bronger et.al., 1987. *Quaternary Research*, **27**, 167-181

Laboratory Sample Code	Stratigraphic Unit	Soil Horizon	Depth mbas	TL age (years)	Method	Other Ages/Controls/Remarks
DIL-4	Loess		3.3	57800 ±	RGN	
DIL-5	Soil	Bwt	6.1	111000 ±	RGN	

Country: India
Site: Karapur, Kashmir
Source: Singhvi , A.K.; Bronger, A.; Pant, R.K. and Saur, W (1987), Thermoluminescence dating and its implications for the chronostratigraphy of loess-plaeosol sequences in Kashmir *Chemical Geology*, **65**, 45-56
Bronger et.al., 1987. *Quaternary Research*, **27**, 167-181

Laboratory Sample Code	Stratigraphic Unit	Soil Horizon	Depth mbas	TL age (years)	Method	Other Ages/Controls/Remarks
K-1		Bt	1.5	5100 ±	RGN	
K-2		A	4.5	50800 ±	RGN	
K-3		Aht	5.7	52100 ±	RGN	
K-4		Ah	6.4	65300 ±	RGN	
K-5		Aht	8.0	81600 ±	RGN	
K-6	Loess		11.3	130300 ±	RGN	

Country: India
Site: Kanchikhol, Kashmir
Source: Rendell H.M., Gardner R.A.M., Agrawal D.P. and Juyal N (1989). Chronology and stratigraphy of Kasmir loess. *Z.Geomorph N.F.suppl. BD*, **76**, 213-223

Laboratory Sample Code	Stratigraphic Unit	Soil Horizon	Depth mbas	TL age (years)	Method	Other Ages/Controls/Remarks
KK4C	Loess		4.6	31040 ± 3600		
KK4B	Loess		5.0	53100 ± 6200		
KK4A	Loess		5.3	41480 ± 5600		
KK3A	Loess		11.3	81180 ± 7300		
KK2B	Loess		14.1	90000 ± 9000		
KK1C	Loess		20.2	94440 ± 8200		
KK1B	Loess		20.8	93450 ± 8300		
KK1A	Loess		21.6	142500 ± 14900		

Country: India
Site: Dilpur, Kashmir
Source: Rendell H.M., Gardner R.A.M., Agrawal D.P. and Juyal N (1989). Chronology and stratigraphy of Kasmir loess. *Z.Geomorph N.F.suppl. BD*, **76**, 213-223

Laboratory Sample Code	Stratigraphic Unit	Soil Horizon	Depth mbas	TL age (years)	Method	Other Ages/Controls/Remarks
DIL4	Loess		3.3	50780 ± 6020		
DIL3B	Loess		8.5	86080 ± 8600		
DIL2	Loess		12.2	98270 ± 8600		
DIL1	Loess		18.5	122530 ± 12200		

Country: India
Site: Pehru, Kashmir
Source: Rendell H. M., Gardner R.A.M., Agrawal D.P. and Juyal N (1989). Chronology and stratigraphy of Kasmir loess.. *Z.Geomorph N.F.suppl. BD*, **76**, 213-223

Laboratory Sample Code	Stratigraphic Unit	Soil Horizon	Depth mbas	TL age (years)	Method	Other Ages/Controls/Remarks
PE4	B Borizon	Bh	5.7	94110 ± 8350		
PE3	Loess		9.0	98470 ± 8700		
PE2	Loess		15.0	112250 ± 10200		
PE1	Loess		18.0	113680 ± 10800		
PEUK ((Upper karewa lake beds)	Lake silt		21.0	113500 ± 10300		

Country: India
Site: Waghoma, Kashmir
Source: Rendell H.M., Gardner R.A.M., Agrawal D.P. and Juyal N (1989). Chronology and stratigraphy of Kasmir loess. *Z.Geomorph N.F.suppl. BD*, **76**, 213-223

Laboratory Sample Code	Stratigraphic Unit	Soil Horizon	Depth mbas	TL age (years)	Method	Other Ages/Controls/Remarks
W3A	Lightly weathered loess		3.6	47100 ± 5500		
W2AA	Loess		12.2	100800 ± 9100		

Country: India
Site: Burzahom, Kashmir
Source: Rendell H.M., Gardner R.A.M., Agrawal D.P. and Juyal N (1989). Chronology and stratigraphy of Kasmir loess.. *Z.Geomorph N.F.suppl. BD*, **76**, 213-223

Laboratory Sample Code	Stratigraphic Unit	Soil Horizon	Depth mbas	TL age (years)	Method	Other Ages/Controls/Remarks
BURZL	Loess		4.6	47730 ± 4400		
BURZUK	Lake silt		7.2	78480 ± 7200		

Country: India
Site: Humhama, Kashmir
Source: Rendell H.M., Gardner R.A.M., Agrawal D.P. and Juyal N (1989). Chronology and stratigraphy of Kasmir loess. *Z.Geomorph N.F.suppl. BD*, **76**, 213-223

Laboratory Sample Code	Stratigraphic Unit	Soil Horizon	Depth mbas	TL age (years)	Method	Other Ages/Controls/Remarks
HUM4	soil	Bh	5.0	48810 ± 5300		
HUM7((Upper karewa lake beds)	Bloky lake clay		6.6	109000 ± 5800		

Country: India
Site: Pattan, Kashmir
Source: Rendell H.M., Gardner R.A.M., Agrawal D.P. and Juyal N (1989). Chronology and stratigraphy of Kasmir loess.. *Z.Geomorph N.F.suppl. BD*, **76**, 213-223

Laboratory Sample Code	Stratigraphic Unit	Soil Horizon	Depth mbas	TL age (years)	Method	Other Ages/Controls/Remarks
PAT (Upper karewa lake beds)				82400 ± 8000		

Country: New Zealand
Site: North Island and South Island
Source: Berger et.al., Test of thermoluminescence dating of loess from New Zealand and Alaska, 1994. *Quaternary Science Review*, **13**, 309-333

Laboratory Sample Code	Stratigraphic Unit	Soil Horizon	Depth mbas	TL age (years)	Method	Other Ages/Controls/Remarks
AOK-2	Loess			41800 ± 3100	TB	26200 ± 900 ^{14}C
AOK-2	Loess			19800 ± 2000	PB	26200 ± 900 ^{14}C
AOK-2	Loess			24300 ± 1800	PB-R	26200 ± 900 ^{14}C
PNRD-1	Loess			19800 ± 1900	PB	26500 ± 1000 ^{14}C
PNRD-1	Loess			34100 ± 2700	TB	26500 ± 1000 ^{14}C
RTAT-1	Loess			16300 ± 1300	PB	20200 ± 1600 ^{14}C
GTR-1	Loess			15800 ± 1600	PB	23500 ± 600 ^{14}C
GTR-5	Loess			17200 ± 2400	PB	24500 ± 600 ^{14}C
CSL-1	Loess			≥16900 ± 2200	PB	24500 ± 600 ^{14}C
FERY-1	Loess			85000 ± 15000	PB	75000 ± 5000 (ref.6)
FERY-1	Loess			105000 ± 12000	ADD	75000 ± 5000 (ref.6)

RTAT-5	Loess			134000 ± 22000	PB	110000 ± 10000 (ref.3 and 8)
RTAT-5	Loess			89100 ± 7300	PB-R	110000 ± 10000 (ref.3 and 8)
RTAT-13	Loess			168000 ± 17000	TB	190000 ± 20000 (ref.3 and 8)
RTAT-9	Loess			234000 ± 56000	TB	270000 ± 20000 (ref.3 and 8)
RTAT-9	Loess			<406000 ± 76000	ADD	270000 ± 20000 (ref.3 and 8)
GRDQ-2	Loess			194000 ± 22000	TB	300000 ± 20000 (ref.3 and 8)
RTAT-16	Loess			247000 ± 41000	PB	354000 ± 40000
RTAT-16	Loess			257000 ± 30000	ADD	354000 ± 40000
RTP-2	Loess			323000 ± 83000	PB	360000 ± 40000 (Fission track, ref. 3 and 8)
RTP-2	Loess			403000 ± 76000	TB	360000 ± 40000 (Fission track, ref 3 and 8)
RTP-2	Loess			399000 ± 48000	ADD	360000 ± 40000 (Fission track ref 3 and 8)
RTAT-20	Loess			≥370000 ± 57000	PB	475000 ± 25000 (ref. 3 and 8)
RTAT-20	Loess			599000 ± 99000	TB	475000 ± 25000 (ref. 3 and 8)
TMUNA-1	Loess			410000 ± 120000	PB	800000 ± 50000 (magnetic reversal)
TMUNA-1	Loess			730000 ± 25000	TB	800000 ± 50000 (magnetic reversal)

Country: Pakistan
Site: Potwar plateau
Source: Rendell H.M. and Townsend P.D. (1988) Thremoluminescence dating of a 10m loess profile in Pakistan, . *Quaternary Science Reviews*, 7, 251-255

Laboratory Sample Code	Stratigraphic Unit	Soil Horizon	Depth mbas	TL age (years)	Method	Other Ages/Controls/Remarks
PKR891			0.5*	32370 ± 3200	TB	
PKR891			0.5*	33420 ± 3300	RGN	
PKR892			1.0*	39860 ± 4250	TB	
PKR892			1.0*	35820 ± 3600	RGN	
PKR893			1.5*	45770 ± 4100	TB	
PKR893			1.5*	36600 ± 3600	RGN	
PKR894			2.0*	46880 ± 4200	TB	
PKR894			2.0*	39460 ± 4000	RGN	
PKR895			2.5*	58330 ± 5300	TB	
PKR895			2.5*	45440 ± 4500	RGN	
PKR897			3.5*	59420 ± 5900	TB	
PKR897			3.5*	44460 ± 4400	RGN	
PKR899			4.5*	74980 ± 7900	TB	
PKR899			4.5*	62600 ± 6300	RGN	
PKR8911			5.5*	89940 ± 8900	TB	
PKR8911			5.5*	72500 ± 7300	RGN	
PKR8915			7.5*	107960 ± 9190	TB	
PKR8915			7.5*	72830 ± 7300	RGN	
PKR8917			8.5*	135800 ± 12600	TB	
PKR8917			8.5*	72300 ± 7200	RGN	

PKR8919					TB	
PKR8919			8.5*		RGN	

Country: UK
Site: Devensian, England
Source: Wintle A.G. (1981) Thermoluminescence dating of the late Devensian loesses in southern England *Nature*, **289**, 479-480

Laboratory Sample Code	Stratigraphic Unit	Soil Horizon	Depth mbas	TL age (years)	Method	Other Ages/Controls/Remarks
1a				14800 ± 1480	RGN	
1b				13150 ± 1315	RGN	
1c				17880 ± 1788	RGN	
1d				17530 ± 1753	RGN	
1e				15930 ± 1593	RGN	
1f				18620 ± 1862	RGN	

Country: UK
Site: Devensian, Kent England
Source: Wintle A.G. and Catt J.A., (1985). Thermoluminescence dating of soils developed in Late Devesian loess at Pegwell Bay, Kent, *Jounal of Soil Science*, **36**, 293-298

Laboratory Sample Code	Stratigraphic Unit	Soil Horizon	Depth mbas	TL age (years)	Method	Other Ages/Controls/Remarks
QTLz	Surface top soil		1.8	700 ± 100	RGN	
QTLm	Late Holocene hill wash above burried soil		3.3	9800 ± 900	RGN	
QTLn	Late Holocene hill wash above burried soil		7.8	9900 ± 900	RGN	
QTLo	Late Holocene hill wash above burried soil		1.2	8600 ± 800	RGN	
QTLq	Organic horizon in hillwash		6.8	3100 ± 300	RGN	
QTLr	Burried soil		1.9	4600 ± 800	RGN	
QTLs	Burried soil		4.04	7400 ± 700	RGN	
QTLt	Burried soil		6.0	12200 ± 1400	RGN	
QTLu	Burried soil		8.0	11700 ± 1100	RGN	
QTLv	Burried soil		9.7	8000 ± 700	RGN	
QTLw	Burried soil		11.5	9800 ± 900	RGN	
QTLx	Burried soil		13.5	10500 ± 900	RGN	

Country: UK
Site: Northfleet, Southeast, England
Source: Parks D.A. and Rendell H.M. (1992) Thermoluminescence dating and geochemistry of loessic deposits in southeast England. *Journal of Quaternary Science*, **7**, 99-107

Laboratory Sample Code	Stratigraphic Unit	Soil Horizon	Depth mbas	TL age (years)	Method	Other Ages/Controls/Remarks
NF1			2.6	115600 ± 12800	RGN	
NF1			2.6	157900 ± 17500	TB	
NF2/3			3.0	126100 ± 12300	RGN	
NF2/3			3.8	153400 ± 15900	RGN	
NF/4			3.8	182400 ± 18900	TB	

Country: UK
Site: Susex Pad, Southeast, England
Source: Parks D.A. and Rendell H.M.,(1992) Thermoluminescence dating and geochemistry of loessic deposits in southeast England. *Journal of Quaternary Science*, **7**, 99-107

Laboratory Sample Code	Stratigraphic Unit	Soil Horizon	Depth mbas	TL age (years)	Method	Other Ages/Controls/Remarks
T1/2			1.65	87500 ± 10100	RGN	
T1/2			1.65	92300 ± 10600	TB	
T3/4			0.7	73000 ± 8000	RGN	
T3/4			0.7	66600 ± 7300	TB	

Country: UK
Site: Boxgrove, Southeast, England
Source: Parks D.A. and Rendell H.M.,(1992) Thermoluminescence dating and geochemistry of loessic deposits in southeast England. *Journal of Quaternary Science*, **7**, 99-107

Laboratory Sample Code	Stratigraphic Unit	Soil Horizon	Depth mbas	TL age (years)	Method	Other Ages/Controls/Remarks
GTP9			0.6	175300 ± 19500	RGN	
GTP11			0.7	229400 ± 27700	RGN	
GTP14			1.65	184300 ± 20200	RGN	
GTP			1.65	175800 ± 19300	TB	
TP3			0.6	177900 ± 19900	RGN	

Country: UK
Site: Howgate, Southeast, England
Source: Parks D.A. and Rendell H.M.,(1992) Thermoluminescence dating and geochemistry of loessic deposits in southeast England. *Journal of Quaternary Science*, **7**, 99-107

Laboratory Sample Code	Stratigraphic Unit	Soil Horizon	Depth mbas	TL age (years)	Method	Other Ages/Controls/Remarks
HW1/2			1.14	23600 ± 2200	RGN	
HW1/2			1.14	25500 ± 2400	TB	
HW3/4			2.25	21200 ± 2000	RGN	
HW3/4			2.25	24600 ± 2400	TB	

Country: UK
Site: Bebridge, Southeast, England
Source: Parks D.A. and Rendell H.M.,(1992) Thermoluminescence dating and geochemistry of loessic deposits in southeast England. *Journal of Quaternary Science*, **7**, 99-107

Laboratory Sample Code	Stratigraphic Unit	Soil Horizon	Depth mbas	TL age (years)	Method	Other Ages/Controls/Remarks
BF1/3			0.5	18600 ± 2100	RGN	
BF1/3			0.5	17200 ± 1900	TB	

Country: UK
Site: Fresh Water Bay, Southeast, England
Source: Parks D.A. and Rendell H.M., (1992) Thermoluminescence dating and geochemistry of loessic deposits in southeast England. *Journal of Quaternary Science*, **7**, 99-107

Laboratory Sample Code	Stratigraphic Unit	Soil Horizon	Depth mbas	TL age (years)	Method	Other Ages/Controls/Remarks
FB1/3			1.0	21800 ± 2700	RGN	
FB1/3			1.0	24800 ± 3000	TB	

Country: UK
Site: Pegwell Bay, Southeast, England
Source: Parks D.A. and Rendell H.M.,(1992) Thermoluminescence dating and geochemistry of loessic deposits in southeast England. *Journal of Quaternary Science*, **7**, 99-107

Laboratory Sample Code	Stratigraphic Unit	Soil Horizon	Depth mbas	TL age (years)	Method	Other Ages/Controls/Remarks
PB1			2.0	18100 ± 1700	RGN	
PB1			2.0	18800 ± 1800	TB	
PB2			1.5	14600 ± 1600	RGN	
PB2			1.5	14900 ± 1600	TB	
PB3			2.5	17400 ± 1900	RGN	
PB3			2.5	17300 ± 1900	TB	

Country: UK
Site: Reculver, Southeast, England
Source: Parks D.A. and Rendell H.M.,(1992) Thermoluminescence dating and geochemistry of loessic deposits in southeast England. *Journal of Quaternary Science*, **7**, 99-107

Laboratory Sample Code	Stratigraphic Unit	Soil Horizon	Depth mbas	TL age (years)	Method	Other Ages/Controls/Remarks
RC1			4.1	19000 ± 2000	RGN	
RC1			4.1	20800 ± 2200	TB	
RC2			3.5	17600 ± 1800	RGN	
RC2			3.5	18500 ± 1900	TB	
RC3			3.0	17900 ± 1900	RGN	
RC3			3.0	16500 ± 1800	TB	
RC4			2.3	12800 ± 1500	RGN	

RC4			2.3	9600 ± 1100	TB	
RC5			1.3	10100 ± 1200	RGN	
RC5			1.3	9400 ± 1100	TB	

Country: UK
Site: Selsey, Southeast, England
Source: Parks D.A. and Rendell H.M., (1992) Thermoluminescence dating and geochemistry of loessic deposits in southeast England. *Journal of Quaternary Science*, **7**, 99-107

Laboratory Sample Code	Stratigraphic Unit	Soil Horizon	Depth mbas	TL age (years)	Method	Other Ages/Controls/Remarks
SEL1(1/2)			0.55	13600 ± 2100	RGN	
SEL1(1/2)			0.55	17000 ± 2500	TB	

Country: UK
Site: Hope Gap, Southeast, England
Source: Parks D.A. and Rendell H.M., (1992) Thermoluminescence dating and geochemistry of loessic deposits in southeast England. *Journal of Quaternary Science*, **7**, 99-107

Laboratory Sample Code	Stratigraphic Unit	Soil Horizon	Depth mbas	TL age (years)	Method	Other Ages/Controls/Remarks
HG1/3			1.5	109400 ± 14000	RGN	

Country: UK
Site: Southend, Southeast, England
Source: Parks D.A. and Rendell H.M.,(1992) Thermoluminescence dating and geochemistry of loessic deposits in southeast England. *Journal of Quaternary Science*, **7**, 99-107

Laboratory Sample Code	Stratigraphic Unit	Soil Horizon	Depth mbas	TL age (years)	Method	Other Ages/Controls/Remarks
SE1			0.65	15900 ± 1900	RGN	
SE1			0.65	17100 ± 2000	TB	
SE2			1.2	17000 ± 2000	RGN	
SE2			1.2	19300 ± 2300	TB	
SE3			1.65	19900 ± 2200	RGN	
SE3			1.65	21700 ± 2300	TB	

Country: UK
Site: Faversham, Southeast, England
Source: Parks D.A. and Rendell H.M., (1992) Thermoluminescence dating and geochemistry of loessic deposits in southeast England. *Journal of Quaternary Science*, **7**, 99-107

Laboratory Sample Code	Stratigraphic Unit	Soil Horizon	Depth mbas	TL age (years)	Method	Other Ages/Controls/Remarks
FM1			0.95	15000 ± 1800	RGN	

FM1			0.95	23000 ± 2700	TB	
FM2			1.5	17500 ± 2000	RGN	
FM2			1.5	17700 ± 1900	TB	
FM3			2.4	18200 ± 2000	RGN	
FM3			2.4	19400 ± 2400	TB	

Country: UK
Site: Lape Point, Southeast, England
Source: Parks D.A. and Rendell H.M.,(1992) Thermoluminescence dating and geochemistry of loessic deposits in southeast England. *Journal of Quaternary Science*, **7**, 99-107

Laboratory Sample Code	Stratigraphic Unit	Soil Horizon	Depth mbas	TL age (years)	Method	Other Ages/Controls/Remarks
LP1/2			0.6	19900 ± 2600	RGN	
LP1/2			0.6	22800 ± 2900	TB	
LP3/4			0.3	97800 ± 11900	RGN	

Country: UK
Site: Bobbing, Southeast, England
Source: Parks D.A. and Rendell H.M., (1992) Thermoluminescence dating and geochemistry of loessic deposits in southeast England. *Journal of Quaternary Science*, **7**, 99-107

Laboratory Sample Code	Stratigraphic Unit	Soil Horizon	Depth mbas	TL age (years)	Method	Other Ages/Controls/Remarks
BG1/2				20600 ± 2800	RGN	
BG1/2				21800 ± 2800	TB	

Country: UK
Site: Spotlane Quarry, Southeast, England
Source: Parks D.A. and Rendell H.M., (1992) Thermoluminescence dating and geochemistry of loessic deposits in southeast England. *Journal of Quaternary Science*, **7**, 99-107

Laboratory Sample Code	Stratigraphic Unit	Soil Horizon	Depth mbas	TL age (years)	Method	Other Ages/Controls/Remarks
SPQ1(1/22)			0.5	50200 ± 7600	RGN	
SPQ1(1/22)			0.5	51600 ± 7700	TB	

Country: UK
Site: Holbury, Southeast, England
Source: Parks D.A. and Rendell H.M., (1992) Thermoluminescence dating and geochemistry of loessic deposits in southeast England. *Journal of Quaternary Science*, **7**, 99-107

Laboratory Sample Code	Stratigraphic Unit	Soil Horizon	Depth mbas	TL age (years)	Method	Other Ages/Controls/Remarks
HR1				121900 ± 14400	RGN	
HR1				146300 ± 17300	RGN	

Country: UK
Site: Ferring, Southeast, England
Source: Parks D.A. and Rendell H.M., (1992) Thermoluminescence dating and geochemistry of loessic deposits in southeast England. *Journal of Quaternary Science*, **7**, 99-107

Laboratory Sample Code	Stratigraphic Unit	Soil Horizon	Depth mbas	TL age (years)	Method	Other Ages/Controls/Remarks
FE1				11200 ± 1400	RGN	
FE1				10300 ± 1200	TB	

Country: UK
Site: Great Wakering, Southeast, England
Source: Parks D.A. and Rendell H.M., (1992) Thermoluminescence dating and geochemistry of loessic deposits in southeast England. *Journal of Quaternary Science*, **7**, 99-107

Laboratory Sample Code	Stratigraphic Unit	Soil Horizon	Depth mbas	TL age (years)	Method	Other Ages/Controls/Remarks
GW1				16800 ± 1900	RGN	
GW1				16300 ± 1900	TB	

Country: UK
Site: Telscombe, Southeast, England
Source: Parks D.A. and Rendell H.M., (1992) Thermoluminescence dating and geochemistry of loessic deposits in southeast England. *Journal of Quaternary Science*, **7**, 99-107

Laboratory Sample Code	Stratigraphic Unit	Soil Horizon	Depth mbas	TL age (years)	Method	Other Ages/Controls/Remarks
TE1				16400 ± 2000	RGN	
TE1				15000 ± 1900	TB	

Country: UK
Site: Sturt Pond, Southeast, England
Source: Parks D.A. and Rendell H.M., (1992) Thermoluminescence dating and geochemistry of loessic deposits in southeast England. *Journal of Quaternary Science*, **7**, 99-107

Laboratory Sample Code	Stratigraphic Unit	Soil Horizon	Depth mbas	TL age (years)	Method	Other Ages/Controls/Remarks
SP1				29700 ± 3400	RGN	
SP1				35200 ± 4100	TB	

Country: UK
Site: Hordle Cliff, Southeast, England
Source: Parks D.A. and Rendell H.M., (1992) Thermoluminescence dating and geochemistry of loessic deposits in southeast England. *Journal of Quaternary Science*, **7**, 99-107

Laboratory Sample Code	Stratigraphic Unit	Soil Horizon	Depth mbas	TL age (years)	Method	Other Ages/Controls/Remarks
HCL				11800 ± 1400	RGN	

Country: UK
Site: Barton on Sea, Southeast, England
Source: Parks D.A. and Rendell H.M., (1992) Thermoluminescence dating and geochemistry of loessic deposits in southeast England. *Journal of Quaternary Science*, **7**, 99-107

Laboratory Sample Code	Stratigraphic Unit	Soil Horizon	Depth mbas	TL age (years)	Method	Other Ages/Controls/Remarks
B1				16600 ± 2000	RGN	

Country: UK
Site: Chiling, Southeast, England
Source: Parks D.A. and Rendell H.M., (1992) Thermoluminescence dating and geochemistry of loessic deposits in southeast England. *Journal of Quaternary Science*, **7**, 99-107

Laboratory Sample Code	Stratigraphic Unit	Soil Horizon	Depth mbas	TL age (years)	Method	Other Ages/Controls/Remarks
CC1				15500 ± 1900	RGN	
CC1				15100 ± 1800	TB	

Country: UK
Site: Highcliffe, Southeast, England
Source: Parks D.A. and Rendell H.M., (1992) Thermoluminescence dating and geochemistry of loessic deposits in southeast England. *Journal of Quaternary Science*, **7**, 99-107

Laboratory Sample Code	Stratigraphic Unit	Soil Horizon	Depth mbas	TL age (years)	Method	Other Ages/Controls/Remarks
HS1				19500 ± 2400	RGN	

Country: UK
Site: Church St., Southeast, England
Source: Parks D.A. and Rendell H.M., (1992) Thermoluminescence dating and geochemistry of loessic deposits in southeast England. *Journal of Quaternary Science*, **7**, 99-107

Laboratory Sample Code	Stratigraphic Unit	Soil Horizon	Depth mbas	TL age (years)	Method	Other Ages/Controls/Remarks
CSB1				50700 ± 6000	RGN	
CSB1				59600 ± 7000	TB	
CSB2				61400 ± 7200	RGN	
CSB2				79700 ± 9400	TB	

Country: UK
Site: Goring, Southeast, England
Source: Parks D.A. and Rendell H.M., (1992) Thermoluminescence dating and geochemistry of loessic deposits in southeast England. *Journal of Quaternary Science*, **7**, 99-107

Laboratory Sample Code	Stratigraphic Unit	Soil Horizon	Depth mbas	TL age (years)	Method	Other Ages/Controls/Remarks
GS1				15700 ± 1900	RGN	
GS1				17700 ± 2200	TB	